Investigation of Flavoproteins Involved in the Metabolism of Anaerobic Hyperthermophilic Microorganisms

by

Xianqin Yang

A thesis
presented to the University of Waterloo
in fulfillment of the
thesis requirement for the degree of
Doctor of Philosophy
in
Biology

Waterloo, Ontario, Canada, 2007

AUTHOR'S DECLARATION

I hereby declare that I am the sole author of this thesis. This is a true copy of the thesis, including any required final revisions, as accepted by my examiners.

I understand that my thesis may be made electronically available to the public.

ABSTRACT

It was estimated that more than one hundred open reading frames in *Pyrococcus furiosus* and *Thermotoga maritima* could encode flavoproteins based on the results of motif search and comparison of genomic annotation to the experimentally characterized flavoproteins. However, only a few flavoproteins have been characterized from those anaerobic hyperthermophiles. It was found *T. maritima* and *Thermotoga hypogea* were able to grow in the presence of micromolar level of oxygen. As part of an oxygen removal system, the presence of NADH oxidase was detected in both microorganisms. In *T. hypogea*, NADH oxidase activity was constant regardless of the presence of oxygen, while in *T. maritima* it was increased in the presence of oxygen. The purified *T. hypogea* NADH oxidase was a flavin adenine dinucleotide (FAD)-containing homodimer with subunit molecular mass of 50 kDa. In addition to NADH oxidase activity, it also demonstrated activity of dihydrolipoamide dehydrogenase (DLDH), which is probably involved in glycine decarboxylation. The purified NADH oxidase from *T. maritima* was a heterodimeric protein of two subunits with molecular weight of 54 and 46 kDa, which were identified to be encoded by TM1432 and TM1433, respectively. Each subunit bore one FAD and the large subunit had one bacterioferritin-associated ferredoxin (BFD)-like [2Fe-2S]-center. Although the *T. maritima* NADH oxidase had very unusual oxygen sensitivity, the oxygen inactivated enzyme could be fully recovered by incubating with reducing reagents anaerobically. The NADH oxidases from both *T. hypogea* and *T. maritima* catalyzed the reduction of oxygen only to hydrogen peroxide. NADH-dependent peroxidase activities were detected in both *T. maritima* and *T. hypogea*, suggesting the presence of a multi-component oxygen detoxification system in *Thermotoga* species. In addition to its NADH oxidase activity, the enzyme from *T. maritima* exhibited FAD-linked glycerol-3-phosphate dehydrogenase (FAD-GPDH) activity. Along with the glycerol kinase, the FAD-GPDH took part in glycerol utilization in *T. maritima*. Ferredoxin NAD^+ oxidoreductase (FNOR) activity was detected in *T. maritima* using an NADH:benzyl viologen oxidoreductase (BVOR) assay. The purified enzyme was a homodimeric FAD-containing protein with subunit molecular mass of 37 kDa. The purified enzyme was very active in catalyzing the reduction of BV and methyl viologen (MV) using either NADH or NADPH as electron donor and could indeed catalyze the reduction of NAD^+ with the reduced ferredoxin from *T. maritima*. The purified enzyme was further identified to be encoded by TM0869 and annotated as thioredoxin reductase (TrxR). *T. maritima* TrxR could not use commercially available thioredoxin (Trx) from *Spirulina*, but the Trx purified from *T. maritima*. *T. maritima* Trx was identified to be

encoded by TM0868 and annotated as glutaredoxin (Grx)-like protein, which showed both thioredoxin (Trx) and Grx activity. The purified *T. maritima* TrxR could catalyze the Trx-dependent reduction of both insulin and DTNB using NAD(P)H as electron donor. The identified Trx-TrxR system in *T. maritima* is the first one characterized in hyperthermophilic bacteria. *T. hypogea* has great potential in microbial hydrogen production. The key enzyme involved in this process, hydrogenase, has not been studied yet. The growth-dependent hydrogenase activity was detected in *T. hypogea*, from which a homotetrameric hydrogenase was purified. The purified *T. hypogea* hydrogenase did not contain any flavin prosthetic group as speculated, but [Fe-S]-centers. The hydrogenase could catalyze both BV and MV-dependent hydrogen oxidation and MV-dependent hydrogen evolution. Neither NAD(P)H nor NAD(P) could be used as electron carrier for this enzyme. *T. hypogea* hydrogenase could utilize ferredoxin as electron carrier for both production and oxidation of hydrogen, which suggests that the purified hydrogenase plays an important role in hydrogen metabolism of *T. hypogea*. It was concluded that flavoproteins can be involved at least in several very important cellular processes such as detoxification of oxygen, utilization of glycerol, redox regulation, and hydrogen metabolism in hyperthermophiles.

Acknowledgements

I would like to thank my wonderful supervisor, Dr. Kesen Ma, for his endless enthusiasm and guidance throughout my degree. You have been a great mentor and friend to me. You have trusted my capacity and encouraged me to challenge my limits. I would like to thank my committee members, Dr. Bernard Glick and Dr. Trevor Charles, for their invaluable discussions regarding my research and advice about life in general.

I would like to thank all of my friends and colleagues that I have worked with during the past few years. Thank you for your friendship and willingness to share your knowledge with me. Particularly, I would like to thank my friend Xiangxian Ying for sharing his scientific ideas and also helping me through the hard time and happy moments during my study. I would like also to thank Zhenyu Cheng for helping me understand more about protein identification using mass spectrometry.

I would especially like to thank my husband, Ming Jiao, for his dearest love and understanding. I thank him for encouraging me to be confident and optimistic during my study. Lastly, I would like to thank my dearest six-year old daughter for being so understanding throughout my study and letting me concentrate on my thesis writing. I thank her for being so proud of her mother's achievements.

Dedication

This thesis is dedicated to all those I love. Thank you, for everything you do.

Table of Contents

List of Figures

List of Tables

List of Abbreviations

ABTS	2,2'-Azino-bis(3-ethylbenzthiazoline-6-sulfonic acid)
ACN	Acetonitrile
BFD	Bacterioferritin-associated ferredoxin
BV	Benzyl viologen
BVOR	NADH:benzyl viologen oxidoreductase
DCPIP	2,6-Dichlorophenolindophenol
DLDH	Dihydrolipoamide dehydrogenase
DMPD	N, N-dimethyl-*p*-phenylenediamine
DTNB	5,5′-Dithiobis(2-nitrobenzoic acid)
DTT	Dithiothreitol
EPPS	N-(2-hydroxyethyl)-piperazine-N'-3-propanesulfonic acid
FA	Formic acid
FAD	Flavin adenine dinucleotide
FAD-GPDH	FAD-linked *sn*-glycerol-3-phosphate dehydrogenase
FMN	Flavin mononucleotide
FNOR	Ferredoxin:NAD^+ oxidoreductase
FPLC	Fast Performance Liquid Chromatography
G-3-P	Glycerol-3-phosphate
GDC	Glycine decarboxylase complex
Grx	Glutaredoxin
GSSG	Glutathione
HAP	Hydroxyapatite
HRP	Horseradish peroxidase
IAA	Iodoacetamide
ICP-MS	Inductively Coupled Plasma–Mass Spectrometer
MV	Methyl viologen
NAD^+-GPDH	NAD^+-dependent glycerol-3-phosphate dehydrogenase
NBT	Neo blue tetrazolium
PMS	Phenazine methosulfate
POR	Pyruvate:ferredoxin oxidoreductase

ROS	Reactive oxygen species
SDS-PAGE	Sodium dodecyl sulfate-polyacylamide gel electrophoresis
SDT	Sodium dithionite
SHMT	Serine hydroxymethltransferase
Tris-HCl	Tris(hydroxymethyl)aminomethane-HCl
TrxR	Thioredoxin reductase
Trx	Thioredoxin

Chapter 1 General Introduction

The overarching goal of this thesis is to explore the presence of flavoproteins and their roles in the metabolism of hyperthermophiles. Though many different types of flavoproteins have been extensively studied in mesophiles, little is known about their counterparts or new ones in hyperthermophiles, a group of microorganisms with distinct metabolism features. This section of the thesis gives an overview of knowledge about flavoproteins and their diverse functions, and features of the metabolism of hyperthermophiles. The importance of flavoproteins in the metabolism of hyperthermophiles is discussed and the study of flavoproteins in representative microorganisms *Pyrococcus furiosus* and *Thermotoga maritima* is reviewed. The specific goals are described in the last part of this section.

1.1 HYPERTHERMOPHILES

1.1.1 Discovery and diversity of hyperthermophiles

A milestone in microbiology was the isolation of organisms from sulfur-rich, shallow marine volcanic vents, which grow at and even above the boiling point of water (Stetter 1982). Hyperthermophiles are defined as organisms that grow optimally at 80°C and above or capable of growing at 90°C and above (Adams 1994; Baross and Holden 1996; Stetter 1982). In contrast to thermophiles, hyperthermophiles are normally unable to grow below 60^{o}C (Stetter 1996). The majority of them are classified as members of the domains of archaea consisting of four branches: the *Nanoarchaeota*, a group of recently discovered tiny symbiotic cocci (Huber et al. 2002); the *Crenarchaeota* that were isolated from geothermal sites; the *Euryarchaeota* that mainly include methane-producing archaea and halophiles; and the *Korarchaeota* that was discovered recently by DNA sequence analysis and has not yet been fully identified (Barns et al. 1996; Vieille and Zeikus 2001). As the only two branches of bacteria among the hyperthermophiles known, *Thermotogales* and *Aquificales* are deepest in the bacteria genealogy and represent an obvious interest in evolutionary studies (Achenbach-Richter et al. 1987). An archaeal strain, *Pyrolobus aerophilum*, has been recently isolated from hydrothermal vent, which grows at the autoclave temperature and survives up to 130^{o}C (Kashefi and Lovley 2003). Hyperthermophiles have been isolated from the environments with temperatures in the range of 80 to 115^{o}C including continental solfataras, deep geothermally heated oil-producing stratifications, shallow marine and deep-sea hot sediments, hydrothermal vents located up to 4,000 m below the sea level, and hot industrial environments (Vieille and Zeikus 2001). Deep-sea hyperthermophiles live in

the environments with hydrostatic pressures ranging from 200 to 360 atm. Some of these organisms are barotolerant (Reysenbach and Deming 1991) or even barophilic (Erauso et al. 1993; Marteinsson et al. 1999; Nelson et al. 1992). Studies of environmental 16S rRNA sequences and environmental lipid analysis in samples originating from a single continental hot spring (Obsidian pool at Yellowstone National park) suggest that the known hyperthermophiles represent only a fraction of all the hyperthermophiles (Barns et al. 1994; Barns et al. 1996; Hedrick et al. 1992). All hyperthermophiles are found to be located in the extremely short and deep branching-off lineages of the universal phylogenetic tree, indicating a slow rate of evolution (Figure 1-1, Stetter 2006). The tree shows that the archaea and eukarya have a common ancestor that is not shared by bacteria.

1.1.2 Metabolic diversity of hyperthermophiles

Metabolic diversity is one of the approaches microorganisms use for adapting to extreme environments. Although the metabolic pathways used by hyperthermophiles still remain largely unresolved, several dominant characteristics of energy-yielding redox reactions are apparent. The majority of hyperthermophiles in culture take advantage of electron transfer among species of the sulfur redox system. Anaerobes commonly reduce sulfate, sulfite, thiosulfate, or elemental sulfur, while aerobes oxidize sulfide or elemental sulfur to sulfate (Amend and Shock 2001).

1.1.2.1 Chemolithoautotrophic hyperthermophiles

Among all the hyperthermophiles described, some of them are able to utilize inorganic electron donors and acceptors in their energy-yielding reactions. For example, bacterium *Aquifex pyrophilus* can use H_2, S^0, and $S_2O_3^{2-}$ as electron donors, and archaeon *Acidianus infernus* can use S^0 as electron acceptor and donors (Huber et al. 1992; Segerer et al. 1986; Stetter 1996). Autotrophic metabolism is coupled with ATP synthesis *via* the mechanisms of oxidative phosphorylation (Schönheit and Schäfer 1995). In hyperthermophiles, autotrophic energy metabolism is mostly anaerobic or microaerophilic and based on the oxidation of H_2 or sulfur coupled with the reduction of S^0, SO_4^{2-}, CO_2 and NO_3^-, but rarely O_2 (Stetter 2006). Carbon dioxide is the only carbon source required for building up organic cell material.

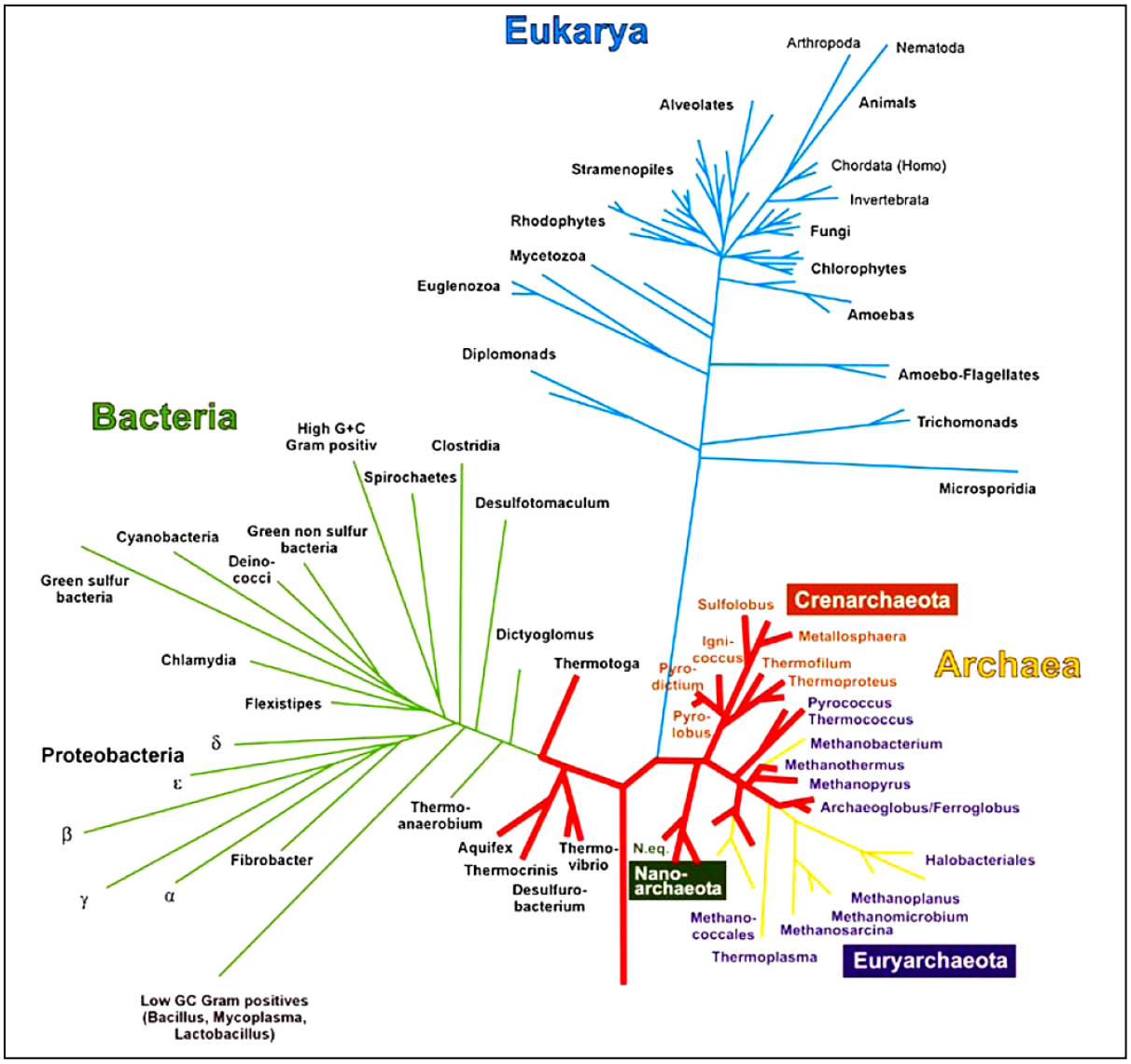

Figure 1-1 Small subunit 16s rRNA based universal phylogenetic tree.

The red bulky lineages represent hyperthermophiles (modified from Stetter 2006) that contain the branches of both bacteria and archaea.

1.1.2.2 Heterotrophic hyperthermophiles

The majority of known hyperthermophiles are obligately heterotrophs that reduce elemental sulfur to hydrogen sulfide, preferentially using complex mixtures of polypeptides and/or carbohydrates as energy and carbon sources in laboratory growth environments (Adams 1994). Among heterotrophic hyperthermophiles, the most extensively studied species from biochemical perspectives are the archaeon, *Pyrococcus furiosus,* and the bacterium, *Thermotoga maritima*. Their facultative dependence on sulfur makes these organisms attractive sources for native versions of hyperthermophilic enzymes (Adams et al. 1995; Adams and Kelly 1998; Bauer et al. 1996; Sunna et al. 1997), as well as good model systems for physiological studies (Kengen et al. 1994; Rinker and Kelly 1996; Schicho et al. 1993).

P. furiosus belongs to the genus of *Pyrococcus*, which includes *P. abyssi* (Erauso et al. 1993), *P. furiosus* (Fiala and Stetter 1986), *P. horikoshii* (Gonzälez et al. 1998) and *P. woesei* (Zillig et al. 1987). *P. furiosus* is a strictly anaerobic, heterotrophic, hyperthermophilic archaeon isolated from geothermally heated marine sediments Vulcano, Italy (Fiala and Stetter 1986). It grows optimally at 100^{o}C and is able to utilize a broad range of sugars as primary carbon source (Bauer et al. 1996; Driskill et al. 1999; Koning et al. 2001, 2002). These include cellobiose, lamimarin, chitin, maltose, barley glucan and starch. It can also grow on pyruvate through gluconeogenesis (Schäfer and Schönheit 1993). Maltose is fermented to pyruvate *via* a modified Embden-Meyerhof pathway involving novel ADP-dependent kinases (Figure 1-2; Sakuraba et al. 2004; Selig et al. 1997; Tuininga et al. 1999). The pyruvate produced is converted to acetate, alanine, CO_2 and H_2. Ferredoxin serves as primary electron carrier for oxidoreductase instead of NAD^+ or $NADP^+$ in the fermentation. *T. maritima* was originally isolated from Volcano Island, Italy (Huber et al. 1986). It belongs to the genus of *Thermotoga* comprising a group of extremely thermophilic, rod shaped, nonsporeforming bacteria with an outer sheath-like envelope also known as 'toga'. They demonstrate heterotrophic growth, with acetic acid, L-lactate, CO_2 and H_2 as the main products from fermentation (Huber et al. 1986; Van Ooteghem et al. 2002, 2004). H_2S is produced when elemental sulfur or sodium thiosulfate is added, the presence of which decreases the production of H_2. In addition to *T. maritima*, eight species in the genus have been isolated, *T. neapolitana* (Jannasch et al. 1988), *T. elfii* (Ravot et al. 1995), *T. subterranae* (Jeanthon et al. 1995), *T. hypogea* (Fardeau et al. 1997); *T. petrophila* and *T. naphthophila* (Takahata et al. 2001), *T. lettingae* (Balk et al. 2002), and *T. thermarum* (Windberger et

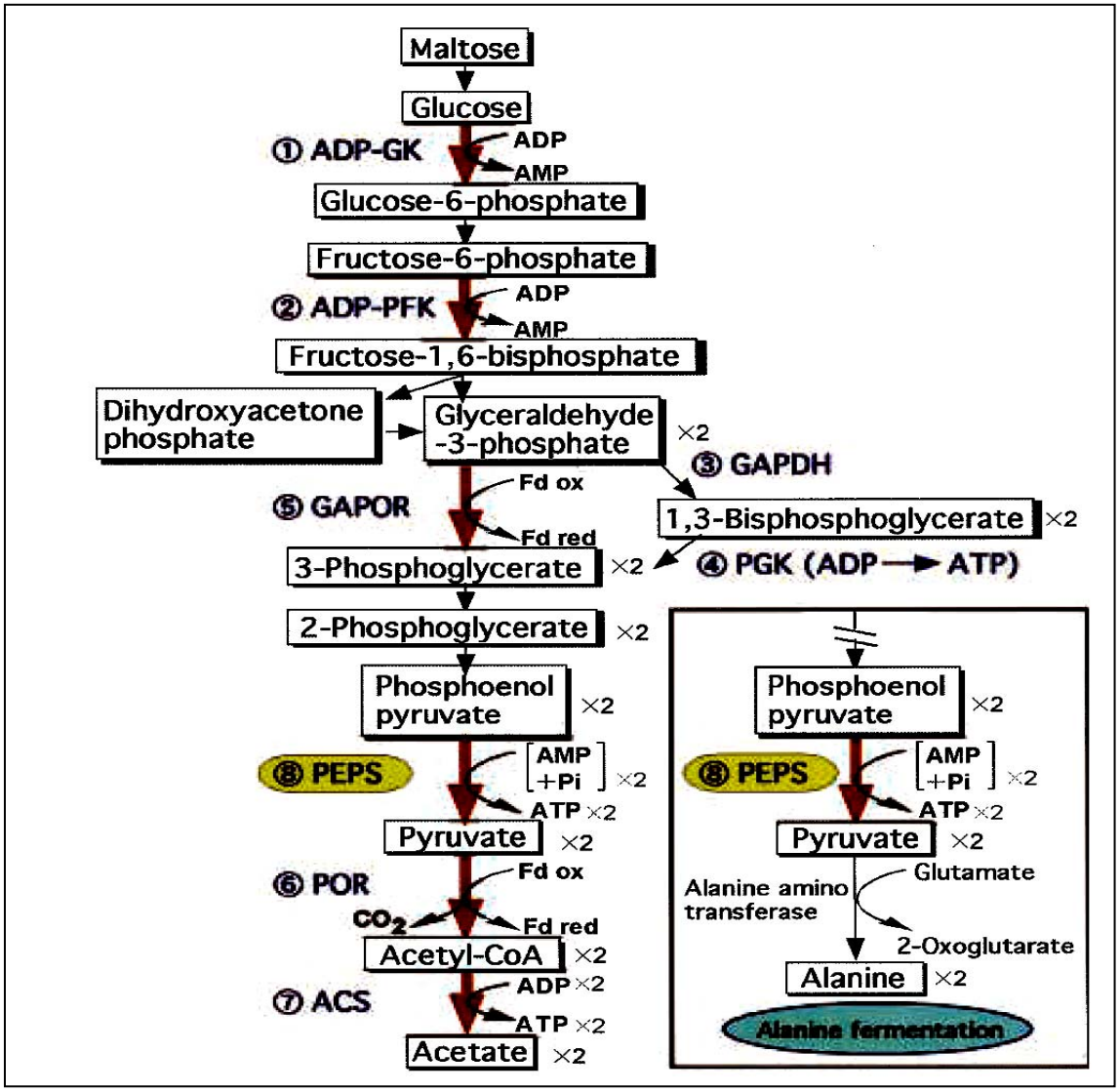

Figure 1-2 Proposed pathway of maltose metabolism in *P. furiosus*

Novel enzymes such as ADP-dependent glucokinase, ADP-dependent phosphofructokinase, and glyceraldehyde-3-phosphate ferreoxin oxidoreductase are invloved in the pathway (Modified from Sakuraba et al. 2004).

al. 1989). *T. maritima* has great potential to use a wide range of simple and complex carbohydrates confirmed by the inventory of glycoside hydrolases encoded in its genome (Nelson et al. 1999) and experimental results (Chhabra et al. 2002). It is known to metabolize both polysaccharides and simple sugars, including carboxymethylcellulose, barley glucan, starch, galactomannan, xylan, pectin, mannose, xylose, and glucose (Bronnenmeier et al. 1995; de Vos et al. 1998). Complex sugars are processed by a series of glycoside hydrolases and then transported by ATP-binding protein cassette (ABC) transporters but not phosphoenolpyruvate phosphotransferase system (Chhabra et al. 2003; Galperin et al. 1996; Nelson et al. 1999; Nguyen et al. 2004). Glucose is fermented through the conventional Embden-Meyerhof (EM 85%) and Entner-Doudoroff (ED 15%) pathways (Selig et al. 1997). It has been reported that genes encoding enzymes catalyzing NADH oxidation are up-regulated by both lactose and maltose (Nguyen et al. 2004). The mechanisms involved in such regulation remain unclear. Although the picture of the metabolism in hyperthermophiles is far from clear, a group of enzymes, flavoenzymes, are known to be involved in many important cellular processes.

1.2 OVERVIEW OF FLAVOPROTEINS

1.2.1 Discovery of flavin and flavoprotein

Riboflavin (vitamin B2), a bright yellow pigment, was first isolated from cow's milk whey by English chemist, A. Wynter Blyth more than 100 years ago as lactochrome (Blyth 1879). In subsequent years, yellow pigments extracted from various biological sources called ovoflavin, lactoflavin, heptoflavin, or verdoflavin, depending on either the source of isolation or physical appearance, were described. It was recognized that the yellow compound was a constituent of vitamin B, the structure of which was determined *via* chemical synthesis by two important groups (Karrer et al. 1935; Kuhn et al. 1934) and the name of riboflavin was given to the compound (Müller 1991). Flavin is a generic term for a group of compounds that have the heterocylic isoalloxazine chromophore in common. Riboflavin consists of the tricyclic isoalloxazine moiety connected to a ribityl side-chain at N-10 (Figure 1-3).

Flavoproteins are ubiquitous proteins using flavins as prosthetic groups and mostly catalyzing redox reactions. They occur in all organisms and are known to be involved in various processes essential for

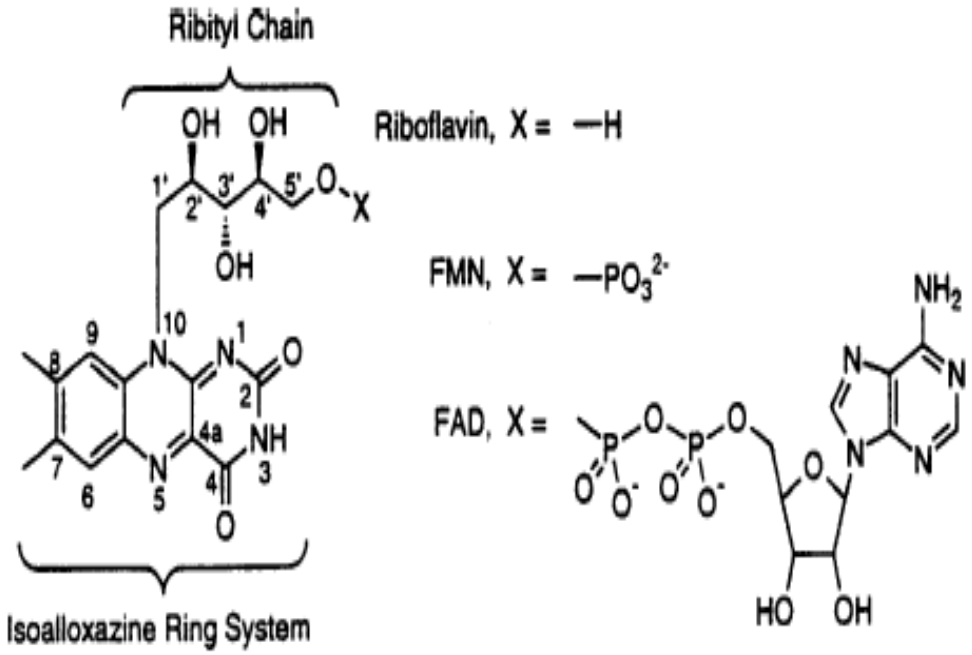

Figure 1-3 The structures of riboflavin, flavin mononucleotide, and flavin adenine dinucleotide (FAD) and the numbering system for isoalloxazine ring (Adapted from Massey 2000).

sustaining the living conditions for each organism (Miura 2001). The first flavoprotein was discovered in yeast and named as yellow enzyme by the German biochemist Otto Heinrich Warburg, a pioneer in research on mechanism of biological respiration process (Warburg and Christian 1933). Since their pioneering work, hundreds of flavoenzymes have been known till 1989 (Ghisla and Massey 1989) and new features of some flavoproteins have been continuously presented every year.

1.2.2 Commonly used flavin cofactors

The common flavin cofactors in flavoproteins are present mainly in the form of flavin adenine dinucleotide (FAD) and in less amount flavin mononucleotide (FMN) (Palfey and Massey 1996). They are synthesized from riboflavin by riboflavin kinase and FAD synthetase (Karthikeyan et al. 2003; Spencer et al. 1976). FMN is produced from the phosphorylation of riboflavin at the ribityl 5-OH and FAD is the combination of FMN with AMP (Figure 1-3). In bacteria, the functions of FAD synthetase and riboflavin kinase are carried out by one bifunctional flavoprotein (Mack et al. 1998; Manstein and Pai 1986).

Although most flavoenzymes utilize FAD and FMN as prosthetic groups, there are some exceptional cases in which the modification on isoalloxazine ring or ribityl side-chain occurs. A derivative of riboflavin called coenzyme F_{420} (7, 8-dimethyl-8-hydroxy-5-deazariboflavin) because of its strong absorbance at 420 nm is widely used by some redox enzymes including hydrogenase, formate dehydrogenase, and methyltetrahydrofolate dehydrogenase (Lin and White 1986; Tzeng et al. 1975 a, b). These enzymes have been isolated from methanogenic archaea involved in methane formation (Weiss and Thauer 1993; Wolfe 1991), *Streptomyces* involved in the synthesis of antibiotic lincomycin (Coats et al. 1989; Kuo et al. 1989; Piepersberg 1994) and tetracycline (McCormick and Morton 1982), and *Mycobacterium* involved in the oxidation of glucose-6-phosphate (Klein et al. 1996; Purwantini and Daniels 1996).

The known crystal structures of flavoproteins reveal that the majority of the flavin-protein interactions are with the N-10 ribityl side chain of FMN and FAD (Massey 2000). A recent study based on the sequence-structure relationship in 32 families of FAD-containing proteins shows that the pyrophosphate moiety binds to the most strongly conserved sequence motif in every case, suggesting

that pyrophosphate binding is a significant component of molecular recognition in flavoproteins (Dym and Eisenberg 2001).

In most cases the flavin prosthetic group is tightly but not covalently bound to the enzyme and does not dissociate during catalysis. However, in a subset of flavoproteins, the flavin is covalently bound to the polypeptide chain, at either the 8-α (methyl) or 6-positions of the isoalloxazine ring (Mewies et al. 1998). The typical enzymatic residues attaching to the isoalloxazine ring are histidines at either of the imidazole nitrogens, cysteines at the sulfur and tyrosines at the phenolic oxygen.

1.2.3 Oxidation-reduction properties of flavin

The most prominent feature of flavin is its capability to undergo redox reactions and there is no other coenzyme known in nature showing the same great variety of reactions (Müller 1991). Flavoproteins have been recognized by their ability of participating in both one- and two-electron transfer processes, which means that flavin can exist in three different redox states: oxidized (flavoquinone), one-electron reduced (flavosemiquinone), and two-electron reduced states (flavohydroquinone) (Figure 1-4; Miura 2001). Each of the redox state has three ionic states: neutral, cationic, and anionic state, because of its amphotericity. On binding to a specific protein, this equilibrium can change dramatically.

In addition to chemical attractions, flavin has aesthetic benefits as well. The fully oxidized flavin is bright yellow. Different ionic states of flavin or reaction intermediates show different colors, such as red flavosemiquinone, blue flavosemiquinone, purple intermediates, green complex, etc. The property of being highly colored at different states makes optical spectrometry very useful to study the redox changes of flavin and flavoprotein (Stanley 2001). Figure 1-5 shows absorption spectra in the visible region of flavin in different redox, ionic, and charge-transfer states, which are origins of the different colors of flavins and flavoproteins, and serve as monitoring probes for studying the functions of flavoproteins (Miura 2001).

The redox potential for two electron reduction of both free FAD and FMN is around -210 mV at pH 7.0 (Müller 1991). However, this redox potential can vary greatly among the flavoproteins, spanning a range from approximately -400 mV to +60 mV (Fraaije et al. 1999; Ghisla and Massey 1989).

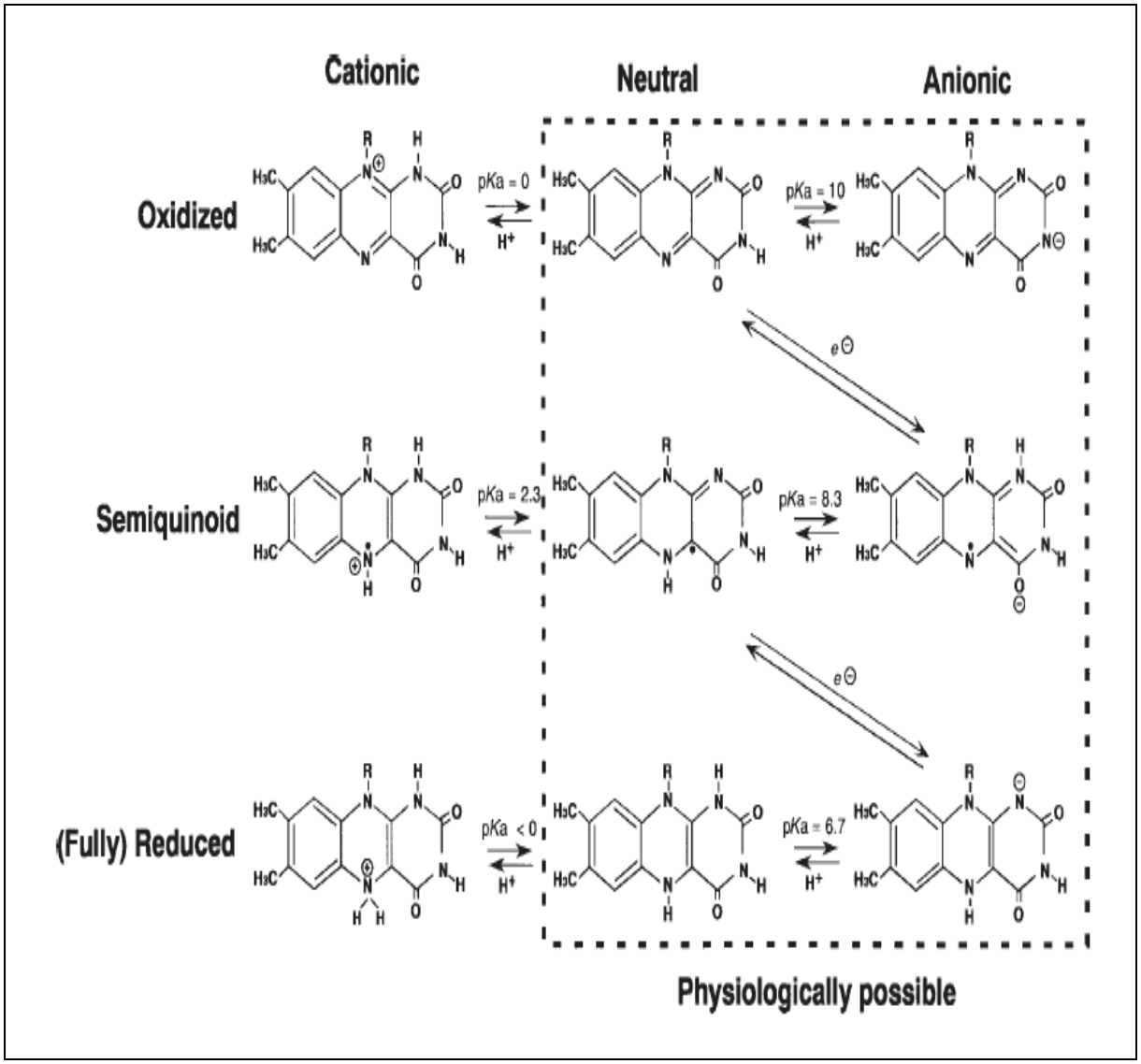

Figure 1-4 Redox and ionic states of flavin (Modified from Miura 2001).

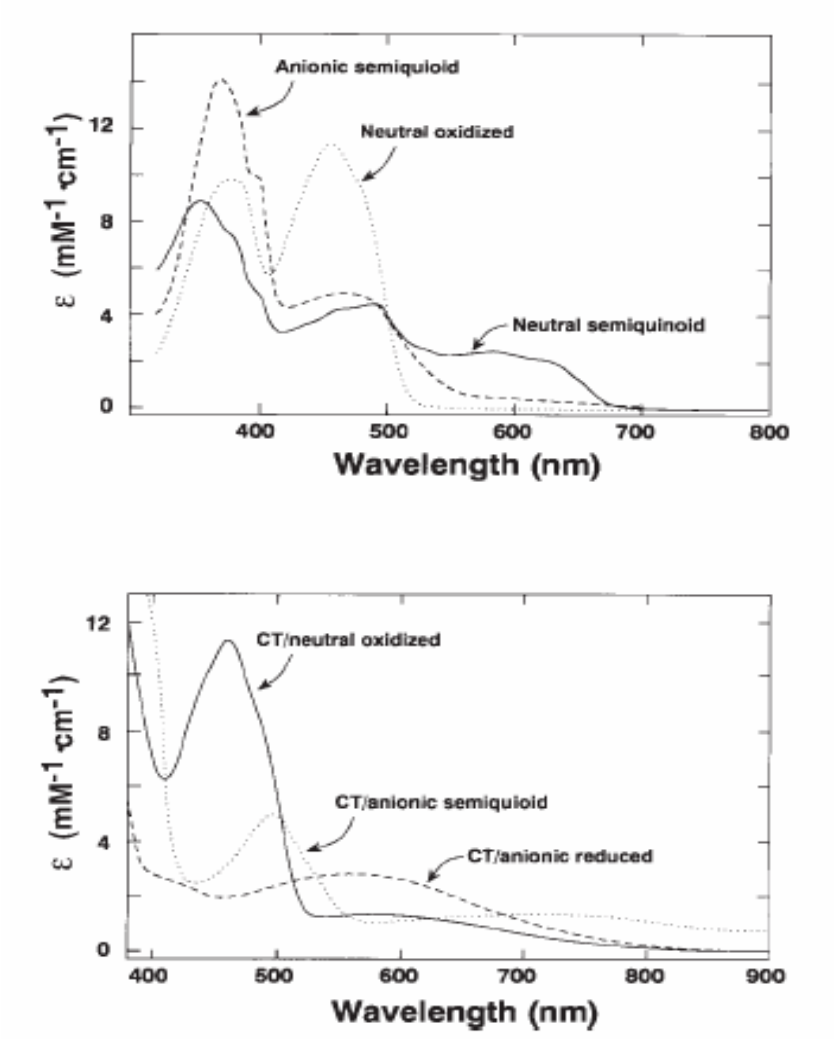

Figure 1-5 Absorption spectra of D-amino-acid oxidase at different states of flavin (Adapted from Miura 2001).

Redox properties of flavoproteins depend not only upon the features of the prosthetic group they contain, but also are affected by the metal ions (in the metal flavoprotein) as well as by the protein environment (Ksenzhek and Petrova 1983). In general, the proximity of a positive charge is thought to increase the redox potential, whereas that of a negative charge or a hydrophobic environment is expected to lower it (Fraaije and Mattevi 2000; Massey 1995). A change of redox potential may be made by the environment provided by the apoprotein and the specific interaction between the apoprotein and the prosthetic group.

The ability to participate in redox reactions as either one- or two-electron mediator makes flavoproteins very versatile in terms of substrate and type of reactions catalyzed, which enables flavoproteins to play a pivotal role in coupling the two-electron oxidation of most organic substrates to the one-electron transfers of the respiratory chain. This property and the capability of catalyzing a variety of biochemical reactions make flavoproteins to be at crossroads of cellular redoxchemistry (Ghisla and Massey 1989; Palfey and Massey 1996). The majority of flavoprotein-reducing substrates are dehydrogenated in a two-electron reduction step. The resulting reduced flavin is then re-oxidized by its oxidizing substrate, either in a two-electron step (Figure 1-6) or in a single one electron-step, in which the flavosemiquinone would be observed as an intermediate by the spectral study (Figure 1-5). For the convenience to describe the catalytic process, the reaction catalyzed by flavoprotein normally is split to two parts: reductive half-reaction and oxidative half-reaction.

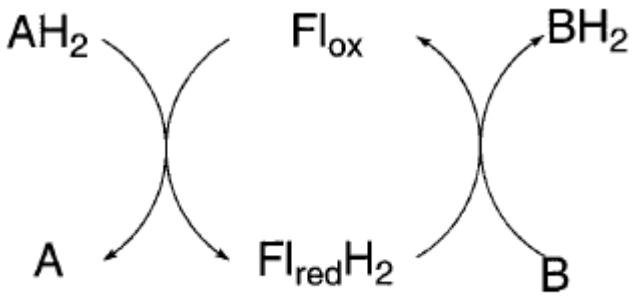

Figure 1-6 Reductive and oxidative half-reaction of flavoproteins (Adapted from Massey 2000).

1.2.4 Catalytic versatility of flavoproteins

Flavoproteins catalyze a large variety of different reaction types. According to the composition of flavoproteins, they are divided into two big groups, simple flavoproteins that only use flavins as prosthetic group and complex flavoproteins, the latter contain one or more prosthetic groups involved in the overall catalytic cycle in addition to flavin (Palfey and Massey 1996).

1.2.4.1 Simple flavoproteins

Simple flavoproteins can be classified on the basis of their reactivity towards a number of reagents, their ability to stabilize the flavin semiquinone, the reaction they catalyze, substrate subjected to catalysis, and their properties upon substitution with artificial flavins (Palfey and Massey 1996). Each of these characteristics is affected by the protein residues of the active sites that are optimized to promote certain type of reaction. Members of a particular group share common mechanistic properties, and some have evolved to catalyze reactions in addition to those common to the group (Massey 1994; Palfey and Massey 1996). According to those criteria, simple flavoproteins are further classified into five families: oxidases, flavoprotein disulfide oxidoreductases, electron transferases, monooxygenases, and flavoproteins that do not catalyze any net redox reduction.

1.2.4.1.1 Oxidases

Oxidases catalyze the oxidation of a substrate single bond to a double bond, followed by the oxidation of the flavin by oxygen. This group includes D-amino-acid oxidase (EC 1.4.3.3; Konno and Yasumura 1992), L-amino acid oxidase (EC 1.4.3.2; Ponnudurai et al. 1994), α-hydroxy acid oxidases with subgroups of glycolate oxidase (EC 1.1.3.15), L-lactate monooxygenase (EC 1.13.12.4), flavocytochrome b_2 (EC 1.1.2.3), and L-lactate oxidase (EC 1.1.3.2; Diêp Lê and Lederer 1991), and glucose oxidase (EC 1.1.3.4; Kelley and Reddy 1986). These enzymes dehydrogenate at the α-carbon atom of the substrates, yielding the 2-oxo (α-keto) acid or α-imino acid as the primary products, respectively (Massey 2000). The reduced enzyme reacts with oxygen very rapidly and hydrogen peroxide is produced (Massey 1994). The reaction is essentially irreversible because of the high redox potential of the couple O_2/H_2O_2 (E_m= +270 mV) versus that of oxidized/reduced flavin (**E_m** = -209 mV). Among this group of enzymes, D-amino-acid oxidases have been so extensively studied that they are regarded as model flavooxidase catalysts. D-Amino-acid oxidases are found in numerous eukaryotic organisms, including fungi, insects, amphibians, reptiles, birds and mammals (Friedman

1999). The presence of D-amino-acid oxidases in microorganisms is related to the well established ability to use D-amino acid for growth (LaRue and Spencer 1967). However, the significance of D-amino-acid oxidase in higher organisms remains unclear. The enzymes in this group have some common catalytic properties including reacting rapidly with oxygen in reduced form, stabilizing the red anionic flavin radical *via* one electron reduction (Pilone 2000).

1.2.4.1.2 Flavoprotein disulfide oxidoreductases (FDR)

Flavoprotein disulfide oxidoreductases catalyze the pyridine-dinucleotide-dependent reduction of a variety of substrates, including disulfide-bonded substrates (lipoamide dehydrogenase (EC 1.8.1.4), glutathione reductase (EC 1.8.1.7) and functional homologues, thioredoxin reductase (EC 1.8.1.9), and coenzyme A disulfide reductase (EC 1.8.1.14), alkylhydroperoxide reductase, mercuric ion (mercuric ion reductase; EC 1.16.11), hydrogen peroxide (NADH peroxidase; EC 1.11.1.1), molecular oxygen (NADH oxidase), and the reductive cleavage of a carbonyl-activated carbon-sulfur bond followed by carboxylation (2-ketopropyl-coenzyme-M carboxylase/oxidoreductase) (Argyrou and Blanchard 2004; Williams 1992). Normally, pyridine nucleotide reduces the flavin and the reduced flavin reduces an active-site disulfide, followed by the reduced enzymes containing thiols undergo thiol-disulfide interchange with a disulfide substrate. All the members in this group use at least one redox center in addition to flavin to transfer electrons from reduced pyridine nucleotide to their substrates through FAD (Argyrou and Blanchard 2004). Three types of nonflavin redox center adjacent to the flavin have been identified: catalytic disulfide, catalytic cysteine sulfenic acid (NADH peroxidase and NADH oxidase), and mixed Cys-S-S-CoA disulfide (coenzyme A disulfide reductase).

Flavoprotein disulfide oxidoreductases have high sequence and structural homology. Homology in the FAD-binding region and in the pyridine nucleotide binding region is a common feature in all members of this family (Carothers et al. 1989). Lipoamide dehydrogenase, glutathione reductase, mercuric ion reductase and trypanothione reductase have a high degree of homology in amino acid sequence which expands to all domains (Brown et al. 1983; Greer and Perham 1986; Shames et al. 1988; Williams et al. 1982). The level of sequence identity between the four enzymes varies between 24 and 40%. The region of the active site disulfide in thioredoxin reductase (TrxR) was different from the other four enzymes mentioned above (Russel and Model 1988). Enzymes in flavoprotein disulfide

oxidoreductase family are normally involved in cellular energy metabolism and protection from damage by molecular oxygen and other toxic agents. Since most work of this thesis is focused on the enzymes from this family, the representative enzymes, such as lipoamide dehydrogenase, NADH oxidase, and TrxR will be introduced in later chapters.

1.2.4.1.3 Monooxygenases

The flavoprotein monooxygenases (flavin-dependent aromatic hydroxylase) are a group of enzymes that catalyze the addition of a single oxygen atom from molecular oxygen into the substrate and the reduction of the second oxygen atom in the substrate to form water. Those enzymes are involved in a wide range of biological process including drug detoxification, biodegradation of aromatic compounds in the environment, biosynthesis of antibiotics and siderophores (Ballou et al. 2005). They activate molecular oxygen through the formation of a reactive flavin hydroperoxide which can attack the substrate by an electrophilic or nucleophilic process depending on the protonation state of the flavin hydroperoxide and the nature of the protonation state of the substrate (Leahy et al. 2003; Moonen et al. 2002). The mammalian microsomal flavin-containing monooxygenase (FMO; EC 1.14.13.8) catalyzes the monooxygenation of nitrogen-, sulfur, phosphorus, selenium, or iodine-containing compounds at the expense of NADPH and O_2 and is considered to have evolved as xenobiotic detoxification catalyst to protect mammals from liponucleophilic plant chemicals in the early environments (Cashman 2005; Ziegler 1990, 1991). These enzymes are of deep interest for the bio-catalytic production of fine chemicals and food ingredients and play important roles in soil detoxification process *via* the hydroxylation of many aromatic compounds due to their high regioselectivity and stereoselectivity (Massey 1994, 2000; Moonen et al. 2002).

Cyclohexanone monooxygenase (EC 1.14.13.22) catalyzes the reaction of hydrocarbon, cyclohexane to form the cyclic ester ε-caprolactone with NADPH and O_2 to enable the microorganisms containing the enzyme to grow on cyclohexane as sole carbon and energy source (Donoghue et al. 1976; Trower et al. 1989). Bacterial luciferase (EC 1.14.14.3) catalyzes the oxidation of a long chain aldehyde with oxygen and reduced FMN to cause bioluminescence in bacteria (Fisher et al. 1995). Other aromatic compounds such as *p*-hydroxyphenylacetate (p-hydroxyphenylacetate 3-hydroxylase; Arunachalam et al. 1992), salicylate (salicylate hydroxylate; You et al. 1991), anthranilate (anthrannilate hydroxylase; Powlowski et al. 1987), and 2-methyl-3-hydroxypyridine-5-carboxylic acid (2-methyl-3-

hydroxypyridine-5-carboxylic acid oxygenase; Sparrow et al. 1969) can also be oxidized by the enzymes in this group.

1.2.4.1.4 Electron transferases, reductases, and dehydrogenases

There are a lot of flavoproteins involved solely in the oxidation and reduction of inorganic, organic, and protein substrates and form the bridge between the catabolism of small molecules and respiratory chains, or photosynthesis and soluble cellular reductants (Massey 2000). The flavin semiquinone, the catalytically competent intermediate, is always stable and observable in the reaction catalyzed by enzyme in this group because they are often reduced by hydride-donating substrate and pass the electrons to redox proteins one at a time. Pyridine nucleotides and alkenes conjugated to carbonyls are the frequent small-molecule substrates (or products) (Palfey and Massey 1996). This group includes many enzymes with representatives of cytochrome P450 reductase (EC1.6.2.4) that catalyzes hydroxylation reactions of primary importance in the metabolism of lipids, drugs, and other foreign compounds working together with other microsomal mixed function oxidase system (Kurzban et al. 1990; Vermilion et al 1981). Acyl-CoA dehydrogenases that are involved in fatty acids metabolism (Thorpe and Kim 1995), NAD(P)H:quinone oxidoreductase (EC 1.6.99.20) that is in involved in chemo- and bio-detoxification (Ross et al. 2000), ferredoxin:NAD^+ oxidoreductase (FNOR; EC 1.18.1.2) that serves as switch between one- and two-electron carrier (Carrillo and Ceccarelli 2003), old yellow enzyme (EC 1.6.99.1) that can catalyze many reactions but without physiological substrate identified yet (Massey 2000; Stott et al. 1993) and UDP-N-acetylenolpyruvylglucosamine reductase (EC 1.1.1.15B) that is important for cell wall biosynthesis (Sylvester et al. 2001) are members of this group of enzyme. Interestingly, cytochrome P450 reductases contain both FAD and FMN and both flavins have distinct roles and distinct reactive properties (Kurzban et al. 1990; Vermilion et al. 1981). They reductively activate molecular oxygen and oxidize a variety of compounds for biosynthetic and detoxification purpose (Porter and Kasper 1986).

1.2.4.1.5 Flavoproteins not catalyzing a net redox reaction

Some flavoproteins may only have structural role and do not catalyze a redox transformation of substrates to products (Palfey and Massey 1996). This group consists of DNA photolyase (EC 4.1.99.3; Sancar 1994), N-methylglutamte synthase (EC 2.1.1.21; Pollock and Hersh 1973),

hydroxyacyl-CoA dehydratase (Scherf and Buckel 1993), chorismate synthase (EC 4.6.1.4; Bornemann et al. 1995), acetolactate synthase (EC 4.1.3.18; Joo and Kim 2001), glycoxalate carboligase (EC 4.1.1.47; Cromartie and Walsh 1976), and oxynitrilase (EC 4.1.2.10; Petrounia et al. 1994).

1.2.4.2 Complex flavoproteins

In addition to flavin, some flavoproteins may contain one or more prosthetic groups involved in the catalysis. Frequently, the additional prosthetic groups are iron-sulfur centers, heme, pterins, thiamine pyrophosphate, pyridoxal, etc. (Palfey and Massey 1996). These enzymes have been studied as soluble model of respiratory chains because their redox-active cofactors often function as self-contained electron transport chains. The role of flavins in these complex redox systems is a bridge between components that are obligate one-electron reactants, such as iron-sulfur centers, and two-electron reactants, such as pyridine nucleotides. The well studied enzymes in this group include xanthine oxidase (EC 1.1.3.22) and xanthine dehydrogenase (EC 1.1.1.204) which contain FAD, iron-sulfur center, and molybdenum involved in the metabolism of purines and pyrimidines in various organisms (Hille and Nishino 1995), glutamate synthase (EC 1.4.1.13) that contains iron-sulfur center, FAD, and FMN and is involved in ammonium ion assimilation in many organisms (Suzuki and Knaff 2005), phthalate dioxygenase reductase (EC 1.14.12.7) that contains FMN and iron-sulfur center and is involved in breaking down of unactivated aromatic compounds in soil bacteria (Gassner et al. 1995), and 2-aminobenzoyl-CoA monooxygenase/reductase (EC 1.14.13.40) containing two identical polypeptides and two active centers (FAD) which differ substantially in their catalytic properties (Langkau et al. 1995). One center belongs to monooxygenase, the other one to the dehydrogenase.

1.3 CURRENT STUDY OF FLAVOPROTEINS IN HYPERTHERMOPHILES

Some flavoproteins involved in energy metabolisms in hyperthermophilic lithotrophs have been studied, which include succinate dehydrogenase (respiratoty complex II) in S^0 or O_2 reducing organisms *Acidianus amibivalens, Acidianus infernus, Sulfolobus solfataricus, Sulfolobus metalicus, Sulfolobus acidocaldarius,* and *Sulfolobus* strain 7 (Gomes et al. 1999); adenylysulphate (APS) reductase in sulphate reducer *Archaeoglobus* species (Fritz et al. 2002; Schönheit and Schäfer 1995;

Speich et al. 1994); $F_{420}H_2$ dehydrogenase, a redox-driven proton pump closely related to NADH:ubiquinone oxidoreductase in methanogenic archaea, involved in converting CO_2 to CH_4 with H_2 as electron donor (Bäumer et al. 2000).

Several flavoproteins have been purified and characterized from *P. furiosus*, including NADH oxidase (Ward et al. 2001) and rubredoxin oxidoreductase involved in oxygen defensive system (Ma and Adams 1999), sulfide dehydrogenase (Ma and Adams 1994) and hydrogenase I and II involved in hydrogen and hydrogen sulfide production (Ma et al. 1993; Ma et al. 2000), and thymidylate synthase catalyzing the conversion of dUMP and 5,10-methlenetetrahydrofolate to dTMP and dihydrofolate (Kanai et al. 2006). Though *P. furiosus* is an obligate anaerobe, studies of hydrothermal vent systems have shown that it can be exposed to significant levels of oxygen at low temperatures when hot, anaerobic vent fluids mix with cold, oxygen-saturated seawater (Huber et al. 1990). An NADPH-dependent superoxide reduction pathway including rubredoxin oxidoreductase has been constructed *in vitro* for *P. furiosus* (Grunden et al. 2005). Hydrogenases are essential in energy metabolism and fermentation for anaerobic thermophilic heterotrophs catalyzing the reversible oxidation of hydrogen gas (Adams 1990b). Three flavoproteins related to H_2 and H_2S metabolism were purified from *P. furiosus*, two soluble FAD-containing Ni-Fe hydrogenases which also possess sulfur reductase activity, and one FAD-containing sulfide dehydrogenase which also functions as FNOR (Ma and Adams 1994; Ma et al. 1993; Ma et al. 2000). A pathway of electron transfer in *P. furiosus* has been proposed: reduced ferredoxin as major electron carrier is used to reduce $NADP^+$ by FNOR, and NADPH formed can be used by the soluble hydrogenases to produce H_2 and H_2S respectively (Ma and Adams 1994). Based on the characterization of a membrane bound hydrogenase, it is thought that the membrane bound hydrogenase may be responsible for H_2 formation. However, this hydrogenase could not reduce sulfur *in vitro* and neither NAD(P)H nor ferredoxin serves as electron donor as the cytoplasmic hydrogenases do (Sapra et al. 2000; Silva et al. 2000). One ORF encoding a putative flavoprotein is up-regulated by the presence of sulfur in the medium and seems to be involved in the metabolism of sulfur in *P. furiosus* (Schut et al. 2001). All these studies suggest that flavoproteins play very important roles in the life sustaining hydrogen and hydrogen sulfide metabolism of *P. furiosus*. However, the precise mechanisms of H_2 formation and S^0 reduction are still not clear, including the electron transfers during these processes.

It has been proposed that the excess reductant produced during fermentation in the form of NADH and reduced ferredoxin is disposed ultimately by hydrogenase in *Thermotoga* (Schröder et al. 1994; Verhagen et al. 1999). Hydrogenase has been extensively studied in *T. maritima* (Juszczak et al. 1991; Smith and Adams 1994; Verhagen et al. 1999, 2001). The purified *T. maritima* hydrogenase does not use NADH or reduced ferredoxin as electron donor for H_2 formation *in vitro* (Verhagen et al. 1999). The electron transfer process in hydrogen production in *Thermotoga* is not clear yet. Flavoprotein, FNOR is thought to play a vital role in the bridge of shuttling between one and two-electron carriers (Carrillo and Ceccarelli 2003). Although not purified yet, FNOR activity was found in *T. maritima* (assayed by BVOR activity; Schröder et al. 1994) and *T. neapolitana* (assayed by NADH:methyl viologen oxidoreductase activity; Käslin et al. 1998). It is plausible to reason that there should be some flavoproteins that serve as a switch between one electron carrier (reduced ferredoxin) and two-electron carrier (NAD/P) in the H_2 and H_2S metabolism of these heterotrophic anaerobic hyperthermophiles.

Despite the large number, crucial roles in metabolism and vast diversity of flavoproteins studied, there is no report regarding the global expression of flavoproteins in any particular organism. The short consensus sequence consisting of a pattern of amino acid sequence that characterizes a domain or a protein family is called motif (Bork and Gibson 1996). The sequences of homologous hyperthermophilic and mesophilic proteins are typically as high as 40 to 85% similar (Davies et al. 1993; Vieille et al. 1995; Vieille and Zeikus 2001). The conserved motifs in FAD-binding proteins from mesophilic organisms can be used to search the genome of hyperthermophilic microorganims to quantify the FAD-containing proteins. It was preliminarily predicted in our laboratory that there was 4.89%, 5.97% and 8.02% of the ORFs potentially encoding flavoprotein in *P. furiosus* (104/2125), *T. maritima* (111/1858) and *Escherichia coli* (340/4237) based on motif matching method, respectively (Chiu 2006). A list of experimentally determined flavoproteins was generated by searching the primary articles published in journals in biological science database including Web of Science and Canada Institute for Scientific and Technical Information (CISTI) and flavoprotein encyclopaedia (Müller 1991). Based on name search, there was 2.21%, 1.88% and 3.63% of the ORFs annotated as the enzymes that are flavoproteins in *P. furiosus*, *T. maritima*, and *E. coli*, respectively.

1.4 AIMS OF STUDY

The central goal of this thesis was to study the flavoproteins involved in the metabolism of anaerobic hyperthermophiles. The work was mainly focused on the following specific goals.

Although hyperthermophlic anaerobes live in oxygen-free environment, it has been showed that they can be exposed to significant levels of oxygen when hot, anaerobic vent fluids mix with cold, oxygen-saturated seawater (Huber et al. 1990). How they deal with such substantial amount of oxygen and what mechanisms are involved in the detoxification process attracted our attention. The first goal of this research was to investigate the effect of oxygen on the growth of *Thermotoga* species, namely *T. maritima* and *T. hypogea* and the enzymes involved in their oxygen detoxification systems. As an enzyme catalyzing the reduction of oxygen using NADH as electron donor, the presence of NADH oxidase in these anaerobic hyperthermophilic bacteria had to be proven, and its catalytic properties would be studied. An important aspect of NADH oxidase study was to determine what the product of oxygen reduction was since it may catalyze the formation of either water or hydrogen peroxide. To know the product was critical to evaluate the function of this enzyme and to predict the type of oxygen detoxification system present in such anaerobes. It was known that the NADH remained in the NADH oxidase reaction system could significantly interfere with the H_2O_2 determination. For mesophilic NADH oxidase, the reaction time may be extended in order to consume NADH completely. There was no good approach to consume the NADH completely by hyperthermophilic NADH oxidase because NADH self-decomposes at high temperatures which makes the stoichiometric calculation not accurate. Efforts had to be made to develop a proper way to detect H_2O_2 generated by hyperthermophilic NADH oxidase.

In hyperthermophiles, pyruvate dehydrogenase is replaced by pyruvate:ferredoxin oxidoreductase. However, it was found that the gene encoding E3 component of pyruvate dehydrogenase, dihydrolipoamide dehydrogenase (DLDH), was present in the genome of *Thermotoga* species. There had been no report of the presence of activity of this flavoenzyme in any hyperthermophiles yet. It would be interesting to detect the presence of the activity, investigate the properties, and predict the function of DLDH in hyperthermophiles. Therefore, the second goal of this research was to study DLDH which might be involved in energy conservation process in the cells.

Microbial hydrogen production is of great interest as an alternative fuel. To study the hydrogen metabolism in which flavin may play an important role will provide new information to help enhance the efficiency of hydrogen production. For the heterotrophic and hyperthermophilic anaerobes themselves, hydrogen production serving as electron sink is a very important life sustaining process. Intrigued by the two complex FAD-containing hydrogenases characterized from *P. furiosus* and the unsolved puzzles regarding the presence of flavin in the hydrogenase from *T. maritima*, the third goal of this research was to investigate the properties and functions of hydrogenase in *T. hypogea*.

Thermostable ferredoxin is widely used as electron carrier during fermentation in hyperthermophiles. However, many enzymes require NAD(P)H for their functions in other cellular processes such as hydrogen production or biosynthesis. So, the bridge enzyme, the flavin-containing FNOR catalyzing the electron transfer between the reduced one electron carrier, ferredoxin and two electron carrier, NAD(P) is essential. However, there has been no study of this enzyme in hyperthermophilic bacteria yet. The fourth goal of this research was to detect the presence of FNOR in hyperthermophilic bacterium, *T. maritima*, and characterize its catalytic properties.

The main approaches used to achieve the goals were first to detect the specific activities and then purify the target enzymes from the anaerobic hyperthermophilic microorganisms. After the target enzymes were purified, biophysical and biochemical properties of these purified enzymes and their physiological functions in their anaerobic hosts were examined.

Chapter 2 Determination of Hydrogen Peroxide Generated by NADH Oxidase

The work described in this chapter was published in Analytical Biochemistry.

Yang X. and K. Ma. 2005. Determination of hydrogen peroxide generated by reduced nicotinamide adenine dinucleotide oxidase. Anal. Biochem. 344:130-134.

2.1 ABSTRACT

Hydrogen peroxide can be conveniently determined using horseradish peroxidase (HRP) and 2,2'-azino-bis(3-ethylbenzthiazoline-6-sulfonic acid). However, interference occurs among assay components in the presence of reduced nicotinamide adenine dinucleotide (NADH) that is also a substrate of NADH oxidase. So, depletion of NADH is required before using the HRP method. A simple and rapid procedure to accurately determine hydrogen peroxide generated by NADH oxidase was developed. All procedures developed were based on the extreme acid lability of NADH and the stability of hydrogen peroxide, because NADH was decomposed at pH 2.0 or 3.0 for 10 min, while hydrogen peroxide was stable at pH 2.0 or 3.0 for at least 60 min. Acidification and neutralization were carried out by adjusting sample containing NADH up to 30 μM to pH 2.0 for 10 min before neutralizing it back to pH 7.0. Then, hydrogen peroxide in the sample was measured using the HRP method and its determination limit was found to be about 0.3 μM. Alternatively, hydrogen peroxide in samples containing NADH up to 100 μM could be quantitated using a modified HRP method that required an acidification step only, which was found to have a determination limit of about 3 μM hydrogen peroxide in original samples.

2.2 INTRODUCTION

Hydrogen peroxide (H_2O_2), a reactive oxygen species, can produce hydroxyl radicals and cause injury of cells in the presence of redox-active metal ions such as Fe^{3+} (Rosen et al. 1995). H_2O_2 can be quantitated using several methods including spectrophotometry, enzymatic electrodes, and flow injection (Alexandre et al. 1992; Voraberger 2004). However, detection limits are found to be 0.5 μM, 50 nM, and 5 nM, respectively, for these three types of methods, among which a spectrophotometry method that is based on the reaction of hydrogen peroxide and a certain dye catalyzed by horseradish peroxidase (HRP) is the most convenient and less expensive (Alexandre et al. 1992). For accurate and sensitive determination of H_2O_2 using this HRP method, there must be absolutely no interference between the dye used and any component in the assay mixture. NAD(P)H oxidases can catalyze either a two-electron or a four-electron transfer reaction to oxygen (O_2) to form H_2O_2 or H_2O, respectively (Kawasaki et al. 2004; Toomey and Mayhew 1998). Therefore, it is necessary to determine how much H_2O_2 is produced using NAD(P)H as electron donor. The determination is often done using the HRP method. Because NAD(P)H in the H_2O_2 sample interferes with the dye assay for horseradish peroxidase used, such as 2,2'-azino-bis(3-ethylbenzthiazoline-6-sulfonic acid) (ABTS), any remaining NAD(P)H in the sample must be depleted before the HRP assay (Kengen et al. 2003). The depletion of NAD(P)H is normally achieved by extending the oxidase reaction time which may take up to 4 h as tested in our laboratory. For oxidases from hyperthermophilic sources, it is very difficult to deplete NAD(P)H completely within a reasonable period of time due to lower solubility of O_2 at high temperatures (≥80 °C). In this case, thermal decomposition of NAD(P)H becomes very significant during an extended reaction period, which adds to the difficulty in obtaining an accurate ratio of NAD(P)H utilized by oxidase to H_2O_2 produced. Therefore, any remaining NAD(P)H has to be removed as quickly as possible for an accurate HRP assay for H_2O_2. NAD(P)H can also be removed by adding respiratory membranes or limiting the amount of NAD(P)H added to NAD(P)H oxidase reaction mixture (Kengen et al. 2003; Messner and Imlay 1999). Apparently, it is not practical for most laboratories to do so, and very low concentrations of NAD(P)H often cause greater errors. Here, a simple method based on the acid lability of NAD(P)H and extremely acid stability of H_2O_2 to accurately determine H_2O_2 produced by a hyperthermophilic NADH oxidase. It is also demonstrated that this assay method can be used reliably for determining H_2O_2 in samples containing high concentrations of NADH.

2.3 MATERIALS AND METHODS

2.3.1 Materials

Horseradish peroxidase, ABTS, and NADH were purchased from Sigma (Ontario, Canada); 30% peroxide (H_2O_2) was obtained from EM Science (Germany). All other chemicals were from commercially available sources. NADH oxidase was purified from *Thermotoga maritima* using a fast-performance liquid chromatography system in our laboratory as described in Chapter 4 this thesis (4.3.4 Enzyme purification).

2.3.2 Determination of hydrogen peroxide

Hydrogen peroxide was determined by monitoring the oxidation of ABTS in the presence of horseradish peroxidase at 725 nm (Ward et al. 2001). One milliliter assay mixture contained 100 mM phosphate (pH 7.0) and 150 µl ABTS (0.2 mg/ml). The reaction was started by adding 25 µl horseradish peroxidase (100 U/ml). After incubating the mixture at room temperature for 5 min, absorbance change at 725 nm was monitored to avoid any possible interference observed at around 405 nm previously (Pinkernell et al. 2000) despite higher molar absorbance coefficient of ABTS at the shorter wavelength (Childs and Bardsley 1975). A molar absorbance coefficient of $\varepsilon_{725} = 14{,}200 \pm 200\ M^{-1}\ cm^{-1}$ for the oxidized ABTS was obtained from a standard curve. Reduction of one mole of hydrogen peroxide requires two moles of ABTS.

2.3.3 NADH oxidase reaction

Phosphate buffer (100 mM, pH 7.0) is generally used for NADH oxidase reaction, and it is suitable for H_2O_2 measurement using the HRP method (Alexandre et al. 1992; Mäkinen and Tenovuo 1982; Nishiyama et al. 2001). After incubation of 1 or 2 ml phosphate buffer (100 mM, pH 7.0) saturated with air at 80 °C for 4 min, 100 µM NADH was added and absorbance at 340 nm was recorded before adding *T. maritima* NADH oxidase to start the reaction. Absorbance at 340 nm was recorded after running the reaction for about 1–2 min and the reaction was stopped immediately by adding 2 N HCl to reach a pH of 2.0. The mixture was then ready for H_2O_2 determination using the HRP assay. A control without addition of *T. maritima* NADH oxidase was done the same way to determine the amount of NADH decomposed at the same temperature.

2.4 RESULTS AND DISCUSSION

Prior to measurement of H_2O_2 produced by NADH oxidase, all conditions and procedures for a simple and rapid determination of H_2O_2 were tested using known amounts of H_2O_2 that were prepared using 30% H_2O_2.

2.4.1 Standard curve for determination of H_2O_2

To obtain a standard curve, various concentrations of H_2O_2 from 0 to 16.5 μM in 0.725 ml of 100 mM sodium phosphate (pH 7.0) were prepared from a consecutive dilution of 30% H_2O_2. To each sample, 150 μl solution of ABTS and 25 μl horseradish peroxidase were added. After incubating the mixtures at room temperature for 5 min, absorbance changes at 725 nm were monitored. Values of the absorbance at 725 nm were plotted against known concentrations of H_2O_2 to draw the standard curve. A molar extinction coefficient of 14,200 ± 200 M^{-1} cm^{-1} for the oxidized ABTS was obtained under this condition (Figure 2-1), which was very similar to that reported previously (Duetz and Witholt 2004). This estimated coefficient was used for all calculations for the H_2O_2 determination using the same HRP assay.

2.4.2 Interference of NADH on the determination of H_2O_2 using the HRP assay

Tests were conducted to determine how NADH interfered with H_2O_2 determination using the HRP assay. One milliliter of 100 mM sodium phosphate (pH 7.0) contained 2.2 and 8.8 μM H_2O_2, respectively. Various amounts of NADH were added to reach final concentrations of 0 to 200 μM, respectively. For those with 8.8 μM H_2O_2 in the presence of 0, 10, 30, 50, 100, and 200 μM NADH, the determined H_2O_2 concentrations were 8.68 ± 0.032 μM (100%), 7.81 ± 0.028 μM (90%), 6.22 ± 0.025 μM (72%), 4.72 ± 0.024 μM (54%), 0.14 ± 0.013 μM (16%), and 0.0 μM (0%), respectively. For those with 2.2 μM H_2O_2 in the presence of 0, 10, 30, 50, 100, and 200 μM NADH, the determined H_2O_2 concentrations were 2.29 ± 0.022 μM (100%), 1.67 ± 0.023 μM (73%), 0.36 ± 0.012 μM (16%), 0.0 μM (0%), 0.0 μM (0%), and 0.0 μM (0%), respectively. These results showed clearly that NADH did interfere with H_2O_2 determination; in particular, the lower the H_2O_2 concentration in the sample, the bigger was the interference. To accurately measure H_2O_2 concentration, NADH present in the sample must be removed using a simple and reliable procedure.

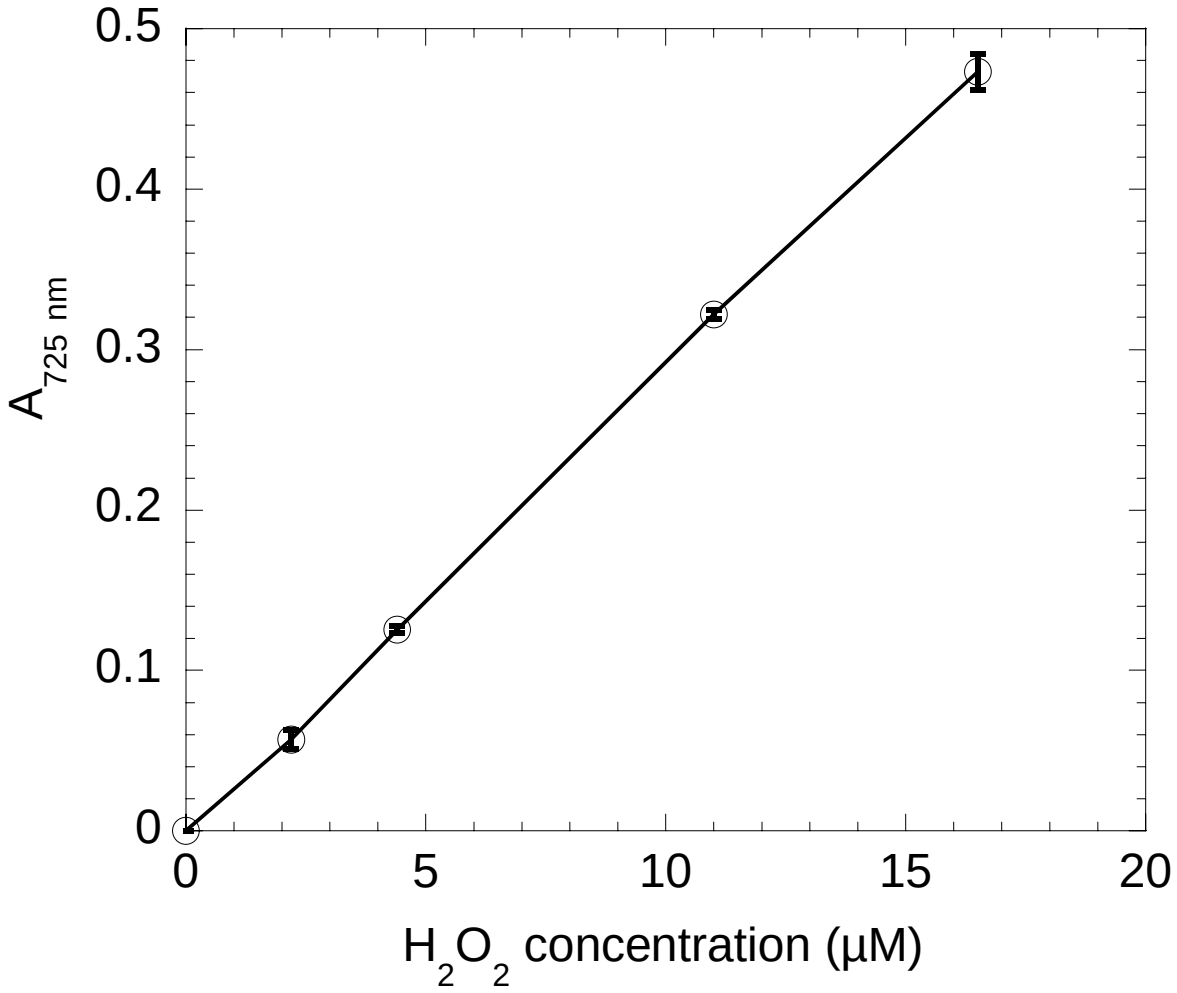

Figure 2-1 Standard curve for H_2O_2 determination

Various concentrations of H_2O_2 from 0 to 16.5 μM were prepared from a consecutive dilution of 30% H_2O_2. To each sample, 150 μl ABTS and 25 μl horseradish peroxidase solutions were added. The absorbance changes at 725 nm were monitored after the mixtures were incubated at room temperature for 5 min.

2.4.3 Lability of NADH at low pH values

It is well known that NADH is not stable under acidic conditions (Hentall et al. 2001), but it is not clear how quickly it can be decomposed at lower pH values. At first, pH changes of 50 ml of 100 mM sodium phosphate (pH 7.0) were made by adding 2 N HCl, and their pH values were monitored using a pH meter (AB15, Fisher, Canada). Amounts of 2 N HCl required for adjusting pH to 7.0, 6.0, 5.0, 4.0, 3.0, and 2.0 were recorded, and they were scaled down for 1 ml or another required volume to each pH value accordingly. The corresponding amounts of 2 N HCl were then used for adjusting acidities of 1-ml solutions of 100 mM sodium phosphate (pH 7.0) that contained 50 μM NADH to pH 7.0, 6.0, 5.0, 4.0, 3.0, and 2.0, respectively. Solutions (1 ml) with different pH values were incubated at room temperature. The decomposition of NADH at different pH values was monitored by the decrease of absorbance at 340 nm (Table 2-1). The results showed that the absorbance of NADH at pH 2.0 and 3.0 decreased by more than 96% (below 0.01) within 10 min. After neutralization using 2 N NaOH, there was no increase in absorbance at 340 nm of the same sample that was adjusted to pH 2.0 for 10 min. In contrast, NADH was relatively stable at other tested pHs≥4.0 within the same period of time. Therefore, both pH 2.0 and 3.0 were suitable for destroying any remaining NADH present in H_2O_2 samples within a very short period of time.

2.4.4 Stability of H_2O_2 at low pH values

It was also necessary to determine whether H_2O_2 was stable under strong acidic conditions compared to that at pH 7.0; 8.8 μM H_2O_2 was added to 100 mM sodium phosphate with pH values of 2.0, 3.0, and 7.0. Concentrations of H_2O_2 in the mixtures at pH 2.0, 3.0, and 7.0 after their incubation at room temperature for 0, 20, 30, and 60 min were determined to be 8.62 ± 0.21, 8.62 ± 0.22, and 8.68 ± 0.16 μM, respectively. The results showed that H_2O_2 was stable at pH 2.0 and 3.0 for at least 60 min, which is consistent with its extreme stability under acidic conditions reported previously (Schumb 1949).

2.4.5 Acidification–neutralization procedures

The stability of H_2O_2 and lability of NADH at pH 2.0 should make it possible to determine H_2O_2 simply and reliably in any sample containing NADH. Mixtures (0.84 ml) with known concentration

Table 2-1 Stability of NADH at various pH values

Incubation time (min)	Absorbance change (340 nm) at pH-values adjusted					
	pH 2.0	pH 3.0	pH 4.0	pH 5.0	pH 6.0	pH 7.0
0	0.276	0.273	0.275	0.277	0.272	0.278
1	0.043	0.115	0.216	0.214	0.219	0.278
5	0.003	0.007	0.215	0.214	0.219	0.281
10	0.005	0.004	0.213	0.212	0.218	0.280
60	0.005	0.004	0.204	0.200	0.212	0.280
120	0.005	0.004	0.180	0.179	0.197	0.277
300	0.003	0.001	0.131	0.133	0.161	0.258
>1,000	0.003	0.004	0.044	0.045	0.072	0.204

of H_2O_2 (9.7 μM) containing various concentrations of NADH (0, 10, 20, 50, and 100 μM) were acidified to pH 2.0 using 2 N HCl (80 μl) and incubated at room temperature for 10 min. Each mixture was then neutralized with the same amount of 2 N NaOH corresponding to that of 2 N HCl to bring the pH back to 7.0. H_2O_2 was measured using the HRP assay by adding 150 μl ABTS and 25 μl horseradish peroxidase solution prepared to the entire mixture immediately after neutralization. The results showed that accurate determination of H_2O_2 was obtained only when the concentration of NADH in the H_2O_2 assay mixture before acidification was between 0 and 30 μM (Figure 2-2). In contrast, H_2O_2 could not be determined accurately in the presence of NADH without acidification and neutralization (Figure 2-2).

Detection limit of H_2O_2 using this procedure was also determined. A series of H_2O_2 solutions from 0.0 to 8.8 μM in 100 mM sodium phosphate (pH 7.0) containing 10 μM NADH was prepared. Both steps of acidification and neutralization were carried out exactly as described above. Then 150 μl ABTS and 25 μl horseradish peroxidase were added to each of the mixtures and H_2O_2 was measured. The results showed that the accuracy was very good and the limit of H_2O_2 determination was about 0.3 μM when an initial NADH concentration was 10 μM by using this method of acidification and neutralization to eliminate NADH present in the original samples (Figure 2-3).

2.4.6 Acidification-only procedures

An alternative way to determine H_2O_2 in the presence of NADH with an initial concentration up to 200 μM was also developed using the same principle of the HRP assay (Figure 2-4). After acidification (pH 2.0) for 10 min, 10% of the mixture (1 ml) was used for determining the H_2O_2 in all samples. After a 100 μl sample was added to 725 μl of 100 mM phosphate buffer (pH 7.0), additions of 150 μl ABTS and 25 μl horseradish peroxidase were carried out. Absorbance at 725 nm was monitored after incubation of the assay mixture for 5 min. It showed that H_2O_2 was accurately determined in the presence of NADH up to 100 μM (Figure 2-4). In contrast, H_2O_2 could not be determined accurately in the presence of NADH without acidification.

To test the determination limit of this alternative procedure, solutions of H_2O_2 (0.92 ml) with concentrations from 0.0 to 88 μM in 100 mM sodium phosphate (pH 7.0) containing 100 μM NADH were prepared. Each solution was acidified to pH 2.0 using 2 N HCl (80 μl) as described above. After

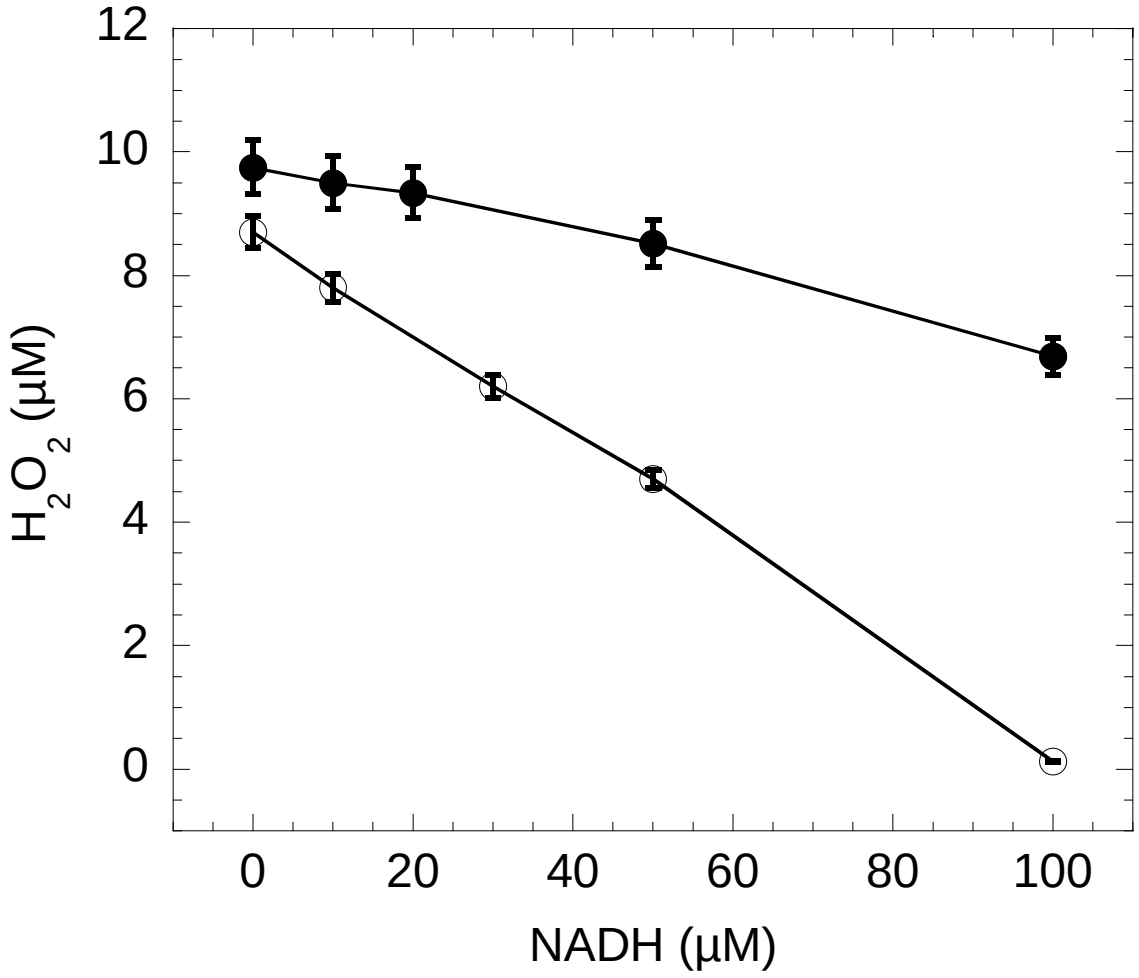

Figure 2-2 Determination of H_2O_2 in the presence of NADH using acidification–neutralization procedures.

One set of 0.84 ml of 9.7 μM H_2O_2 in 100 mM phosphate, pH 7.0, containing 0, 10, 30, 50, 100, and 200 μM NADH, respectively, was prepared. The pH in one set with 9.7 μM H_2O_2 was adjusted to 2.0 using 2 N HCl (80 μl) for 10 min followed by adding 2 N NaOH (80 μl) for neutralization to pH 7.0. Another set of 1 ml of 8.8 μM H_2O_2 in 100 mM phosphate, pH 7.0, containing 0, 10, 30, 50, and 100 μM NADH, respectively, was prepared. Then 150 μl ABTS and 25 μl horseradish peroxidase were added to each set for determining H_2O_2 using the HRP assay. Filled circle, with acidification and neutralization; open circle, without acidification.

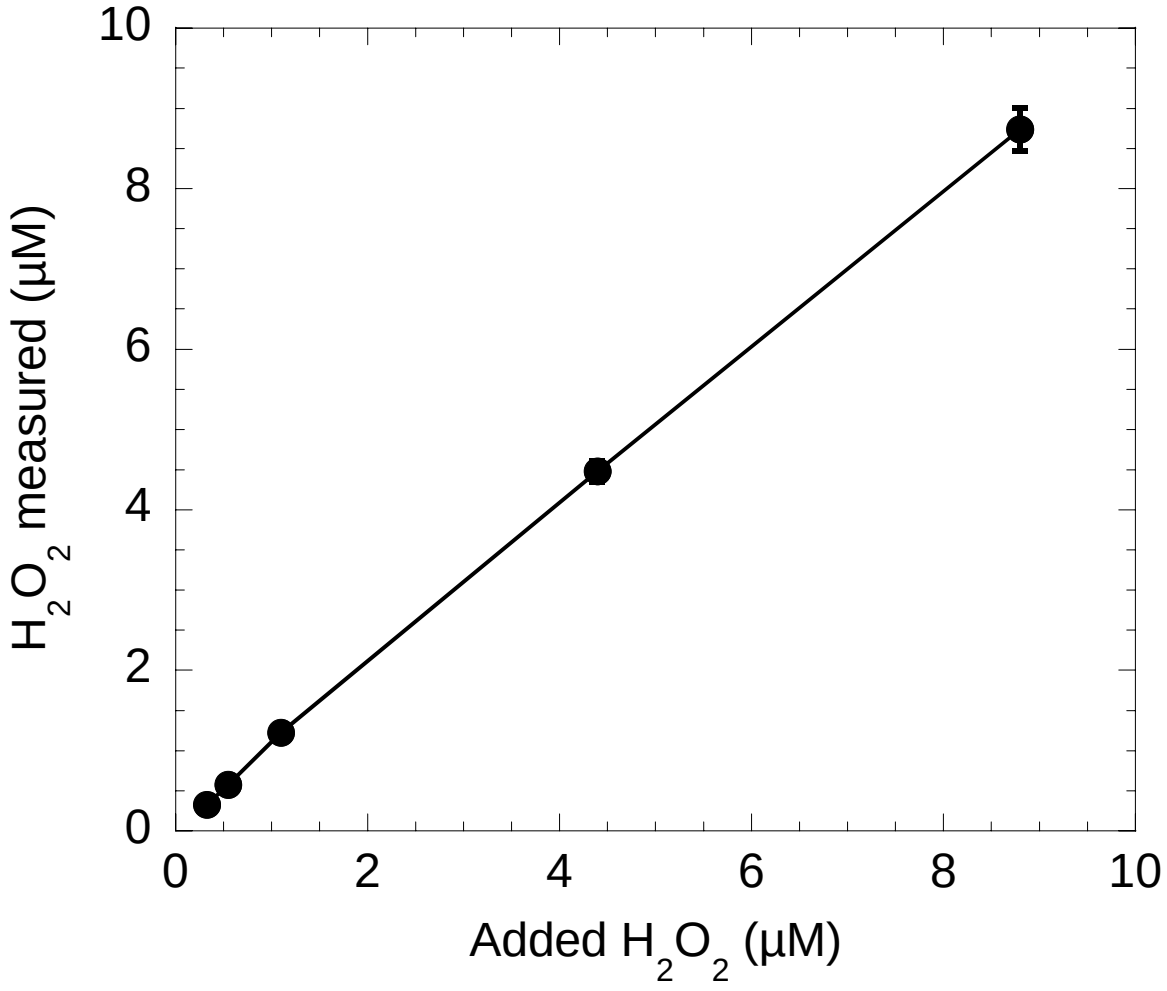

Figure 2-3 Sensitivity of H_2O_2 determination in the presence of NADH using acidification–neutralization procedures.

Mixtures with known concentrations of H_2O_2 in 0.84 ml of 100 mM phosphate (pH 7.0) containing 10 μM NADH were adjusted to pH 2.0 using 2 N HCl (80 μl) for 10 min followed by adding 2 N NaOH (80 μl) for neutralization to pH 7.0. Then 150 μl ABTS and 25 μl horseradish peroxidase were added to each set for determining H_2O_2 using the HRP assay.

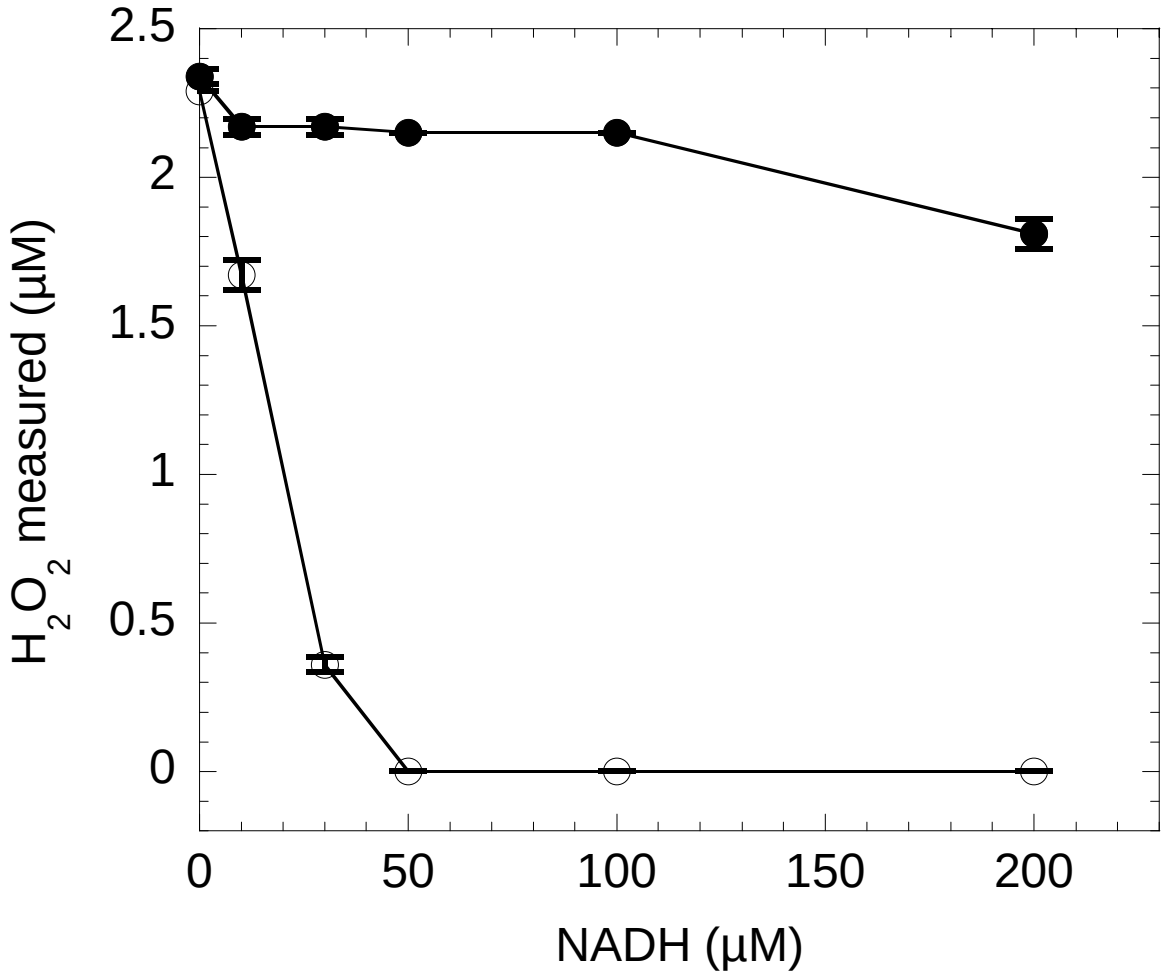

Figure 2-4 Determination of H_2O_2 in the presence of NADH using the acidification-only procedures.

Two sets of 0.92 ml of 22 μM H_2O_2 in 100 mM phosphate, pH 7.0, containing 0, 10, 30, 50, 100, and 200 μM NADH, respectively, were prepared. The pH in one set was adjusted to 2.0 using 2 N HCl (80 μl) for 10 min. Then 100 μl of each of mixture (1 ml) was taken out for determining H_2O_2 using the HRP assay. Filled circle, with acidification; open circle, without acidification.

incubation at room temperature for 10 min, a portion (100 µl) from each of the solutions (1 ml) was taken out for H_2O_2 assay as described above. The H_2O_2 determined was also nearly the same as that added to the mixtures (Figure 2-5). It showed that the accuracy of H_2O_2 determination was about the same when the acidified solutions without neutralization were used directly for the HRP assay, and the detection limit of H_2O_2 was about 3 µM in the sample under this condition, which was comparable in principle with that (0.3 µM) obtained using acidification and neutralization procedures described above.

2.4.7 Determination of H_2O_2 generated by *T. maritima* NADH oxidase

In general, 100 mM phosphate (pH 7.0) was used to measure NADH oxidase activity in the presence of about 100 µM NADH (Reed et al. 2001). Therefore, H_2O_2 produced by a *T. maritima* NADH oxidase was measured using the procedures described above. The oxidase reaction was carried out aerobically in 2 ml of 100 mM phosphate (pH 7.0) containing 100 µM NADH at 80 °C. Consumption of NADH was monitored by the decrease of absorbance at 340 nm. Thermal decomposition of NADH was monitored the same way under the same condition without the NADH oxidase added. With the acidification-only method, 118 ± 4 nmol H_2O_2 was determined while 129 ± 5 nmol NADH was consumed excluding thermally decomposed NADH during the same period of time, indicating that more than 90% of NADH used by the oxidase was converted to H_2O_2 when an initial NADH concentration in the sample was 100 µM. Using the acidification–neutralization method, the NADH oxidase reaction was carried out aerobically in 2 ml of 100 mM phosphate (pH 7.0) containing 20 µM NADH at 80 °C. Similarly, consumption of NADH was monitored by the decrease of absorbance at 340 nm. Thermal decomposition of NADH was monitored the same way under the same condition without the added NADH oxidase. After acidification at pH 2.0 for 10 min, the mixture was neutralized using the same amount of 2 N NaOH to pH 7.0. H_2O_2 was measured using the HRP assay by adding 300 µl ABTS and 50 µl horseradish peroxidase to the entire mixture immediately after neutralization. It was found that 22.3 ± 1.2 nmol H_2O_2 was determined while 23.6 ± 1.4 nmol NADH was consumed excluding thermally decomposed NADH during the same period of time, indicating that more than 94% of NADH used by the oxidase was converted to H_2O_2 when an initial NADH concentration in the sample was 20 µM.

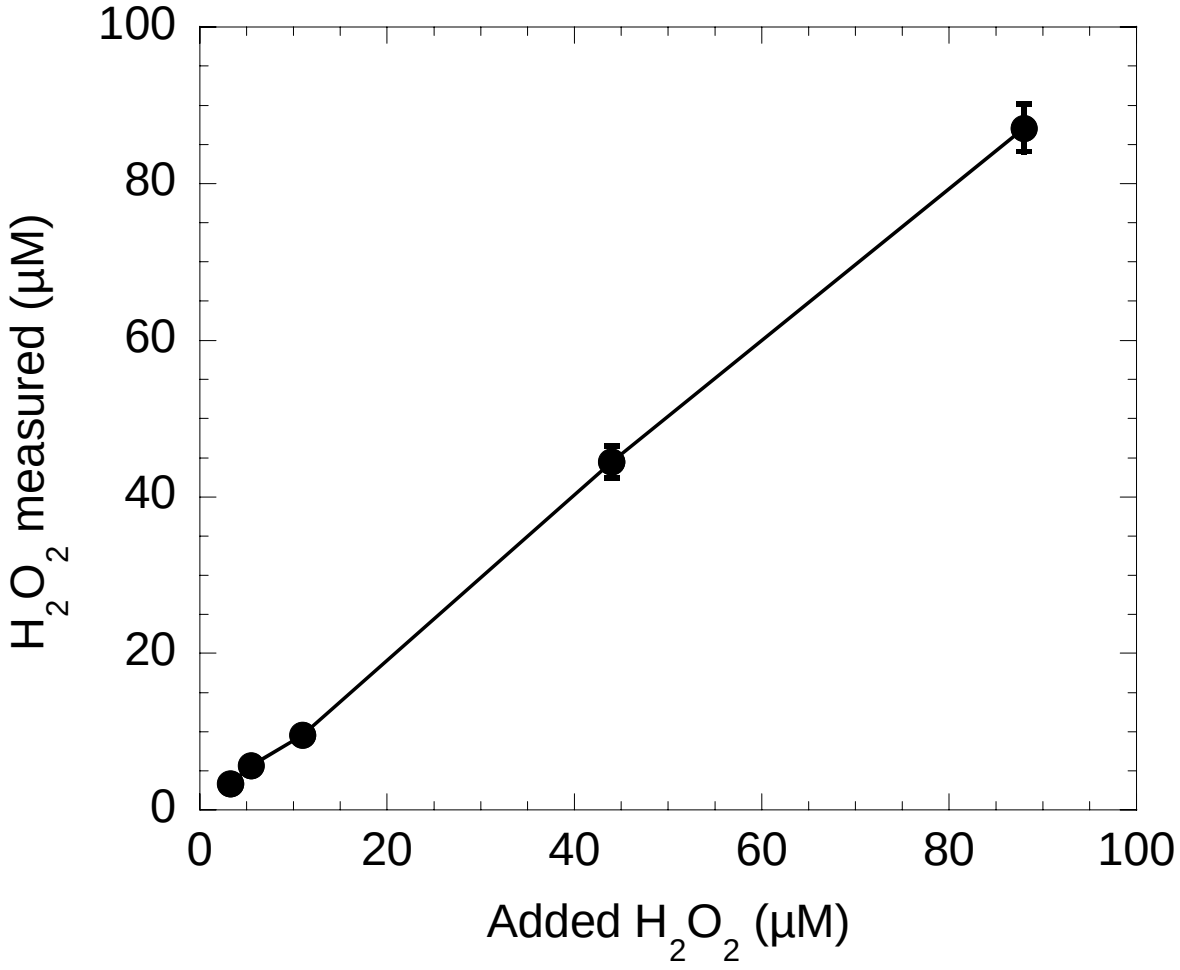

Figure 2-5 Sensitivity of H_2O_2 determination in the presence of NADH using the acidification-only procedures.

Mixtures with known concentrations of H_2O_2 in 0.92 ml of 100 mM phosphate (pH 7.0) containing 100 μM NADH were adjusted to pH 2.0 using 2 N HCl (80 μl) for 10 min. Then 100 μl from each of the mixtures was used for measuring H_2O_2 using the HRP assay.

NADH remaining in any sample could be eliminated by adjusting pH to 2.0 or 3.0 for about 10 min at room temperature. H_2O_2 in any sample containing NADH from 10 to 100 μM could be determined accurately with a detection limit from 0.3 to 3 μM depending on the initial concentration of NADH present in the sample. Acidification was a required step for this method described; however, neutralization was not necessary if just a portion (~10%) of the acidified sample was used for the H_2O_2 determination using the HRP assay, which is simple, sensitive, and reliable.

Chapter 3 Purification and Characterization of an NADH Oxidase from Extremely Thermophilic Anaerobic Bacterium *Thermotoga hypogea*

The work described in this chapter was published in Archives of Microbiology.

Yang X. and K. Ma. 2005. Purification and characterization of an NADH oxidase from extremely thermophilic anaerobic bacterium *Thermotoga hypogea*. Arch. Microbiol. 183: 331-337.

3.1 ABSTRACT

Thermotoga hypogea is an extremely thermophilic anaerobic bacterium capable of growing at 90°C. It was found to be able to grow in the presence of micro-molar level of molecular oxygen. Activity of NADH oxidase was detected in the soluble fraction of the cell-free extract of *T. hypogea*, from which an NADH oxidase was purified to homogeneity using a Fast Performance Liquid Chromatography (FPLC) system. The purified enzyme was a homodimeric flavoprotein with a subunit of 50 kDa revealed by Sodium dodecyl sulfate-polyacylamide gel electrophoresis (SDS-PAGE). It catalyzed the reduction of oxygen to hydrogen peroxide specifically using NADH as electron donor. Its catalytic properties showed that the NADH oxidase had an apparent V_{max} value of 37 μmol NADH oxidized min^{-1}. mg^{-1} protein. Apparent K_m values for NADH and molecular oxygen were determined to be 7.5 μM and 85 μM, respectively. The enzyme exhibited a pH optimum of 7.0 and temperature optimum above 85°C. NADH-dependent peroxidase activity was also present in the cell-free extract, which could reduce hydrogen peroxide produced by the NADH oxidase into water. Although it seems possible that oxygen can be reduced into water by both oxidase and peroxidase, further investigation is required to firmly conclude if the purified NADH oxidase is part of an enzyme system that protects anaerobic *T. hypogea* from accidental exposure to molecular oxygen.

3.2 INTRODUCTION

NAD(P)H oxidases (EC1.6.3.1) catalyze the oxidation of NAD(P)H by simultaneously reducing molecular oxygen (O_2) to form either H_2O_2 in a two-electron transfer process or H_2O in a four-electron transfer process (Kawasaki et al. 2004; Toomey and Mayhew 1998). In aerobic microorganisms, NAD(P)H oxidase activities are generally resulted from a side reaction of membrane-bound enzymes catalyzing electrons transfer from NAD(P)H through quinones and cytochromes to oxygen. Since oxygen is toxic to obligate anaerobic microorganisms, their oxygen-consuming enzymes such as NAD(P)H oxidases were previously found not to be obviously involved in their metabolism (Dolin 1959; Maeda et al. 1992). However, more enzymes catalyzing NADH-dependent reduction of oxygen are found to be present in many anaerobic microorganisms and these enzymes may have important physiological functions (Herles et al. 2002; Kengen et al. 2003; Ward et al. 2001). It is demonstrated that NADH oxidases can be involved in regulation of NAD/NADH ratio in anaerobic bacteria (Niimura et al. 2000). NADH-dependent consumption of O_2 is also considered as a defense mechanism for anaerobes to reduce toxicity from accidental exposure to oxygen in the environment (Kengen et al. 2003; Ward et al. 2001).

T. hypogea is a strictly anaerobic microbe belonging to the order of *Thermotogales* (Fardeau et al. 1997). It produces hydrogen, carbon dioxide, and acetate as fermentation products. Recently, it has been reported that many strictly anaerobic microorganisms including several members in *Thermotogales* can grow in the presence of oxygen, but how oxygen is involved in their metabolism is not known (Van Ooteghem et al. 2001, 2004). The hydrogen production is even stimulated by the presence of oxygen in the growth media of *T. neapolitana*. It was intriguing to elucidate the mechanism of oxygen tolerance by anaerobic *Thermotoga* species, of which *T. hypogea, T. neapolitana* and *T. maritima* were found to have O_2-dependent NADH-oxidation activities. The activity detected in their cell-free extracts showed the presence of NADH oxidases in all three obligate anaerobes. In this study, it was found that *T. hypogea* grew in the presence of low-level of oxygen. One NADH oxidase was purified from *T. hypogea*. The present chapter reports the properties and proposed physiological functions of the purified enzyme.

3.3 MATERIALS AND METHODS

3.3.1 Organism and chemicals

T. hypogea (DSM 11164) was obtained from the Deutsche Sammlung von Mikroorganismen and Zellkulturen GmbH, D-38124 Braunschweig, Germany. All chemicals were from commercially available products unless specified.

3.3.2 Growth of *T. hypogea*

T. hypogea was cultured in a medium modified from Fardeau at 70°C (Fardeau et al. 1997). The medium contains (per liter): 1 g of NH_4Cl, 0.3 g of K_2HPO_4, 0.3 g of KH_2PO_4, 0.2 g of $MgCl_2 \cdot 6H_2O$, 0.1 g of $CaCl_2 \cdot 2H_2O$, 0.1 g of KCl, 2.0 g of yeast extract, 2.0 g of trypticase, 10 ml of trace mineral element solution (Balch et al. 1979**)**, 0.05 mg of resazurin, and 1 liter of de-ionized H_2O. The pH was adjusted to 7.3 at room temperature. It was grown routinely using 50 ml medium in a sealed serum bottle with N_2 as gas phase (160 ml, Wheaton, Millville NJ). Different amount of oxygen was added to the gas phase of the bottle to test the growth in the presence of oxygen. The final dissolved oxygen concentration was calculated based on oxygen partial pressure (Kengen et al. 2003). The growth was monitored by direct cell count using a Petroff-Hausser counting chamber (1/400 SQ MM, 0.0200 MM deep) and a Nikon Eclipse E600 phase-contrast light microscope.

3.3.3 Enzyme assay and protein determination

NADH oxidase was determined in a glass cuvette by monitoring oxygen-dependent oxidation of NADH spectrophotometrically at 340 nm (ε_{340} = 6.22 $mM^{-1}cm^{-1}$) at 80 ^oC. The assay mixture (2 ml) contained 100 μM NADH and 100 mM sodium phosphate buffer, pH 7.0 (Ward et al. 2001). One unit of enzyme activity was defined as 1 μmol NADH oxidized per minute. NADH-dependent peroxidase activity was determined anaerobically using the same type of cuvette by monitoring H_2O_2-dependent oxidation of NADH at 340 nm at 80 °C. The assay mixture (2 ml) contained 200 μM NADH, 200 μM H_2O_2 and 100 mM sodium phosphate buffer, pH 7.0. One unit of peroxidase activity was defined as 1 μmol NADH oxidized per minute. Protein concentration was determined using Bradford method with bovine serum albumin as standard protein (Bradford 1976).

3.3.4 H_2O_2 determination

H_2O_2 was determined using the method described previously (Ward et al. 2001). To obtain a standard curve for assaying H_2O_2, a series of concentrations of H_2O_2 from 0-8.8 μM in 1.0 ml of 100 mM phosphate buffer pH 7.0 was prepared. One ml of 30% H_2O_2 (8.8 M) was diluted 100-fold using 99 ml de-ionized water. Then, one ml of the resulted 8.8 x 10^{-2} M H_2O_2 was diluted 100-fold using another 99 ml de-ionized water. Finally, one ml of the resulted 8.8 x 10^{-4} M H_2O_2 was diluted 8-fold using 7 ml de-ionized water to prepare 1.1 x 10^{-4} M H_2O_2. Different concentrations of 0, 0.55, 2.2, 4.4 and 8.8 μM of H_2O_2 were prepared by adding 0, 5 and 20 μl of 1.1 x 10^{-4} M H_2O_2, 5 and 10 μl of 8.8 x 10^{-4} M H_2O_2 respectively into separated cuvettes containing one ml of 100 mM phosphate buffer pH 7.0. Each concentration was prepared in duplicate. 150 μl of a solution containing ABTS (0.2 mg. ml^{-1}) and horseradish peroxidase (100 U. ml^{-1}, from Sigma) were added. The assay mixture (1.15 ml) in the cuvette was then incubated 30 min at 37 °C. Absorbance change at 725 nm was monitored. A standard curve was obtained by plotting the absorbance at 725 nm against the corresponding H_2O_2 concentration. Please note that two moles of ABTS are required to reduce one mole of H_2O_2. H_2O_2 produced in an assay mixture catalyzed by the purified NADH oxidase at 80°C was measured using the same procedure. However, NADH present in the assay mixture had to be depleted first, which was carried out by either flushing with pure oxygen for 10 min, and left the mixture at room temperature for up to 4 hours with periodic shaking to accelerate the oxidation of NADH. The depletion of NADH was monitored using absorbance value at 340 nm. When the absorbance value reached below 0.010, 100 μl of the reaction mixture was taken out and added into 900 μl of 100 mM phosphate buffer pH 7.0 in the cuvette. After adding 150 μl of the solution containing ABTS and horseradish peroxidase, absorbance at 725 nm was measured and the H_2O_2 concentration in the reaction mixture was calculated based on the standard curve. Since NADH was thermally degraded at a slow rate, a control without adding the NADH oxidase was performed.

3.3.5 Preparation of cell-free extracts

To obtain sufficient amount of biomass for enzyme study, *T. hypogea* grew in the medium described above with addition of 0.5 g/l cysteine-HCl and 5 g/l sodium thiosulfate in a 20-liter glass carboy (Corning, NY). Cells growing at late exponential phase were harvested anaerobically by centrifugation at 13,000x*g* (Sharples super centrifuge). Cells were frozen with liquid nitrogen and stored at -80^{o}C. Frozen cells (50 grams) were suspended in 250 ml of anaerobic buffer that

contained 50 mM tris(hydroxymethyl)aminomethane-HCl (Tris-HCl) pH 7.8, 1 mM dithiothreitol (DTT), l mM sodium dithionite (SDT) and 0.1 mg/ml lysozyme. DNase I (5 µg/ml**)** was added to the mixture after the cells were completely thawed. The mixture was incubated at 37^{o}C for 2 hours with constant stirring and centrifuged at 20,000 x *g* for 30 min (Sorvall RC-5B centrifuge, SS-34 Rotor). The resulting supernatant was cell-free extract used for the purification of NADH oxidase of *T. hypogea*. An aliquot of the cell-free extract was used for ultracentrifugation at 115,000x*g* for 1 hour at 4 ^{o}C. NADH oxidase activities present in both supernatant and pellet were measured.

3.3.6 Enzyme purification

Cell-free extract was prepared anaerobically and applied to a pre-equilibrated DEAE-Sepharose Fast Flow (5 x 5 cm, Amersham Biotech, Quebec, Canada) using buffer A (50 mM Tris-HCl pH 7.8, 5% [vol/vol] glycerol, 1 mM SDT, and 1 mM DTT). The column was eluted with a linear gradient of 0-0.5 M NaCl in buffer A at a flow rate of 2 ml/min. NADH oxidase started to elute as 0.05 M NaCl applied to the column. All activity-containing fractions were pooled together and applied to a hydroxyapatite (HAP, Amersham Biotech, Quebec, Canada) column (2.6 x 10 cm) equilibrated with buffer A. The column was eluted with a linear gradient (0-0.25 M) of potassium phosphate in buffer A at a flow rate of 2 ml/min. NADH oxidase started to elute as 0.065 M potassium phosphate applied to the column. Activity-containing fractions were pooled and applied to a Phenyl-Sepharose Fast Flow column (2.6 x 8 cm, Amersham Biotech, Quebec, Canada) equilibrated with 0.8 M $(NH_4)_2SO_4$ in buffer A. The column was eluted with a $(NH_4)_2SO_4$ gradient (0.8 -0 M) at a flow rate of 2 ml/min. The majority of NADH oxidase was eluted as 0.38 M $(NH_4)_2SO_4$ applied to the column. Fractions containing high NADH oxidase activity were combined and concentrated by ultrafiltration (Amicon Ultrafilter, PM 30 membrane). The concentrated fraction (1.0 ml) was applied to a Superdex 200 column (2.6 x 60 cm, Amersham Biotech, Quebec, Canada) equilibrated with buffer A containing 100 mM KCl. The flow rate of the elution was 2 ml/min. Fractions containing pure NADH oxidase were combined and stored at –20°C, at which it was stable for a few months.

3.3.7 Electrophoresis and molecular weight determination

SDS-PAGE was carried out according to the method of Laemmli (Laemmli 1970). The purity of fractions from various purification steps was examined using SDS-PAGE. The gel was stained with

Coomassie Brilliant Blue R250 after electrophoresis. The subunit molecular mass was estimated using phosphorylase b (97 kDa), bovine serum albumin (66 kDa), ovalbumin (45 kDa), carbonic anhydrase (30 kDa), trypsin inhibitor (20 kDa), and ß-lactalbumin (14.4 kDa) as standard proteins.

Native polyacylamide gel electrophoresis was performed the same way as the SDS-PAGE with the absence of SDS and without denaturing of protein samples. Un-denatured protein samples were run on 7.5% native gels and stained for NADH oxidase by being immersed in standard NADH oxidase assay mixture containing 500µg/ml Neo Blue Tetrazolium. The purple NBT formazan was visualized after the gels were incubated at 80^{o}C for 20 min (López-Huertas et al. 1999). Molecular weight of native NADH oxidase was determined by gel filtration using Superdex 200 column with ferritin (440 kDa), catalase (232 kDa), aldolase (158 kDa), and bovine serum albumin (66 kDa) as protein standard.

3.3.8 Flavin cofactor analysis

Flavin present in the purified NADH oxidase was extracted using previously reported method (Stanton and Jensen 1993). The amount of flavin was estimated using absorbance value at 450 nm (ε_{450} = 11.3 x 10^3 $M^{-1}.cm^{-1}$). The sample was then concentrated using water pump before it was spotted on a thin-layer silica gel plate (5 x 1 0 cm, 200 micron, Selecto Scientific, USA). Other pure flavin compounds, riboflavin, FMN and FAD were applied on the same silica gel as standards. Samples ascended in the dark on the silica gel plate with *n*-butanol-acetic acid-H_2O (12:3:5) as solvent. After drying the silica plate in the air, samples on the plate were visualized using a UV lamp (365 nm).

3.3.9 Determination of free thiol-group of the purified NADH oxidase

Free thiol-group (–SH) present in the purified enzyme was determined using 5,5'-dithio-*bis*-(2-nitrobenzoic acid) (DTNB) based on the method described previously (Ellman 1959). 7.9 mg of DTNB was dissolved in 10 ml in sodium phosphate buffer (pH 7.0, 50 mM). The purified *T. hypogea* NADH oxidase in buffer A was concentrated with Microcon (PM 30) by centrifugation 10,000x*g* for 10 min and washed five times with de-ionized water. 46 µg of the washed enzyme in 100 µl de-ionized water was mixed with 850 µl of Tis-HCl buffer (100 mM, pH 8.0) and 50 µl DTNB solution.

In the control, the enzyme sample was replaced by 100 µl of the last pass through during previous wash step. The mixture was incubated at room temperature for 30 min and the absorbance at 412 nm was read for both sample and control. A molar coefficient of ε_{412}=13,600 M^{-1} cm^{-1} was used for the calculation of free thiols present in the purified *T. hypogea* NADH oxidase.

3.4 RESULTS

3.4.1 Growth of *T. hypogea* in the presence of oxygen

T. hypogea was isolated and reported as an obligate anaerobic bacterium (Fardeau et al. 1997). We found that this organism grew well in a culture bottle that was accidentally contaminated with trace amount of oxygen from the air. The growth in the presence of small amount of oxygen was confirmed by further experiments when various oxygen concentrations (0-13.8 μM) were introduced into the growth media. *T. hypogea* in a static culture could tolerate up to 6.9 μM dissolved oxygen in the growth media. However, the tolerated level of dissolved oxygen was reduced to 4.1 μM when *T. hypogea* grew in a sealed bottle with constant shaking (Figure 3-1&Figure 3-2). The decrease in oxygen tolerance level indicated that *T. hypogea* had a limited ability to remove dissolved oxygen that diffused into the liquid phase from the gasphase much quicker under shaking conditions. Therefore, it was plausible to assume there must be an oxygen-removing system in *T. hypogea*.

3.4.2 Activities of NADH oxidase and peroxidase

To determine if an oxygen-scavenging activity was present in this obligate anaerobic bacterium, NADH oxidase activity was measured. Cell-free extracts from *T. hypogea* growing under different conditions were prepared. Only NADH-specific oxidase activity was detected. The NADH oxidase from cells that were grown either in the presence or absence of oxygen had a higher activity (0.13±0.02 U/mg) in the late log phase than that in the stationary phase (0.05±0.01 U/mg). These results showed the NADH oxidase activity was not induced by the presence of oxygen in the growth media.

Interestingly, an NADH-specific peroxidase activity was also detected in the cell-free extract of *T. hypogea* (0.031±0.002 U/mg). An apparent K_m-value for H_2O_2 was determined to be 98±11 μM and apparent V_{max} to be 0.045±0.005 U/mg protein in the cell-free extract of *T. hypogea*.

In principle, O_2 would be reduced to water by both oxidase and peroxidase in the cell-free extract. However, a complete reduction of O_2 to water happened only if the O_2 in the gasphase was removed 5 min after the start of the reaction and the reaction time was extended for one hour (Table 3-1).

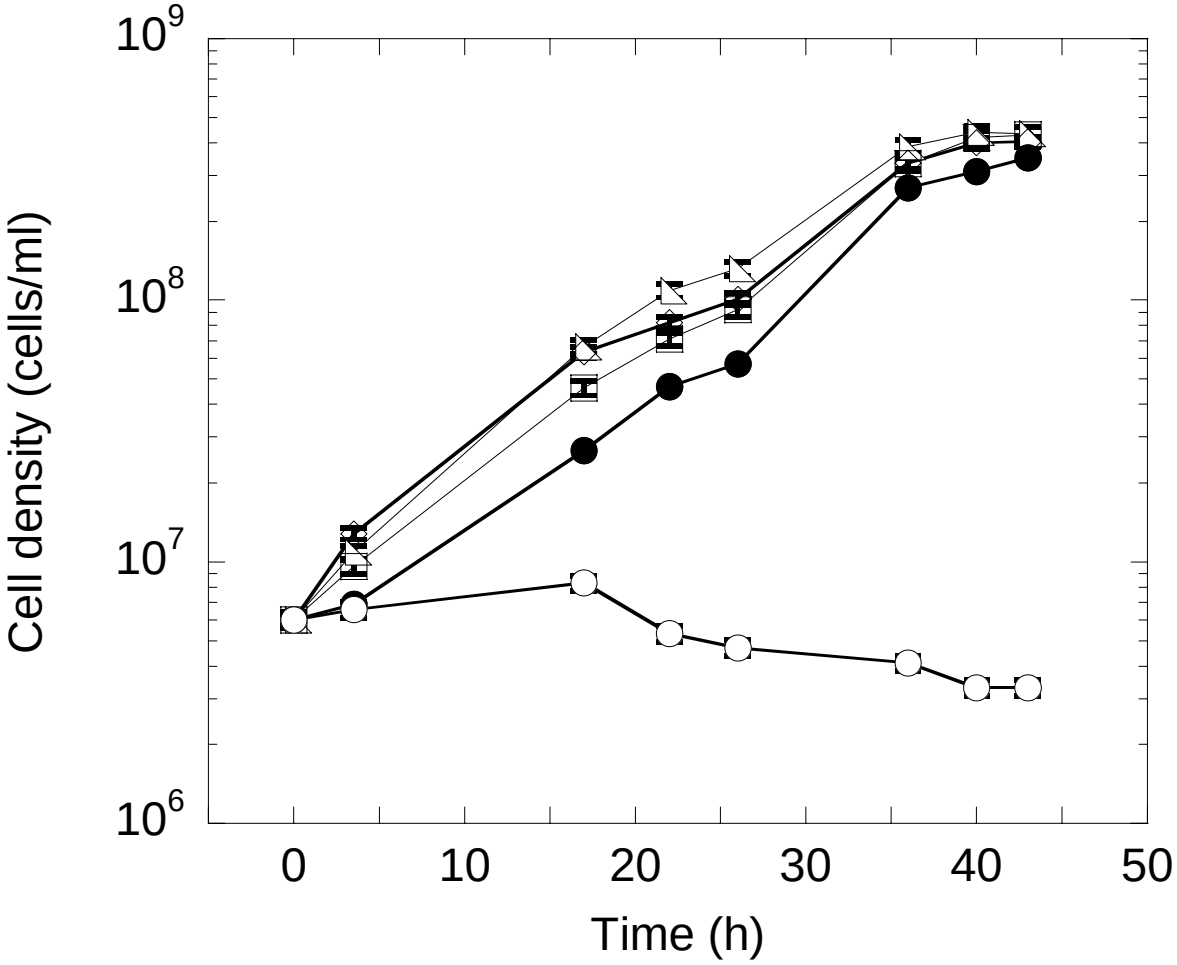

Figure 3-1 Growth of *T. hypogea* in the presence of oxygen in the static culture.

The growth experiments were carried out in sealed serum bottles without shaking at 70°C with various dissolved oxygen concentrations. Open triangles, without oxygen; open diamonds, 0.14 μM; open squares, 0.70 μM; closed circles, 6.9 μM; open circles, 13.8 μM.

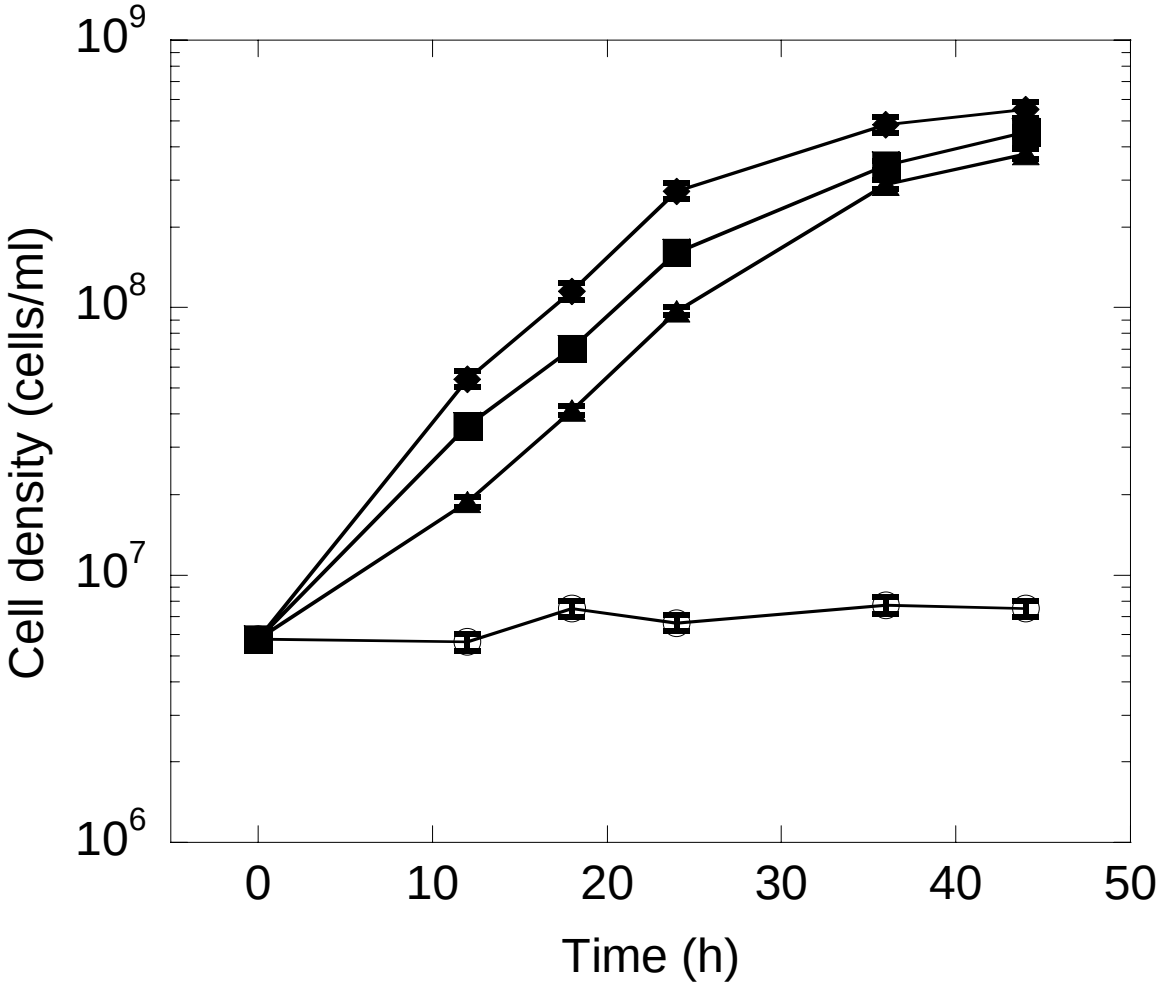

Figure 3-2 Growth of *T. hypogea* in the presence of oxygen under shaking conditions.

The growth experiments were carried out in sealed serum bottles with shaking (180 rpm) at 70°C with different dissolved oxygen concentrations. Filled diamonds, without oxygen; filled squares, 2.7 μM; filled triangles, 4.1 μM; open circles, 6.9 μM.

Table 3-1 H_2O_2 production catalyzed by the cell-free extract of *T. hypogea*

O_2-concentration (%, v/v)	NADH consumed (nmoles)	H_2O_2 produced (nmoles)	H_2O_2 produced/ NADH consumed (%)
20[a]	122±7	32±3	26
20[b]	310±11	0	0
100[a]	204±4	82±5	40

[a], The assay was performed in a mixture (2 ml) containing 100 mM phosphate buffer pH 7.0, 100 μM NADH and cell-free extract of *T. hypogea* (260 μg) 5 min at 80°C.

[b], The assay was performed in a mixture (2 ml) containing 100 mM phosphate buffer pH 7.0, 400 μM NADH and cell-free extract of *T. hypogea* (260 μg) 5 min at 80°C, however, the gasphase of the assay mixture was exchanged with 100% N_2 5 min after the reaction started. So, the H_2O_2 produced by the NADH oxidase was then reduced to water by the peroxidase present in the cell-free extract of *T. hypogea*.

Otherwise, an amount of H_2O_2 that was equal to 26% of the consumed NADH molar equivalents was detected. The production of H_2O_2 increased to 40% of the consumed NADH molar equivalents when 100% of O_2 was used (Table 3-1). Apparently, only part of the O_2 was reduced into water in the latter conditions. These results indicate that the cell-free extract of *T. hypogea* could only convert lower concentration of O_2 to water, which may well serve the purpose of scavenging micromolar level of O_2 that was observed by our growth experiments.

3.4.3 Purification of NADH oxidase

Although the cell-free extract could reduce O_2 to water completely, it was not clear if the detected NADH oxidase alone can catalyze the reduction of O_2 to water. It is required to obtain a pure NADH oxidase for determining its catalytic properties.

NADH oxidase activity was located in the cytoplasm of the strictly anaerobic bacterium *T. hypogea,* since more than 90% of the activity was present in the supernatant fraction after ultracentrifugation (115,000 x *g*, 1 h) of the cell-free extract. This also contained 90% of the cellular glutamate dehydrogenase activity, a known cytoplasmic enzyme (Ma and Adams 1994; Robb et al. 2001). Several chromatographic columns were used for purifying NADH oxidase from *T. hypogea* (Table 3-2). During the purification, NADH oxidase activity was eluted out as a predominant single peak in all purification steps except Phenyl-Sepharose HP, from which near 80% of NADH oxidase activities were eluted out when 0.38 M $(NH_4)_2SO_4$ applied and about 20% of NADH oxidase activities were eluted out when 0.0 M $(NH_4)_2SO_4$ applied. Therefore, there might be two different NADH oxidases present in *T. hypogea*. The major peak eluted from the column when 0.38 M $(NH_4)_2SO_4$ was applied was further purified using Superdex 200 gel filtration column, and the native NADH oxidase was estimated to have a molecular weight of 100 kDa. The enzyme was purified to homogeneity and had a single subunit with a molecular weight of 50 kDa revealed by SDS-PAGE (Figure 3-3). These results suggested that the NADH oxidase purified from *T. hypogea* was a homodimer.

3.4.4 Cofactor of the purified NADH oxidase

The solution that contained the purified NADH oxidase was yellowish, which was an indication of presence of flavin. A yellowish cofactor was released after the enzyme mixed with methanol was

Table 3-2 Purification of the NADH oxidase from *T. hypogea*

Steps	Total protein (mg)	Total activity (U)	Sp act (U/mg)	Purification fold	Recovery (%)
Cell-free extract	1694	227	0.13	1	100
DEAE-Sepharose	320	154	0.48	3.6	68
HAP	93	128	1.37	10	56
Phenyl-Sepharose	15.8	55	3.48	27	24
Superdex 200	0.7	21	30	230	9

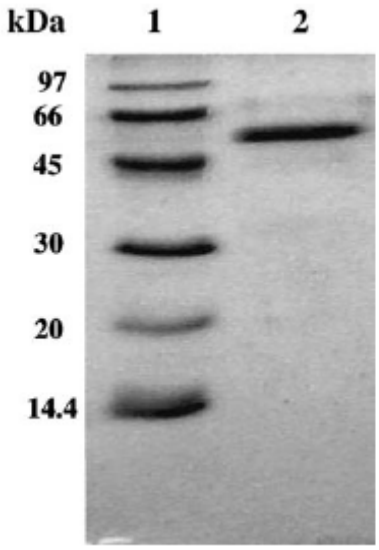

Figure 3-3 SDS-PAGE of the purified NADH oxidase from *T. hypogea*.

The purified NADH oxidase (lane 2, 1.2 μg) and low molecular weight standards (lane 1) are indicated along with their corresponding molecular masses.

boiled for 10 min in the dark. The absorbance spectrum of the oxidized cofactor released in solution had a characteristic peak of flavin at 450 nm that was lost upon addition of a reducing reagent SDT. This flavin cofactor was further identified as FAD using thin-layer chromatography (Figure 3-4). The NADH oxidase contained 1.8±0.1 mol of FAD per mol native enzyme based on the absorbance value at 450 nm and protein amount from which the FAD was extracted. Since the enzyme was a homodimer, each subunit contained approximately one non-covalently bound FAD moiety, which is a common feature of NADH oxidases.

3.4.5 Presence of sulfhydryl group in the NADH oxidase

The purified NADH oxidase in solution was incubated with various metal ions (1 mM) at room temperature for 1 hour and NADH oxidase activities were determined before and after the incubation. The remaining activities were found to be 6%, 56%, 69%, 71%, 85% and 93% after the incubation with $HgCl_2$, $FeSO_4$, $ZnSO_4$, $NiCl_2$, $CuSO_4$, $MgCl_2$, respectively. It appeared that sulfhydryl group susceptible to heavy metal ions was involved in catalysis of the enzyme. Incubation of the purified enzyme with DTNB **(**1 mM**)** for 7 min resulted in a 50% loss of activity, which further suggested that the sulfhydryl group of the enzyme was part of the catalytic site of the enzyme. The number of active free thiols of the enzyme was determined to be 1.8±0.1 per subunit of 50 kDa, which means there are four free –SH groups per dimer.

3.4.6 Product of oxygen reduction

Since NADH oxidases can catalyze both bivalent and tetravalent reduction of oxygen to H_2O and H_2O_2 respectively, production of H_2O_2 by the purified NADH oxidase from *T. hypogea* was determined. At first, a standard curve was made for the quantification of H_2O_2 produced. An apparent molar coefficient of the oxidized ABTS at 725 nm was determined to be 11,000 $M^{-1}.cm^{-1}$. NADH oxidation catalyzed by the enzyme in a sealed glass cuvette containing 158 nmol of NADH was allowed to go to completion ($OD_{340} < 0.010$). 100 µl of the assay mixture (equal to 7 nmol NADH consumed) was taken for assaying H_2O_2 using horseradish peroxidase and ABTS as electron donor. The results from assays in triplicate showed that near 90% of NADH consumed (7±0.2 nmol) in the assay mixture was used for reducing O_2 to H_2O_2 (6.2±0.3 nmol). While there was a slow

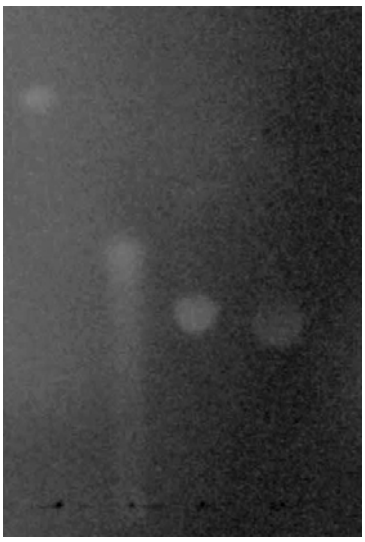

1 2 3 4

Figure 3-4 Thin layer chromatography of FAD cofactor extracted from the purified *T. hypogea* NADH oxidase.

The sample extracted from purified T. hypogea NADH oxidase was co-migrated with commercially available flavins: lane 1, riboflavin; lane 2, FMN; lane 3, FAD; lane 4, flavin extracted from the purified *T. hypogea* NADH oxidase. The R_f values for riboflavin, FMN, and FAD were determined to be 0.75, 0.46, and 0.33, respectively. The R_f value for the extracted flavin was 0.32.

thermal degradation of NADH at high temperatures (0.5±0.1 nmol), it was concluded that the NADH oxidase from *T. hypogea* exclusively catalyzed the reduction of oxygen to H_2O_2 using NADH as electron donor.

3.4.7 Catalytic properties of the purified NADH oxidase

The pH dependence of the NADH oxidase activity was determined using different buffers (100 mM phosphate pH 6.0-8.0; 100 mM glycylglycine pH 8.0-9.0). Maximum activity was found to be at pH 7.0 while the enzyme was very active at a pH range from 6.5 to 8.5, which might indicate NADH oxidase functions optimally under physiological conditions of *T. hypogea* (Figure 3-5). This is also true for NADH oxidases from acidophilic archaea *Acidianus ambivalens* and *Sulfolobus solfataricus*, which have much lower pH optima between 3 and 5 (Gomes and Teixeira 1998; Masullo et al. 1996). The activity of the NADH oxidase from *T. hypogea* increased along with the elevation of temperatures and the highest catalytic activity could be reached at temperatures above 85°C (Figure 3-6). However, no enzyme assay was performed at higher temperatures because of the thermal lability of NADH. The enzyme was very stable at 70°C, which is the optimal growth temperature of *T. hypogea*. There was no apparent activity loss after the enzyme was incubated for 8 hours at 70°C, while 50% of total activity was lost when incubated during a period of about 100 min at 90°C (Figure 3-7). The lost of NADH oxidase activities at 70°C and 90°C did not follow first order kinetics.

The purified oxidase could not use NADPH as electron donor for the reduction of oxygen. Its activity was dependent on concentrations of both NADH and oxygen. The catalysis followed Michaelis-Menten kinetics. Apparent K_m-value for NADH and apparent V_{max}–value were determined to be 7.5 µM and 37 µmol $min^{-1}.mg^{-1}$, respectively. Apparent K_m-value for oxygen was 85 µM, which is similar to that of NoxA-1 (NADH oxidase A-1, 60 µM) and much lower than that of NoxB-1 (NADH oxidase B-1, 2.9 mM) from *Archaeoglobus fulgidus* (Kengen et al. 2003). The relative high affinity towards O_2 suggested that this NADH oxidase might have physiological roles in the anaerobic *T. hypogea*.

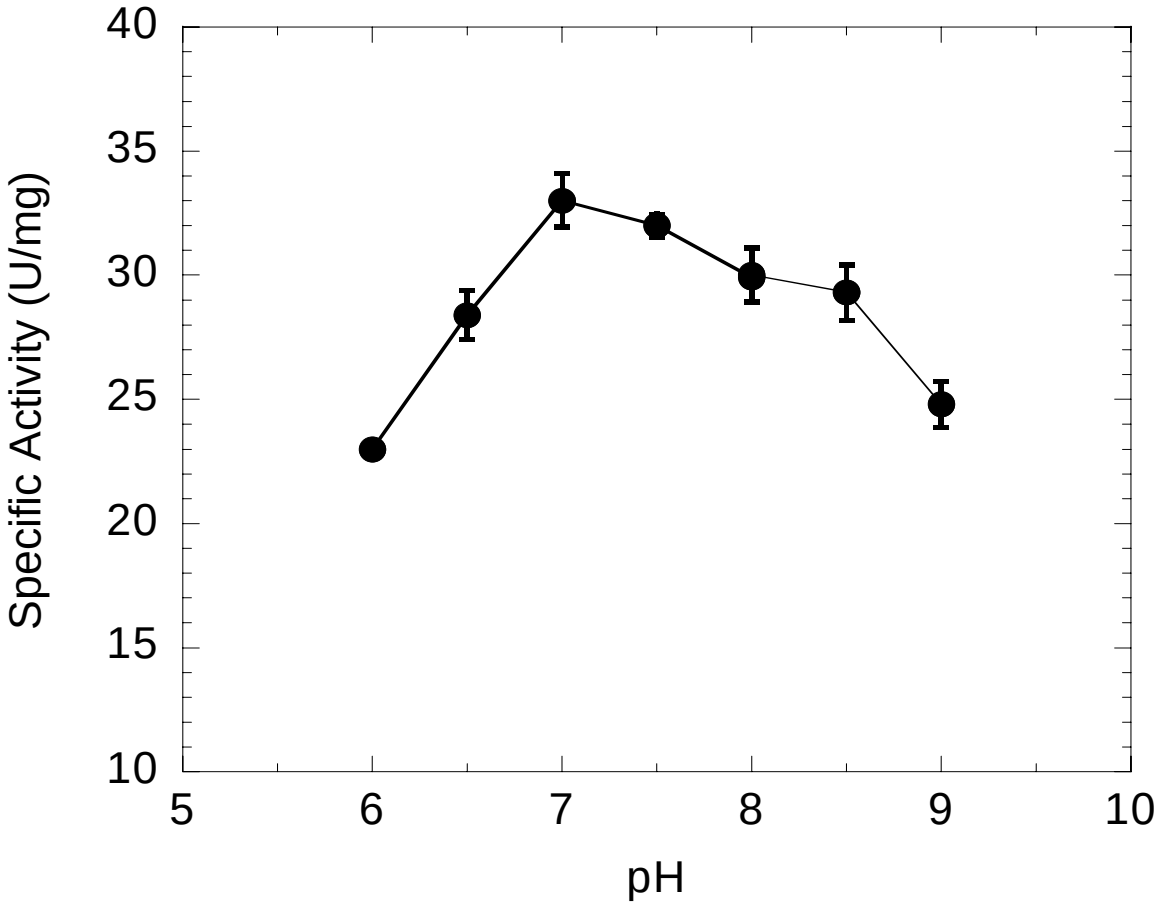

Figure 3-5 pH dependency of the purified NADH oxidase from *T. hypogea*.

Optimal pH for NADH oxidase was determnined at 80^{o}C. Buffers used: 100 mM phosphate (pH 6.0 – 8.0), 100 mM Glycine-NaOH (pH 8.0-9.0).

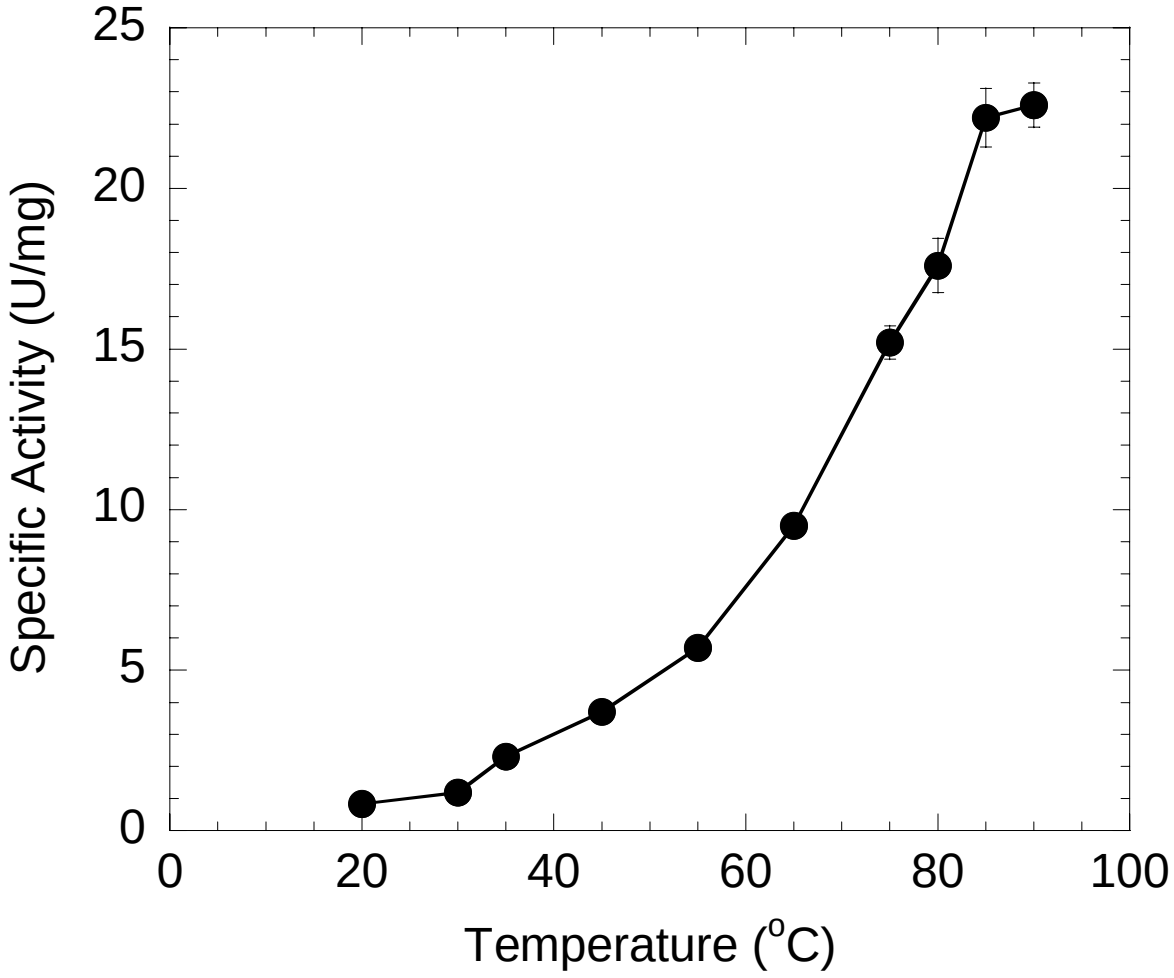

Figure 3-6 Temperature dependency of the purified NADH oxidase from *T. hypogea*.

The standard assay conditions were used as described in the Materials and Methods section with the assay temperature varied from 20 to 95°C.

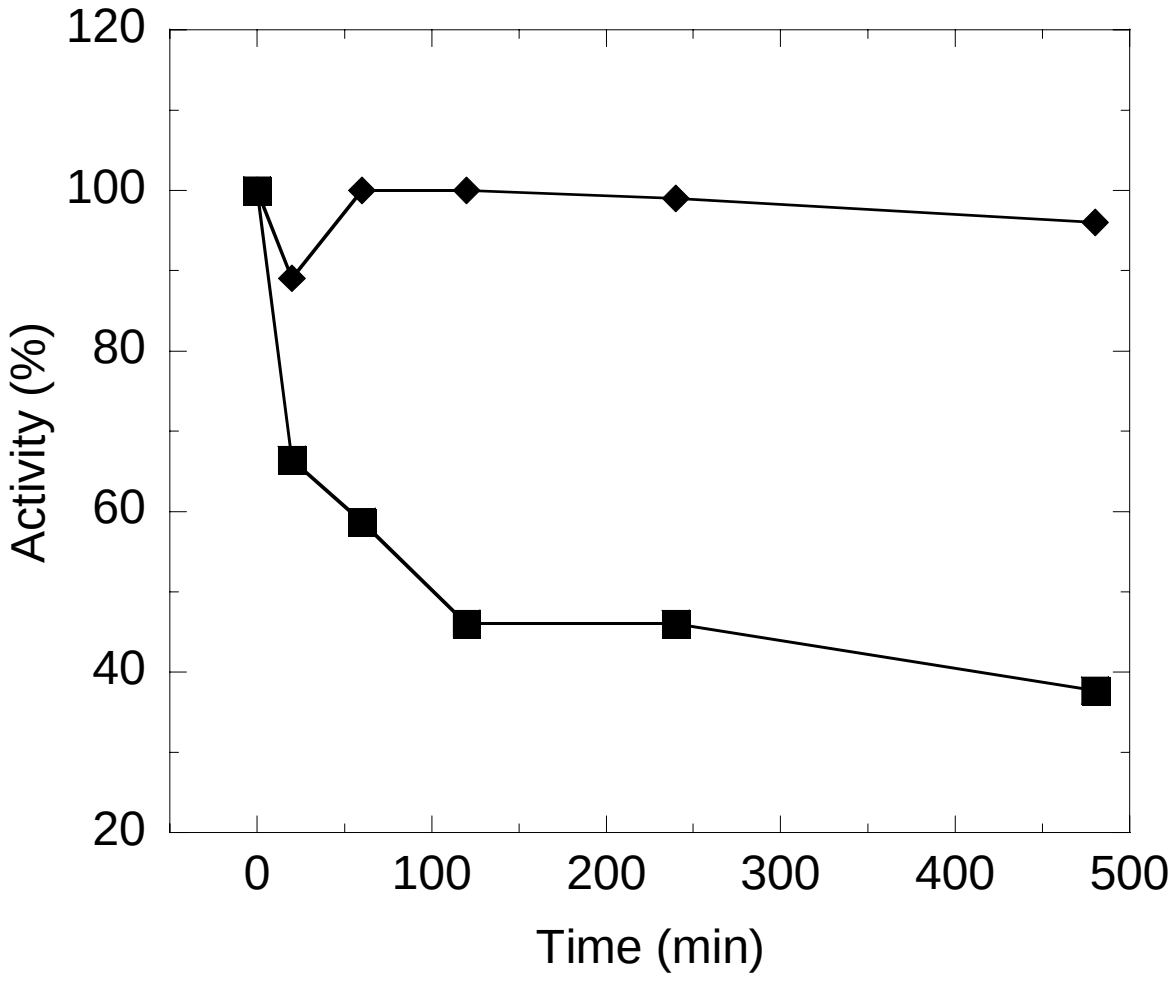

Figure 3-7 Thermostability of the purified NADH oxidase from *T. hypogea*.

The purified NADH oxidase (0.04 $mg.ml^{-1}$) in buffer A containing 0.1 M KCl was incubated at 70°C (filled diamonds) and 90°C (filled squares) respectively. The residual activities were assayed under standard conditions. 100% = 30 U/mg.

3.5 DISSCUSSION

It was demonstrated that *T. hypogea* could grow in the presence of limited amount of oxygen. The oxygen tolerance level of 6.9 μM in static culture might be an overestimated value because the level was decreased to 4.1 μM in culture with constant shaking that accelerated the diffusion rate of oxygen into the liquid medium. Therefore, *T. hypogea* is still considered as one of the strict anaerobes, which in general can not grow when the dissolved oxygen is higher than 5 μM (Engelkirk et al. 1992). Other species including *T. neapolitana* and *T. elfii* have also been found to grow in the presence of oxygen in the gas phase (Van Ooteghem et al. 2001). However, the ability of oxygen tolerance of strictly anaerobic microorganisms is not unique for *Thermotoga* species. An obligate anaerobic bacterium *Clostridium aminovalericum* (Kawasaki et al. 2004) and another strict anaerobe *Bacteroides fragilis* can grow in the presence of trace amount of oxygen (Baughn and Malamy 2004). More data have been obtained to show that various oxygen-consuming systems are present in strict anaerobes. For example, cytochrome *bd* oxidase is essential for oxygen consumption in *B. fragilis* (Baughn and Malamy 2004). NADH oxidase has been assumed to be responsible for the oxygen detoxification for anaerobes, and it has been found to be an oxygen-responsive enzyme in *C. aminovalericum* (Kawasaki et al. 2004). Its cellular NADH oxidase activity (41.6 mU/mg) was doubled after 10 min, and increased five-fold after 30 min of flushing with 3% O_2/97% N_2. NADH oxidase activity in *T. hypogea* was not inducible by the presence of oxygen, indicating it is a constitutive enzyme.

Several NADH oxidases have been characterized from thermophilic anaerobes (Table 3-3). Unlike most of the mesophilic enzymes that produce H_2O (Kawasaki et al. 2004), virtually all of the thermophilic enzymes contain an FAD cofactor and catalyze the reduction of oxygen to H_2O_2, and they have apparent K_m values for NADH and oxygen from 4 to 130 μM and 60 to 2,900 μM, respectively. NADH oxidase from *T. hypogea* had all the common features of this type of enzymes known and showed a much higher apparent V_{max} value (37 U $mg^{-1}.min^{-1}$) with a relatively low apparent K_m-value for O_2 (85 μM). The enzyme is also constitutive and stable at optimal growth temperature of 70°C, indicating it is essential in *T. hypogea*. All these features support at least one possible role of the NADH oxidase in tolerating oxygen by the anaerobic bacterium *T. hypogea*. However, a puzzle remains, which is that all types of NADH oxidases from obligate anaerobic

Table 3-3 Properties of NADH oxidases from extremely thermophilic anaerobic microorganisms

Organisms	Subunit (kDa)	Cofactor	Product of O_2-reduction	Apparent K_m (μM)		Apparent V_{max} ($U.mg^{-1}.min^{-1}$)	Ref.
				NADH	O_2		
A. fulgidus NoxA-1	48 α_2	FAD	H_2O_2	130	60	8.7	Kengen et al. 2003
A. fulgidus NoxB-1	69 α	FAD	H_2O_2	11	2900	4.1	Kengen et al. 2003
P. furiosus	50 α_2	FAD	H_2O_2/ H_2O	<4	>110	13.3	Ward et al. 2001
T. hypogea	50 α_2	FAD	H_2O_2	7.5	85	37	Yang and Ma 2005a

microorganisms produce H_2O_2 (Herles et al. 2002; Kengen et al. 2003; Maeda et al. 1992; Ward et al. 2001), a more harmful species than O_2. It seems inconsistent with the possible role of the enzyme in detoxification of oxygen. Therefore, it would only make sense if the H_2O_2 generated could be further reduced to H_2O by other enzyme(s), such as peroxidase (Niimura et al. 2000; Toomey and Mayhew 1998). It was reported that rubrerythrin from *Pyrococcus furiosus* functioned as a peroxidase using electrons indirectly from the oxidation of NAD(P)H (Weinberg et al. 2004). *T. hypogea* may also have such an enzyme since rubrerythrin is present in other *Thermotoga* sp. In fact, the activity of peroxidase was detected in cell-free extract of *T. hypogea*, though it was lower compared to its oxidase activity. It is plausible to assume that accidentally encountered O_2 can be reduced by both oxidase and peroxidase to water using NADH as electron donor. Since both activities appeared not to be high and O_2 was reduced to water only when the O_2-level was low (Table 3-1), it seems to be consistent with its lower capacity of scavenging the O_2 encountered (< 5 μM). However, more studies are required to further determine and confirm physiological roles of the NADH oxidase in this strictly anaerobic microorganism.

Since the purified NADH oxidase was extremely stable and catalyzed the formation of H_2O_2 exclusively at a very high rate, it may have application as a biosensor acting as a mediator between a dehydrogenase and an electrode (Liu et al. 1999). A k_{cat}/K_m-value for the *T. hypogea* enzyme is calculated as 4.1 x 10^6 $M^{-1}.s^{-1}$, which is higher than the value reported for the NADH oxidase of *Thermus thermophilus* (k_{cat}/K_m = 2.3 x 10^6 $M^{-1}.s^{-1}$) (Park et al. 1992). Potential applications of this enzyme are worthy of further exploration.

NADH-oxygen reaction by NADH oxidases *in vitro* may occur due to the lack of protection of flavin portion of flavoprotein. It was proposed that NADH oxidase from a thermophile, *Thermoanaerobium brokii* could play other roles under physiological conditions (Maeda et al. 1992). This type of NADH-utilizing flavoproteins may transfer electrons to acceptors other than oxygen. Therefore, it is also reasonable to speculate that the NADH oxidase in *T. hypogea* may play other roles *in vivo*. It was found that *T. hypogea* NADH oxidase indeed was able to use other electron acceptor other than oxygen, dihydrolipoamide. The dihydrolipoamide dehydrogenase activity of *T. hypogea* NADH oxidase was investigated and its properties are reported in Chapter 5 of this thesis.

Chapter 4 A Highly Active NADH Oxidase from Anaerobic Hyperthermophilic Bacterium *Thermotoga maritima*

Part of the work described in this chapter was published in Journal of Bacteriology.
Yang X. and K. Ma. 2007. Characterization of an exceedingly active NADH oxidase from the anaerobic hyperthermophilic bacterium *Thermotoga maritima*. J. Bacteriol. 189:3312-3317.

4.1 ABSTRACT

Thermotoga maritima is an anaerobic bacterium capable of growing at 90°C. It was found that *T. maritima* could grow in the presence of oxygen (up to 5.5 μM) and had a high activity of NADH oxidase. The NADH oxidase was purified from *T. maritima* cells using a FPLC system. The purified enzyme was a heterodimeric flavoprotein with molecular weights of 54 kDa and 46 kDa respectively, which were revealed by SDS-PAGE. The enzyme catalyzed the reduction of oxygen to hydrogen peroxide exclusively using NADH specifically as electron donor. It exhibited an optimal pH between 7.0 and 7.5 and an optimal temperature of 80^{o}C. The catalytic properties of *T. maritima* NADH oxidase showed characteristics of Michaelis-Menten kinetics with K_m values for NADH and oxygen of 46.1 and 37.4 μM respectively, and V_{max} value of 213 U/mg calculated with SigmaPlot10. The NADH oxidase activity was the highest compared to all other known NADH oxidases from hyperthermophilic anaerobes, indicating that this enzyme may play an important role in scavenging accidentally exposed oxygen. The purified NADH oxidase could not catalyze the reduction of hydrogen peroxide, but *T. maritima* cell-free extract did so with a specific activity of 0.1 U/mg using NADH as electron donor. It can be concluded that the purified NADH oxidase is part of an oxygen-detoxification system present in the *T. maritima* cell. The NADH oxidase was oxygen sensitive, however, the inactivated enzyme was fully recovered in the presence of reducing reagent under anaerobic conditions. This reversibility of enzyme activity can be considered to have regulatory function *in vivo*.

4.2 INTRODUCTION

Thermotoga maritima is a hyperthermophilic anaerobic bacterium capable of growing at 90^{o}C. It utilizes carbohydrates and cell extracts such as yeast extract as energy and carbon sources, and produces H_2, CO_2, acetate, and lactate (Huber et al. 1986). H_2S is also produced in the presence of sulfur or sodium thiosulfate. Amino acids cannot be used as carbon, energy, and nitrogen sources for the growth of *T. maritima* (Rinker and Kelly 2000). Although oxygen is toxic and sparse in the natural habitat for anaerobes, it has been reported that some strictly anaerobic microbes including a few *Thermotogales* species could grow in the presence of micro-molar level of oxygen (Van Ooteghem et al. 2002, 2004). However, it is not clear which system is present in the cell to enable this oxygen tolerance. In addition to enzymes such as superoxide dismutase, superoxide reductase, catalase and peroxidase, NADH oxidase is considered to be an important enzyme involved in oxygen scavenging systems because of its potential to reduce transiently encountered oxygen by anaerobes (Herles et al. 2002; Kawasaki et al. 2004; Kengen et al. 2003).

NADH oxidases are flavoproteins, which react with oxygen to produce either water in a four-electron transfer process or hydrogen peroxide in a two-electron transfer process (Sakamoto et al. 1996). A H_2O_2-forming NADH oxidase from *T. hypogea* has been purified and characterized, and its catalytic properties are similar to other anaerobic hyperthermophilic NADH oxidases (Yang and Ma 2005a). The *T. hypogea* enzyme is a typical NADH oxidase that has a structure of homodimer of 50 kDa and contains one FAD per subunit. To our surprise, NADH oxidase activity in *T. maritma* cell-free extract was about six times higher than that in *T. hypogea*, indicating that a much more active NADH oxidase in *T. maritima* may have a better ability to remove accidentally encountered oxygen. The present chapter reports that a highly active NADH oxidase from *T. maritima* was purified and characterized, and physiological function of the purified enzyme is proposed to be part of an oxygen–scavenging system in the *T. maritima* cell.

4.3 MATERIALS AND METHODS

4.3.1 Organism and chemicals

T. maritima (DSM3109) was obtained from the Deutsche Sammlung von Mikroorganismen and Zellkulturen, Braunschweig, Germany. All chemicals were from commercially available products except dihydrolipoamide was prepared by reduction of *dl*-lipoamide with sodium borohydride (Patel et al. 1995; Reed et al. 1958). A suspension of 200 mg *dl*-lipoamide in 4 ml methanol and 1 ml de-ionized H_2O was cooled down by sitting on ice for 10 min and then flushed with nitrogen for 5 min. A solution of 200 mg sodium borohydride in 1 ml de-ionized H_2O was cooled down by sitting on ice for 10 min. The cooled sodium borohydride solution was added to *dl*-lipoamide suspension with 1 ml gas tight syringe. The mixture was flushed with nitrogen for 5 min and then stirred on ice until it became clear (approximately 3 hours). The solution was acidified with 1 N HCl to pH 1-2 and then extracted with chloroform for three times. The chloroform extract was combined, evaporated and dried with water pump overnight. The white powder, ~100 mg, was collected and stored in -20^{o}C till use.

4.3.2 Growth of *T. maritima*

T. maritima was cultured in a medium modified from that of Huber at 80°C (Huber at al. 1986). The medium contains (per liter) 20 g of NaCl, 1.14 g of $(NH_4)_2CO_3$, 2.0 g of KCl, 1.72 g of $MgSO_4 \cdot 6H_2O$, 1.42 g of $MgCl_2 \cdot 6H_2O$, 0.05 g of $CaCl_2 \cdot 2H_2O$, 2.5 g of yeast extract, 4.0 g of glucose, 0.5 g of KH_2PO_4, 0.05 mg of Resazurin, 10 ml of trace mineral element solution (Balch et al. 1979**)**. The pH was adjusted to pH 6.8. Cultures were grown routinely using 50 ml medium in a sealed 160 ml-serum bottle (Wheaton, Millville, N.J., USA). For determining the maximum level of oxygen tolerance, various amounts of pure oxygen were added to the gasphase of the bottles before inoculation. The culture bottles were incubated in a shaking water bath that was set at 160 rpm at 80^{o}C. The growth was monitored by direct cell count using a Petroff-Hausser counting chamber (1/400mm^2, 0.02 mm deep) and a Nikon Eclipse E600 phase contrast light microscope. For observing the effects of oxygen on the expression of NADH oxidase, *T. maritima* was grown anaerobically till late exponential phase, and various amounts of pure oxygen gas was added to separated bottles in duplicate to bring final oxygen concentrations in the gas phase to be 0, 2.5, 5.0% (v/v) respectively. All bottles were then incubated at the same temperature for another 30 min before the cells were

harvested. To test whether the increase of NADH oxidase activity in the presence of oxygen was caused by stimulating of enzyme activity or increasing enzyme expression amount, chloramphenicol was applied (Huber et al. 1986; Jiang et al. 2006). *T. maritima* was grown routinely till late log phase. Pure oxygen was added to the gas phase of the culture bottle to make 5% (v/v) final concentration. In the mean while, Chloramphenicol solution was added to bring the concentration to 100 mg/L. Control bottles were either with no chloramphenicol or oxygen added. Then all the bottles were incubated for another 30 min under the same temperature. The cells were harvested and used to prepared cell-free extract routinely. To obtain sufficient *T. maritima* cell mass for the purification of NADH oxidase, large-scale culture (15-liter) was grown routinely at 80°C.

4.3.3 Enzyme assay and protein determination

NADH oxidase was determined in a glass cuvette by monitoring O_2-dependent oxidation of NADH spectrophotometrically at 340 nm (ε_{340} = 6.22 mM^{-1} cm^{-1}) at 80 °C. The assay mixture (2 ml) contained 200 μM NADH and 100 mM air-saturated sodium phosphate buffer, pH 7.0 (Ward et al. 2001). One unit of NADH oxidase activity was defined as 1 μmol NADH oxidized per minute. When other electron acceptors were tested, different wavelengths and extinction coefficients were used to monitor the reaction and calculate the specific activities: potassium ferricyanide (ε_{420} = 1.00 mM^{-1} cm^{-1}), 2,6-dichlorophenolindophenol (DCPIP) (ε_{600} = 20 mM^{-1} cm^{-1}), DTNB (ε_{412} = 13.6 $mM^{-1}cm^{-1}$), benzyl viologen (BV; ε_{578} = 8.6 mM^{-1} cm^{-1}), cytochrome *c* (ε_{550} = 21.1 mM^{-1} cm^{-1}) (Kengen et al. 2003); methyl viologen (MV; ε_{578} = 9.7 mM^{-1} cm^{-1}) (Ma and Adams 2001); riboflavin (ε_{450} = 12.2 mM^{-1} cm^{-1}), FAD (ε_{450} = 11.3 mM^{-1} cm^{-1}), and FMN (ε_{450} = 12.2 mM^{-1} cm^{-1}) (Whitby 1953).

Other enzymes including DLDH, glutamate synthase, glutathione reductase, hydrogenase, NADH peroxidase, nitrate reductase, and sulfite reductase were measured using NADH or NAD as electron carrier depending on the direction of enzymatic reactions at 80°C. Decreasing of absorbance of NADH at 340 nm was monitored for glutamate synthase (Sodek and Silva 1977), glutathione reductase (Patel et al. 1998), NADH peroxidase (Diaz et al. 2002), nitrate reductase (Moorhead et al. 2003), and sulfite reductase (Siegel et al. 1974) under anaerobic conditions. For hydrogenase assay, both SDT-reduced MV and NADH were used as electron donors (Ma et al. 1994b). The hydrogen evolved was quantitatively determined using a gas chromatograph (Model 910, Buck Scientific, East Norwalk, CT). Hydrogen oxidation activity was tested spectrophotometrically by monitoring the H_2-

dependent reduction of BV at 578 nm or NAD^+ at 340 nm (Ma and Adams 2001). One unit of hydrogenase activity was defined as 1 μmol H_2 oxidized or produced per minute. Sarcosine dehydrogenase activity was measured by reduction of nitro blue tetrazolium (NBT) with phenazine methosulfate (PMS) being used as prior electron acceptor anaerobically (Kato et al. 2003). Sarcosine oxidase activity was measured aerobically by monitoring sarcosine-dependent production of H_2O_2, and the H_2O_2 produced was measured using the ABTS method described previously (Yang and Ma 2005b). One unit activity was defined as 1 μmol sarcosine oxidized or 1 μmol H_2O_2 produced per minute.

Peroxidase activity was determined under anaerobic conditions at 80°C using a modified method described previously (Diaz et al. 2002). Two ml assay mixture contained 100 mM phosphate buffer (pH 7.0), 0.1 mM NADH and 0.25 mM hydrogen peroxide. The hydrogen peroxide dependent oxidation of NADH was monitored at 340 nm. One unit activity was defined as 1 μmol NADH oxidized per minute. For the determination of apparent K_m of hydrogen peroxide, 0.2 mM NADH and 0-0.36 mM hydrogen peroxide were used. For the determination of apparent K_m of NADH, 0.5 mM hydrogen peroxide and 0-0.2 mM NADH were used. FNOR was determined with a modified method described previously (Ma and Adams 2001). The assay mixture contained 25 μg *T. maritima* ferredoxin, 4 μg *T. maritima* pyruvate: ferredoxin oxidoreductase (POR), 0.5 mM NAD^+, 0.4 mM CoA, 10 mM pyruvate, 2 mM $MgCl_2$, and varied amount of purified *T. maritima* NADH oxidase or Cell-free extract in pH 8.4, 100 mM EPPS buffer. The increase of absorbance at 340 nm was monitored at 80°C.

Protein concentration was determined using Bradford method with bovine serum albumin as the standard protein (Bradford 1976).

4.3.4 Enzyme purification

T. maritima cell-free extracts were prepared anaerobically using similar procedures described previously (Yang and Ma 2005a). The cell–free extract was applied at a flow rate of 4 ml/min to a DEAE-Sepharose Fast Flow column (5 x 10 cm; Amersham Biotech, Quebec, Canada) that was pre-equilibrated using buffer A [50 mM Tris-HCl, pH 7.8, 5% (v/v) glycerol, 1 mM SDT, and 1 mM DTT]. The column was eluted with a linear gradient of 0-0.3 M NaCl in buffer A at a flow rate of 4

ml/min. The NADH oxidase activity started to elute out as 0.10 M NaCl was applied to the column. The fractions with increased NADH oxidase specific activity (>4-fold of purification) were pooled together and applied to a HAP (Bio-Rad) column (2.6 x 10 cm) equilibrated with buffer A. The column was eluted with a linear KH_2PO_4 (0-0.15 M) in buffer A at a flow rate of 2 ml/min. The NADH oxidase started to elute out as 0.065 M KH_2PO_4 applied to the column. NADH oxidase activity-containing fractions were pooled together and applied to a Phenyl-Sepharose HP column (2.6 x 8 cm, Amersham Biotech, Quebec, Canada) equilibrated with 0.8 M $(NH_4)_2SO_4$ in buffer A. The column was eluted with a $(NH_4)_2SO_4$ gradient (0.8-0 M) at a flow rate of 2 ml/min. The NADH oxidase was eluted as 0.52 M $(NH_4)_2SO_4$ was applied to the column. Fractions contained high NADH oxidase activity were pooled together and concentrated by ultra filtration (Amicon Ultra filter, PM 30 membrane). The concentrated fraction (3.0 ml) was applied to a Superdex 200 column (2.6 x 60 cm, Amersham Biotech, Quebec, Canada) equilibrated with buffer A containing 100 mM KCl. The flow rate of the elution was 2 ml/min. Fractions containing high NADH oxidase activity were combined and applied to a Q-Sepharose HP column (1 x 10 cm, Amersham Biotech, Quebec, Canada) equilibrated with buffer A. The column was eluted with a linear gradient of NaCl (0-0.5 M) at a flow rate of 1.0 ml/min. NADH oxidase was eluted out as 0.25 M NaCl applied to the column. Fractions containing pure NADH oxidase as revealed by SDS-PAGE (Laemmli 1970) were stored at -20°C till use. *T. maritime* POR and ferredoxin were purified with the methods reported previously (Blamey and Adams 1994; Blamey et al. 1994).

4.4 RESULTS

4.4.1 Growth and NADH oxidase activities in the presence of oxygen

It was found that *T. maritima* could grow well in a culture bottle that was contaminated with air. Further tests confirmed that it grew in the presence of oxygen in the gas phase up to 1% (v/v) corresponding to a dissolved oxygen concentration of 5.5 μM in the medium and that no growth occurred when the oxygen concentration increased to 1.5% (v/v) corresponding to a dissolved oxygen concentration of 7.7 μM in the medium (Figure 4-1). NADH oxidase activities from cells being exposed to oxygen concentrations of 0, 2.5 and 5% (v/v) for 30 min at 80°C when the cells grew at their late log phase were determined to be 1.0, 1.4, 1.5 U/mg, respectively. When chloramphenicol was added, there was no increase of the NADH oxidase activity if exposed to oxygen (5%, v/v), and there was no change in the NADH oxidase activity if there was no exposure to oxygen. Therefore, the slight increase of the NADH oxidase activities were likely resulted from the enzyme production in response to oxygen in the growth media. The increase of the NADH oxidase activities resulted from the presence of oxygen in the growth media might be an inducible response of an oxygen detoxifying system in *T. maritima*. On the other hand, there was a fairly constant NADH oxidase activity of 1.0±0.1 U/mg from *T. maritima* cells grown in the absence of oxygen, and even with addition of cysteine HCl (0.4 g/l) and sodium thiosulfate (3.2 g/l) to the growth medium, which was used later to grow large-scale culture for obtaining sufficient cell mass for purification of the NADH oxidase.

4.4.2 Purification of *T. maritima* NADH oxidase

Cell-free extract was prepared routinely from 50 g of *T. maritima* cells, and it was loaded to a DEAE-Sepharose column, the first of five columns that were used for the purification. NADH oxidase activity was eluted out as a predominant single peak after each column, and the enzyme was purified approximately 130-fold, which indicates that this enzyme is present in the cell in a quantity slightly less than 1% (Table 4-1). It's plausible to conclude that the purified NADH oxidase was the major NADH oxidase activity present in *T. maritima* cell-free extract. The purity of the enzyme after the final column was confirmed using SDS-PAGE that revealed two types of subunits with a molecular weight of 54 and 46 kDa respectively (Figure 4-2). The native molecular weight of the purified enzyme was estimated to be 90±10 kDa using a Superdex-200 gel filtration column that was

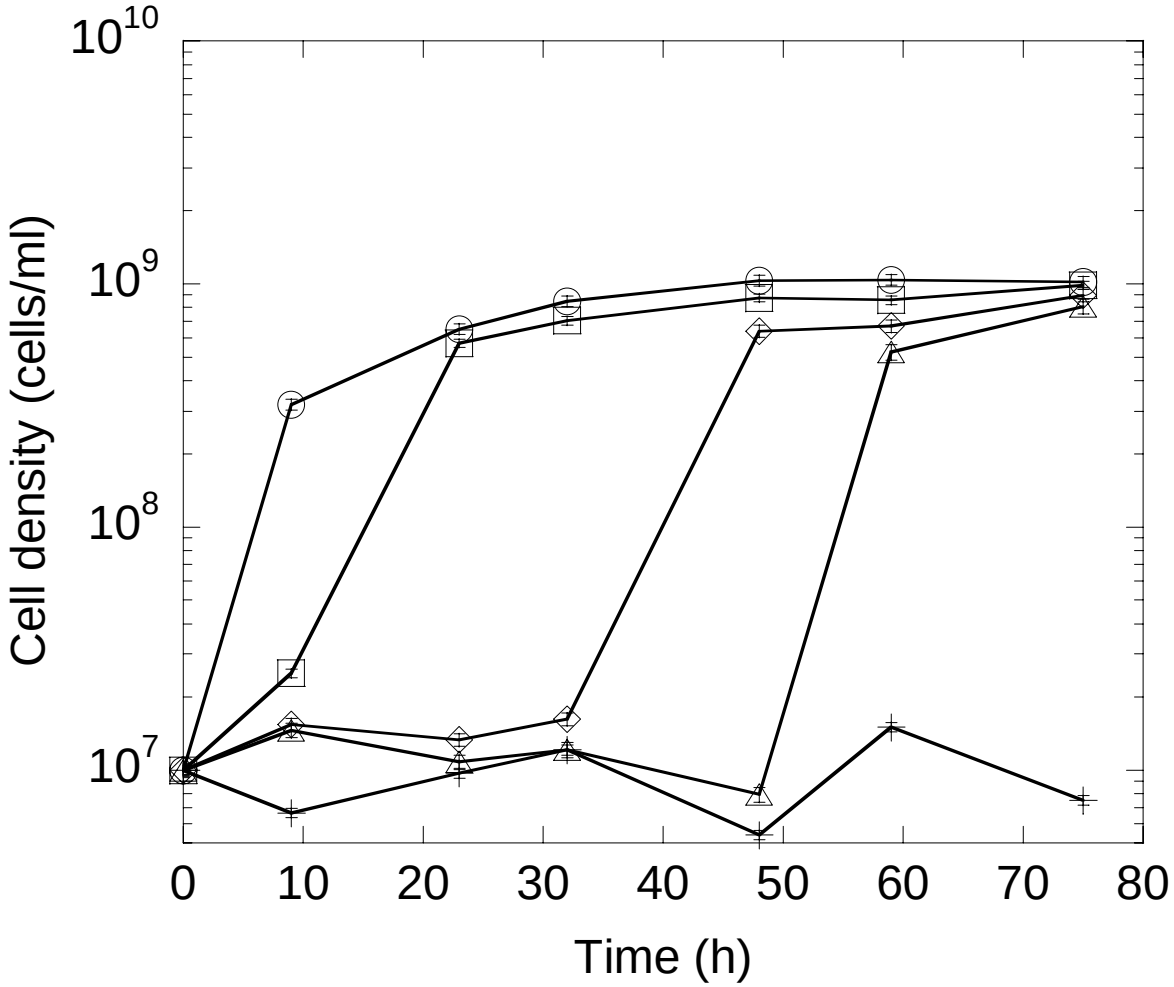

Figure 4-1 Growth of *T. maritima* in the presence of oxygen.

The experiments were carried out in sealed serum bottles with shaking (160 rpm) at 80°C with various dissolved oxygen concentrations. Open circles, without oxygen; open squares, 1.1 μM; open diamonds, 3.3 μM; open triangles, 5.5 μM; crosses, 7.7 μM.

Table 4-1 Purification of NADH oxidase from T. maritima

Steps	Total protein (mg)	Total activity (U)	Sp act (U/mg)	Purification fold	Recovery (%)
Cell-free extract	1,689	1,858	1.1	1	100
DEAE-Sepharose	401	1,502	3.8	3.5	80
HAP	138	1,003	7.2	6.5	54
Phenyl-Sepharose	13.8	678	49	45	37
Superdex 200	1.9	212	112	102	11
Q-Sepharose	0.75	108	144	131	6

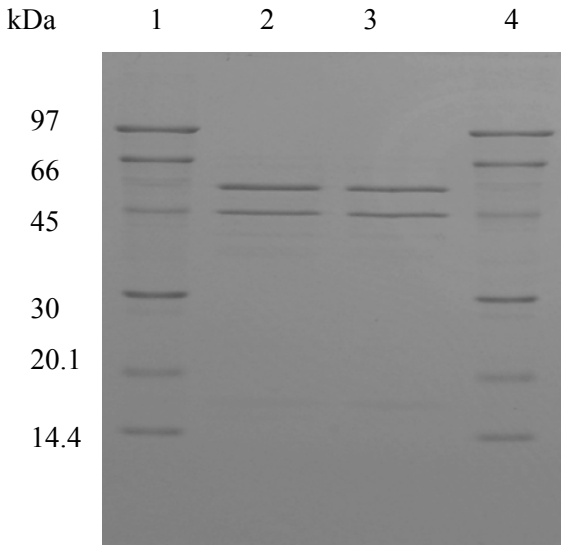

Figure 4-2 SDS-PAGE of the purified NADH oxidase from *T. maritima*.

The purified NADH oxidase (lane 2 and 3, 1.7 μg) and low molecular weight standards (lane 1 and lane 4) are indicated along with their corresponding molecular weights.

calibrated using proteins with known molecular weights. These results suggested that the purified NADH oxidase was a heterodimer, which is different from typical NADH oxidases previously characterized (Ward et al. 2001).

4.4.3 Flavin cofactor

The solution that contained the purified NADH oxidase was yellowish, which was an indication of the presence of flavin. The oxidized enzyme solution (0.25 mg in 1 ml pH 7.8, 50 mM Tris-HCl buffer) in a quartz cuvette was scanned to obtain an absorption spectrum from 190 nm to 600 nm (Varian Bio 50 UV-visible spectrophotometer). Absorbance peaks at 274, 366, and 445 nm were observed as characteristic of oxidized flavoprotein (Figure 4-3). The flavin cofactor was extracted with hot methanol and a yellowish compound was released after the enzyme mixed with methanol was boiled for 10 min in the dark (Yang and Ma 2005a). The released flavin was further identified to be FAD using thin layer chromatography by co-migrating with commercially available FAD, FMN, and riboflavin as standards (Figure 4-4). The NADH oxidase contained 1.9±0.1 mol of FAD per mol native enzyme based on the absorbance value at 450 nm and protein amount from which the FAD was extracted.

4.4.4 Catalytic properties of the purified NADH oxidase

All NADH oxidases can be classified into two categories: H_2O-forming or H_2O_2-forming NADH oxidases. The product of oxygen reduction is an important factor to evaluate the physiological function of NADH oxidase. Production of H_2O_2 by the purified *T. maritima* NADH oxidase was determined using the ABTS method described previously (Yang and Ma2005b).It was found that more than 94±3% of NADH oxidized was used to produce stoichiometrical H_2O_2. Therefore, it was concluded that the purified NADH oxidase from *T. maritima* catalyzed the reduction of O_2 to H_2O_2 exclusively using NADH as electron donor.

The pH dependence of the NADH oxidase activity was determined using different buffers at various pH ranges. Maximum activity was found to be between pH 7.0 and 7.5 with phosphate buffer (Figure 4-5), which is similar to the enzyme from *T. hypogea* reported (Yang and Ma 2005a). The activity of NADH oxidase from *T. maritima* increased along with the elevation of temperatures (Figure 4-6).

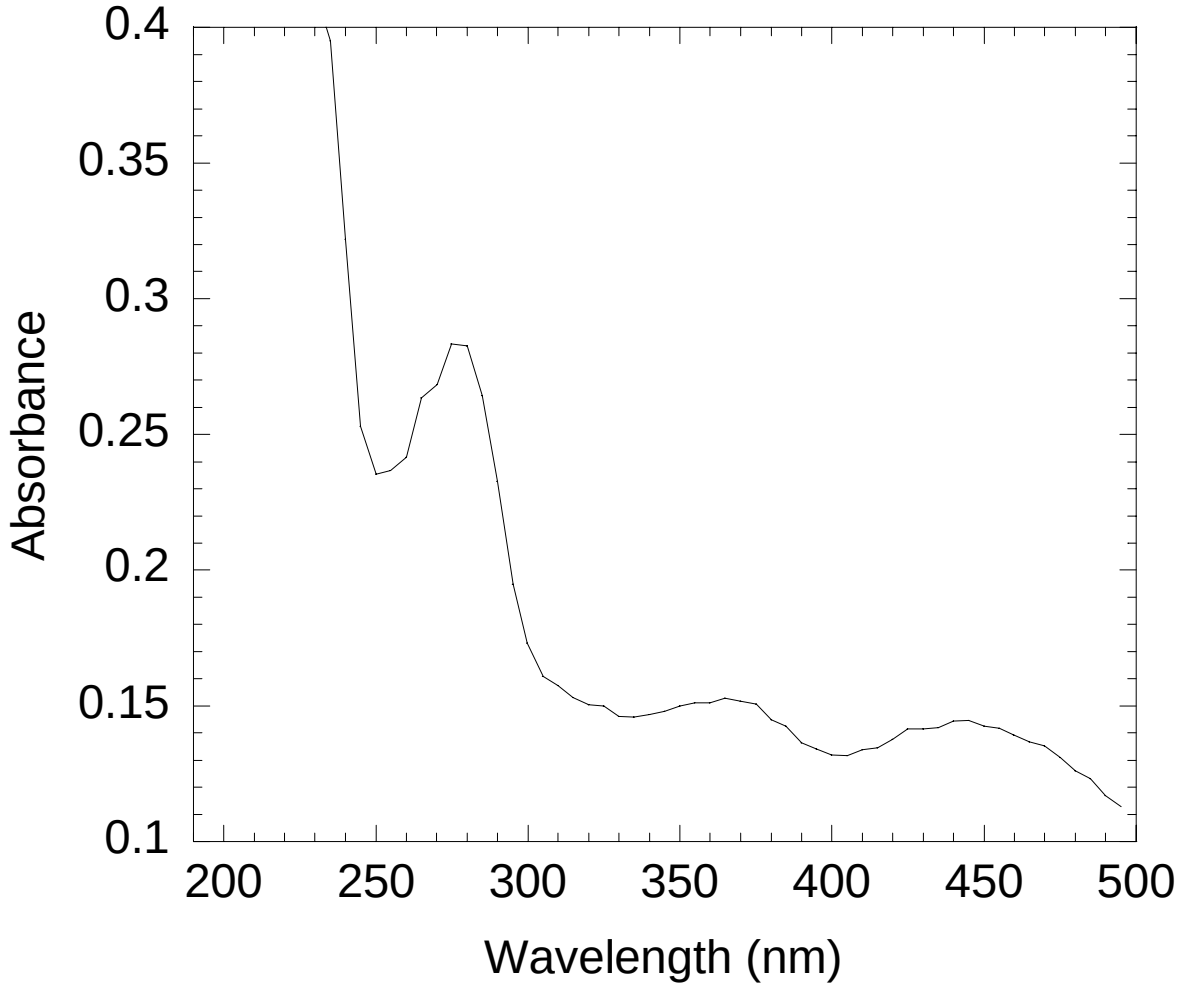

Figure 4-3 Spectrum scanning of *T. maritima* NADH oxidase.

The oxidized enzyme solution (0.25 mg in 1 ml pH 7.8, 50 mM Tris-HCl buffer) in a quartz cuvette was scanned to obtain an absorption spectrum from 190 nm to 600 nm using Varian Bio 50 UV-visible spectrophotometer.

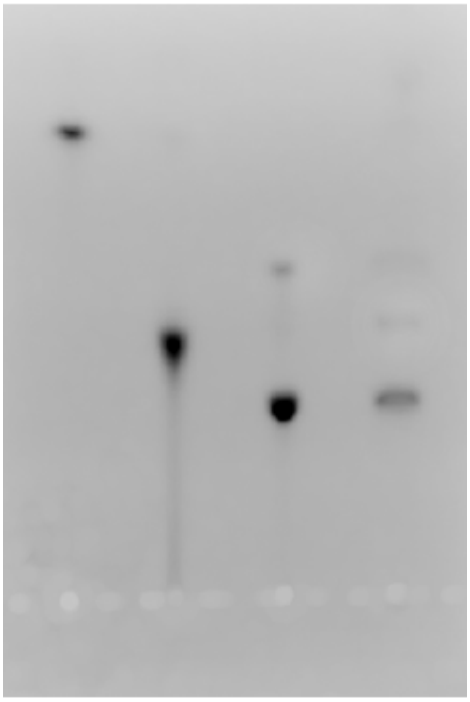

Figure 4-4 Identification of flavin cofactor of *T. maritima* NADH oxidase by thin layer chromatography.

The extracted sample from *T. maritima* NADH oxidase was ascended on thin-layer plate in dark together with commercial standards. Lane 1, riboflavin; lane 2, FMN; lane 3, FAD; lane 4, flavin extracted from the purified enzyme.

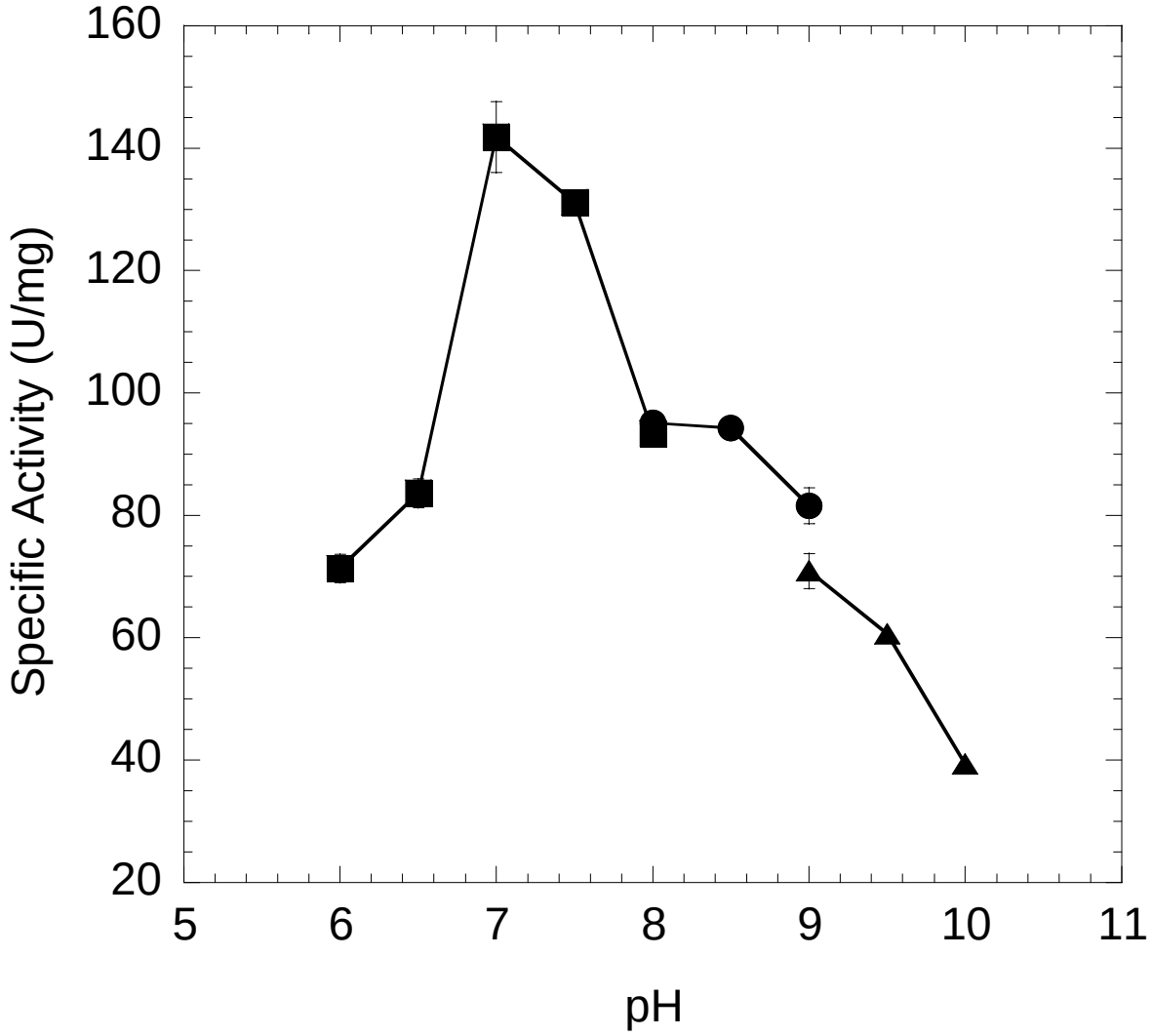

Figure 4-5 pH dependency of the purified NADH oxidase from *T. maritima*.

The enzyme activity was assayed at 80°C. Squares, 100 mM sodium phosphate buffer, pH 6.0-8.0; Circles, 100 mM glycylglycine-NaOH buffer (pH 8.0-9.0); Triangles, 100 mM glycine-NaOH buffer (9.0-10.0).

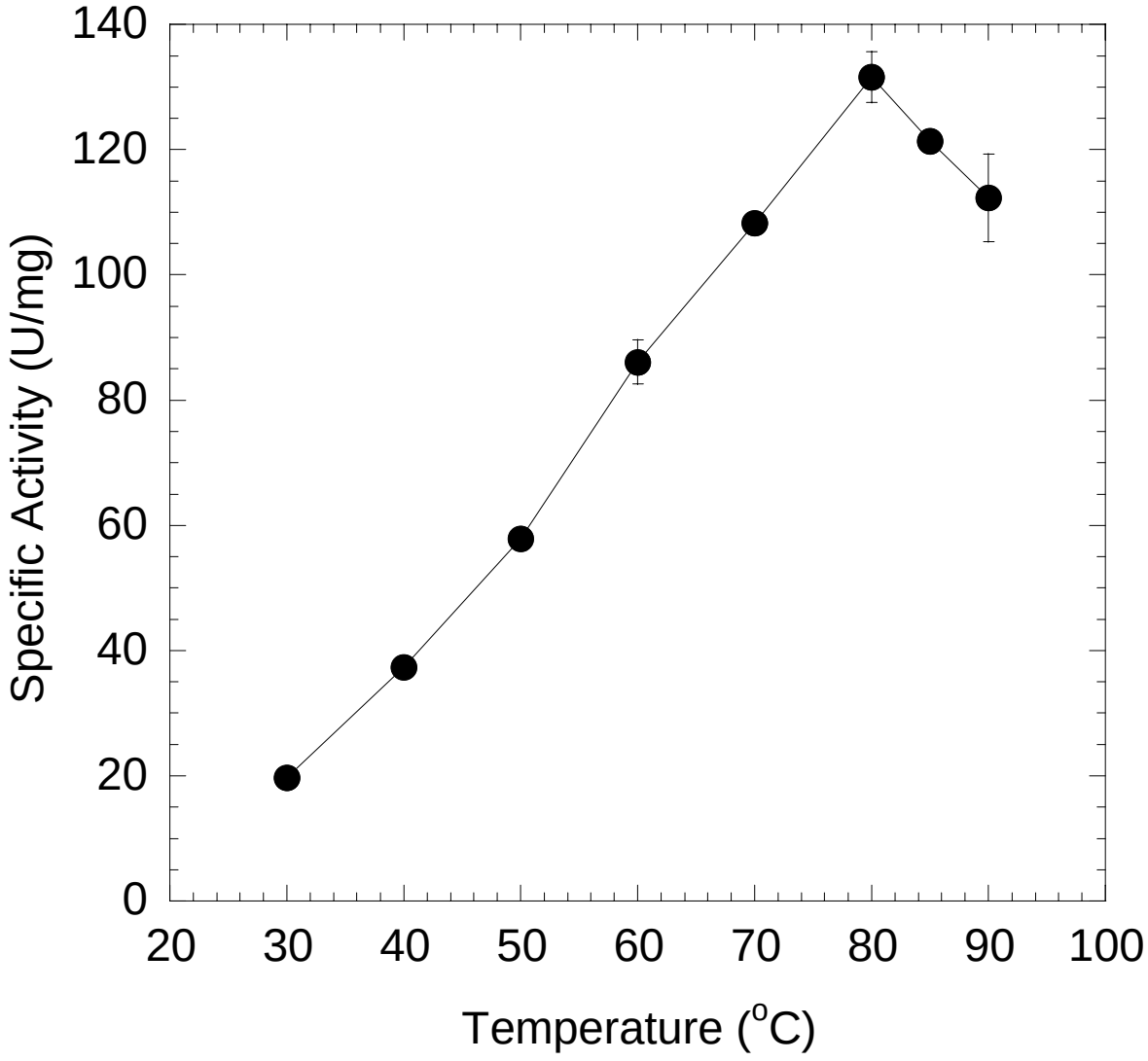

Figure 4-6 Temperature dependency of the purified NADH oxidase from *T. maritima.*

The assay was carried out same as standard assay conditions as described in section 4.2.3 with the temperature range from 30 to 90°C.

The highest activity was found to be at 80 ^{o}C, which is the optimal growth temperature for *T. maritima*. Tests for the thermostability of the enzyme were carried out at 80^{o}C and the lost of activity did not follow first order kinetics (Figure 4-7). The estimated time for the loss of 50% activity ($t_{1/2}$) was about 100 min. Kinetic parameters of NADH oxidase were determined by using specific assay systems. K_m value for NADH was determined by measuring the initial rate (within 10-20 seconds) at different concentrations of NADH (0, 0.025, 0.05, 0.1, 0.2 mM) and oxygen (0, 7.8, 16, 24, 38, 55, 103 μM) in 100 mM phosphate buffer (pH 7.0) at 80°C. The buffer used for determining K_m for oxygen was prepared by adding different amount of oxygen to stoppered glass cuvettes containing anoxic 100 mM phosphate buffer (pH 7.0) followed by vigorous shaking the cuvettes. The dissolved oxygen concentration in 100 mM phosphate buffer was estimated to be 0.086 mM at 80^{o}C when the partial pressure of oxygen was $0.2x10^5$ Pa as reported previously (Kengen et al. 2003) and this value was used for other calculations when partial pressure of oxygen varied. NADH oxidase activity was dependent on concentrations of both NADH and O_2, and the catalysis fitted Michaelis-Menten kinetics using SigmaPlot10 (Figure 4-8&Figure 4-9). Both Lineweaver-Burk plots of the NADH-dependent oxidase activities at different oxygen concentrations (7.8, 16, 24, 38, 55, 103 μM) and oxygen-dependent oxidase activities at different concentrations of NADH (0.025, 0.05, 0.1, 0.2 mM) showed parallel lines, indicating a ping-pong catalytic mechanism (Figure 4-10&Figure 4-11).The K_m values for NADH, O_2, and V_{max} value were calculated to be 46.1, 37.4 μM and 213 μmol min^{-1} mg^{-1}, respectively using SigmaPlot10 (Table 4-2). The K_m value for O_2 (37.4 μM) is the lowest among all known NADH oxidases from hyperthermophilic anaerobes (Kengen et al. 2003; Ward et al. 2001; Yang and Ma 2005a). Its low K_m value for O_2 and high specificity constant (K_{cat}/K_m) of 569,000 min^{-1} mM^{-1} may suggest that the purified NADH oxidase is very efficient at removing transiently encountered oxygen by *T. maritima*.

4.4.5 Alternative electron acceptors and donors

The purified NADH oxidase could not use NADPH as electron donor for the reduction of oxygen. It could transfer electrons from NADH to other electron acceptors under anaerobic conditions (Table 4-3). This enzyme exhibited the highest activity using O_2 as electron acceptor (140 U/mg, 100%) compared to lower activities for BV (20%) and DTNB (7%) while no activity was observed when FAD or FMN or riboflavin was used as electron acceptor. Its incapability to catalyze the reduction of external flavins is similar to that of a water-forming

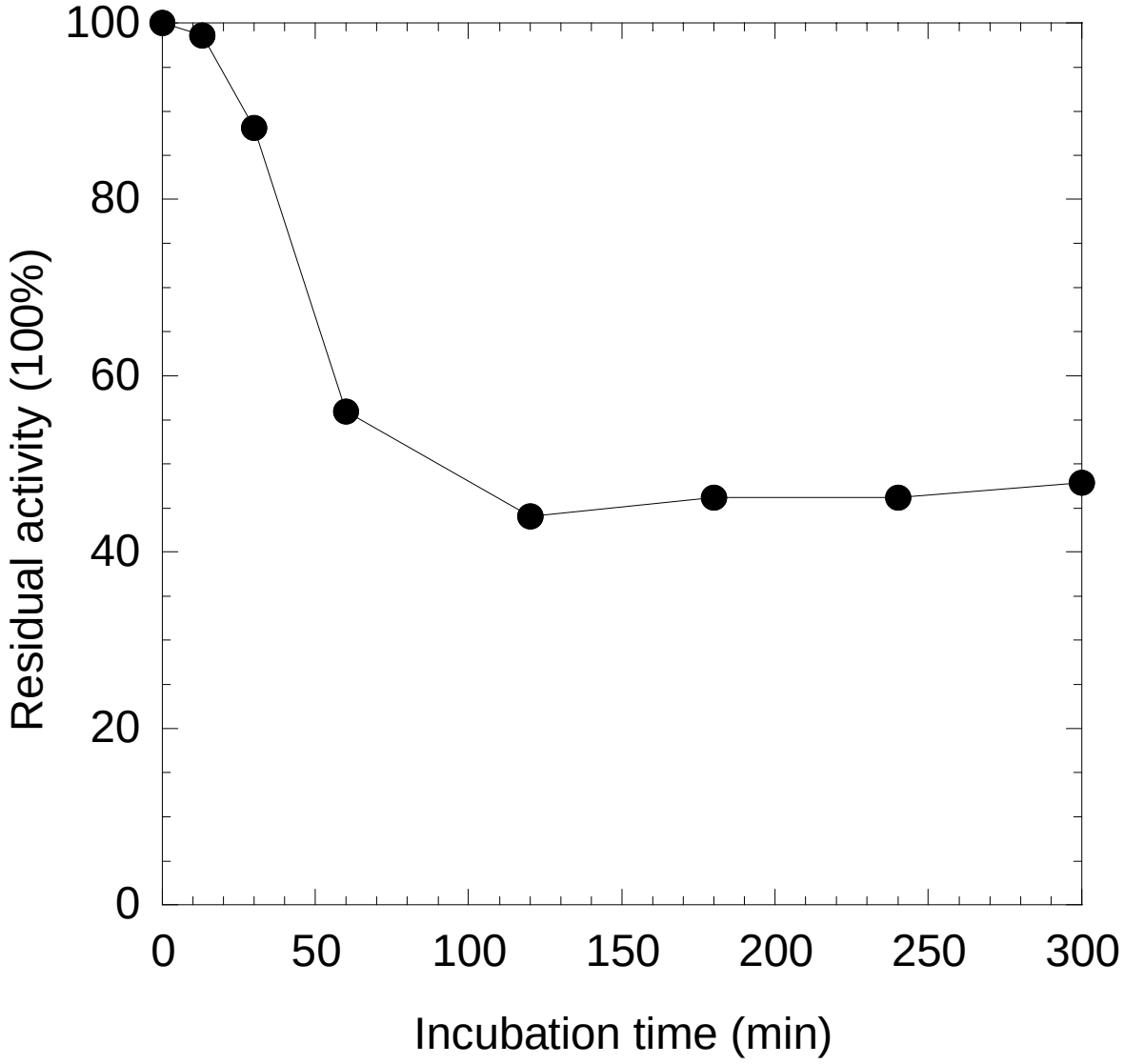

Figure 4-7 Thermostability of the purified NADH oxidase from *T. maritima*.

The purified NADH oxidase in 50 mM Tris-HCl buffer (pH 7.8) containing 5% glycerol was incubated at 80^{o}C. 100% of activity was 140 U/mg.

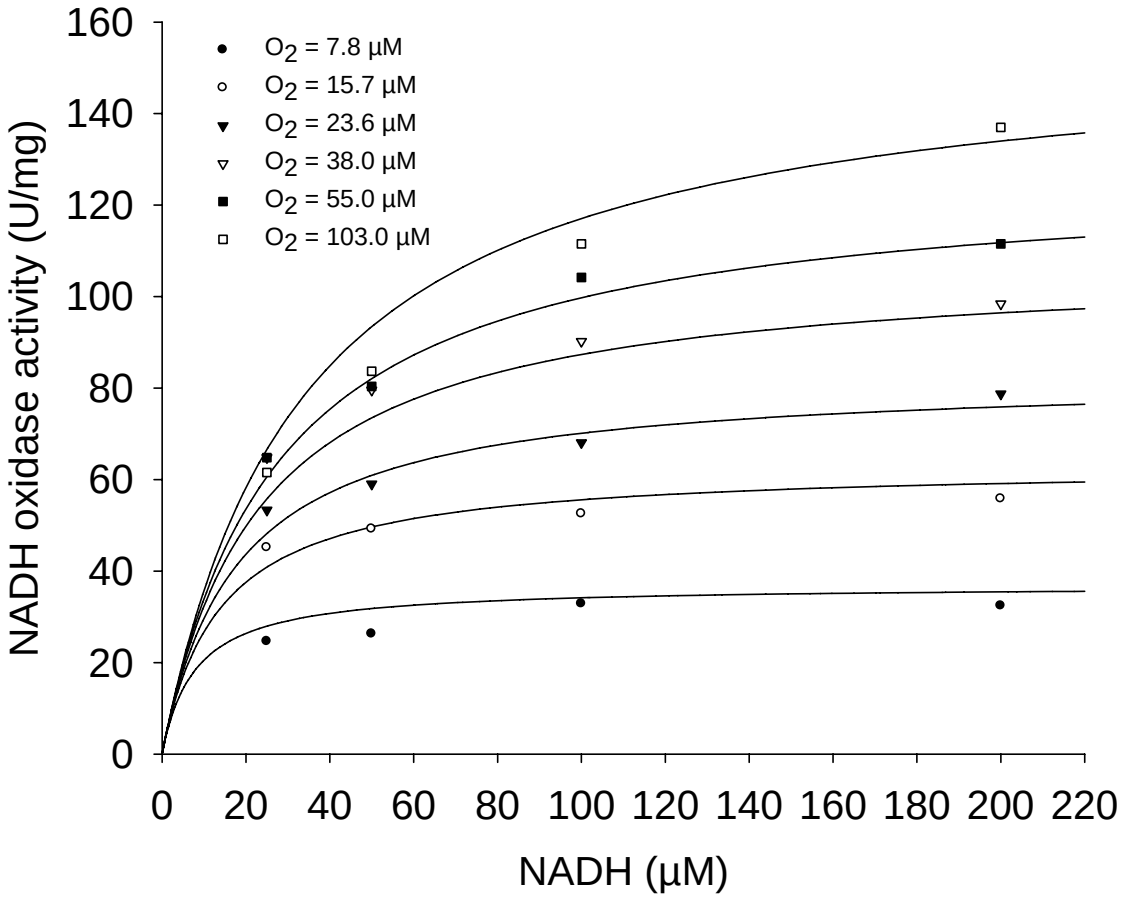

Figure 4-8 Dependency of *T. maritima* NADH activity on the concentration of NADH.

The dependency of NADH oxidase activity on the concentration of NADH was fitted to Michaelis-Menten kenetics using SigmaPlot10. O_2 was varied from 7.8 µM to 103 µM while NADH concentration was varied from 25 µM to 200 µM.

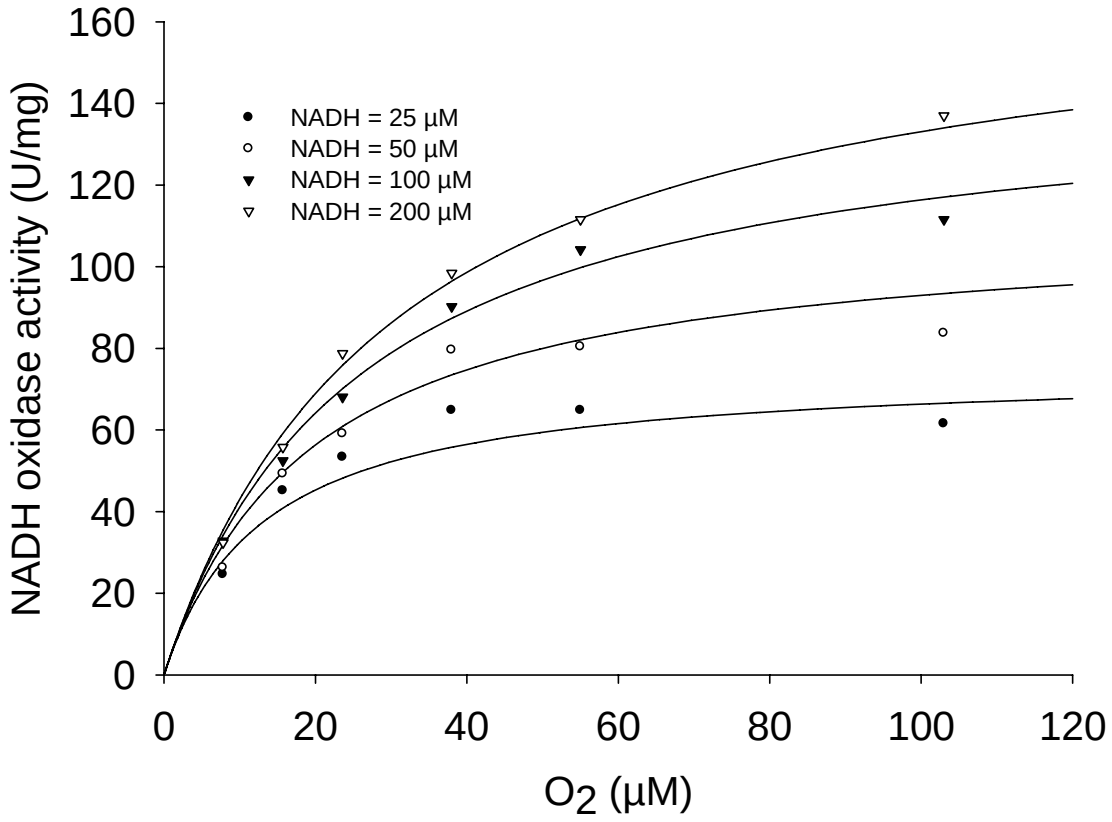

Figure 4-9 Dependency of *T. maritima* NADH activity on the concentration of O_2.

The dependency of NADH oxidase activity on the concentration of O_2 was fitted to Michaelis-Menten kenetics using SigmaPlot10. NADH concentration was varied from 25 µM to 200 µM while O_2 was varied from 7.8 µM to 103 µM.

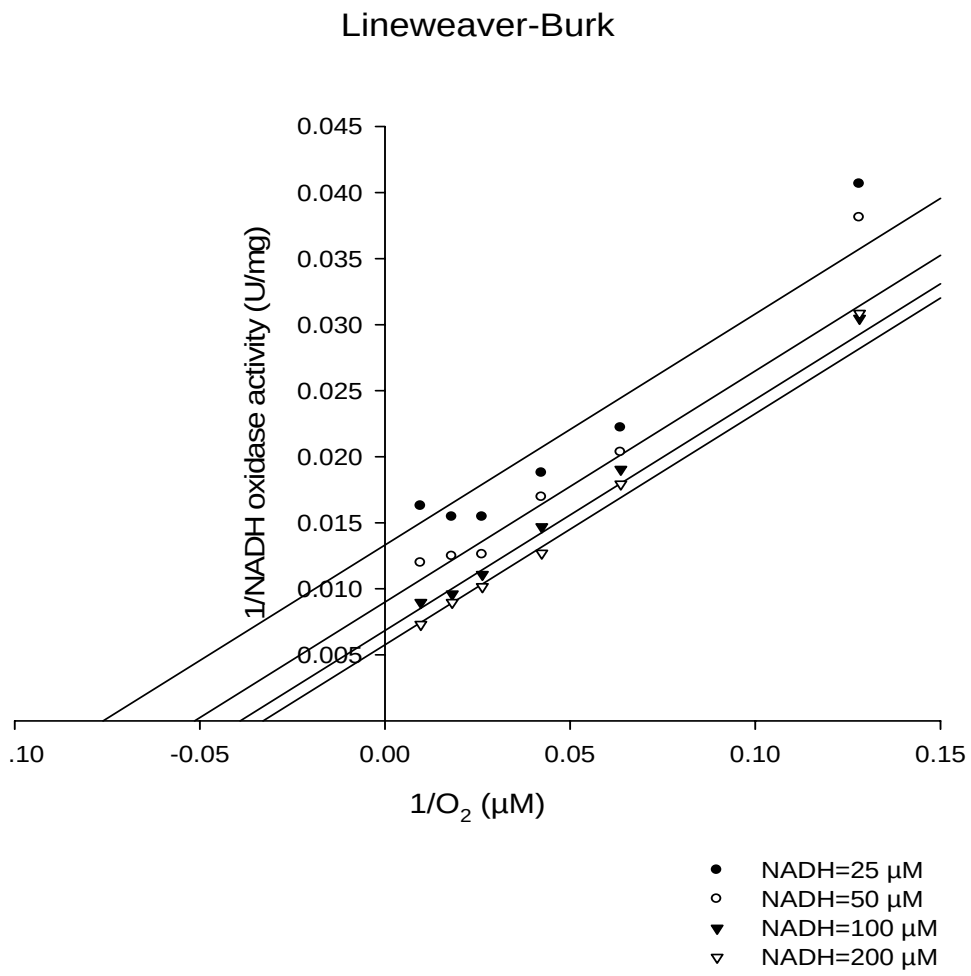

Figure 4-10 Lineweaver-Burk plots of steady kinetic analysis of *T. maritima* NADH oxidase (A).

The data in Figure 4-9 were fitted to Lineweaver-Burk kinetics using SigmaPlot10 to analyze the catalysis mechanism of *T. maritima* NADH oxidase when the concentration of O_2 was varied.

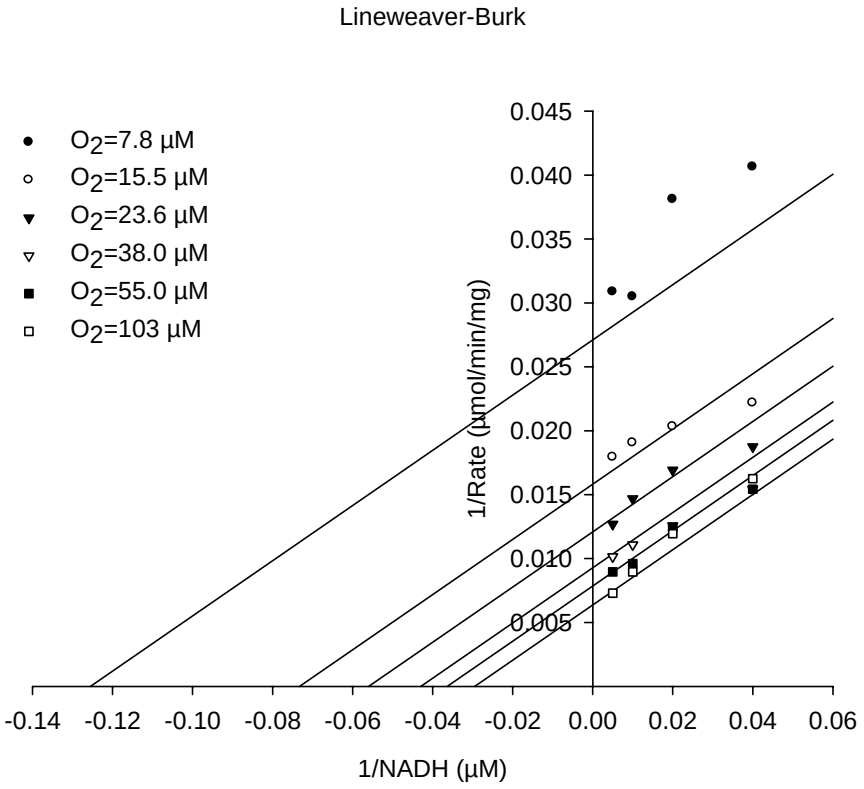

Figure 4-11 Lineweaver-Burk plots of steady kinetic analysis of *T. maritima* NADH oxidase (B).

The data in Figure 4-8 were fitted to Lineweaver-Burk kinetics using SigmaPlot10 to analyze the catalysis mechanism of *T. maritima* NADH oxidase when the concentration of NADH was varied.

Table 4-2 Kinetics parameters of the purified *T. maritima* NADH oxidase

Substrate (mM[a])	Co-substrate (mM)	K_m (mM)	k_{cat} (min^{-1})[b]	k_{cat} / K_m (min^{-1} mM^{-1})
O_2 (0-0.1)	NADH (0.2)	0.037	21,300	569,500
NADH (0-0.2)	O_2 (0-0.10)	0.046	21,300	463,000
BV (0-0.8)	NADH (0.2)	0.18	2,900	16,000
DCPIP (0-0.086)	NADH (0.2)	0.26	20,000	77,000

[a] Concentration range used to determine the kinetic constants.

[b] A molecular weight of 100,000 Da was used for the calculation of apparent k_{cat} values.

Table 4-3 Substrate specificity of the purified *T. maritima* NADH oxidase

Substrate (mM)	Redox potential (mV)[a]	Activity (%)[b]
O_2 (0.1)	+830	100
Ferricyanide (0.5)	+360	98
Cytochrome *c* (0.05)	+250	5[c]
DCPIP (0.1)	220	94
DTNB (0.1)	-40[d]	7
FMN (0.12)	-190	0
FAD (0.15)	-220	0
Riboflavin (0.05)	-222[e]	0
BV (1.0)	-350	20
Ferredoxin ($1.8x10^{-3}$)[f]	-338[g]	3
MV (1.0)	-440	10

[a] Value at 25°C from reference (Ma and Adams 1994) unless specified.

[b] 100% activity is 140 μmol of NADH oxidized per min. All assays but O_2 were carried out under anaerobic conditions (in the absence of O_2).

[c] Assay was performed at 50°C.

[d] Data from (Casero et al. 1999).

[e] Data from (Malinauskas et al. 1999).

[f] The ferredoxin purified from *T. maritima* was used in the assay for FNOR.

[g] Data from (Smith et al. 1995)

NADH oxidase from *Lactococcus lactis* (Lopez de Felipe and Hugenholtz 2001). Although DCPIP had a comparable activity with O_2 (94%), the apparent K_m value was five times higher (0.26 mM) and apparent k_{cat} /apparent K_m value was six times lower (Table 4-2). It can be concluded that O_2 is the best substrate among all tested. Although the activity was low (3% of the NADH oxidase activity), the purified *T. maritima* NADH oxidase could catalyze the reduction of NAD^+ with the POR reduced ferredoxin as electron donor.

To determine if the purified NADH oxidase from *T. maritima* had functions other than NADH oxidation with oxygen as electron acceptor, various enzyme activities were tested. The purified enzyme could not reduce H_2O_2 (NADH peroxidase), α-ketoglutaric acid plus glutamine (glutamate synthase), oxidized glutathione (glutathione reductase), H^+ (hydrogenase), sodium nitrate (nitrate reductase), and sulfite (sulfite reductase) when NADH was used as electron donor. Neither would this enzyme oxidize H_2 (hydrogenase), dihydrolipoamide (DLDH) when NAD^+ was used as electron acceptor. No activities of MV dependent hydrogenase, sarcosine dehydrogenase and sarcosine oxidase were observed. Therefore, oxygen was the only possible physiological electron acceptor identified for the purified *T. maritima* NADH oxidase.

4.4.6 Inhibition of the purified NADH oxidase

The following chemicals were tested for their effects on the activity of NADH oxidase: $HgCl_2$, $CuCl_2$, quinine, quinacrine, hydrocortisone, and NaCN. After the enzyme was pre-incubated anaerobically with the chemicals (3 mM) on ice for 1 hour, NADH oxidase activity assay was performed. The enzyme sample without addition of any of the compounds served as a control (100%). The residual activities of *T. maritima* NADH oxidase were 1.7%, 40%, 54%, 77%, 95%, and 100% when it was incubated with $HgCl_2$, $CuCl_2$, quinacrine, quinine, hydrocortisone, and NaCN, respectively.

4.4.7 Oxygen sensitivity

T. maritima NADH oxidase was purified under strictly anaerobic conditions. However, during the purification, it was found that enzyme samples exposed to air exhibited a decrease of enzyme activity. Therefore, oxygen sensitivity of the NADH oxidase was further determined for both cell-free extract

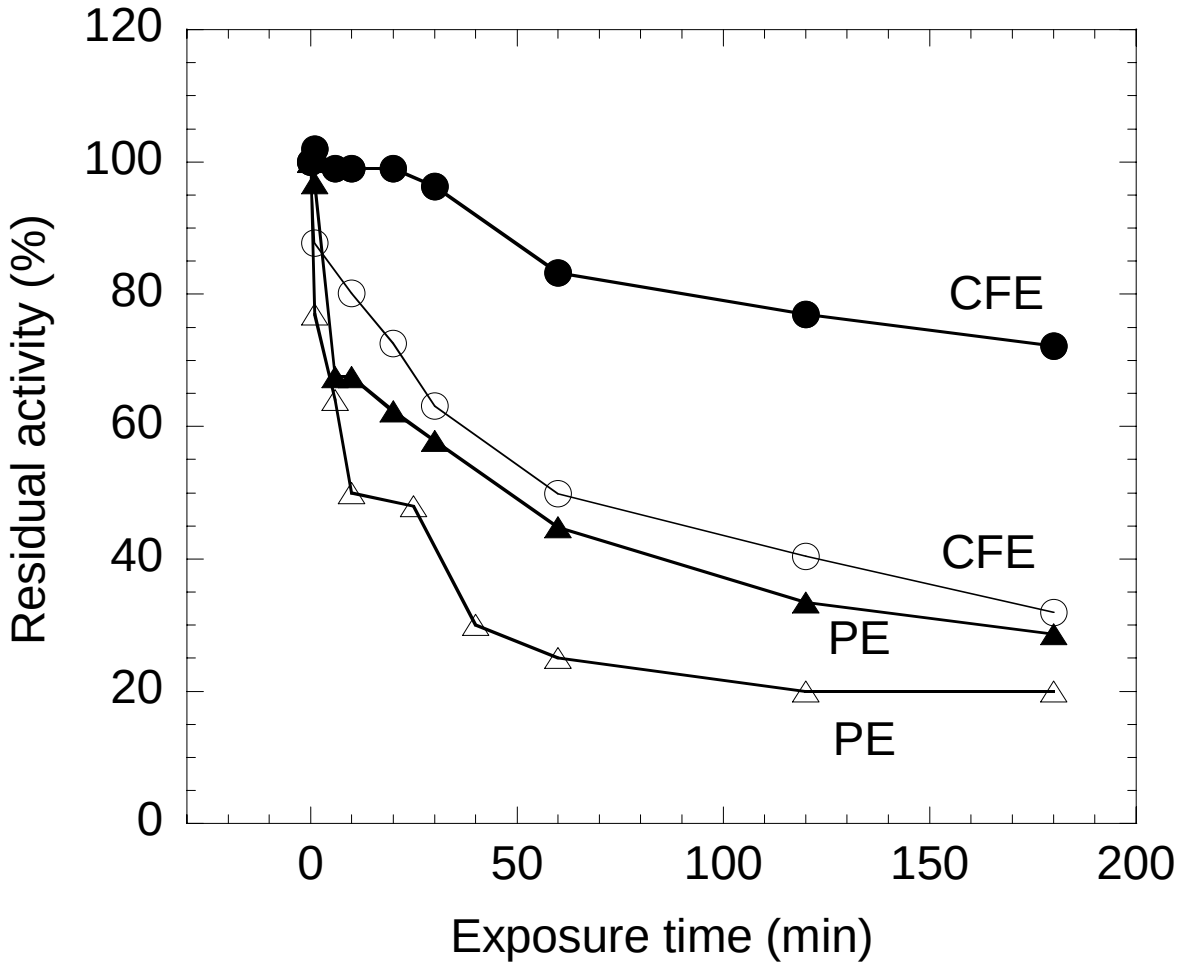

Figure 4-12 Oxygen sensitivity of NADH oxidase activities of the cell-free extract and the purified enzyme.

Filled circles, cell-free extract (CFE) exposed to 1% (v/v) of O_2; open circles, CFE exposed to 20% (v/v) of O_2; filled triangles, the purified NADH oxidase (PE) exposed to 1% (v/v) of O_2; open triangles, PE exposed to 20% (v/v) of O_2. The NADH oxidase activity assay was carried out under standard conditions. 100% of activity for cell-free extract (CFE) and the purified enzyme (PE) were 0.9 U/mg and 140 U/mg, respectively.

and the purified enzyme (Figure 4-12). The results showed that the inactivation rate of NADH oxidase activity was dependent on oxygen concentrations. The time required for the loss of 50% of the enzyme activity from the purified enzyme was about 20 min and 40 min for oxygen concentration of 20% (v/v) and 1% (v/v), respectively. However, the time required for the loss of 50% of the enzyme activity from the cell-free extract was about 60 min and 360 min for oxygen concentration of 20% (v/v) and 1% (v/v), respectively. Apparently, the enzyme in the cell-free extract was more resistant to oxygen-inactivation than the purified enzyme. There might be unknown factors present in the cell-free extract, which protected the NADH oxidase from inactivation by exposure to oxygen. These results together with the observation that there was only one predominant peak of NADH activity after each column during the purification steps, lead to a conclusion that the NADH oxidase accounting for the major activity in *T. maritima* was oxygen-sensitive, which was unexpected.

It has been showed that some inactivated oxygen-sensitive enzymes can be recovered by incubating with reducing reagents (Pan and Imlay 2001). Therefore, recoverability of the inactivated *T. maritima* NADH oxidase was achieved using reducing reagents SDT and DTT under anaerobic conditions. Either SDT (2 mM) or DTT (2 mM) could achieve only partial recovery of the inactivated enzyme (~54%). A full re-activation (100%) of the enzyme activity was achieved only in the presence of both SDT (2 mM) and DTT (2 mM). Interestingly, the recoverability for NADH oxidase activity from both purified enzyme and cell-free extract was dependent on exposure time to oxygen (Figure 4-13). There was a quick recovery of approximately 80% of the activity in the cell-free extract within 10 min incubation with SDT and DTT, and a 100% recovery of the activity required a longer incubation time (>10 hours). For the purified enzyme, it seemed that there was only a quick recovery process (within half hour) and no significant reactivation was observed after further incubation (>10 hours). However, the full activity recovery in the cell-free extract and of the purified NADH oxidase was achieved only if the exposure time to air were less than 2 hours and 0.3 hour respectively. Apparently, a longer exposure time to oxygen resulted in less recoverability (Figure 4-13). It is concluded that the purified enzyme is much more subject to oxygen damage compared to the cell-free extract, and it is not clear yet regarding mechanisms involved in both inactivation and reactivation processes.

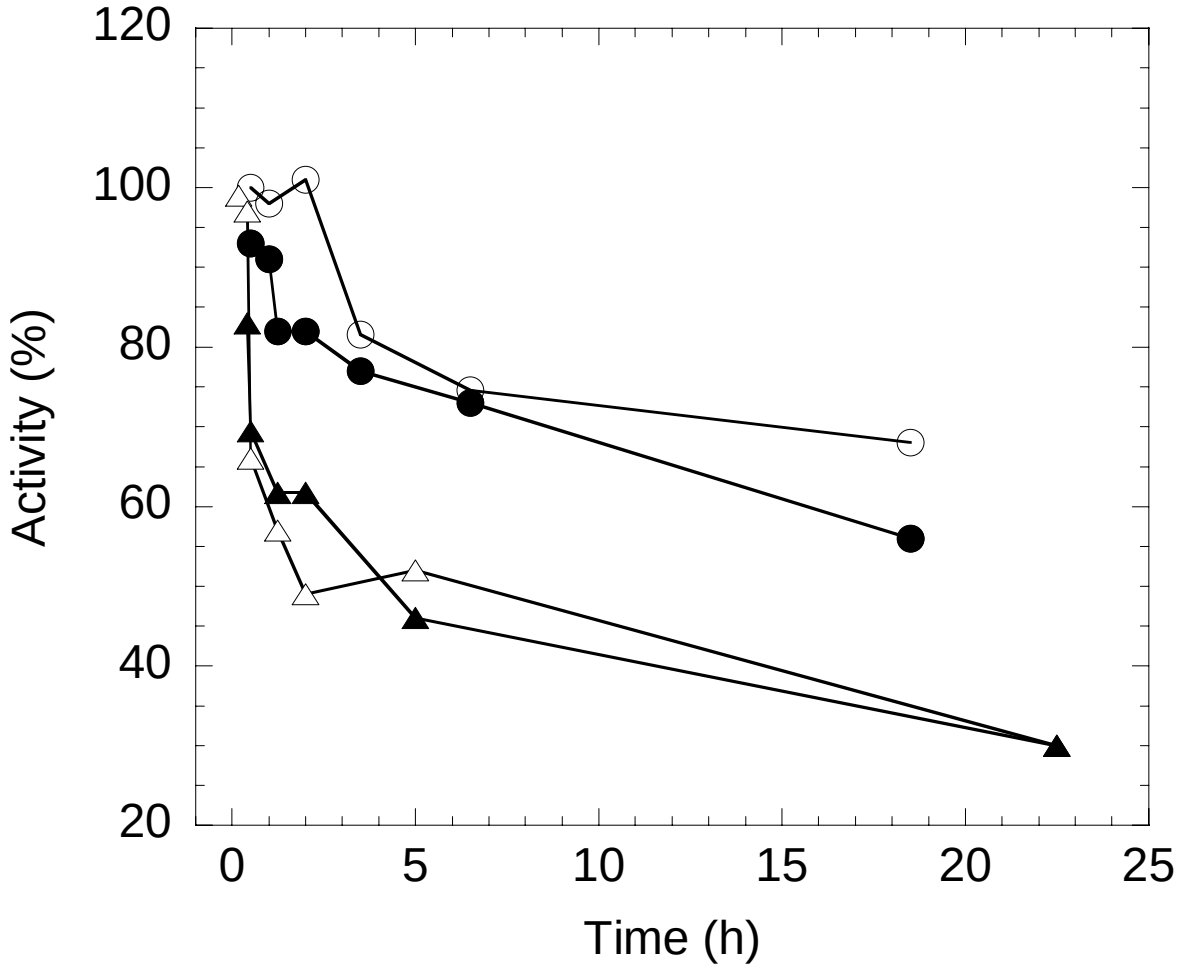

Figure 4-13 Recoverability of inactivated NADH oxidase from *T. maritima*.

Filled circles, recovered activity from cell-free extract (CFE) exposed to air with an incubation time of about 20 min in the presence of SDT and DTT; open circles, recovered activity from CFE exposed to air with an incubation time of about 20 hours in the presence of SDT and DTT. Open triangles, recovered activity from purified NADH oxidase exposed to air with an incubation time of 20 min in the presence of SDT and DTT; filled triangles, recovered activity from purified NADH oxidase exposed to air with an incubation time of about 20 hours in the presence of SDT and DTT; 100% re-activation represents a full recovery of the lost NADH oxidase activity.

4.4.8 NADH-dependent peroxidase activity in *T. maritima* cell-free extract

The purified enzyme did not have either NADH- or NADPH-dependent peroxidase activity. However, it was found that NADH-dependent peroxidase activity was present in cell-free extract of *T. maritima*. The peroxidase activity was dependent on concentrations of both NADH (0-0.2 mM) and H_2O_2 (0-0.36 mM). The catalysis followed Michaelis-Menten kinetics. Apparent K_m values for NADH and H_2O_2 were determined to be 6.5 μM and 0.25 mM, respectively. Apparent V_{max} was determined to be 0.1 U/mg, which is much lower than that of NADH oxidase activity (1 U/mg) in the cell-free extract. There was no H_2O_2 produced with a consumption of NADH up to 130±10 μmol in the presence of oxygen up to 5% (v/v) in the gas phase and 186 μg *T. maritima* cell-free extract within 5 min at 80^{o}C. However, the value of H_2O_2 produced over NADH consumed increased from 0.2±0.1% to 8.3±0.6% when oxygen concentration increased from 8 to 20% (v/v) with a consumption of NADH from 186±12 to 286±18 μmol respectively under the same assay conditions. These results showed that *T. maritima* was in principle capable of reducing oxygen completely to H_2O with no accumulation of H_2O_2 when the concentration of exposed oxygen was low.

4.5 DISCUSSION

T. maritima, an obligate anaerobe, exhibited a very high NADH oxidase activity in the cell-free extract to be 1.0 U/mg compared to 0.13 U/mg in *T. hypogea* (Yang and Ma 2005a), 0.55 U/mg in *Thermotoga neapolitana* (Yang and Ma, unpublished data), 0.29 U/mg in *Thermococcus guaymasensis* (Yang and Ma, unpublished data), 0.042 U/mg in *Clostridium aminovalercum* (Kawasaki et al. 2004), and 0.073 U/mg in *Amphibacillus xylanus* (Niimura et al. 1993). The specific activity of the purified *T. maritima* NADH oxidase is also the highest among all known hyperthermophilic enzymes (Yang and Ma 2005a). This property is consistent with the relatively higher tolerance to exposed oxygen level up to 5.5 μM for the growth of *T. maritima*.

T. maritima NADH oxidase is a flavoprotein containing non-covalently bound FAD as prosthetic group, which is a common feature of NADH oxidases. Its sensitivity to several inhibitors such as quinacrine and quinine is also similar to that of other NADH oxidases (Sakamoto et al. 1996**)**. However, unlike typical NADH oxidases, which are homodimers, *T. maritima* enzyme is a heterodimeric protein containing two subunits with molecular weights of 46 and 54 kDa respectively, which is similar to a small number of NADH oxidases with different subunits (Reinards et al. 1981), and the first of this type of NADH oxidase found in hyperthermophiles.

In contrast to most of the mesophilic enzymes that catalyze the formation of H_2O (Kawasaki et al. 2004), the purified NADH oxidase from *T. maritima* catalyzed the electron transfer from NADH to molecular oxygen and produce hydrogen peroxide exclusively, which is a distinctive property of NADH oxidases from hyperthermophilic microorganisms (Yang and Ma 2005a). No H_2O-forming NADH oxidase from this group of microbes has been reported, but a recombinant NADH oxidase from *Pyrococcus furiosus* could produce both hydrogen peroxide (77%) and water (23%) (Ward et al. 2001). The production of hydrogen peroxide remains a puzzle for all NADH oxidases from hyperthermophilic microorganisms because hydrogen peroxide, a reactive oxygen species, is obviously more toxic than molecular oxygen. If the accumulated hydrogen peroxide cannot be removed fast enough, it will produce hydroxyl radicals and cause injury of cells in the presence of redox-active metal ions such as Fe^{3+} (Rosen et al. 1995). In the case of *T. maritima*, an NADH-dependent peroxidase activity was detected in its cell free-extract. Therefore, *T. maritima* showed capability to reduce oxygen completely to H_2O. The significantly high affinity of NADH-dependent

peroxidase towards NADH (apparent K_m 6.5 μM) suggests that the hydrogen peroxide produced can be removed very efficiently. However, the low affinity towards hydrogen peroxide (apparent K_m = 0.25 mM) may result in low efficiency of this NADH-dependent peroxidase activity when hydrogen peroxide concentration becomes higher. This may provide an explanation to why *T. maritima* can only tolerate low oxygen concentration and it is still considered as an anaerobe.

Surprisingly, there is no NADH peroxidase homologue present in the genome sequence of *T. maritima* (Nelson et al. 1999). Although a possibility that new type of NADH peroxidase may not show homology to any known ones cannot be excluded, the reduction of peroxide to H_2O can be carried out alternatively by an NADH-independent peroxidase, such as rubrerythrin (Weinberg et al. 2004). In fact, there are two such peroxidase homologues, TM0657 (rubrerythrin) that may function as peroxidase similar to that in *Desulfovibrio vulgaris* (Coulter et al. 1999) and *P. furiosus* (Weinberg et al. 2004), and TM 0807 (alkyl hydroperoxide reductase Ahpc) that can be the catalytic subunit for reducing alkyl hydroperoxide or hydrogen peroxide to H_2O when other components (NADH and AhpF) are supplemented (Bryk et al. 2000). So, the oxygen removing system present in *T. maritima* may work in two steps: first, converting O_2 to hydrogen peroxide by the NADH oxidase, and secondly, reducing the hydrogen peroxide to water by rubrerythrin or akyl hydroperoxide reductase (Figure 4-14**A**). NADH may not be used directly as electron donor in the peroxidase reaction in this proposed system due to the failure to identify NADH peroxidase genes from the genome sequence (Nelson et al. 1999; Weinberg et al. 2004).

NADH oxidases from thermophilic anaerobes have apparent K_m values for NADH and O_2 from 4 - 130 μM and 60 - 2,900 μM, respectively (Yang and Ma 2005a). K_m values of *T. maritima* NADH oxidase for NADH is 46 μM that is in the middle of the range, and for O_2 is 37 μM that is lower than that of all known hyperthermophilic NADH oxidases (Yang and Ma 2005a). The extremely high apparent V_{max} value (213 U/mg) and low apparent K_m value for O_2 (37 μM) suggest that this enzyme can be very efficient to remove oxygen encountered by *T. maritima*.

The NADH oxidase activity in *T. maritima* cell-free extract lost 70-80% of activity upon incubating in the air at ambient temperature for 3 hours so did the purified enzyme with an accelerated rate (Figure 4-12). This is the first oxygen-sensitive NADH oxidase ever reported. The unexpected

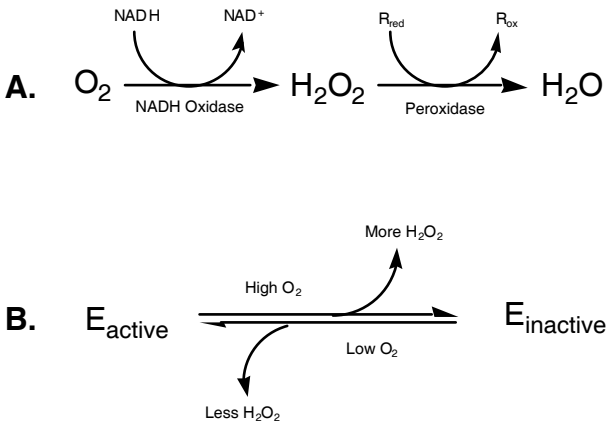

Figure 4-14 Proposed physiological function and regulatory model of the purified NADH oxidase from *T. maritima.*

A. The NADH oxidase as part of an oxygen-detoxification system in *T. maritima*. R_{red}, reduced electron carrier other than NADH; R_{ox}, oxidized electron carrier other than NAD^+. **B.** Tentative model of regulation of NADH oxidase activity depending on oxygen level and redox potential in the cell. E_{active}, active *T. maritima* NADH oxidase; $E_{inactive}$, inactivated *T. maritima* NADH oxidase; high or low, high or low concentration; more or less, arbitrary levels or amounts.

oxygen sensitivity of this enzyme seems to be contrary to the presumed function of detoxifying oxygen. However, the anaerobe *T. maritima* might benefit from the oxygen sensitivity of the NADH oxidase. As described previously, this enzyme has very high specific activity and present in the cell at high quantity. Once the cells are exposed to oxygen, the oxygen would be reduced rapidly to hydrogen peroxide, which is then reduced to water. If the hydrogen peroxide cannot be removed in a reasonable rate, it becomes more toxic than molecular oxygen (Rosen at el. 1995). Since the peroxidase activity (0.1 U/mg) is much lower than the NADH oxidase (1 U/mg), hydrogen peroxide produced could be accumulated at a level which would damage the cells. By inactivating a certain amount of the NADH oxidase only when oxygen concentration is too high, *T. maritima* may regulate the concentration of hydrogen peroxide at a low level to minimize oxidative damage caused by high concentration of hydrogen peroxide accumulated. The growth of *T. maritima* had a long lag-phase (near 45 hours, Figure 4-1) in the presence of 5.5 μM dissolved oxygen in the medium, however, there was no growth when dissolved oxygen concentration increased to 7.7 μM. Apparently, *T. maritima* can only tolerate a lower level of oxygen. As reported previously by Fucci, substrate concentration of glutamine synthetase in *Escherichia coli* plays important role in the regulation of enzyme inactivation and consequently in the enzyme turnover (Fucci et al. 1983). It is important to point out that the inactivated *T. maritima* NADH oxidase can be fully activated upon incubation with SDT and DTT (Figure 4-13), therefore, it is reasonable to speculate that such inactivated enzyme would be fully activated when low redox potential in the cells returns or the concentrations of oxygen and hydrogen peroxide become low (Figure 4-14**B**). If the oxygen level is too high, the proposed oxygen-scavenging system fails and no growth occurs. To obtain more detailed information about how the redox potential and concentrations of oxygen and hydrogen peroxide affect the NADH oxidase activity *in vivo*, further investigation is required. On the other hands, it was proposed that NADH oxidase from *Thermoanaerobium brokii* may play other roles under physiological conditions (Maeda et al. 1992). These NADH-utilizing flavoproteins may transfer electrons to acceptors other than molecular oxygen. Therefore, it is probably reasonable to speculate that the purified NADH oxidase in *T. maritima* might play other roles *in vivo*. Electron acceptor for *T. maritima* NADH oxidase was extensively studied. It was found that this enzyme was able to use *sn*-glycerol-3-phosphate as subsrate and therefore exhibited glycerol-3-phosphate dehydrogenase activity, which is reported in Chapter 6 of this thesis.

Chapter 5 Dihydrolipoamide Dehydrogenase of *Thermotoga hypogea*

A manuscript has been prepared for submission based on the work presented in this chapter.

5.1 ABSTRACT

Thermotoga hypogea is an extremely thermophilic anaerobic bacterium capable of growing at 90°C. It was found that dihydrolipoamide dehydrogenase (DLDH) activity was overlapped and proportional to NADH oxidase activity during all steps of purification. The purified enzyme revealed as a single band on SDS-PAGE exhibited both DLDH and NADH oxidase activities. The NADH oxidase activity of this enzyme was previously desribed in Chapter 3 of the thesis. The purified enzyme exhibited a specific DLDH activity of 180 U/mg in dihydrolipoamide oxidation. It used NAD(H) as electron carrier exclusively. When DLDH catalyzed the forward reaction, the oxidation of dihydrolipoamide, the catalysis that was analyzed with SigmaPlot10 followed Michealis-Menten kinetics. The apparent K_m values for NAD^+ and dihydrolipoamide were determined to be 0.30 mM and 0.80 mM, respectively. In the reduction of lipoamide by NADH, it showed apparent inhibition by higher concentration of NADH, which is one of the typical properties of DLDH. The inhibition of NADH was fitted to Hanes-Woolf plot using SigmaPlot10. The K_i value for NADH was estimated to be 57.6 μM, which was lower than K_m value of NADH, 79.8 μM. In addition to use lipoic acid, lipoamide, and dihydrolipoamide as substrate, *T. hypogea* DLDH could catalyze the reduction of various artificial electron acceptors using NADH as electron donor. The purified DLDH was partially sequenced by mass spectrometry. The peptide sequences significantly matched other DLDH sequences, especially within *Thermotogales* order in the BLAST search. The partial sequence of *T. hypogea* DLDH was found to be closely related to the other three sequences of DLDHs from *Thermotogales* whose genome sequences are known. *T. hypogea* DLDH is the first one that has been characterized from anaerobic hyperthermophilic sources. Further sequence analysis showed that all species with genome sequences known in *Thermotogales* contained genes encoding all components of glycine decarboxylase complex, but not pyruvate dehydrogenase. However, both *T. hypogea* and *T. maritima* had not been found to be able to use glycine as sole carbon source. It is speculated that the function of glycine decarboxylase complex may be involved only in contribution to one-carbon pool instead of energy metabolism.

5.2 INTRODUCTION

Thermotoga hypogea, a rod shape and strict anaerobe, was first isolated from African oil-producing well (Fardeau et al. 1997). It can tolerate up to 6.9 μM of oxygen dissolved in the growth media under static conditions and an NADH oxidase has been proposed to be functioning in the oxygen defensive system (Yang and Ma 2005a). The NADH oxidase is a homodimeric flavoprotein with subunit molecular mass of 50 kDa. During purification, it was found that dihydrolipoamide DLDH activity always stayed together with the NADH oxidase.

DLDH (EC1.8.1.4) was first isolated from pig heart (Straub 1939). It catalyzes the reversible conversion between lipoamide and dihydrolipoamide (equation 1).

$$NAD^+ + \text{dihydrolipoamide} \leftrightarrow \text{lipoamide} + NADH + H^+ \qquad (1)$$

Since then DLDHs have been purified from various sources including mitochondria of eukaryotes, aerobic mesophilic prokaryotes (Williams 1992) and also from halophilic archaeon, *Haloferax volcanii* (Vettakkorumakankav and Stevenson 1992). All the DLDHs studied are in the cytoplasm except the one from *Trypanosoma brucei*, which has been found in the purified plasma membrane (Danson et al. 1987). The DLDH from different sources is a homodimer with one FAD and one redox-active disulfide on each subunit with molecular weight of about 50 kDa (Williams 1992). The catalysis of DLDH follows ping-pong mechanism and it has been studied in significant details in mesophiles (Argyrou et al. 2003; Williams 1992). Crystal structures of DLDH from eukaryotes and bacteria have been determined (Mattevi et al. 1992; Toyoda et al. 1998a, b).

DLDH is well known as E_3 component of 2-oxo acid dehydrogenase, which is a large multienzyme complex consisting of three catalytic components: 2-oxo acid dehydrogenase (E_1), dihydrolipoamide acyltransferase (E_2), and DLDH (E_3) (de Kok et al. 1998; Neveling et al. 1998; Patel and Korotchkina 2003). Four 2-oxo acid dehydrogenase complexes are known, which are the complexes of pyruvate dehydrogenase, 2-oxoglutarate dehydrogenase, branched-chain dehydrogenase, and acetoin dehydrogenase. In most prokaryotes, these complexes share some common structural features, and E_3 is shared by different complexes (Berg and de Kok 1997; Reed 1974; Reed and Hackert 1990). 2-oxo acid dehydrogenase in all aerobic organisms splits a carbon-carbon bond of the 2-oxo acid with the

reduction of NAD^+, and acetyl-coenzyme A, CO_2 and NADH are generated, which couples the oxidative decarboxylation to energy conservation (Berg and de Kok 1997; Perham 2000). Unlike the universal distribution of 2-oxo acid dehydrogenases in mesophiles, they are replaced by POR, which do not contain DLDH component among hyperthermophilic bacteria and all archaea tested (Schönheit and Schäfer 1995). Homologues of 2-oxo acid multienzyme are present in the genome sequences of halophilic archaeon *Haloferax volcanii* but no enzymatic activity is detectable (Jolley et al. 2000; Wanner and Soppa, 2002).

DLDH is involved in another mitochondrial multienzyme complex, glycine decarboxylase multienzyme (GDC), also named as glycine-cleavage system in prokaryotes and eukaryotes (Dietrichs et al. 1990; Freudenberg et al. 1989b; Ichinohe et al. 2004). DLDH is shared by GDC and 2-oxo acid dehydrogenase (Bourguignon et al. 1996). GDC catalyzes the decarboxylation of glycine (equation 2) and consists of four proteins, P-, H-, L-, and T-proteins. P-protein is a pyridoxal phosphate dependent enzyme and catalyzes the decarboxylation of glycine in concert with H-protein. The aminomethyl group attached on H-protein is cleavaged by T-protein to form ammonia and formaldehyde or methylene-tetrahydrofolate. The reaction cycle is completed by reoxidation of H-protein and formation of NAD(P)H by L-protein, DLDH (Walker and Oliver 1986).

$$\text{Glycine} + H_4\text{folate} + NAD^+ \leftrightarrow \text{methylene-}H_4\text{folate} + NH_3 + CO_2 + \text{NADH} + H^+ \qquad (2)$$

It has been showed that some obligately anaerobic bacteria including *Eubacterium acidaminophilum* (Zindel et al. 1988) and *Clostridium* species (Barker 1981) contain GDC and can use glycine as sole fermentation substrate. The reducing equivalents generated from oxidation of glycine to CO_2 are channeled to the selenoprotein, P_A, a component of glycine reductase complex for energy conservation (Freudenberg et al. 1989b). Both enzymes, GDC and glycine reductase are essential for utilizing glycine as sole carbon source (Freudenberg et al. 1989b; Zindel et al. 1988). In addition to the involvement in glycine utilization, GDC is also very important for generating one- carbon moieties, which are essential for the biosynthesis of purine and pyrimidine nucleotide (Arinze 2005). GDC, together with serine hydroxymethltransferase (SHMT), is responsible for the inter-conversion of glycine and serine and contributes to one-carbon pool through tetrahydrofolate (Douce et al. 2001). In *Eshcherichia coli*, 15% of all carbon atoms assimilated from glucose is estimated to pass through the glycine-serine pathway (Wilson et al. 1993).

Unlike the universal distribution and extensive study of mesophilic DLDH, there has been no report about the DLDH in hyperthermophiles yet. Here, the DLDH activity of NADH oxidase and its possible physiological role in the metabolism of *Thermotogales* species are presented.

5.3 MATERIALS AND METHODS

5.3.1 Organism and chemicals

T. hypogea (DSM 11164) was obtained from the Deutsche Sammlung von Mikroorganismen and Zellkulturen GmbH, D-38124 Braunschweig, Germany. All chemicals were commercial except dihydrolipoamide which was prepared by reduction of *dl*-lipoamide with sodium borohydride (Patel et al. 1995; Reed et al. 1958). The details were described in section 4.3.1 Organism and chemicals.

5.3.2 Growth of *T. hypogea* and *T. maritima* with glycine

The ability to use glycine as sole carbon and energy source of *T. maritima* and *T. hypogea* was tested. *T. hypogea* was grown at 70^{o}C anaerobically in the medium modified from that of Fardeau (Fardeau et al. 1997). The composition of the media was described in Chapter 3 (3.3.2 Growth of *T. hypogea*). *T. maritima* was grown at 80^{o}C anaerobically in the medium modified from that of Huber (Huber et al. 1986). The composition of the media was described in Chapter 4 (4.3.2 Growth of *T. maritima*). In both media yeast extract was lowered to 1.0 g/L from 2.5 g/L and glucose was omitted (basal medium). The seed culture was prepared in the basal medium, i.e. without any carbohydrate added. Three conditions of growth were tested, basal medium, basal medium with 1.25 g/L of glucose added, and basal medium with 1.25 g/l of glycine added. The growth was monitored by direct cell count as described in Chapter 3 (3.3.2 Growth of *T. hypogea*).

5.3.3 Cell-free extract preparation and enzyme purification

Details were described in Chapter 3 (3.3.6 Enzyme purification).

5.3.4 Localization of DLDH in *T. hypogea*

Fractionation of cell-free extract of *T. hypogea* was carried out by ultracentrifugation. After each centrifugation, the supernatant and pellet were collected anaerobically and the pellet was re-suspended to its original volume (6 ml). The crude extract of *T. hypogea* (6.0 ml) was centrifuged at 20,000x*g* for 30 min. The resulting supernatant was centrifuged further at 30,000x*g* (1 hour, 10^{o}C). The supernatant obtained was centrifuged at 115,000x*g* (1 hour, 10^{o}C). DLDH activity was detected

with the samples including, cell free extract, 30,000xg supernatant, re-suspended 30,000x*g* pellet, 115,000x*g* supernatant and re-suspended 115,000x*g* pellet, to locate the enzyme.

5.3.5 Enzyme assays and protein determination

DLDH was determined spectrophotometrically at 80°C by monitoring the substrate-dependent absorbance change of NAD(H) at 340 nm (ε_{340} =6.22 $mM^{-1}cm^{-1}$; Tsai 1980). The assay mixture contained 1.2 mM NAD^+ and 1.8 mM dihydrolipoamide that was dissolved in 100% acetone for forward reaction (oxidation of dihydrolipoamide) or 200 µM NADH and 1 mM lipoamide that was prepared in 100% methanol or acetone for the reverse reaction (reduction of lipoamide) in 2 ml pH 7.0, 100 mM potassium phosphate buffer. One unit of enzyme was defined as the oxidation of 1 µmol NADH or reduction of 1 µmol NAD^+ per min. NADH oxidase assay was carried out with 100 µM NADH in the same buffer by monitoring the decrease of absorbance at 340 nm (Yang and Ma 2005a). The diaphorase activities with artificial electron acceptors were monitored anaerobically at different wavelengths and the specific activities were calculated with the extinction coefficients of BV (ε_{578} = 8.8 mM^{-1} cm^{-1}) (Kengen et al. 2003) and MV (ε_{578} = 9.7 mM^{-1} cm^{-1}) (Ma and Adams 2001). Protein concentration was determined using the Bradford method with bovine serum albumin as the standard protein (Bradford 1976).

5.3.6 Calculation of $t_{1/2}$

The thermostability of DLDH was characterized by $t_{1/2}$, the time to 50% of initial activity upon heating at 70 and 95°C. Kinetics was modeled as first order decay rates of percent initial activity. $t_{1/2}$ was calculated from relative activity over time using equation: $y=e^{-kt}$; where y=percent of residual activity, k=(ln2)/ $t_{1/2}$ and t=incubation time (Tessier et al. 1996).

5.3.7 Partial sequence of DLDH

The purified DLDH was partially sequenced using mass spectrometry. SDS-PAGE was run with the procedures described in Chapter 3 (3.3.7 Electrophoresis and molecular weight determination) except that the Coomassie Brilliant Blue R-250 staining solution was replaced by Gel-code Blue. The protein band was cut with scalpel in flowhood and mapped by Biological Mass Spectrometry Laboratory at University of Western Ontario using MS/MS method (Lange et al. 1994).

5.4 RESULTS

5.4.1 DLDH activity

Similar DLDH activities were detected in the cell-free extract of *T. hypogea* grown with either xylose (0.79±0.10 U/ mg) or glucose (0.77±0.014 U/mg) as carbon source. The activity was higher at middle (0.66±0.03 U/mg) and late log-phase (0.79±0.10 U/mg) than that at stationary phase (0.54±0.026 U/mg). DLDH activity was located in the cytoplasm of the anaerobic bacterium *T. hypogea*, since more than 97% of the activity was present in the supernatant fraction after ultracentrifugation (115,000xg, 1 h) (Table 5-1). This supernatant fraction also contained 90% of the glutamate dehydrogenase activity, a known cytoplasmic enzyme (Ma and Adams 1994; Robb et al. 1992).

5.4.2 Purification and properties of *T. hypogea* DLDH

DLDH activity was eluted as a single peak overlapped with NADH oxidase activity after each chromatographic column and proportional to NADH oxidase activity in all active fractions (Table 5-2). The enzyme was purified 264-fold after four columns. The purified enzyme revealed as a single band of 50 kDa by SDS-PAGE showed both NADH oxidase activity and DLDH activity. It has been reported that the DLDH from *Mycobacterium smegmatis* and porcine heart also demonstrate NADH oxidase activity (Grinblat et al. 1991; Igamberdiev et al. 2004; Marcinkeviciene and Blanchard 1997). *T. hypogea* DLDH, like other bacterial and mammalian DLDHs, is specific for NAD(H) and no reaction could be detected with NADP or NADPH. In addition to lipoamide (54.3±1.0 U/mg), the purified *T. hypogea* DLDH could also reduce lipoic acid (10.3±0.8 U/mg), oxygen (33.8±2.4 U/mg), BV (17.5±0.2 U/mg), and MV (2.4±0.0 U/mg) when 50 μM of NADH was used as electron donor.

The optimal pH for dihydrolipoamide oxidation and lipoamide reduction was determined to be 7.0 (Figure 5-1). It was showed that the dihydrolipoamide oxidation activity was about ten times higher than that of lipoamide reduction at pH 7.0, indicating this enzyme is more efficient in catalyzing the NADH formation in the cell. Thermoactivity and thermostability of *T. hypogea* were determined by monitoring the temperature-dependent change of dihydrolipoamide oxidation activity. The activity of the purified DLDH increased along with the elevation of temperature up to 90^{o}C (Figure 5-2). Thermostability of DLDH was carried out at 90^{o}C and 70^{o}C (Figure 5-3). The lost of activity over

Table 5-1 Cellular localization of DLDH

Enzymes	20Kxg S[a] U/ml	20Kxg P[b] U/ml	30Kxg S U/ml	30Kxg P U/ml	115Kxg S		115,Kxg P	
					U/ml	%	U/ml	%
DLDH	2.26±0.11	0.87±0.07	2.33±0.15	0.07±0.01	2.4±0.12	97	0.07±0.01	3
GDH[c]	0.41±0.03	0.36±0.03	0.44±0.32	0.03±0.01	0.41±0.03	90	0.05±0.01	10
Protein (mg/ml)	4.79±0.19	4.29±0.21	4.45±0.17	0.17±0.01	4.27±0.25		0.38±0.02	

Note:

[a] S stands for the resulting supernatant from ultracentrifugation.

[b]P stands for the pellet resulted from ultracentrifugation.

[c]GDH stands for glutamate dehydrogenase.

Table 5-2 Co-purification of DLDH and NADH oxidase

Purification steps	Total protein (mg)	DLDH activity (U)	DLDH sp act (U/mg)	NADH oxidase actvity (U)	NADH oxidase sp act (U/mg)	Ratios*
Cell-free extract	1750	1156	0.68	227	0.13	5.2
DEAE-Sepharose	320	676	2.1	154	0.48	4.4
HAP	89	458	5.15	123	1.38	3.7
Phenyl-Sepharose	15.8	233	14.7	55	3.48	4.2
Superdex 200	0.7	126	180	23.5	33.6	5.3

* Ratios stand for the ratios between the total activity of DLDH and NADH oxidase in the cell-free extract and the overlapped active fractions during purification steps.

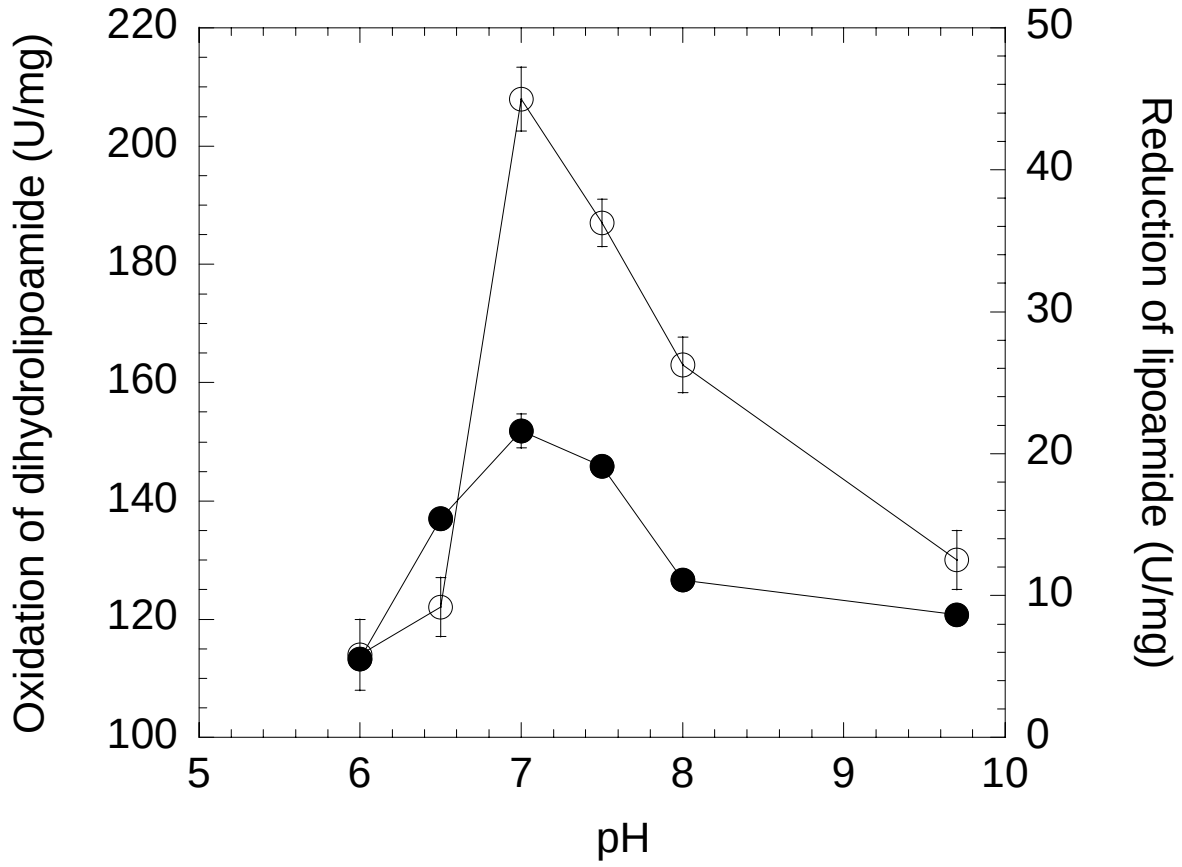

Figure 5-1 pH dependency of *T. hypogea* DLDH.

Filled circles, oxidation of dihydrolipoamide; open circles, reduction of lipoamide. All the assays were carried out using the method described in section 5.3.5.

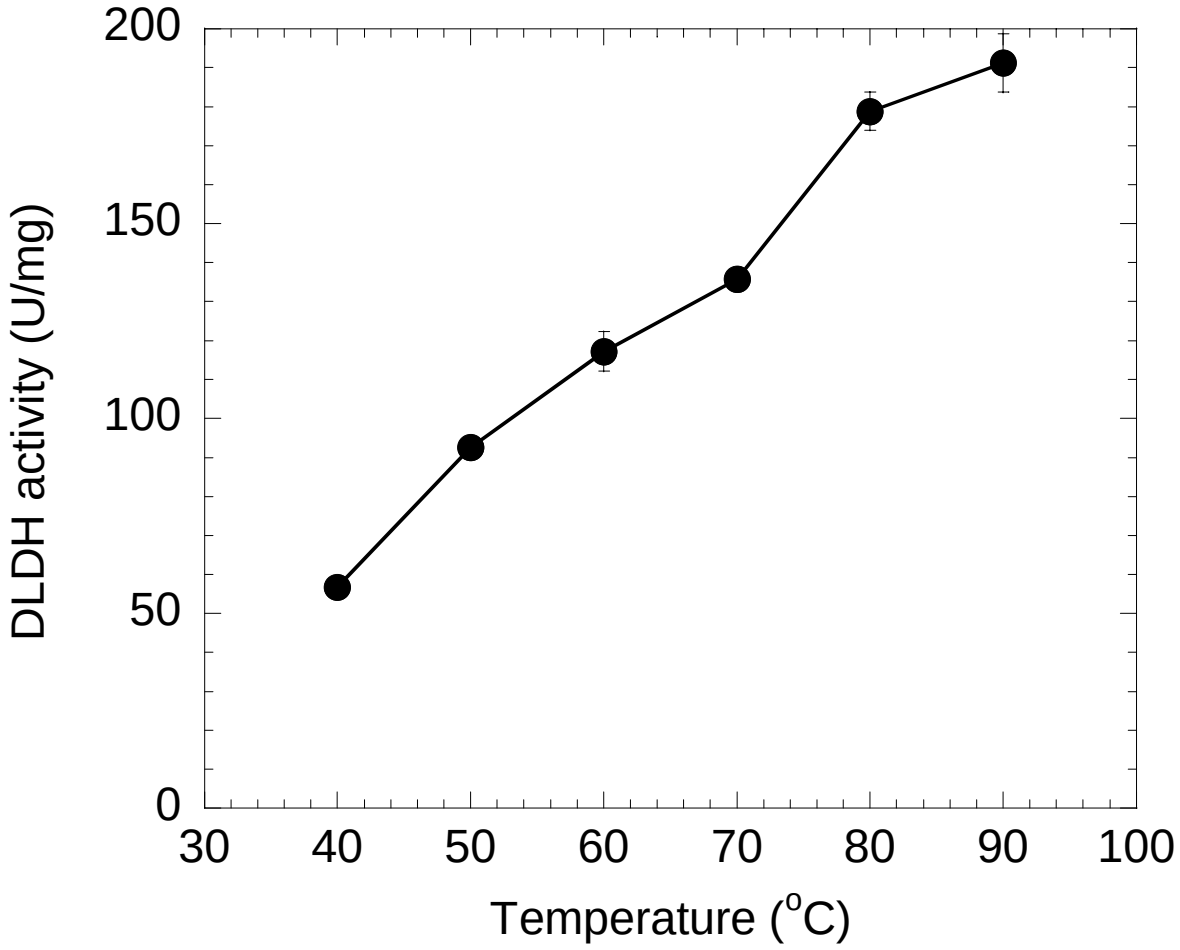

Figure 5-2 Thermoactivity of *T. hypogea* DLDH.

DLDH activity was determined by the oxidation of dihydrolipoamide by using the method described in section 5.3.5.

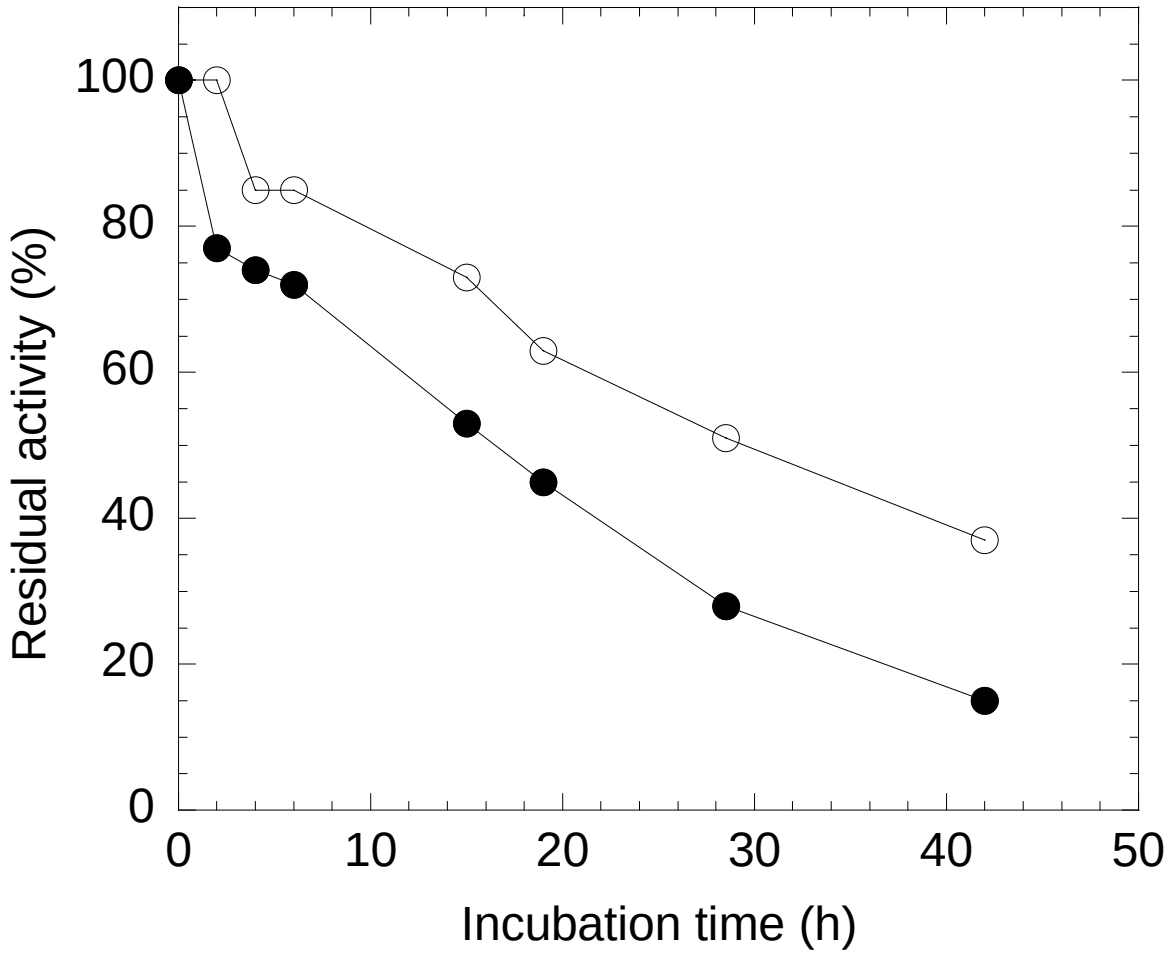

Figure 5-3 Thermostability of *T. hypogea* DLDH.

The enzyme sample (0.011 mg/ml) in a mixture containing 50 mM Tris-HCl buffer pH 7.8, 5% glycerol, 100 mM KCl, 1 mM SDT and DTT was incubated at 70^{o}C (open circles) and 90^{o}C (filled circles). DLDH activity was determined by the oxidation of dihydrolipoamide at different time intervals.

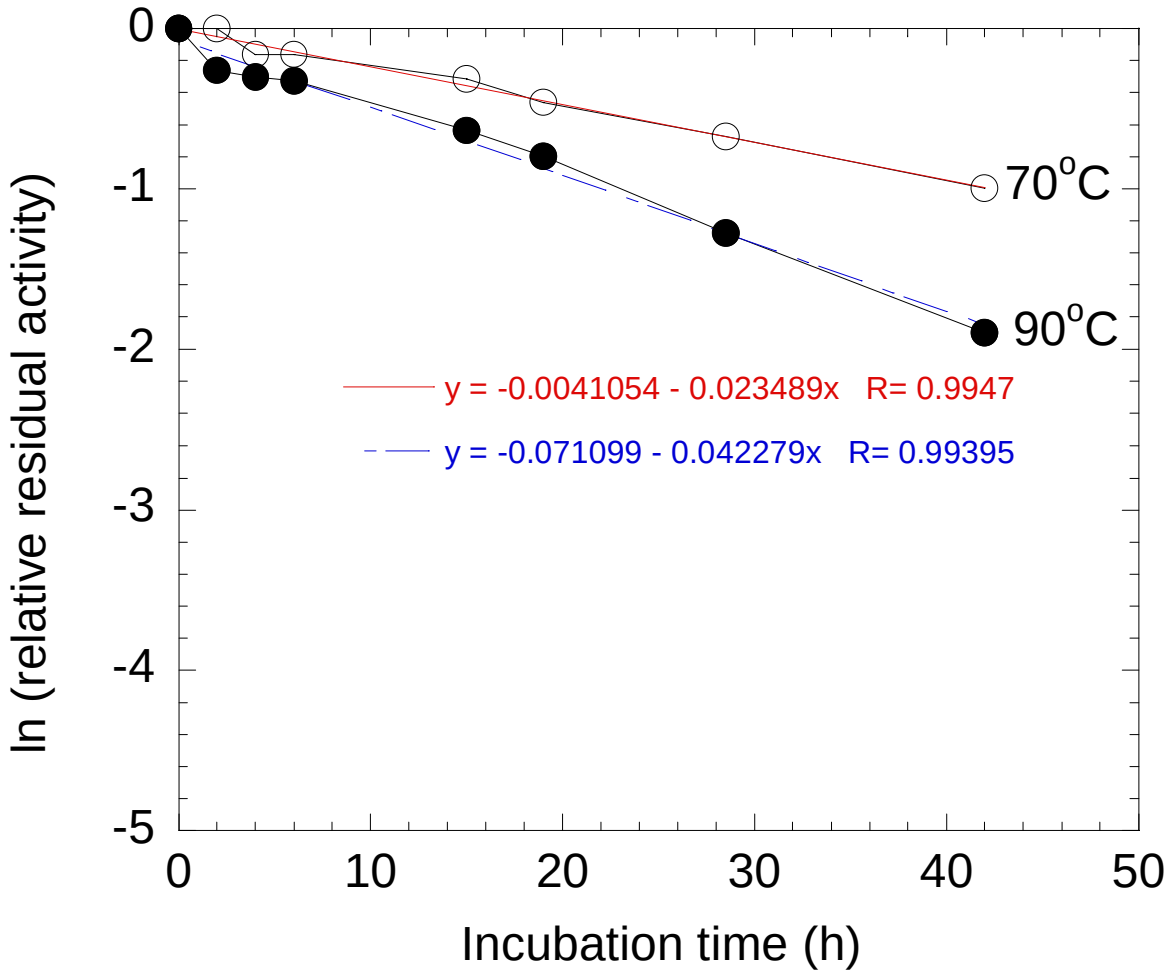

Figure 5-4 Linear plot of DLDH thermostability.

The conditions were described in the legend of Figure 5-3. Filled cirles, 90°C; open circles, 70°C.

time followed first order kinetics (Figure 5-4). The time required for a loss of 50% activity ($t_{1/2}$) was 29.5 and 16.4 hours at 70 and 90°C, respectively, indicating *T. hypogea* DLDH is very thermostable. The dependency of DLDH activity on the concentrations of substrates was determined and the data were fitted to Michaelis-Menten kinetics using SigmaPlot10. Dihydrolipoamide oxidation activity of the purified *T. hypogea* DLDH was dependent on concentrations of both NAD^+ and dihydrolipoamide. The catalysis followed Mechaelis-Menten kinetics **(**Figure 5-5&Figure 5-6). Apparent K_m value for NAD^+ and apparent V_{max} value were determined to be 0.3 mM and 226.3 U/mg, respectively. Apparent K_m value for dihydrolipoamide and apparent V_{max} value were determined to be 0.80 mM and 249.4 U/mg, respectively. The lipoamide reduction activity of the purified *T. hypogea* DLDH was dependent on the concentration of lipoamide and the catalysis followed the Michaelis-Menten kinetics (Figure 5-7). The apparent K_m value and V_{max} value were determined to be 2.2 mM and 166.7 U/mg. The lipoamide reduction activity of the purified *T. hypogea* DLDH was increased along with the increase of NADH concentration when the NADH concentration was below 100 μM, and the higher NADH concentration resulted in the decrease of its activity (Figure 5-8), which is a common feature for DLDH. It has been reported that this property is important for the regulation of the overall enzyme activity in the cell as a mechanism of feedback control (Bunik 2003; Snoep et al. 1993). The data of NADH inhibition were fiited to Hanes-Woolf kinetics (Figure 5-9). The apparent K_m and K_i values for NADH were determined to be 79.8 μM and 57.6 μM, respectively.

5.4.3 Partial sequence of *T. hypogea* DLDH

The partial amino acid sequence of the purified *T. hypogea* DLDH was obtained by mass spectrometry. The peptide-sequences were queried using blast over the entire NCBI database and they matched DLDH from different sources. The sequences showed high similarity to the gene encoding DLDH in *Thermotoga netrophila* (http://img.jgi.doe.gov/cgi-bin/pub/main.cgi?section=TaxonDetail&page=proteinCodingGenes&taxon_oid=639857041), *T. maritima* (Nelson et al. 1999), and *Thermosipho melanesiensis* (http://www.ncbi.nlm.nih.gov/entrez/query.fcgi?cmd=Retrieve&db=genome&dopt=Protein+Table&list_uids=5600). The short peptide sequences were aligned with DLDH from other *Thermotoga* species (Figure 5-10). In *T. hypogea* DLDH sequence, there is a FAD-binding motif, GXGXGG, at the N-

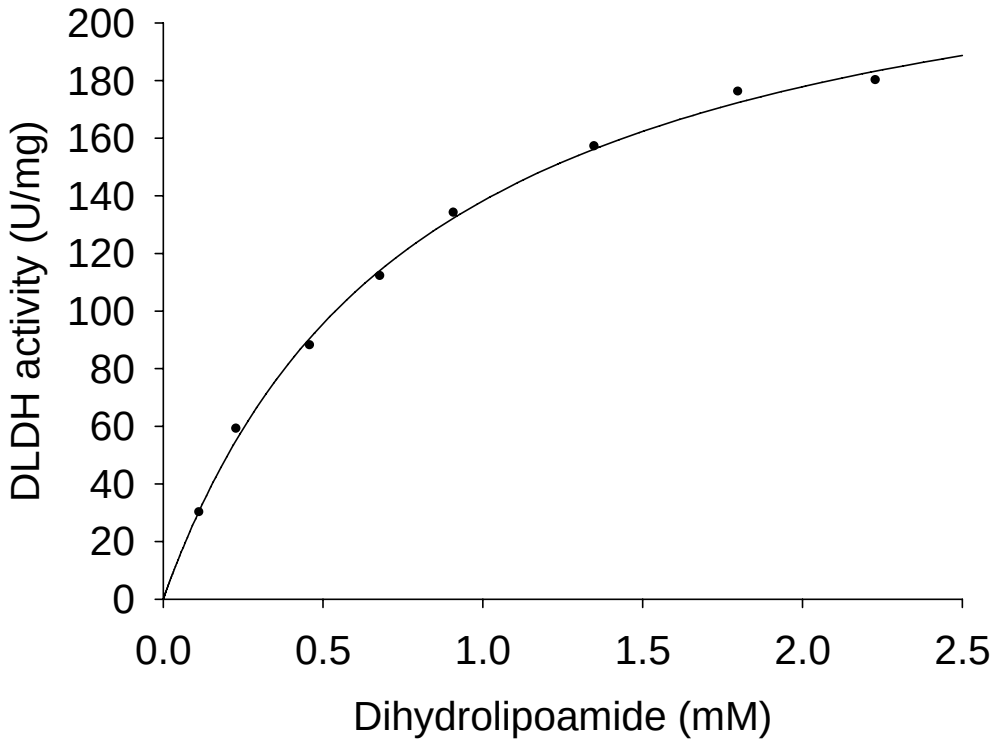

Figure 5-5 Dependency of DLDH activity on the concentration of dihydrolipoamide.

The assay was carried out at 80^{o}C with the standard assay for oxidation of dihydrolipoamide by varying the concentration of dihydrolipoamide (0-2.5 mM). The data were fitted to Michaelis-Menten kinetics by using SigmaPlot10.

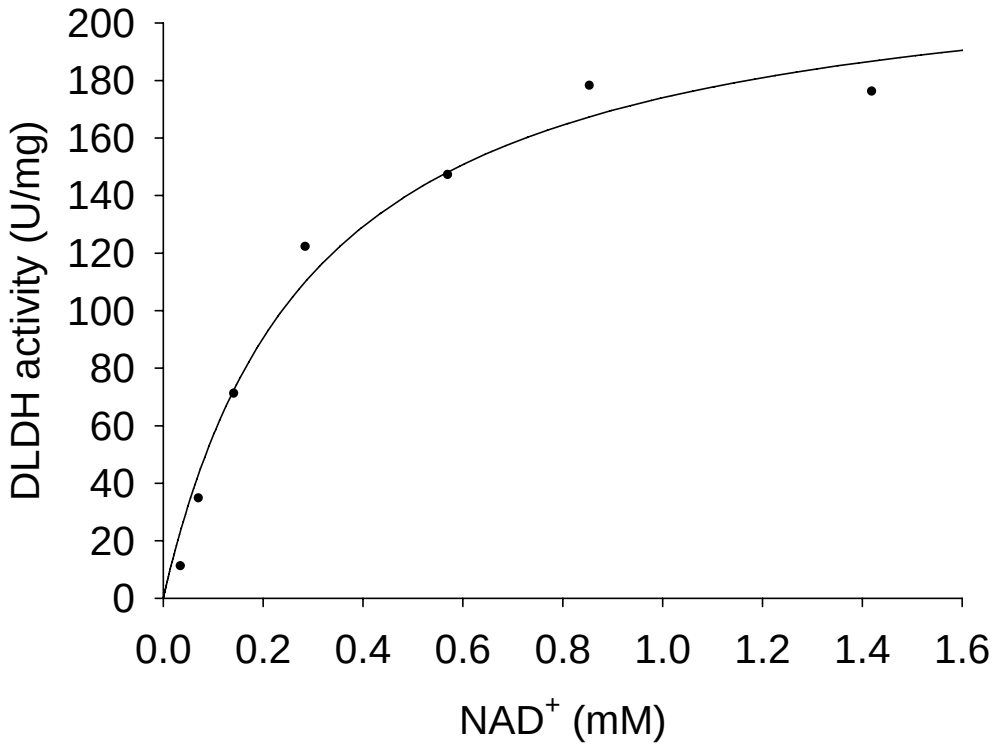

Figure 5-6 Dependency of DLDH activity on the concentration of NAD^+.

The assay was carried out at 80°C with the standard assay for oxidation of dihydrolipoamide with NAD by varying the concentration of NAD^+ (0-1.5 mM). The data were fitted to Michaelis-Menten kinetics by using SigmaPlot10.

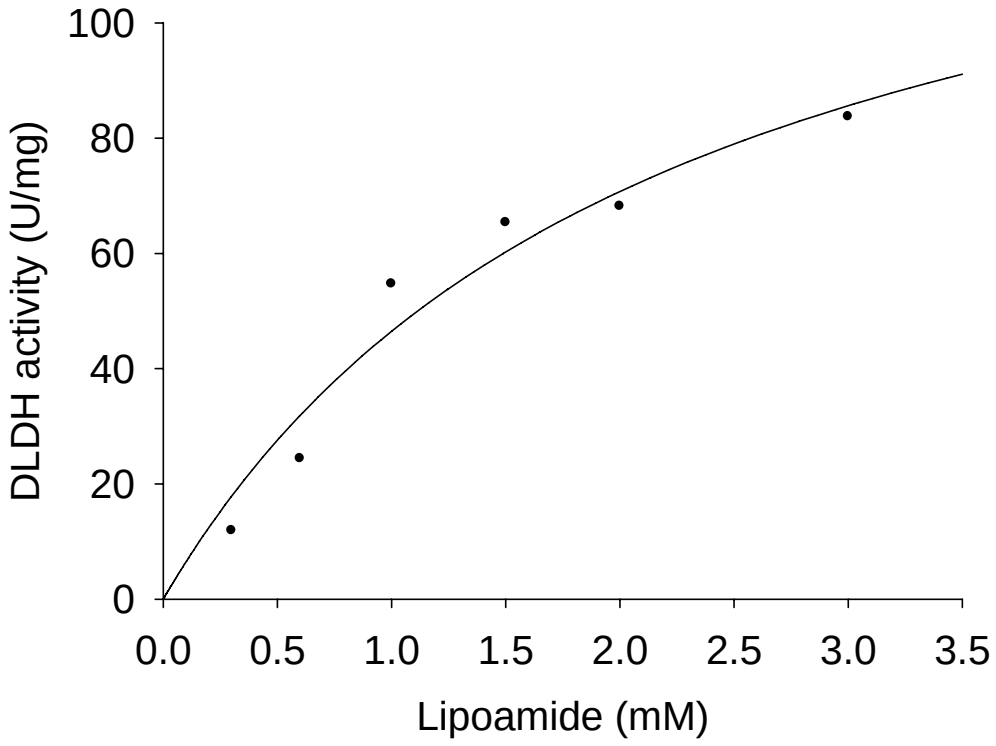

Figure 5-7 Dependency of DLDH activity on the concentration of lipoamide.

The assay was carried out at 80^{o}C with the standard assay for reduction of lipoamide with NADH by varying the concentration of lipoamide (0-3 mM). The data were fitted to Michaelis-Menten kinetics by using SigmaPlot10.

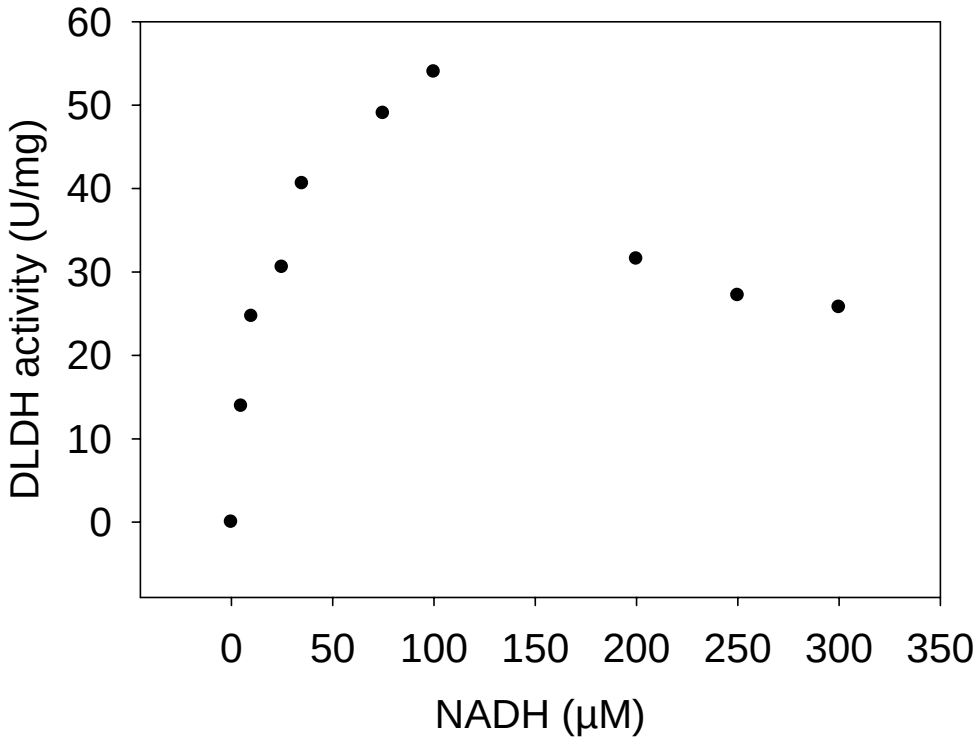

Figure 5-8 Dependency of DLDH activity on the concentration of NADH.

The dependency of DLDH activity on the concentration of NADH was determined with the method described in Materials and Methods (5.3.3). The assays were carried out at 80^{o}C with the standard assay for reduction of lipoamide with NADH by varying the concentration of NADH (0-300 μM).

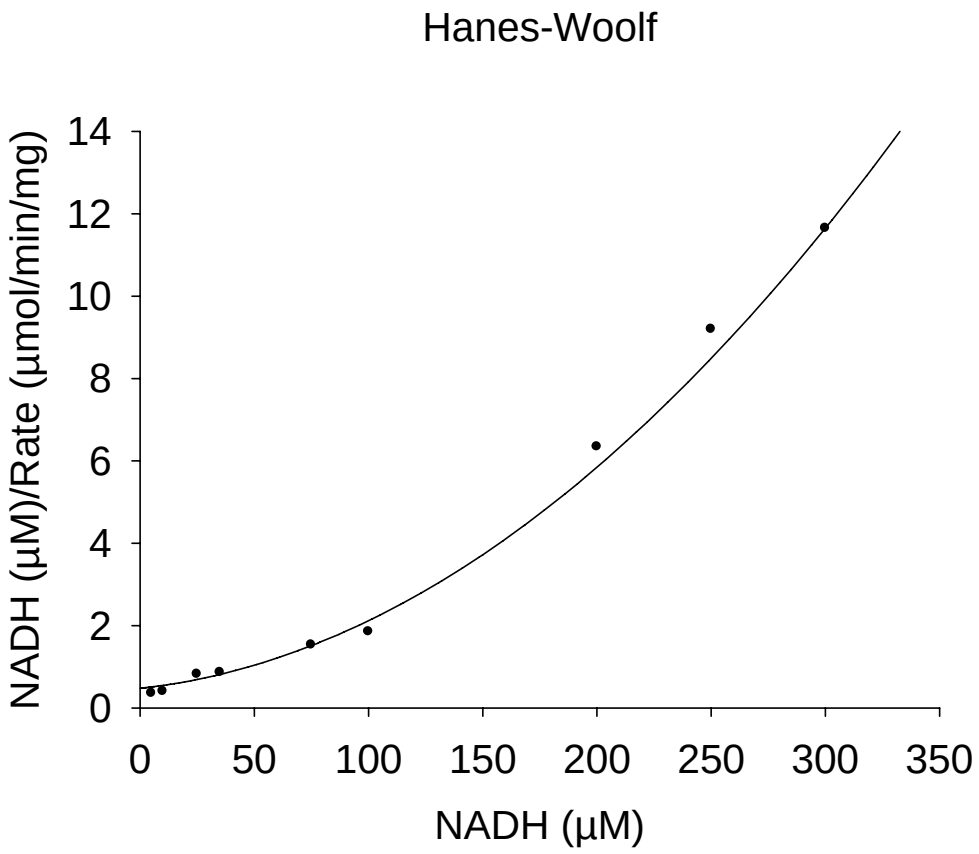

Figure 5-9 Inhibition of NADH on DLDH activity.

The data in Figure 5-8 were fitted to Hanes-Woolf inhibition kinetics by using SigmaPlot10. The K_m value was estimated to be 79.8 µM and K_i value was estimated to be 57.6 µM.

```
                                  10         20         30         40         50
Thermotoga hypogea                MYDALLLGAG PGGYVAALKA LLTSAHLATL ALVEKSFVGG TCTNWGCLPT
Thermotoga maritima               MYDAVIIGGG PGGYVCAIKL AQLG---KKV ALVEKDALGG TCTNRGCIPT
Thermotoga petrophila             MYDAVIIGGG PGGYVCAIKL VQLG---KKV ALVEKDALGG TCTNRGCIPT
Thermosipho melanesiensis         MYDVVVIGGG PGGYIASIRL SQLG---KKV AIIEKEELGG TCTNKGCIPT
Fervidobacterium nodosum          MFDAVIIGGG PGGYVCAIKL AHLG---KNV ALVEKENLGG TCTNWGCIPT
Clustal Consensus                 *:*.:::*.* ****:.:::     .    .: *::**. :** **** **:**

                                   60         70         80         90        100
Thermotoga hypogea                KKRG--AELY ESSKE----- ---------- ---------- ----------
Thermotoga maritima               KAMLTVSHLM DEMKEKASKY GLKVSGVEYD VAAIMKHVQK SVMMSRKGIE
Thermotoga petrophila             KAMLTVSHLM DEMKEKASKY GLKVSGVEYD VDTIMKHVQK SVMMSRKGIE
Thermosipho melanesiensis         KALLTSAHLY RDIKEKASKF GIKVDSVDFE LSGIMKHMQK AVTMSRKGIE
Fervidobacterium nodosum          KALLTATHLI DEIREKADKY GVKATFEGYD ISKVMAHAQK SVTLSRKGIE
Clustal Consensus                 *     :.*   . :*

                                  110        120        130        140        150
Thermotoga hypogea                -----NGVEL LNGEALVESN PSVRKELG-- -------VLA ENVS------
Thermotoga maritima               YLLKKNGVEV FKGTAVVENK NTVVVQETGE KLEAKNLVLA HGSVPSVFSP
Thermotoga petrophila             YLLNKNGVEV FKGTAVVENK NTVVVQETGE KLEAKNLVLA HGSVPSVFSP
Thermosipho melanesiensis         FLMKKNKIDV FKDKGIIKDN ETVLLENEGK EIKGRYLILA QGSIPSVFPP
Fervidobacterium nodosum          FLMKKNNVTL IKGTAEVVNK NQVKIKESGE IFEGKNLVLA HGSVPVVFPP
Clustal Consensus                      * : : ::. . : .:   *  :            :** ..

                                  160        170        180        190        200
Thermotoga hypogea                ---------- ------FDFS KSLVIVGGGV LGVELATFFS SLNVKLVVVE
Thermotoga maritima               FDIDG-VWTS DDVFNLKEFP KSLVIVGGGV IGVEFATFFG SFGVDVTIVE
Thermotoga petrophila             FDIDG-VWTS DDVFNLKEFP KSLVIIGGGV IGVEFATFFG SFGVDVTIVE
Thermosipho melanesiensis         FDKLEGIWTS DDVFKIKEFP KSLLIIGGGV IGVEFATFFS SFGVDVTIVE
Fervidobacterium_nodosum          FDSIEGIWTS NDVFKLQSVP QSLLIIGGGV IGVEFATFFS SLGTKVRIVE
Clustal Consensus                                 ... :**:*:**** :***:****. *:...: :**

                                  210        220        230        240        250
Thermotoga hypogea                LLDHLLPNED ADAAKLVAKK PK-------- ------LSDD LKSLGLALER
Thermotoga maritima               IAEHILPYED SDVAEEVKKA LKRKGVKILE KTKISSLSKV DDGFEVALEN
Thermotoga petrophila             IAEHILPYED SDVAEEVKKA LKRKGVKILE KTKVSSLSKV DDGFEVALEN
Thermosipho melanesiensis         LADHILPNED KDVAEEIKKE LKKKKVNVLE GKKVEEIKKE LN--YIAIVD
Fervidobacterium nodosum          LAEHILPTED SDVAEEVKKA MIRKGVEIQE KSKVTNIEKL EKSYRVTIKD
Clustal Consensus                 : :*:** **  *.*: : *                  :..   .   :::

                                  260        270        280        290        300
Thermotoga hypogea                GLK------- TDVLVAVGRK P--------- --------KT DETMTLNLPN
Thermotoga maritima               GE----TLKA EKVLLAAGRK PNIPEDVKAL GVKIEKGVVT DSRMRTNVEN
Thermotoga petrophila             GE----TLKA EKVLLAAGRK PNIPEDVKAL GVKIEKGVVT DSRMRTNVEN
Thermosipho melanesiensis         GE----TIEA EKVLLAVGRR PNITDDIKEL GVKIDRGVIT DKKMKTNIDN
Fervidobacterium nodosum          NNEKENVVEV ERILLAVGRR PNIPEDVRAL DVEIERGIKT NRKMQTNIEG
Clustal Consensus                 .           :*:*.**: *                   * :  *  *: .
```

```
                                310        320        330        340        350
Thermotoga hypogea              LYAVGDVR-- QGIMVAMYE GLVAAENLCG KPTKMDYSAV PSVLFSEPEV
Thermotoga maritima             VYAIGDIRSG IMLAHVAMYE GIVAAKNIAG EEEEMDYSAV PSIIFSSPEV
Thermotoga petrophila           VYAIGDIRSG IMLAHVAMYE GIVAAKNIAG EEEEMDYSAV PSIIFSSPEV
Thermosipho melanesiensis       IYAIGDIRGQ IMLAHVAMYE GIIAAHNIAG KEIEMDYSAV PAIIFSTPEI
Fervidobacterium nodosum        VYAIGDIRGH IMLAHVASYE GITAALNIAG IEAEMDYSAV PSIIFSNPEV
Clustal Consensus               :**:**:*        ** ** *: ** *:.*    :****** *:::** **:

                                360        370        380        390        400
Thermotoga hypogea              ASVRK-EKDM D--------- ---------- LTVNLGTVRM GG--------
Thermotoga maritima             ASVGVREKDV NPEEVVISKF PVSANGRART MLENIGFAKV IADKKDGTVL
Thermotoga petrophila           ASVGVREKDV NPEEVVISKF PVSANGRART MLENIGFAKV IADKKDRTVL
Thermosipho melanesiensis       ASVGLREKDI EADKINVWKF PVSANGRART MEERAGFAKV IEDKKTGKVL
Fervidobacterium nodosum        ASVGLREKDI DHEKVKISKF PLSANGRART MLENIGFAKV IADKETGTVL
Clustal Consensus               ***   ***: :                    :  . * .::

                                410        420        430        440        450
Thermotoga hypogea              ---------- ---------- ---------- ---------- ----------
Thermotoga maritima             GMSIVSPSAT DMIMEGVIAV KFRMKAEDLE KAIHPHPTLT ETILGALEGV
Thermotoga petrophila           GMSIVSPSAT DMIMEGVIAV KFRMKAEDLE KAIHPHPTLT ETILGALEGV
Thermosipho melanesiensis       GVTVVSPSAT DMIMEGVLAV KYGMTSHQVS EAIHPHPTLT ETLLGAFEGK
Fervidobacterium nodosum        GMSIVSPVAT ELIMEGVVAV KNKLTAHQLE ESIHPHPTLS ETLLGALEGI
Clustal Consensus

Thermotoga hypogea              -------
Thermotoga maritima             SGKPIHL
Thermotoga petrophila           SGKPIHL
Thermosipho melanesiensis       WAIHI--
Fervidobacterium nodosum        TDKPLHL
Clustal Consensus
```

Figure 5-10 Amino acid sequences alignment of partial sequence of *T. hypogea* DLDH and annotated DLDH sequences of *Thermotogales*.

The sequences were aligned using CLUSTAL W method (Higgins and Sharp 1988). The alignment was plotted with reference to a standard sequence, i.e. the partial sequence of *T. hypogea* DLDH at the top. Any residues in a column which are identical to the standard at that point are shown as stars (*) and similar to the standard at that point are shown as dot (·). Black - stands for gap. Red - stands for the unknown sequence of *T. hypogea* DLDH. Green letters: FAD-binding motif. Red letters: redox active disulfide. Blue letters: NAD-binding motif.

terminal, and an NAD-binding motif, GXGXXG, in the middle of the sequence. The catalytic mechanism of DLDH entails the participation of a redox active disulfide formed by two cysteines separated by four amino acid residues (Carothers et al. 1989). Such sequence is also present in *T. hypogea* DLDH (CTNWGC). Both *T. maritima* and *T. netrophila* have the genes encoding all the components of GDC in their genome (Nelson et al. 1999; http://img.jgi.doe.gov/cgi-bin/pub/main.cgi?section=TaxonDetail&page=proteinCodingGenes&taxon_oid=639857041). The genome of *T. maritima* contains the gene TM0380 encoding DLDH, TM0212 encoding H-protein, TM0213 and TM0214 encoding P-protein, and TM0211 encoding T-protein. The gene encoding methylene-tetrahydrofolate dehydrogenase/cyclohydrolase that converts methylene-tetrahydrofolate to formyl-tetrahydrofolate is present in the genome of *T. maritima* as well. However, there was no GDC activity detectable in the cell-free extract of *T. maritima* and *T. hypogea* grown on glucose and they could not grow with glycine as sole carbon and energy source. Growth was actually inhibited by the presence of glycine (Figure 5-11&Figure 5-12), which has not been reported previously and the possible reason will be discussed.

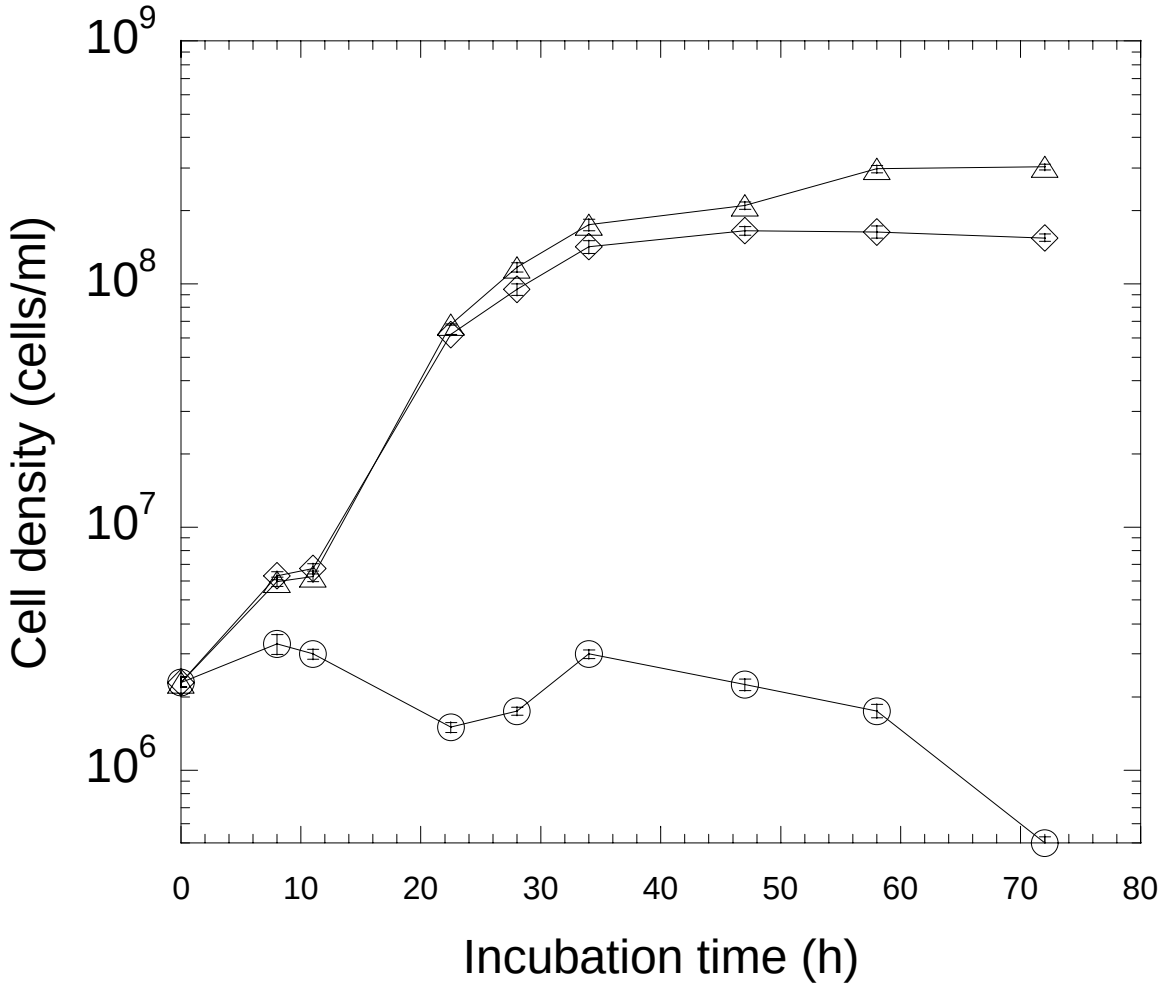

Figure 5-11 Growth of *T. hypogea* with glycine.

T. hypogea was grown anaerobically at 70°C in different media. Diamonds, the culture without extra carbohydrate added to the basal media; circles, the culture containing glycine; triangles, the culture containing glucose.

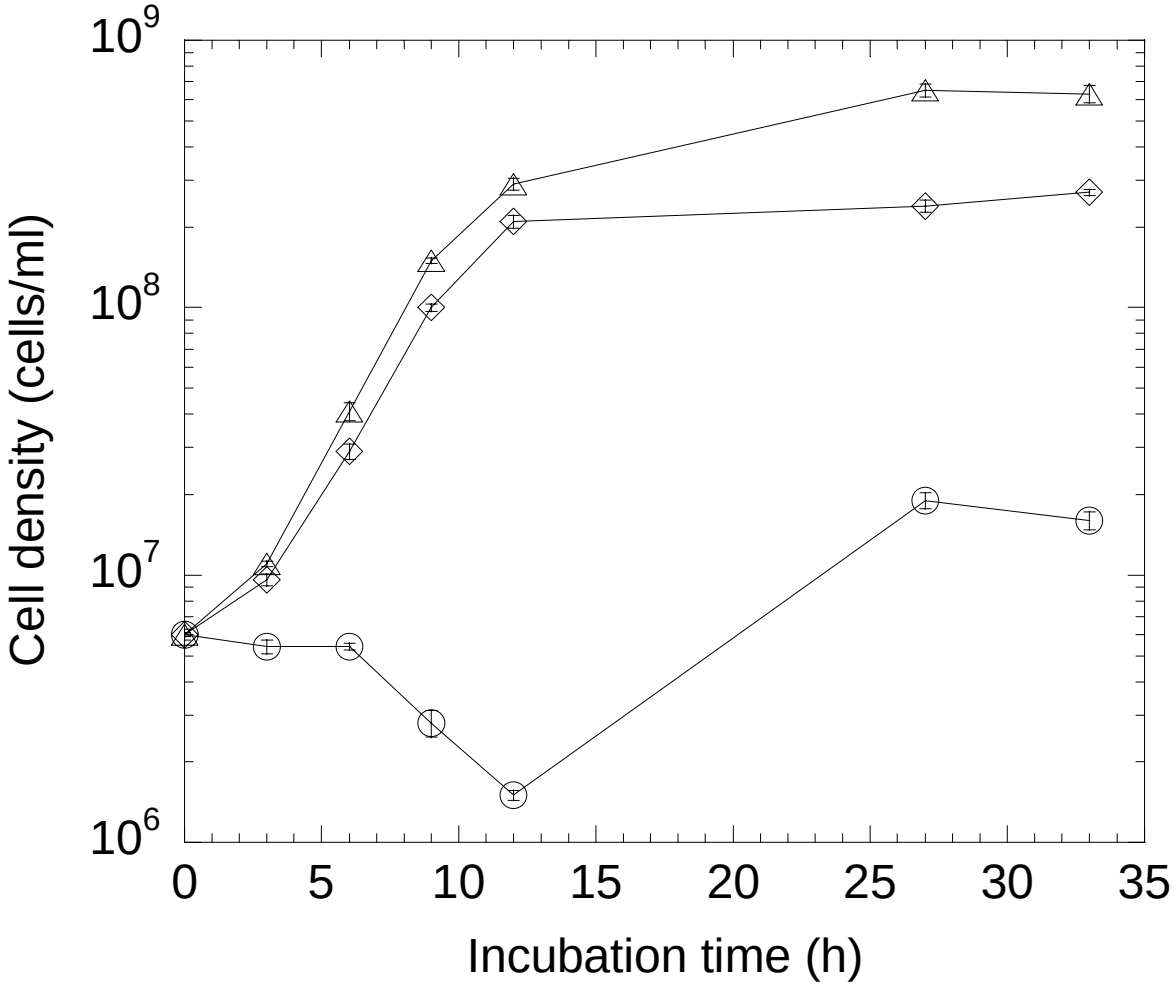

Figure 5-12 Growth of *T. maritima* with glycine.

T. maritima was grown anaerobically at 80°C in different media. Diamonds, the culture without extra carbohydrate added to the basal media; circles, the culture containing glycine; triangles, the culture containing glucose**.**

5.5 DISCUSSION

This is the first report of the presence of DLDH and its purification from hyperthermophiles. Both DLDH and NADH oxidase activities were detected in the cell-free extract of *T. hypogea*. They were all located in the cytoplasm (Table 5-1, Yang and Ma 2005a). Efforts were made to purify both enzymes from *T. hypogea*. However, both activities were always overlapped and the ratios of the NADH oxidase activity to DLDH activity were constant in the fractions during all purification steps (Table 5-2). Finally, the purified enzyme exhibiting both NADH oxidase and DLDH activities showed a single band on SDS-PAGE. Its NADH oxidase properties were reported previously (Yang and Ma 2005a) and in chapter 3 of this thesis. Its DLDH properties were determined and reported in this chapter. DLDH activity was similar in the cell-free extract of xylose grown cells (0.79±0.1 U/mg) and glucose grown cells (0.77±0.014 U/mg), while the DLDH gene in *T. maritima* was slightly differentially expressed in the cells grown on different sugars based on whole genome expression profile (Chhabra et al. 2003; Nguyen et al. 2004).

The NADH-specific *T. hypogea* DLDH is a homodimeric FAD-containing protein with a molecular mass of about 100 kDa, which is similar to most of DLDHs isolated from different sources since this enzyme is conserved during evolution (Williams 1992). In contrast to the majority of DLDHs, a new type of DLDH isolated from some anaerobic glycine-utilizing bacteria diverges from classical enzyme in the aspects of molecular mass and nicotinamide-nucleotide specificity (Dietrichs and Andreesen 1990; Dietrichs et al. 1990; Freudenberg et al. 1989a). A homodimer with subunit molecular mass of 34.5 kDa has been isolated from *E. acidaminophilum* and this enzyme can use both NADPH and NADH with preference for NADPH in the reduction of lipoamide (Freudenberg et al. 1989a). Like most DLDHs, it was demonstrated that the enzyme from *T. hypogea* catalyzed the reduction of lipoamide and the oxidation of dihydrolipoamide with neutral pH optima and exhibited high thermostability. The purified DLDH exhibited versatile catalytic capability including diaphorase activity by catalyzing the reduction of BV and MV with NADH as electron donor, oxidase activity by catalyzing the reduction of molecular oxygen with NADH as electron donor, and DLDH activity by reducing lipoamide and oxidizing dihydrolipoamide.

The activity of the purified enzyme from *T. hypogea* increased along with the increase of NADH concentration up to 100 μM and the activity decreased dramatically when the NADH concentrations

were higher than 100 μM (Figure 5-8). The regulation of NADH on its activity is a feature of DLDH and is a widely observed phenomenon (Massey and Veeger 1961; Wilkinson and Williams 1981). Inhibition of DLDH by NADH is a feedback control for the regulation of enzyme complexes GDC and pyruvate dehydrogenase complex *in vivo* (Douce et al. 2001; Harmych et al. 2002; Kisaki et al. 1971; Snoep et al. 1993). In addition to the regulation effect of NADH inhibition on GDC and pyruvate dehydrogenase complex activity, it has been reported that the NADH/NAD ratio is intimately related to the cellular level of reactive oxygen species (ROS) because pyridine nucleotides participate in both ROS formation *via* NAD(P)H oxidases and degradation *via* thiol oxidation using NADPH and thioredoxin and glutaredoxin-dependent peroxidases (Bunik 2003).

Although genomes of *Thermotogales* species contain the genes encoding all the components of GDC, *T. hypogea* and *T. maritima* were unable to grow with glycine as sole carbon and energy source (Figure 5-11&Figure 5-12) and there are also no GDC activity detectable in the cell-free extract from glucose grown cells. The lack of such activity might result from the dissociation of components of the complex. In addition to GDC, glycine reductase is also required for utilizing glycine in enegy conservation because it produces acetyl phosphate, a substrate for ATP synthesis (Andreesen 1994; Barnard and Akhtar 1979). There was no glycine reductase homologues present in *Thermotogales* species, which may be one reason why *T. maritima* and *T. hypogea* were unable to use glycine as sole carbon and energy source. The growth with glycine was lower than the negative control that had same media composition except with glycine omitted. The possible role of GDC in *T. hypogea* is involved in the process of contribution to one carbon-pool in which the production of N^5N^{10} -methylene-5,6,7,8-tetrahydrofolate is needed. However, the presence of large amount of glycine might have consumed up all the tetrahydrofolate and made other reactions with tetrahydrofolate as cofactor unable to carry on, which may cause the inhibition effect of the glycine on growth. It is reasonable to conclude that the DLDH in *T. hypogea* has typical physical and catalytic properties of DLDHs and it is not involved in the glycine utilization process as glycine fermenting bacteria that can use glycine as sole carbon and energy source and not involved in pyruvate dehydrogenase complex in *T. hypopgea*. DLDH has also been found in halophilic archaeon, *H. colcanii* (Jolley at al. 2000). The pyruvate dehydrogenase and GDC activities were not detected in this organism and there was no difference found between the growth of wild type and DLDH-minus mutant with various substrates including glycine (Jolley et al. 1996). Further study is required to further understand the function of DLDHs in those non-glycine-fermenting and POR containing archaea and hyperthermophilic bacteria.

Chapter 6 FAD-linked *sn*-Glycerol-3-Phosphate Dehydrogenase of *Thermotoga maritima*

A manuscript has been prepared for submission based on the work presented in this chapter.

6.1 ABSTRACT

Thermotoga maritima is an anaerobic hyperthermophilic bacterium growing optimally at 80°C. It was found that glycerol could be used as sole carbon and energy source. The activity of FAD-linked glycerol-3-phosphate dehydrogenase (FAD-GPDH), a key enzyme involved in glycerol dissimilation, was detected in the cell-free extract. The enzyme was then purified using FPLC. The purified enzyme was reported as NADH oxidase previously in Chapter 4. The two subunits of the protein were identified to be encoded by TM1432 annotated as hypothetical protein with high similarity to glycerol-3-phosphate dehydrogenase (GPDH) and TM1433 annotated as hypothetical protein showed high similarity to NADH oxidase, respectively. Further analysis showed that TM1432 and TM1433 were adjacent genes, which is similar to the gene organization of *glpAB* in *Escherichia coli* that encodes anaerobic FAD-GPDH, although the latter was not reported to have NADH oxidase activity. It was found that FAD-GPDH from *T. maritima* indeed could catalyze the *sn*-glycerol-3-phosphate (G-3-P)-dependent reduction of neo blue tetrazolium (NBT), a typical reaction catalyzed by FAD-GPDH. This catalysis showed characteristics of Michaelis-Menten kinetics with an apparent K_m value of 0.98 mM for *sn*-G-3-P and an apparent V_{max} value of 14.7 U/mg at 50°C. It exhibited an optimal pH of 7.5. There was no activity of NAD-dependent GPDH, but glycerol kinase (2 mU/mg), found to be present in the cell-free extract of *T. maritima*. It is plausible to speculate that *T. maritima* possesses a functional glycerol dissimilation pathway involving the glycerol kinase and the FAD-GPDH whose end product, dihydroxyacetone phosphate, produced can enter the Embden-Meyerhof pathway. It was concluded that the heterodimeric NADH oxidase purified from *T. maritima* described in Chapter 4 was a bi-functional flavoenzyme with FAD-GPDH activity, which is the first one characterized in hyperthermophiles.

6.2 INTRODUCTION

Growth on glycerol as sole carbon and energy source has been reported from many types of yeast and some bacteria (Barnett et al. 1983; Lin 1976). It has been demonstrated that glycerol is utilized *via* a glycerol kinase (EC 2.7.1.30) converting glycerol to G-3-P, which is subsequently oxidized to dihydroxyacetone phosphate by an FAD-linked glycerol-3phosphate dehydrogenase (FAD-GPDH) (EC 1.1.99.5). In some organisms, another type of glycerol-3-phosphate dehydrogenase (GPDH), NAD^+-GPDH (EC 1.1.1.8) may also be present and catalyzes the reduction of dihydroxyacetone phosphate to glycerol-3-phosphate (G-3-P) with NADH as reducing equivalent (Daiyasu et al. 2002). FAD-GPDHs are mainly isolated and characterized from mitochondria of eukaryotes (Cole at al. 1978; Larsson et al. 1998; Shen et al. 2003). From bacteria sources, the enzyme has only been purified and characterized from *Escherichia coli* (Schryvers et al. 1978; Schryvers and Weiner 1981). The gene encoding FAD-GPDHs have been identified in *E. coli* (Cole et al. 1988), *Bacillus subtilis* (Lindgren and Rutberg 1974; Wiame et al. 1954) and *Pseudomonas aeruginosa* (Schweizer and Po 1994). *E. coli* contains two different FAD-GPDHs. One enzyme is expressed during aerobic growth called aerobic FAD-GPDH that is a membrane-bound homodimeric flavoprotein (Schryers et al. 1978). The other FAD-GPDH is not membrane-bound and expressed under anaerobic growth conditions composed of two types of subunits, 62 and 43 kDa (anaerobic FAD-GPDH; Schryvers and Weiner 1981). Both FAD-GPDHs carry out the same reaction in the cell, the oxidation of *sn*-G-3-P to dihydroxyacetone phosphate.

Thermotoga maritima is an anaerobic bacterium with an optimum growth temperature at 80^{o}C (Huber et al. 1986). *T. maritima* employs fermentative metabolism converting carbohydrates to pyruvate *via* Embden-Meyerhof (85%) and Enter-Doudoroff (15%) glycolytic pathways (Selig et al. 1997). It was found that *T. maritima* can tolerate trace amounts of oxygen and its cell-free extract had an NADH oxidase activity of 1.0 U/mg (Yang and Ma 2007). The NADH oxidase has been purified to homogeneity, which was a heterodimeric flavoprotein with two subunits with molecular mass of 54 and 46 kDa. In this chapter, we report that the sequence analysis of the purified *T. maritima* NADH oxidase and characterization of its FAD-GPDH activity, which is the first one studied from hyper/thermophiles and strict anaerobes.

6.3 MATERIALS AND METHODS

6.3.1 Growth of *T. maritima*

T. maritima was cultured routinely as described in chapter 4 (4.3.2 Growth of *T. maritima*). For determining the effect of oxygen in the growth media on the activity of both FAD-GPDH and NADH oxidase, *T. maritima* was grown anaerobically in the media without cysteine (500 ml liquid medium, 650 ml gas phase). At late log-phase, 0, 12, 30, 65, or 130 ml pure oxygen was added to each bottle after the pressure in the bottle was released to bring oxygen concentration to 0, 1.8, 4.6, 10, or 20%. One bottle was flushed with pure oxygen. The bottles were continued to be incubated at 80^{o}C for another 2 hours. After the bottles were cooled down, the cells were harvested and used for preparing cell-free extract to determine activities of FAD-GPDH and NADH oxidase.

6.3.2 Enzyme assays

NAD^+-dependent GPDH activity was measured anaerobically at 80^{o}C by monitoring the G-3-P or dihydroxyacetone phosphate-dependent absorbance change of NADH at 340 nm (Kito and Pizer 1969; van Eys et al. 1959). The oxidation of G-3-P was carried out with the assay mixture (2 ml) containing varied amount of *T. maritima* cell-free extract or purified enzyme, 1.2 mM NAD^+ and 3.0 mM α-glycerol phosphate or *sn*-G-3-P in pH 7.5, 100 mM sodium phosphate or pH 9.5, 100 mM glycine-NaOH buffer. The reduction of dihydroxyacetone phosphate was carried out in the assay mixture (2 ml) containing varied amount of *T. maritima* cell-free extract or purified enzyme, 0.25 mM NADH, 1 mM dihydroxyacetone phosphate in 100 mM sodium phosphate buffer (pH 7.0) . One unit of GPDH activity was defined as 1 μmol NADH formed or oxidized per min. FAD-GPDH assay was carried out at 50^{o}C by monitoring the increase of absorbance at 570 nm of neo blue tetrazolium (NBT) diformazan (ε_{570nm}=26 $mM^{-1}cm^{-1}$, Kern et al. 1999; Kistler and Lin 1972). Since four electrons are required to reduce NBT to NBT diformazan, the formation of one mol NBT diformazan will need two mols of G-3-P. The assay mixture contained 0.6 mM NBT, 0.4 mM phenazine methosulfate (PMS), and 3 mM G-3-P in 2 ml pH 7.0, 100 mM sodium phosphate buffer. One unit of FAD-GPDH activity was defined as 1 μmol G-3-P oxidized per min. The oxidase activity of FAD-GPDH was detected in aerobic pH 7.0, 100 mM sodium phosphate buffer containing 3 mM *sn*-G-3-P and cell-free extracts or purified enzyme at 50^{o}C. After the reaction mixture cooled down, H_2O_2 was measured with ABTS method (Yang and Ma 2005) and dihydroxyacetone phosphate was measured with

commercial rabbit muscle NAD^+-GPDH assay (Kito and Pizer 1969). Glycerol kinase was determined *via* FAD-GPDH (the activity present in *T. maritima* cell-free extract) by measuring the formation of H_2O_2 (method A) or dihydroxyacetone phosphate (method B). In method A, the reaction mixture containing 1 mM ATP, 3 mM glycerol, 0.7 mg *T. maritima* cell-free extract, 1 mM $MgCl_2$ in pH 7.5, 100 mM sodium phosphate buffer was incubated at 80°C for 10 min anaerobically to let G-3-P accumulate. Then the stopper was open and the anaerobic cuvett was shaken vigoursly to let the solution become aerobic. The mixtures were incubated for 5 min after 0.7 mg cell-free extract was added. After the mixtures cooled down, hydrogen peroxide was detected. The negative control was without glycerol added in the first incubation step and followed all the other procedures. In method B, the same condition was used as in method A except that after the reaction cooled down, rabbit muscle NAD^+-GPDH and NADH were added to half of the assay mixture to detect the presence of dihydroxyacetone phosphate. The decrease of the absorbance at 340 nm was monitored at 30°C. The control with only NADH added to the other half of the reaction mixture was performed in the same way.

6.3.3 Purification of FAD-GPDH

The enzyme was purified as described in Chapter 4 (4.3.4 Enzyme purification).

6.3.4 Iron and acid labile sulfur determination

The enzyme sample in Buffer A was concentrated and washed with freshly prepared anaerobic Tris-HCl buffer (pH 7.8, 10 mM) containing 2 mM DTT in the anaerobic chamber and ambient air using Microcon YM-10 (Millipore, MA, USA) to remove SDT that would interfere with metal determination. The oxygen level in the anaerobic chamber was about 1.4 ppm when the experiment was carried out. 100 µg of the resulting samples (both aerobic and anaerobic) were used for metal analysis using Inductively Coupled Plasma–Mass Spectrometer (VG Elemental PlasmQuad 3 ICP-MS at the Chemical Analysis Laboratory, University of Georgia, USA). The same set of protein samples was used for acid labile sulfur determination using methylene blue formation method described previously (Beinert 1983). Subsequently, 300 µl freshly prepared 1% zinc acetate and 15 µl 12% NaOH were added to 100 µl enzyme sample. 75 µl freshly prepared 0.1% N, N-dimethyl-*p*-phenylenediamine (DMPD) monohydrochloride in 5.5 N HCl and 30 µl 47 mM $FeCl_3$ in 1.2 N HCl

were added to the mixture. After incubation at room temperature for 30 min, the samples were centrifuged for 15 min at 10,000x*g* to remove protein. The absorbance at 670 nm of the resulting supernatant was measured. The molar absorbance of 34.5 mM^{-1} cm^{-1} was used to calculate the amount of methylene blue formed which is equal to the amount of H_2S present in the sample (Beinert 1983).

6.3.5 Gene identification and sequence analysis

Each of the two bands on SDS-PAGE was cut and digested in-gel with the method modified from Schevchenko (Shevchenko et al. 1996). Protein samples from each of the two subunits on SDS-PAGE were excised with scalpel and cut into small cubes in flowhood. The gel pieces were destained with 50 mM NH_4HCO_3/50% acetonitrile (ACN) (2x10 min) after they were washed three times with HPLC grade water by vortexing. The gels were dehydrated with 100 µl 100% ACN (2x5min). Subsequently, proteins were reduced by incubation with 100 µl of 10 mM DTT in 100 mM NH_4HCO_3 at 50^oC for 30 min, dehydrated with 100 µl 100% ACN and alkylated by incubating with 100 µl 55 mM iodoacetamide (IAA) in 100 mM NH_4HCO_3 for 30 min in dark. Then, the gels particles were washed with 100 µl 100% ACN and air-dried. For the digestion of the proteins with trypsin, the gel particles were rehydrated for 10 min in a trypsin solution to bring a ratio to approximately 1:100 to 1:1000 (W/W) of trypsin: protein. Then 50 µl of 50 mM NH_4HCO_3 was added to the gel pieces and the proteins were digested at 37^oC for 16-18 hours. The mixture was bath-sonicated for 10 min after 50 µl of ultra-pure water was added. The supernatant was removed to a collecting tube, which contained 5 µl of 50% formic acid (FA) in 50% ACN. The gels were washed once with 75 µl of 5% FA in 50% ACN. The supernatant was combined. The volume in the collecting tube was reduced to 10-15 µl in a Speedvac. The resulting samples were cleaned using the C-18 ZipTip system (Millipore). 2 µl of 1% FA was added to the cleaned sample to protonate the peptides and the resulting samples were applied for mass spectrometry analyses (Mass Spectrometry Facility at the University of Waterloo on a Waters Micromass Q-TOF Ultima using nano-spray injection as the sample delivery method). PEAK software (BSI, Waterloo, ON) was used for MS/MS profiling.

6.4 RESULTS

6.4.1 Growth and FAD-GPDH activity

It was found that there was FAD-GPDH activity (0.15 U/mg) in the cell-free extract of *T. maritima.* In addition to FAD-GPDH that converts G-3-P to dihydroxyacetone phosphate, glycerol kinase can also be required for any organism that dissimilates glycerol (Kistler and Lin 1972). Glycerol kinase was detected to be 2 mU/mg in the cell-free extract of *T. maritima* by determining the formation of both H_2O_2 and dihydroxyacetone phosphate when the assay mixture contained only glycerol and cell-free extract, while there was neither of the two products detectable in the control omitting glycerol supplied. Therefore, *T. maritima* has the potential to grow with glycerol as sole carbon and energy source, which was verified (Ronholm and Ma 2006). Since NADH oxidase activity in *T. maritima* exhibited oxygen induction and oxygen sensitivity as described in Chapter 4 (4.4.7 Oxygen sensitivity), FAD-GPDH was examined for these properties as well. FAD-GPDH and NADH oxidase activities from cells being exposed to certain oxygen concentration for 2 hours showed the same pattern of increase and decrease when the cells grew at their late log-phase (Figure 6-1). Both enzyme activities were increased along with the increase of oxygen concentration up to 5% in the gas phase, and started to decrease when the oxygen concentration was higher than 5%.

6.4.2 Purification of FAD-GPDH

FAD-GPDH was purified by monitoring NADH oxidase activity (Table 4-1). It was a heterodimeric protein with two subunits of 54 and 46 kDa as described in Chapter 4 (Figure 4-2).

6.4.3 Properties of *T. maritima* FAD-GPDH

Acid labile sulfur and iron contents were measured using methylene blue formation (Beinert 1983) and ICP-MS, respectively. The purified enzyme contained 2.0 g-atoms of acid labile sulfur and 2.2 g-atoms of iron per mol, which confirmed the presence of a [2Fe-2S]-cluster as predicted based on the sequence analysis described later in this chapter (6.4.4 Gene identification and sequence analysis). This type of [2Fe-2S]-cluster can have low redox potential of -254 mV (Quail et al. 1996), which may be subject to damage by exposure to oxygen.

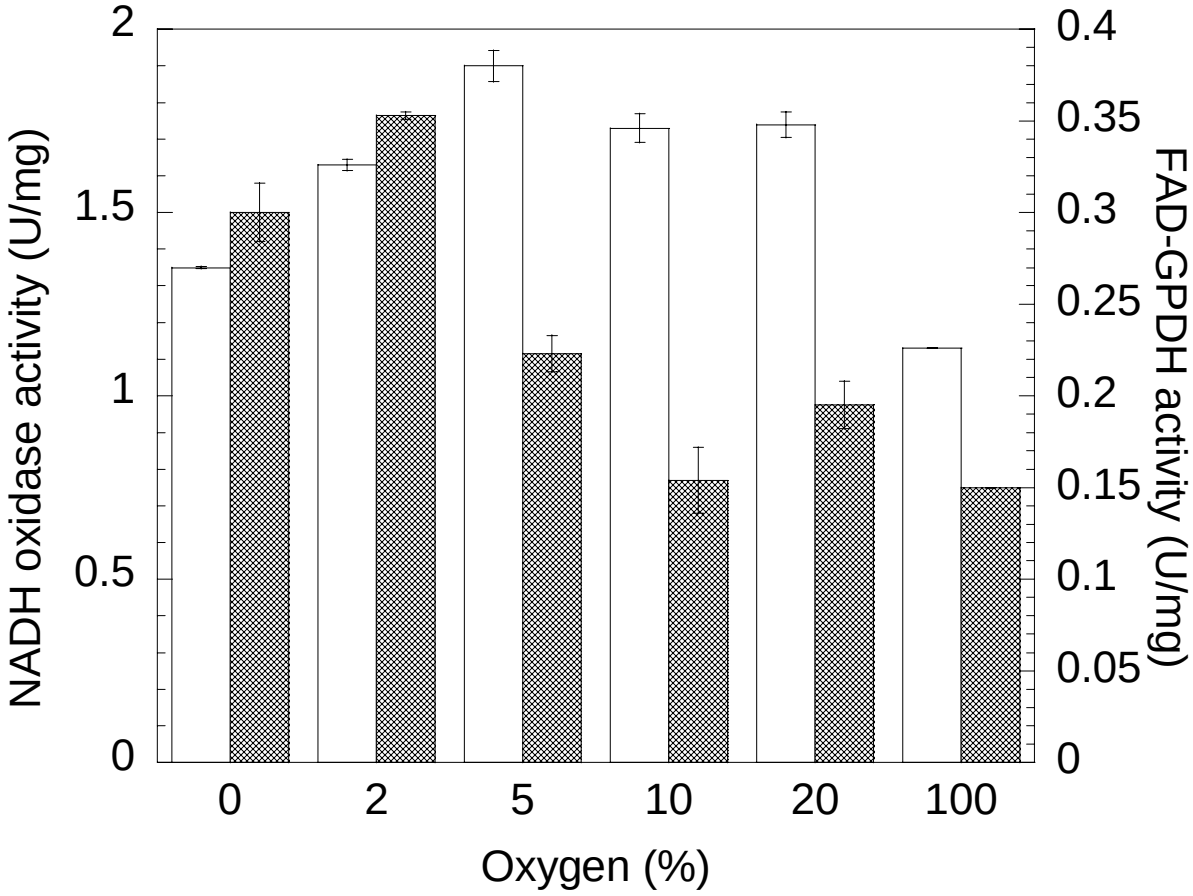

Figure 6-1 Activities of FAD-GPDH and NADH oxidase in the cell-free extract of *T. maritima* exposed to oxygen in the growth media.

Oxygen was added to the late log-phase *T. maritima* to bring oxygen concentration in the gas phase from 0 to 100% and incubated for another two hours. FAD-GPDH and NADH oxidase assays were performed for the cell-free extracts resulted from cells exposed to different level of oxygen. Filled bars, FAD-GPDH; open bars, NADH oxidase.

The iron content of *T. maritima* FAD-GPDH is similar to that of anaerobic FAD-GPDH in *E. coli* (Schryvers and Weiner 1981).

The purified *T. maritma* FAD-GPDH exhibited a specific activity of 11.9 U/mg when it catalyzed the PMS mediated reduction of NBT with *sn*-G-3-P as substrate at 50^{o}C, which was 28% of its NADH oxidase activity (42.4 U/mg) at the same assay temperature. The optimal pH for *T. maritima* FAD-GPDH was determined to be 7.5 (Figure 6-2), which is a common feature for all the FAD-GPDH (Kistler and Lin 1972; Ringler 1961; Shen et al. 2003). Since PMS and NBT are not stable at alkaline condition, all later assays were carried out at pH 7.0, which is the close activity to 7.5. The activity of FAD-GPDH was dependent on *sn*-G-3-P concentrations. The data were fitted to Michaelis-Menten kinetics using SigmaPlot10. The catalysis followed Michealis-Menten kinetics. The apparent K_m and V_{max} values were determined to be 0.98 mM and 14.7 μmol mg^{-1} min^{-1} (Figure 6-3). In addition to dehydrogenase activity, *T. maritima* FAD-GPDH could also oxidize *sn*-G-3-P with molecular oxygen and the products of this reaction were identified to be hydrogen peroxide and dihydroxyacetone phosphate using ABTS method and rabbit muscle NAD^{+}-GPDH, respectively.

The oxygen sensitivity of the purified FAD-GPDH was also examined. It was found that the dehydrogenase activity of FAD-GPDH was more resistant to oxygen inactivation compared to that of *sn*-G-3-P oxidase and NADH oxidase activities (Figure 6-4). There was a quick loss of activity (30%) when the enzyme sample was exposed to air in the first hour, then the residual activity remained at 60% for at least 24 hours. It was speculated that substrates may provide protection against oxygen damage, so the stabilization effect of *sn*-G-3-P on FAD-GPDH was tested. However, the presence of such substrate would interfere with the assay, therefore, NADH oxidase activity was measured as an indicator of the residual activity. Results showed that *sn*-G-3-P did not have protective effect on the oxygen sensitivity of *T. maritima* FAD-GPDH (Figure 6-5). The enzyme lost its NADH oxidase activity at the same rate as that of no *sn*-G-3-P present.

6.4.4 Gene identification and sequence analysis

Protein samples from each of the two subunits *T. maritima* FAD-GPDH on SDS-PAGE were treated and analyzed with mass spectrometry (Table 6-1). The results revealed that the large subunit (54 kDa)

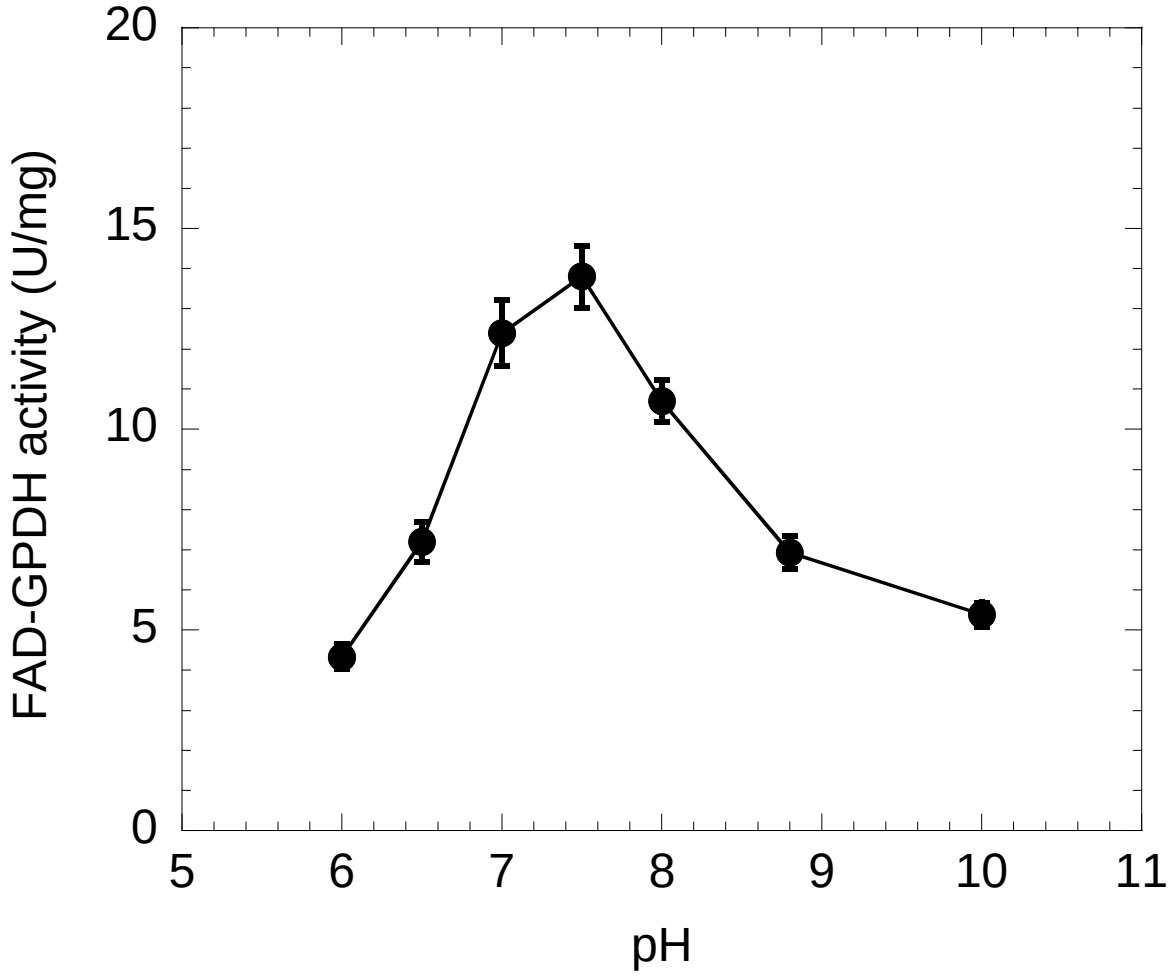

Figure 6-2 pH dependency of *T. maritima* FAD-GPDH activity.

The assay was carried out at 50°C as described in section 6.3.2 with different buffers. Buffers used: 100 mM sodium phosphate, pH 6.0-8.0; 100 mM glycine-NaOH, pH 8.8-10.0.

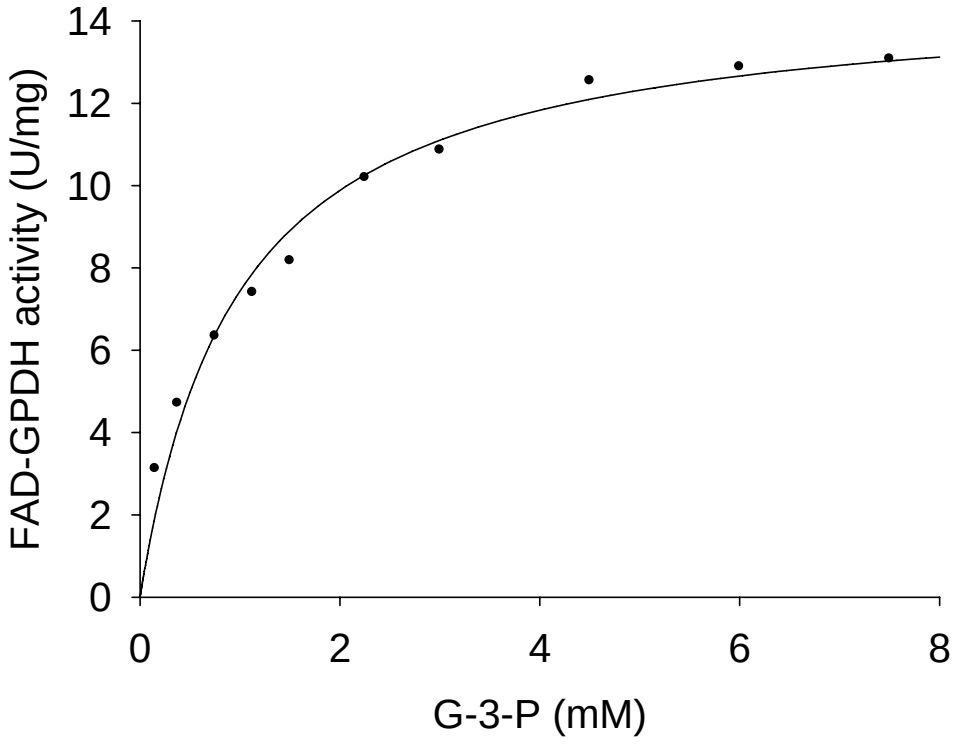

Figure 6-3 Dependency of FAD-GPDH activity on *sn*-G-3-P concentration.

The reactions were carried out at 50^{o}C with standard assay system by varying the concentration of *sn*-G-3-P from 0-7.5 mM. The data were fitted to Michaelis-Menten kinetics using SigmaPlot 10.

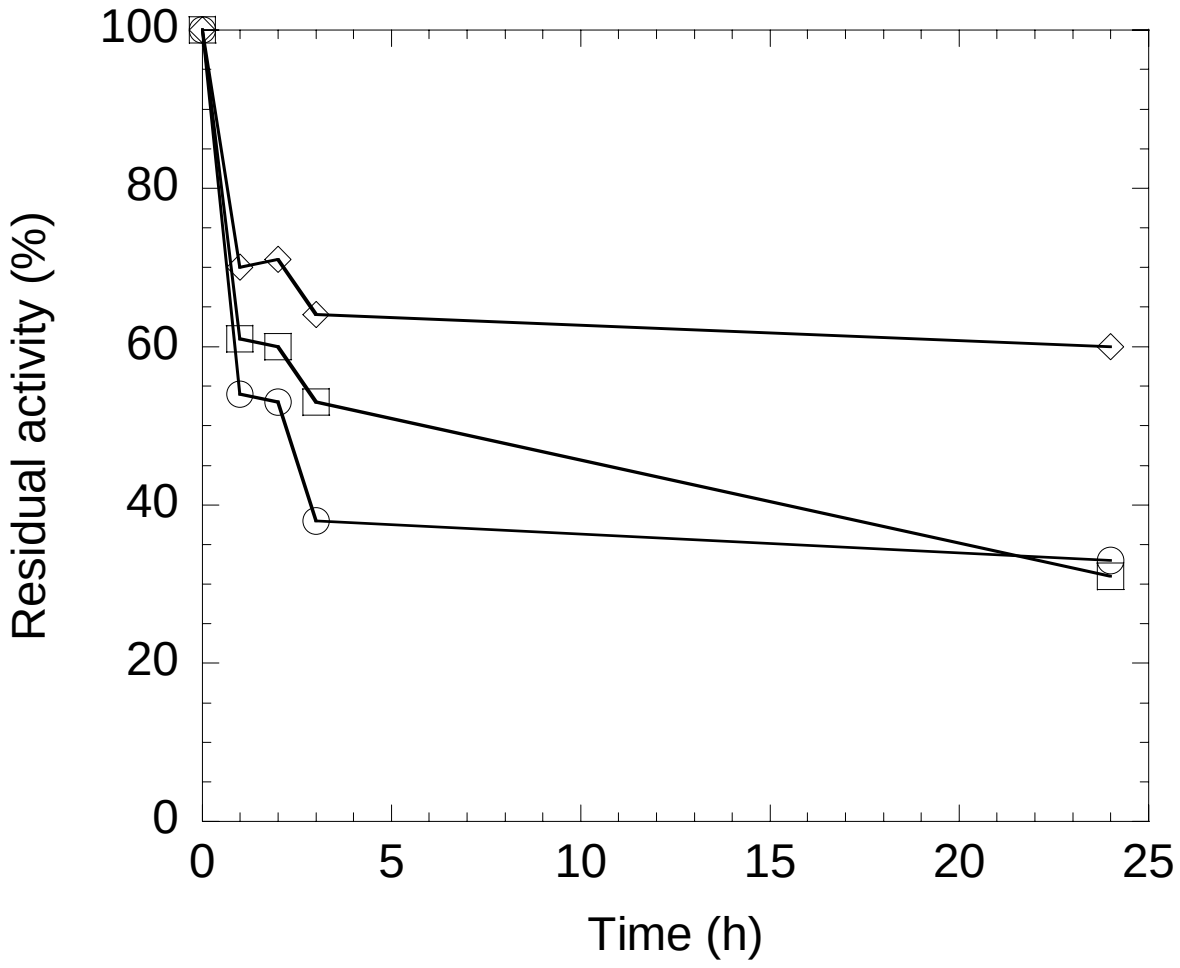

Figure 6-4 Oxygen sensitivity of *T. maritima* FAD-GPDH and NADH oxidase.

FAD-GPDH (diamnods), oxidase activity of GPDH (GPO; squares), and NADH oxidase activity (circles) activities were tested for the purified *T. maritima* NADH oxidase sample exposed to air at different time intervals.

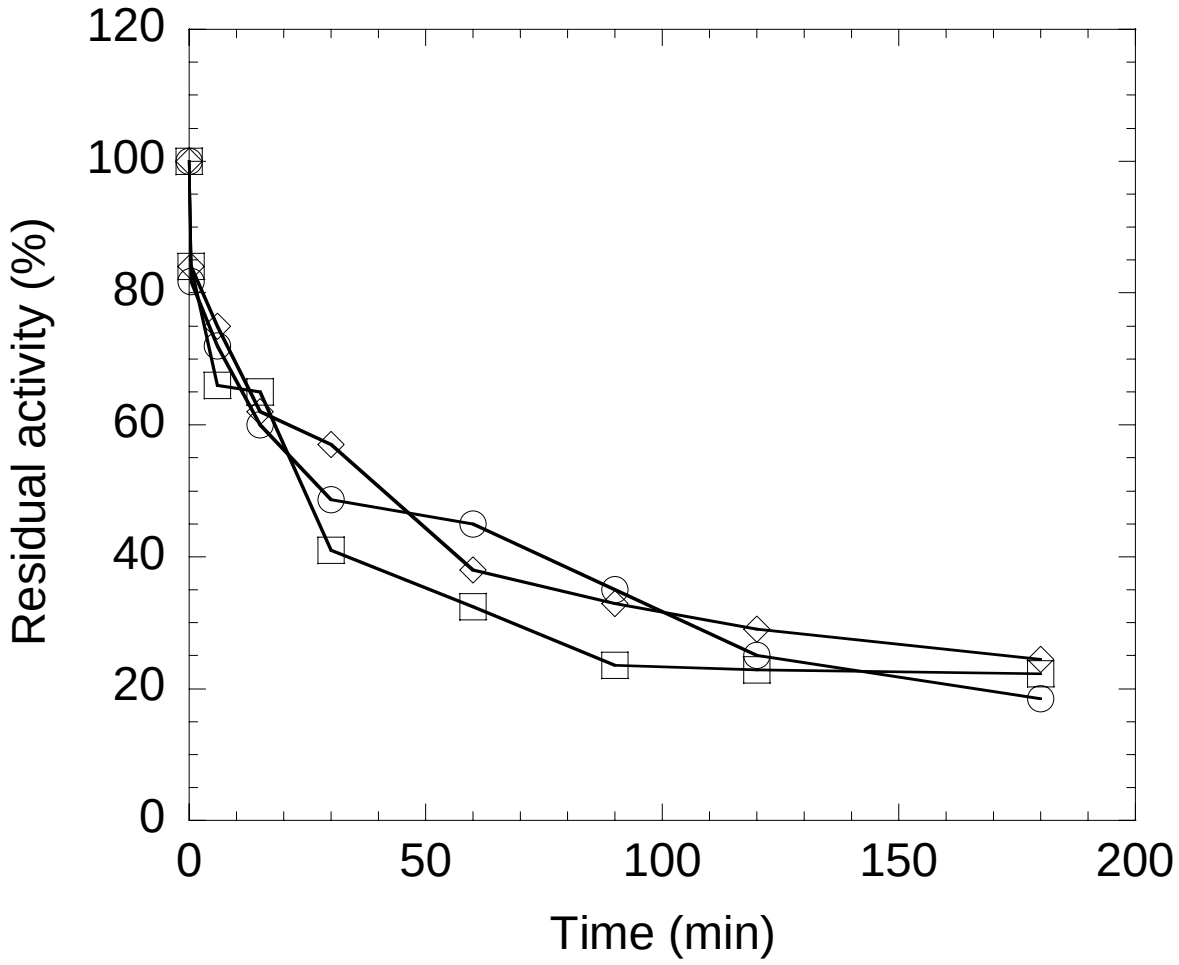

Figure 6-5 Effect of *sn*-G-3-P on the oxygen sensitivity of the *T. maritima* FAD-GPDH.

Enzyme sample in 1 mM *sn*-G-3-P in Tris-HCl buffer (pH 7.8, 50 mM, 5% glycerol; diamonds), 1 mM *sn*-G-3-P and 2 mM SDT and DTT in Tris-HCl buffer (circles), or only in Tris-HCl buffer (squares) was exposed to air. NADH oxidase activity was measured at different time intervals.

Table 6-1 Gene identification

Peptide sequences	LPYAGGLLR VDEQFRPIPR GVGVSNIGQTSR AKEEGAEVLLVERDER EFEDLVPSEMLR	SPGLTAAPAVAK YVVEELIQEK IGSFVVAFNDEELKELER
Sequence coverage (%)	17.37	8.35
Score (%)	97.95	71.71
Accession number	TM1433	TM1432
Annotated name	Conserved hypothetical protein	Hypothetical protein
Apparent Mr (kDa)	46	54
Calculated M_r (Da)	44861	53628

and small subunit (46 kDa) were the products of *T. maritima* genes TM1432 and TM1433, respectively (Nelson et al. 1999). A conserved flavin-binding site (-$GXGX_2GX_3A$-) was present at the N-terminus of each protein encoded by the genes, which is consistent with the experimental value of ~2 FAD moieties per native enzyme (4.4.3 Flavin cofactor). A conserved NAD(P) binding site ($GXGX_2GX_3A$) was present in the middle of TM1433. In addition, a bacterioferritin-associated ferredoxin (BFD)-like binding region (-$CXCX_{32}CX_4C$-) was found to be present near the C-terminus of the large subunit (TM1432), which presumably binds a [2Fe-2S] cluster. BLAST search was performed for both subunits and the results showed that they had 41-94% protein sequence identity and 59-96% protein sequence similarity to genes (locus tag numbers) present in anaerobes (Table 6-2&Table 6-3), which are, TpetDRAFT_0258 and TpetDRAFT_0257 in *Thermotoga petrophila* (http://img.jgi.doe.gov/cgi-bin/pub/main.cgi?section=TaxonDetail&page=proteinCodingGenes&taxon_oid=639857041), FnodDRAFT_1202 and FnodDRAFT_1201 in *Fervidobacterium nodosum* (http://genome.ornl.gov/microbial/fnod/), TmelDRAFT_1688 and TmelDRAFT_1689 in *Thermosipho melanesiensis* (http://www.ncbi.nlm.nih.gov/entrez/query.fcgi?cmd=Retrieve&db=genome&dopt=Protein+Table&list_uids=5600), TK1393 and TK1392 in *Thermococcus kodakaraensis* (Fukui et al. 2005), PF2005 and PF 2006 in *Pyrococcus furiosus* (Robb et al. 2001a), PAB0183 and PAB0184 in *Pyrococcus abyssi* (Cohen et al. 2003), TTE2001 and TTE2000 in *Thermoanaerobacter tengcongensis* (Bao et al. 2002), Teth39DRAFT_0751 and Teth39DRAFT_0752 in *Thermoanaerobacter ethanolicus* (http://www.ncbi.nlm.nih.gov/entrez/viewer.fcgi?val=AAKQ00000000), CsacDRAFT_2355 and CsacDRAFT_2356 in *Caldicellulosiruptor saccharolyticus* (http://www.ncbi.nlm.nih.gov/entrez/viewer.fcgi?val=AALW00000000), CA_C1322 and CA_C1323 in *Clostridium acetobutylicum* (Nölling et al. 2001), CbeiDRAFT_3784 and CbeiDRAFT_3783 in *Clostridium beijerinckii* (http://www.ncbi.nlm.nih.gov/entrez/viewer.fcgi?val=AALO00000000), CPE2551 and CPE2550 in *Clostridium perfringens* (Shimizu et al. 2002), CTC_02436 and CTC_02435 in *Clostridium tetani* (Brüggemann et al. 2003). These pairs of genes were found to be organized as adjacent open reading frames within a putative operon in the genome, and the big subunit was generally annotated as either hypothetical protein or GPDH and the small subunit was annotated as FAD-dependent oxidoreductase or NADH oxidase. However, none of them has been characterized.

Table 6-2 Comparison of the sequence of TM1432 (big subunit) with homologues in the genomes of other anaerobes

Microorganisms	Locus tag	Annotated name	Length (aa)	Identity (%)	Similarity (%)	Optimal growth (^{o}C)
T. maritima	TM1432	Hypothetical protein	479	100	100	80
Thermotoga petrophila	TpetDRAFT_0258	FAD OR [a]	479	94	96	80
Fervidobacterium nodosum	FnodDRAFT_1202	FAD OR	480	63	75	65-70
Thermosipho melanesiensis	TmelDRAFT_1688	FAD OR	478	57	72	70
Pyrococcus furiosus	PF2005	GPDH	496	46	63	100
Thermococcus kodakaraensis	TK1393	GPDH	496	46	62	85
Pyrococcus abyssi	PAB0183	GPDH	497	44	62	100
Thermoanaerobacter tengcongensis	TTE2001	Predicted DH [b]	498	43	61	75
Thermoanaerobacter ethanolicus	Teth39DRAFT_0751	FAD dependent OR	502	43	61	65
Clostridium perfringens	CPE2551	Probable GP DH	476	42	61	43-47

[a] FAD OR stands for probable FAD-dependent oxidoreductase.

[b] DH stands for dehydrogenase.

Table 6-3 Comparison of the sequence of TM1433 (small subunit) with homologues in the genomes of other anaerobes

Microorganisms	Locus tag	Annotated name	Length (aa)	Identity (%)	Similarity (%)	Optimal growth (^{o}C)
T. maritima	TM1433	OR [a]	403	100	100	80
T. petrophila	TpetDRAFT_0257	FAD PDOR [b]	403	89	90	80
F. nodosum	FnodDRAFT_1201	FAD PDOR	412	52	72	65-70
T. melanesiensis	TmelDRAFT_1689	FAD PDOR	406	46	61	70
C. perfringens	CPE2550	Probable OR	417	44	63	43-47
P. abyssi	PYRAB02700	NADH oxidase	407	42	60	100
T. kodakarensis	TK1392	NADH oxidase	413	42	61	85
T. ethanolicus	Teth39DRAFT _0752	FAD-OR	419	42	59	65
T. tengcongensis	TTE2000 (HcaD2)	NAD(FAD)-DH [c]	419	42	59	75
P. furiosus	PF2006	NADH oxidase	413	41	60	100

[a] OR stands for oxidoreductase.

[b] FAD PDR stands for FAD-dependent pyridine nucleotide disulfide oxidoreductase.

[c] DH stands for dehydrogenase.

No NADH-dependent dihydroxyacetone phosphate reduction or NAD^+-dependent *sn*-G-3-P oxidation activity was detected using both of the purified enzyme and *T. maritima* cell-free extract at pH 7.0 or 9.5. Further sequence analysis and literature search were performed to see if there was any clue to indicate any activity for the purified *T. maritima* FAD-GPDH. It was found that the gene organization was also similar to the genes encoding anaerobic FAD-GPDH in *E. coli* (Blattner et al. 1997), i.e. a big flavin- and iron-containing subunit (*glpA*), a medium flavin-containing subunit, and a third iron-sulfur binding domain-containing subunit that did not appear in the purified enzyme (Cole at al. 1988; Nelson et al. 1999). The big subunit (TM1432) showed 42% similarity and 22% identity to the sequence of the big subunit of of *E. coli* FAD-GPDH encoded by *glpA*. Sequence comparison showed that *T. maritima* NADH oxidase and *E. coli* FAD-GPDH belonged to different subgroups of the FAD-GPDHs, i.e. the *T. maritima* enzyme was in the group of enzymes from hyper/thermophilic anearobes (Figure 6-6&Figure 6-7). Therefore, based on activity verification, i.e. the reduction of NBT mediated by PMS with *sn*-G-3-P as substrate, and gene sequence analysis, it is reasonable to conclude that the purified FAD-GPDH was bifunctional. It had activities of both NADH oxidase and FAD-GPDH.

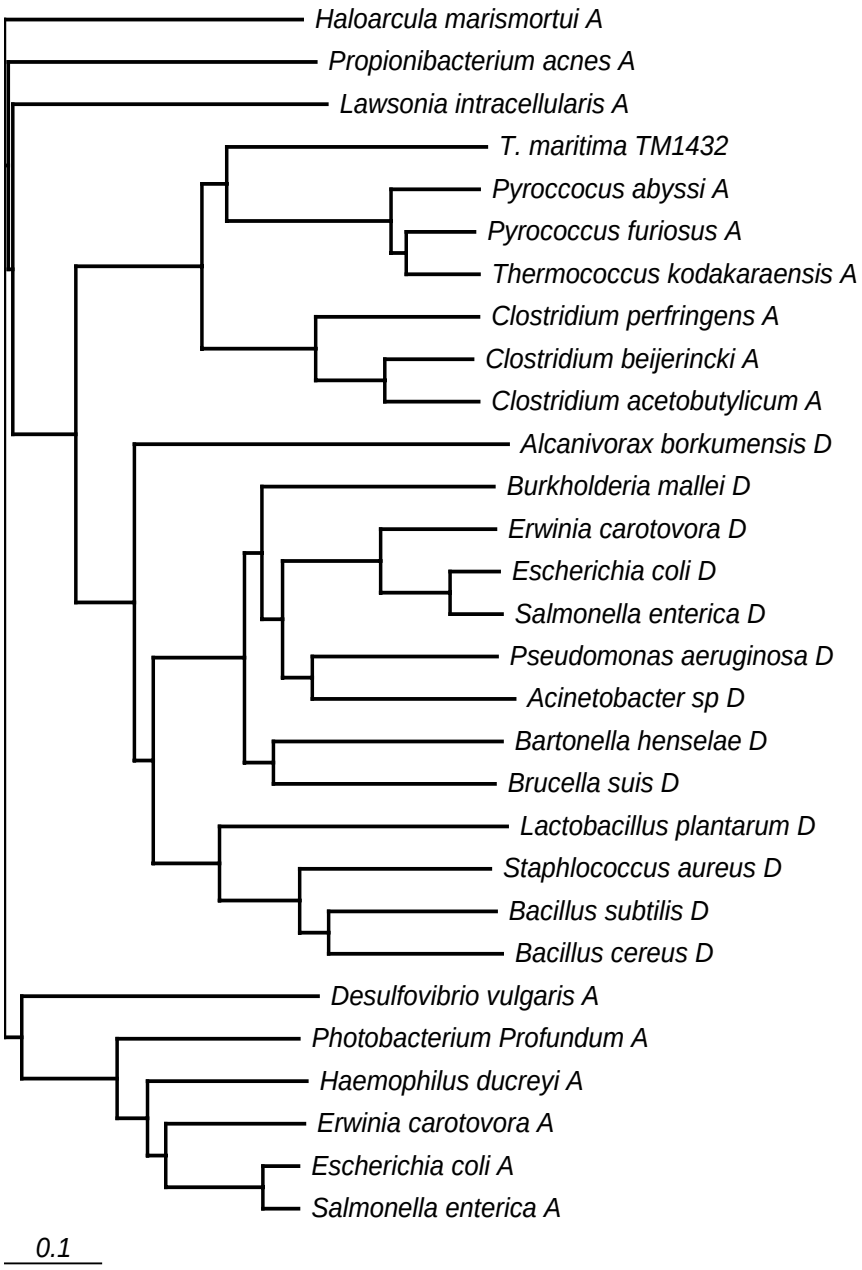
Haloarcula marismortui A
Propionibacterium acnes A
Lawsonia intracellularis A
T. maritima TM1432
Pyroccocus abyssi A
Pyrococcus furiosus A
Thermococcus kodakaraensis A
Clostridium perfringens A
Clostridium beijerincki A
Clostridium acetobutylicum A
Alcanivorax borkumensis D
Burkholderia mallei D
Erwinia carotovora D
Escherichia coli D
Salmonella enterica D
Pseudomonas aeruginosa D
Acinetobacter sp D
Bartonella henselae D
Brucella suis D
Lactobacillus plantarum D
Staphlococcus aureus D
Bacillus subtilis D
Bacillus cereus D
Desulfovibrio vulgaris A
Photobacterium Profundum A
Haemophilus ducreyi A
Erwinia carotovora A
Escherichia coli A
Salmonella enterica A
0.1

Figure 6-6 Sequence comparison of the big subunit of *T. maritima* NADH oxidase TM1432 with the big subunit of the anaerobic FAD-GPDH (A) and aerobic FAD-GPDH (D).

The sequences were aligned using the CLUSTAL W method and a phylogenetic tree was constructed (Higgins and Sharp 1988). The tree was viewed and edited with Tree View (Page 1996).

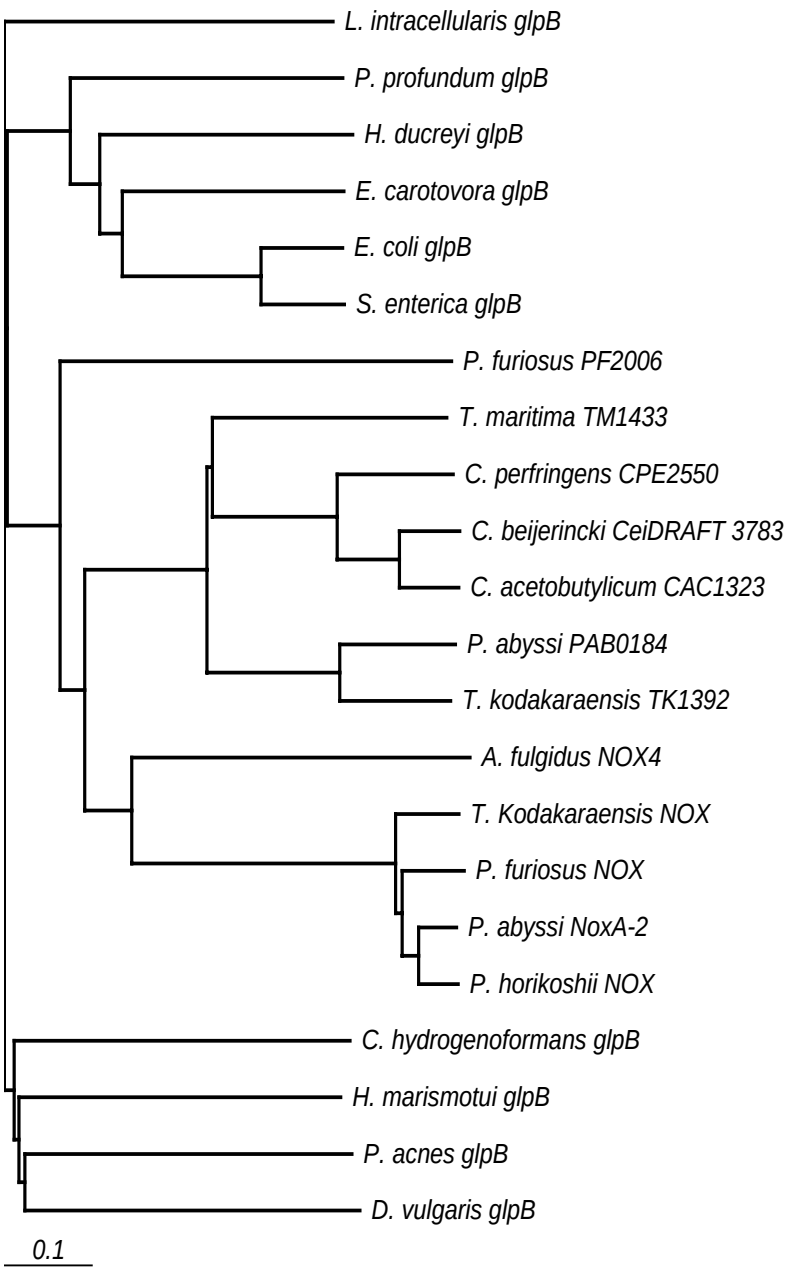
L. intracellularis glpB
P. profundum glpB
H. ducreyi glpB
E. carotovora glpB
E. coli glpB
S. enterica glpB
P. furiosus PF2006
T. maritima TM1433
C. perfringens CPE2550
C. beijerincki CeiDRAFT 3783
C. acetobutylicum CAC1323
P. abyssi PAB0184
T. kodakaraensis TK1392
A. fulgidus NOX4
T. Kodakaraensis NOX
P. furiosus NOX
P. abyssi NoxA-2
P. horikoshii NOX
C. hydrogenoformans glpB
H. marismotui glpB
P. acnes glpB
D. vulgaris glpB
0.1

Figure 6-7 Sequence comparison of the small subunit of *T. maritima* NADH oxidase (TM1433) with the small subunit of anaerobic FAD-GPDH (glpB), NADH oxidases (NOX), and their homologues (named with locus tags).

The sequences were aligned using the CLUSTAL W method and a phylogenetic tree was constructed (Higgins and Sharp 1988). The tree was viewed and edited with Tree View (Page 1996).

6.5 DISCUSSION

The organization of the two genes encoding the two subunits of *T. maritima* NADH oxidase showed very similar pattern to some putative GPDH/oxidoreductase in hyper/thermophilic anaerobes (Table 6-2&Table 6-3). None of these predicted enzymes has been characterized yet. Further sequence analysis showed that this is a subgroup of anaerobic FAD-GPDH (Figure 6-6&Figure 6-7). The only anaerobic FAD-GPDH characterized is that from *E. coli* (Schryvers and Weiner 1981). TM1432 showed 22% identity and 42% similarity to *E. coli glpA*, which encodes the big subunit of anaerobic FAD-GPDH, while TM1433 did not show any significant similarity to the *E. coli glpB*. *E. coli glpA* showed similarity not only to TM1432, but also 22-23% identity and 39-42% similarity to PF2005 in *P. furiosus*, TK1393 in *T. kodakaraensis* and *glpA* in *P. abyssi*, which are annotated as encoding gene of the big subunit of anaerobic FAD-GPDH. *glpB* of *E. coli* did not show significant similarity to any gene in hyperthermophiles. Unlike TM1433 and its hyperthermophilic homologues, *glpB* of *E. coli* does not have a conserved NAD(P) binding domain in the middle of its amino acid sequence. The FAD-GPDH homologues in hyperthermophiles carries NAD(P) binding site in their small subunit and represents a new type of FAD-GPDH, represented by the purified one from *T. maritima*. They may have NADH oxidase activity besides their FAD-GPDH activity, like the enzyme from *T. maritima* and are likely to be multifunctional enzymes.

The first step of glycerol utilization is the phosphorylation of glycerol to G-3-P. Subsequently, G-3-P could be converted to dihydroxyacetone phosphate, which would be converted to pyruvate then further oxidized to acetate and coupled to energy conservation. There would be two net ATPs, one NADH, and two reduced ferredoxins produced from one glycerol to acetate in *T. maritima* (Schröder et al. 1994). The growth of *T. maritima* using glycerol as sole carbon source was observed in our laboratory (Ronholm and Ma 2006). It was reported that *Thermotoga neapolitana* could use both DL-α-glycerol phosphate and glycerol as carbon source (Van Ooteghem et al. 2004), but there were no report about the enzymes involved. *T. maritima* FAD-GPDH exhibited an optimal pH of 7.5, which is a characteristic feature of FAD-GPDHs studied to date when tetrazolium dye is used as the electron acceptor (Kistler and Lin 1972; Ringler 1961). In contrast, the NAD^+-GPDH requires a higher pH at 9.5 for maximal activity (Kito and Pizer 1969; Shen et al. 2003).

The growth of *E. coli* with glycerol under anaerobic conditions requires fumarate added (Kistler and Lin 1972). Anaerobic FAD-GPDH and fumarate dehydrogenase in *E. coli* form a complex that can catalyze the dehydrogenation of G-3-P without any added cofactor (Lin 1976; Miki and Lin 1973). Whether exogenous electron acceptor that may serve as the electron acceptor for FAD-GPDH and hence stimulates the growth of *T. maritima* on glycerol requires further study. FAD-GPDH is essential for the catabolism of glycerol. It was reported that *E. coli* mutant lacking *glpD* encoding aerobic FAD-GPDH or *glpA* encoding anaerobic FAD-GPDH could not grow with glycerol as sole carbon source like the wild type (Lin 1976). The *glpD* deficient *B. subtilis* could not grow on glycerol either (Lindgren and Rutberg 1974). Therefore, besides its role in oxygen defensive system (Yang and Ma 2007), *T. maritima* FAD-GPDH may also play an important role in the glycerol dissimilation in *T. maritima* cells.

Chapter 7 Purification and Characterization of Thioredoxin Reductase and Thioredoxin from Hyperthermophilic Bacterium *Thermotoga maritima*

A manuscript has been prepared for submission based on the work presented in this chapter.

7.1 ABSTRACT

The cell-free extract of *Thermotoga maritima* was found to have a high BVOR activity, which is a normal catalytic property of FNOR. An enzyme was purified to homogeneity from *T. maritima* cell-free extract using FPLC system by following BVOR activity. The purified enzyme was a homodimeric flavoprotein with a subunit of 37 kDa revealed by SDS-PAGE. Based on peptides mass fingerprints, this protein was identified to be NP_228678 (TrxB), which was annotated as thioredoxin reductase (TrxR) in *T. maritima*. The protein sequence showed high identities and similarities to typical bacterial TrxRs with molecular weight around 35 kDa. The purified enzyme catalyzed the reduction of BV preferably with either NADH or NADPH as electron donor. Its catalytic properties showed characteristics of Michaelis-Menten kinetics with an apparent V_{max} value of 1111 μmol NADH oxidized min^{-1} mg^{-1}. The apparent K_m values were determined to be 89 and 73 μM for BV and NADH, respectively. When NADH was used as electron donor it exhibited high activity within a broad pH range and maximum activity with 100 mM, glycine buffer at pH 9.5. When NADPH used as electron donor, the optimal pH was found to be 6.5 and the K_m and V_{max} values were determined to be 0.78 mM and 115 U/mg, respectively. The BVOR activity elevated along with the increasing of temperature up to 95°C. This enzyme exhibited very high thermostability, similar to other TrxRs. More than 60% of the activity remained after incubation for 28 hours at 80°C, which is the optimal growth temperature of *T. maritima*. Thioredoxin (Trx) was also purified to homogeneity following the DTT-dependent reduction of insulin. The purified Trx was a monomer with molecular weight of 31 kDa revealed by SDS-PAGE. The single band on SDS-PAGE was identified to be glutaredoxin (Grx)-like protein by mass spectrometry. Trx exhibited both insulin reduction and thiotransferase activity. It was found that the purified *T. maritima* TrxR and Trx could act as NAD(P)H-dependent protein disulfide reductase system for the reduction of insulin and DTNB. This is the first Trx-TrxR system described in hyperthermophilic bacteria.

7.2 INTRODUCTION

Thermotoga maritima is a hyperthermophilic anaerobic bacterium capable of growing at 90°C. It utilizes carbohydrates and cell extract as energy and carbon sources, and produces H_2, CO_2 and acetate (Huber et al. 1986). During fermentation, reduced ferredoxin and NADH are produced as the major reducing equivalent and eventually used by hydrogenase to produce hydrogen in order to get fermentation going (Schröder et al. 1994). FNOR, a bridge enzyme to shuttle between one electron and two electron carrier, was detected in *T. maritima* and *T. neapolitana* by following BVOR activity assay (Käslin et al. 1998; Schröder et al. 1994). There is no FNOR reported from hyperthermophilic bacteria yet.

In contrast to the oxidized environment in the cell surface, the inside of the cell is kept reduced and proteins contain many free sulfhydryl groups and disulfides are rare (Arnér and Holmgren 2000; Gilbert 1990). Disulfide bonds in protein are very important either as structural features to stabilize protein or part of catalytic cycles (Ritz and Beckwith 2001). The major ubiquitous disulfide reductase responsible for maintaining proteins in their reduced state is Thioredoxin (Trx), which is reduced by thioredoxin reductase (TrxR) using NADH or NADPH as electron donor in archaea, bacteria, and eukaryotes (Bindoli and Rigobello 2002; Hirt et al. 2002; Holmgren 1985). TrxRs are enzymes belonging to the flavoprotein family of pyridine nucleotide-disulfide oxidoreductase including lipoamide dehydrogenase, mercuric reductase, glutathione reductase, and NADH oxidase (Williams 1992). TrxRs can reduce oxidized Trxs, a group of small (10-12 kDa) peptides that can supply reducing equivalents to ribonucleotide reductase, thioredoxin peroxidase and certain transcription factors through thiol-disulfide exchange (Figure 7-1; Baker et al. 1997; Chae et al. 1994; Laurent et al. 1964). The study of Trx-TrxR system in hyperthermophilic microorganisms is not as extensive as that in the mesophiles and some distinct properties have shown up. The Trx from *Aeropyrum pernix* is 37 kDa, several times bigger than the conventional Trx and the TrxR has different substrate spectrum to other TrxR characterized from microbial sources (Jeon and Ishikawa 2002). Based on the sizes, TrxRs can be classified in to two types: one type with high molecular weight (~55 kDa, designated H-TrxR) and containing selenocysteine characterized from animals and protozoan malaria parasite (Gladyshev et al. 1996; Tamura and Stadtman 1996); the other type with low molecular weight (~35 kDa, designated L-TrxR) characterized from archaea, bacteria, and lower eukarya (Hirt

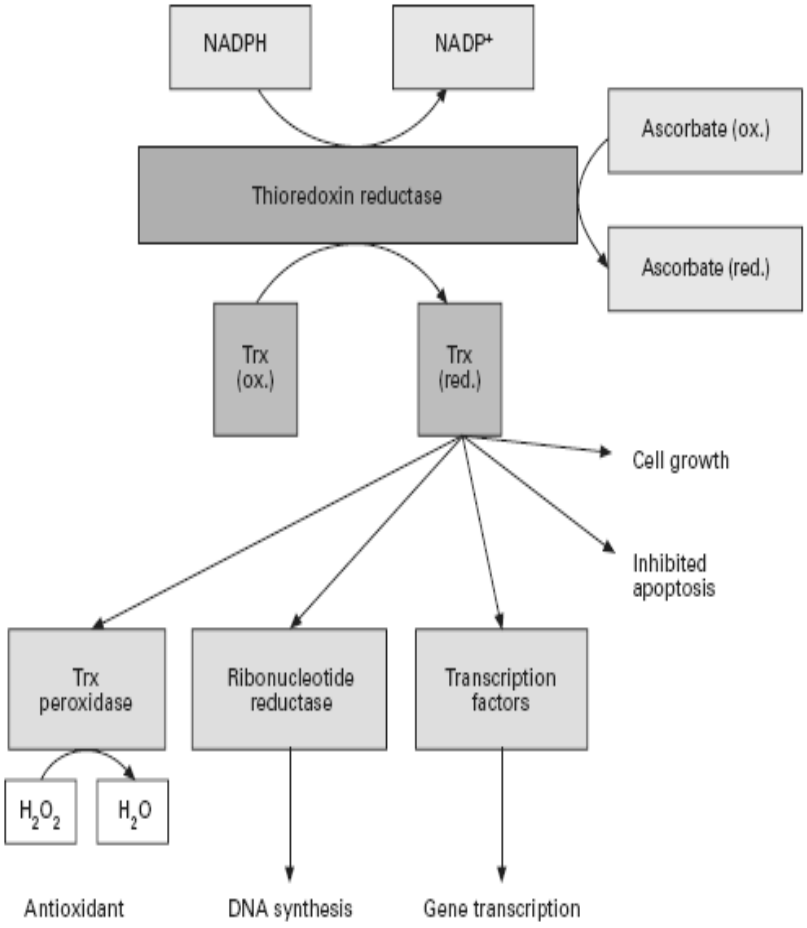

Figure 7-1 General reactions and functions of TrxR in the cell (Modified from Mustacich and Powis 2000).

TrxR utilizes NADPH to reduce oxidized (ox.) Trx or ascorbate into reduced (red.) Trx and ascorbate, respectively. Reduced Trx then provides reducing equivalents to (i) Trx peroxidase, which breaks down H_2O_2 to water, (ii) ribonucleotide reductase, which reduces ribonucleotides to deoxyribonucleotides for DNA synthesis, and (iii) transcription factors, which leads to their increased binding to DNA and altered gene transcription. In addition to the above functions, Trx increases cell growth and inhibits apoptosis.

et al. 2002). These two groups have distinct amino acid sequences and catalytic mechanisms. H-TrxRs are related to glutathione reductase, tryptophane reductase, mercuric reductase, and lipoamide dehydrogenase, while the L-TrxRs are related to the alkyl hydroperoxide reductase F52A (AphF) (Poole et al. 2000). TrxR has been characterized from hyperthermophilic archaea, *Pyrococcus horikoshi* (Jeon and Ishikawa 2002), *Aeropyrum pernix* (Kashima and Ishikawa 2003), and *Sulfolobus solfataricus* (Ruocco et al. 2004). The study indicates that TrxRs are involved in redox regulation and oxidative stress defence systems. There is no Trx-TrxR system known in hyperthermophilic bacteria yet. Here we report the purification and characterization of TrxR and Trx from *T. maritima*.

7.3 MATERIALS AND METHODS

7.3.1 Organism and chemicals

T. maritima (DSM3109) was obtained from the Deutsche Sammlung von Mikroorganismen and Zellkulturen, Braunschweig, Germany. All chemicals were from commercially available products except dihydrolipoamide was prepared by reduction of *dl*-lipoamide with sodium borohydride (Reed et al. 1958). Details were described in Chapter 4 (4.3.1 Organism and chemicals).

7.3.2 Growth of *T. maritima*

T. maritima was cultured at 80°C in a 15 L carboy in a medium modified from that of Huber (Huber et al. 1986). The detailed composition of the media was described in Chapter 4 (4.3.2 Growth of *T. maritima*). The cells were harvested by centrifugation at 13,000x*g* and the cell pellet obtained was frozen at -80^{o}C until use.

7.3.3 Enzyme assays and protein determination

BVOR activity was determined in an anaerobic glass cuvette by monitoring the NADH-dependent BV reduction spectrophotometrically at 580 nm (ε_{580}=8.8 $mM^{-1}cm^{-1}$) at 80^{o}C (Ma and Adams 1994). The assay mixture (2 ml) contained 1 mM BV and 0.2 mM NADH in pH 9.5, 100 mM glycine-NaOH buffer. One unit of enzyme activity was defined as 2 μmol BV reduced per min. The NADH oxidase activity was determined in a glass cuvette by monitoring O_2-dependent oxidation of NADH spectrophotometrically at 340 nm (ε_{340}=6.22 mM^{-1} cm^{-1}) at 80°C (Yang and Ma 2005a). Lipoamide dehydrogenase and glutathione reductase activity were monitored by following the substrate-dependent absorbance change of NADH at 340 nm (Patel et al. 1998; Tsai 1980). Trx activity was monitored by following the insulin reductase activity according to Holmgren (1979). The standard assay mixture contained 100 mM sodium phosphate buffer pH 7.0, 0.13 mM bovine insulin, 1 mM DTT, aliquot of fractions from purification steps or purified *T. maritima* Trx. The increase of absorbance at 650 nm was monitored at 30^{o}C. Grx activity was tested with thiotransferase assay (Gan and Wells 1986). The assay mixture contained varied amount of *T. maritima* Trx, 0.35 mM NADPH, and 0.5 mM reduced glutathione, 1 U glutathione reductase from yeast (Sigma), 2.5 mM 2-hydroxyethyl disulfide or 2.5 mM L-cystine, 1 mM EDTA in pH 8.0, 100 mM sodium phosphate

buffer. The absorbance change at 340 nm was monitored at 30°C. The control without *T. maritima* Trx added was subtracted.

TrxR activity was evaluated with two methods at 30°C. In the insulin reduction method (Arner et al. 1999), the purified *T. maritima* TrxR (50 nM) was added to the assay mixture (0.5 ml) containing 0.2 mM NAD(P)H, 0.13 mM insulin, and 0-1.4 μM *T. maritima* Trx, 1 mM EDTA, in pH 7.0, 100 mM sodium phosphate buffer. The increase of absorbance at 650 nm was monitored. In the DTNB reduction method (Kashima and Ishikawa 2003), purified *T. maritima* TrxR (50 nM) was added to the assay mixture (0.5 ml) containing 0.2 mM NAD(P)H, 0.1 mM DTNB, and 0-1.4 μM *T. maritima* Trx, 1 mM EDTA, in pH 7.0, 100 mM sodium phosphate buffer. The activity was calculated from the increase of absorbance at 412 nm (ε_{412}=13.6 mM^{-1} cm^{-1}) and the reduction of DTNB by 1 mole NAD(P)H forms 2 moles of 2-nitro-5-thiobenzoate. Protein concentration was determined using Bradford method with bovine serum albumin as the standard protein (Bradford 1976).

7.3.4 Enzyme purification

T. maritima cell-free extracts were prepared anaerobically by using similar procedures described previously (Yang and Ma 2005a). Though Trx and TrxR are not oxygen sensitive, the purification was carried out along with other anaerobic enzymes, so all the purification steps were carried out anaerobically. 100 mM sodium phosphate buffer pH 7.0, instead of glycine-NaOH, was used for BVOR assay during TrxR purification. The cell–free extract was applied at a flow rate of 3 ml/min to a DEAE-Sepharose Fast Flow column (5 x 10 cm; Amersham Biotech, Quebec, Canada) that was pre-equilibrated using buffer A [50 mM Tris-HCl, pH 7.8, 5% (v/v) glycerol, 2 mM SDT, and 2 mM DTT]. The column was eluted with a linear gradient of 0-0.3 M NaCl in buffer A at a flow rate of 3 ml/min. The TrxR and Trx started to elute out as 0.08 M and 0.17 M NaCl was applied to the column, respectively. The fractions with high activities were pooled and applied to a HAP (Bio-Rad) column (2.6 x 10 cm) equilibrated with buffer A. The column was eluted with a linear KH_2PO_4 (0-0.15 M) in buffer A at a flow rate of 2 ml/min. The TrxR and Trx started to elute out as 0.05 M and 0.08 M KH_2PO_4 applied to the column. Activity-containing fractions were pooled together and applied to a Phenyl-Sepharose HP column (2.6 x 8 cm, Amersham Biotech, Quebec, Canada) equilibrated with 0.8 M $(NH_4)_2SO_4$ in buffer A (for Trx, SDT and DTT were omitted in all buffers for Phenyl-Sepharose and columns applied later on). The column was eluted with a $(NH_4)_2SO_4$ gradient (0.8-0

M) at a flow rate of 2 ml/min. TrxR was eluted as 0.8 M $(NH_4)_2SO_4$ was applied to the column. While Trx was eluted as 100% buffer A was applied to the column. Fractions containing high activities were pooled and concentrated by ultra filtration separately (Amicon Ultra filter, YM 10 membrane). The concentrated fraction (3.0 ml) was applied to a Superdex 200 column (2.6 x 60 cm, Amersham Biotech, Quebec, Canada) equilibrated with buffer A containing 100 mM KCl. The flow rate was 2 ml/min. Fractions containing high enzyme activities were combined and applied to a Q-Sepharose HP column (1 x 10 cm, Amersham Biotech, Quebec, Canada) equilibrated with buffer A. The column was eluted with a linear gradient of NaCl (0-0.5 M) at a flow rate of 1.0 ml/min. TrxR and Trx started to elute out as 0.13 M and 0.1 M NaCl was applied to the column, respectively. Fractions containing pure TrxR and Trx as revealed by SDS-PAGE (Laemmli 1970) were stored at -20°C till use.

7.3.5 Determination of molecular mass and protein identification

The native molecular mass of both *T. maritima* TrxR and Trx were estimated by gel filtration on Superdex 200 column (2.6 x 60 cm). The column was calibrated with commercial protein standard (Pharmacia, NJ, USA) that contained blue dextran (2000,000 Da), thyroglobulin (669,000 Da), ferritin (440,000 Da), catalase (232,000 Da), aldolase (158,000 Da), bovine serum albumin (67,000 Da), ovalbumin (43,000 Da), chymotrypsinogen A (25,000 Da), and ribonuclease A (13,700). The subunits molecular weights were determined by SDS-PAGE (Laemmli 1970) and a standard curve obtained using the low molecular weight standard from Bio-Rad (Bio-Rad Laboratories, ON, Canada). The single band of TrxR and Trx on SDS-PAGE were cut separately in flow hood and digested in-gel with trypsin. The resulting peptides were extracted and cleaned with the procedures described previously (Shevchenko et al. 1996). The cleaned peptides samples were used for protein identification using mass spectrometry. The details were described in Chapter 6 (6.3.5 Gene identification and sequence analysis).

7.3.6 Analysis of flavin cofactor

The oxidized and NADH-reduced enzyme samples were scanned with Carry 50 UV-visible spectrophotometer from 190-600 nm. FAD was released from TrxR by boiling in methanol (1:9) for 10 min (Stanton and Jensen 1993). The amount of FAD was estimated using the absorbance value at 450 nm (ε_{450}=11.3 $mM^{-1}cm^{-1}$, Whitby 1953). The sample was concentrated by flushing with nitrogen

before it was spotted on a thin layer silica gel plate (5x10 cm, 200 μm; Selecto Scientific, USA) together with commercially available flavin standards, riboflavin, FMN, FAD. Samples were ascended in the dark with *n*-butanol-acetic acid-H_2O (12:3:5) as solvent. Samples on the plate were visualized using FluorChem (FluorChem 8000 Chemiluminescence and Visible Imaginng System, Alpha Innotech Corporation, CA, USA) under UV light after drying the silica plate with a hair dryer.

7.4 RESULTS

7.4.1 Purification of *T. maritima* TrxR and Trx

Cell-free extract from 50 g of *T. maritima* was prepared anaerobically and loaded to a DEAE-Sepharose column. After the first of five columns that were used for the purification, BVOR activity appeared in two peaks. The major one (70% of the total activity) started to elute out when 0.08 M NaCl was applied to the column. The second peak (30%), corresponding to a highly active NADH oxidase (Yang and Ma 2007), started to elute out when 0.1 M NaCl was applied to the column. The active fractions in the first peak were pooled together and applied to HAP column for further TrxR purification. BVOR activity was eluted out as predominant single peak for all the columns thereafter. The enzyme was purified 378-fold after five columns (Table 7-1). The purity of the enzyme after the last column was confirmed using SDS-PAGE that showed a single band with molecular weight of 37 kDa (Figure 7-2). The native molecular weight of the purified enzyme was estimated to be 67 kDa using a Superdex-200 gel filtration column that was calibrated using standard proteins. Therefore, it is reasonable to conclude that the purified enzyme was a homodimer, which is similar to L-TrxR. Trx activity was eluted out as single peak after all the five columns. Trx bound to Phenyl-Sepharose column tightly. It could not be eluted out with buffer A, but with water alone, which may indicate *T. maritima* Trx is more hydrophobic than most soluble proteins. After Q-Sepharose column, the enzyme was purified which was revealed by a single band with a molecular weight of 31 kDa showing on SDS-PAGE (Figure 7-3). The native molecular weight of *T. maritima* Trx was estimated to be 23 kDa by Superdex 200 gel filtration column calibrated with standard proteins. Therefore, the purified *T. maritima* Trx is very likely to be a monomer.

7.4.2 Mass spectrometry identification and sequence analysis

Since the genome of *T. maritima* is available (Nelson et al. 1999), the purified two enzymes were identified by mass spectrometry. Based on peptides mass fingerprints, the purified TrxR was identified to be NP_228678 (TM0869), which was annotated as TrxR. The amino acid sequence of *T. maritima* TrxR was aligned with other (hyper) thermophilic TrxR sequences, *P. horikoshii* TrxR (PhTrxR), *A. pernix* K1 TrxR (AeTrxR), *S. solfataricus* TrxR (SsTrxR) and *Thermus aquatics* NADH: peroxiredoxin oxidoreductase (TaDpor), and *E. coli* TrxR (EcTrxR) (Figure 7-4). Similar to other L-TrxRs, *T. maritima* TrxR has two active cysteines (CXXC), two FAD-binding regions, one NAD(P)-binding region, and one conserved region of pyridine

Table 7-1 Purification table of *T. maritim*a TrxR

Steps	Total protein (mg)	Total unit (U)	Sp act (U/mg)	Purification fold	Recovery (%)
Cell-free extract	2004	1680	0.7	1	100
DEAE-Sepharose	570	995	1.74	2.5	59
HAP	176	779	4.42	6.3	46
Phenyl-Sepharose	25.2	529	21	30	31
Gel filtration	4.16	458	110	157	27
Q-Sepharose	0.78	206	265	378	12

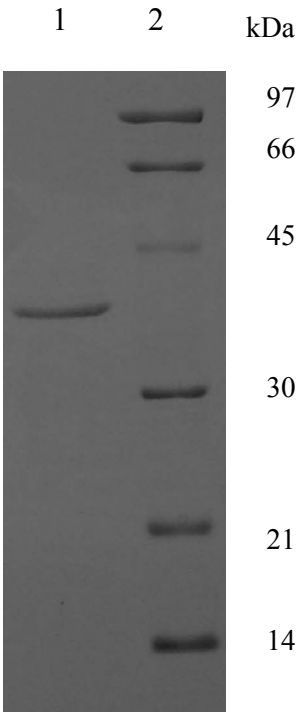

Figure 7-2 12.5% SDS-PAGE of the purified TrxR from *T. maritima*.

The purified *T. maritima* TrxR (lane 1, 1μg) and low molecular weight standards (lane 2) are indicated along with their corresponding molecular masses.

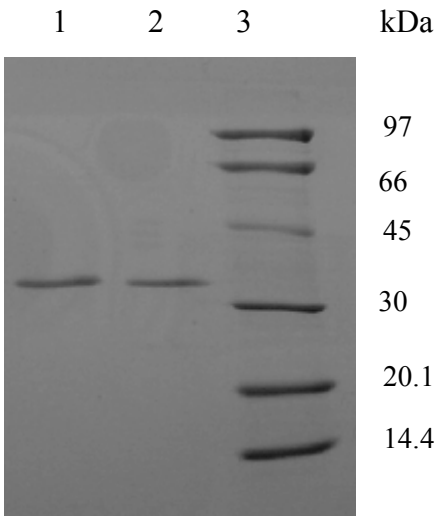

Figure 7-3 12.5% SDS-PAGE of the purified Trx from *T. maritima*.

The purified T. *maritima* Trx (lane 1 and 2, 0.4 and 0.6 ug), low molecular weight standard as indicated along the bands (lane 3).

```
                    10         20         30         40         50
TmTrxR      -------MVF FDTGSLKKKE IKDKYDIVVV GGGPAGLTSA IYARRAGLSV
PhTrxR      -MEVKEMFSL GGGLGRSKVD ESKVWDVIII GAGPAGYTAA IYAARFGLDT
AeTrxR      MIRCVIMPLR LSAVRAPKIP RGEEYDTVIV GAGPAGLSAA IYTTRFLMST
SsTrxR      ---------M SLLPRTTSVK PGEKFDVIIV GLGPAAYGAA LYSARYMLKT
EcTrxR      ---------- --------MG TTKHSKLLIL GSGPAGYTAA VYAARANLQP
Clustal Co                          .  . ::: * ***.  :* :*: *  :.

                    60         70         80         90
100
TmTrxR      LVVEKAIEGG YVNLTHLVEN YPGFPA-ISG EELASKFKEH AEKFGADIYN
PhTrxR      IIITKDLGG- NMAITDLIEN YPGFPEGISG SELSKKMYDQ VKKYGVEVII
AeTrxR      LIVSMDVGG- QLNLTNWIDD YPGMGG-LEA SKLVESFKSH AEMFGAKIVT
SsTrxR      LVIGETPGG- QLTEAGIVDD YLGLIE-IQA SDMIKVFNKH IEKYEVPVLL
EcTrxR      VLITGMEKGG QLTTTTEVEN WPGDPNDLTG PLLMERMHEH ATKFETEIIF
Clustal Co  :::     *   :  :  ::: : *    : .   : . : .:    : . :

                   110        120        130        140        150
TmTrxR      AEVVKLEVQG DKK------- VVELDDGKRI EAPVVIVATG ANPKKLNVPG
PhTrxR      DEVIRIDPAE CAYYEGPCNF VVKTANGKEY KAKTIIIAVG AEPRKLNVPG
AeTrxR      GVQVKTVDRL DDGW-----F LVRGSRGLEV KARTVILAVG SRRRKLGVPG
SsTrxR      DIVEKIENRG DE-------F VVKTKRKGEF KADSVILGIG VKRRKLGVPG
EcTrxR      DHINKVDLQN RPFR------ --LNGDNGEY TCDALIIATG ASARYLGLPS
Clustal Co      :                          .   .  :*:. *    : *.:*.

                   160        170        180        190        200
TmTrxR      EKEFFGKGVS YCATCDGYLF AGK-DVIVVG GGDSACDESI FLSNIVNKIT
PhTrxR      EKEFTGRGVS YCATCDGPLF VGK-EVIVVG GGNTALQEAL YLHSIGVKVT
AeTrxR      EAELAGRGVS YCSVCDAPLF KGKDAVVVVG GGDSALEGAL LLSGYVGKVY
SsTrxR      EQEFAGRGIS YCSVCDAPLF KNR-VVAVIG GGDSALEGAE ILSSYSTKVY
EcTrxR      EEAFKGRGVS ACATCDGFFY RNQ-KVAVIG GGNTAVEEAL YLSNIASEVH
Clustal Co  *  : *:*:*  *:.**. ::  .:  * *:* **::* : :   * .   ::

                   210        220        230        240        250
TmTrxR      MIQLLETLTA AKVLQERVL- --NNPKIEVI YNSTVREIRG KDK-VEEVVI
PhTrxR      LVHRRDKFRA DKILQDRFK- --QAG-IPAI LNTVVTEIKG TNK-VESVVL
AeTrxR      LVHRRQGFRA KPFYVEEAR- --KKPNIEFI LDSIVTEIRG RDR-VESVVV
SsTrxR      LIHRRDTFKA QPIYVETVK- --KKPNVEFV LNSVVKEIKG DKV-VKQVVV
EcTrxR      LIHRRDGFRA EKILIKRLMD KVENGNIILH TNRTLEEVTG DQMGVTGVRL
Clustal Co  :::  : : *   .  .       :   :     :  : *: *  .  *  * :
```

```
                260        270        280        290        300
TmTrxR      ENVKTGETKV -LKADGVFIF IGLDPNSKLL EG-LVELDPY GYVITDEN--
PhTrxR      KNVKTGETVE -KKVDGVFIF IGYEPKTDFV KH-LGITDEY GYIPVDMY--
AeTrxR      KNKVTGEEKE -LRVDGIFIE IGSEPPKELF EAIGLETDSM GNVVVDEW--
SsTrxR      ENLKTGEIKE -LNVNGVFIE IGFDPPTDFA KSNGIETDTN GYIKVDEW--
EcTrxR      RDTQNSDNIE SLDVAGLFVA IGHSPNTAIF EGQLELENGY IKVQSGIHGN
Clustal Co  .:  ..:       . *:*:  ** .* . :  :      :     :  .

                310        320        330        340        350
TmTrxR      -METSVKGIY AVGDVRKK-- NLRQIVTAVA DGAIAVEHAA KHYF------
PhTrxR      -MRTKVPGIF AAGDITN--- VFKQIAVAVG QGAIAANSAK EFIESWNGKT
AeTrxR      -MRTSIPGIF AAGDCTSMWP GFRQVVTAAA MGAVAAYSAY TYLQEKGLYK
SsTrxR      -MRTSVPGVF AAGDCTSAWL GFRQVITAVA QGAVAATSAY RYVTEKKGKK
EcTrxR      ATQTSIPGVF AAGDVMDH-- IYRQAITSAG TGCMAALDAE RYLDGLADAK
Clustal Co    .*.: *:: *.**  .      :*  .:..  *.:*.  *   .

            ....|...

TmTrxR      --------
PhTrxR      IE------
AeTrxR      PKPLTGLK
SsTrxR      --------
EcTrxR      --------
Clustal Co
```

Figure 7-4 Alignment of amino acid sequences of *T. maritima* TrxR and its homologues.

The sequences were aligned using CLUSTAL W method (Higgins and Sharp 1988). The alignment was plotted with reference to a standard sequence, i.e. the partial sequence of *T. maritima* TrxR at the top. Any residues in a column which are identical to the standard at that point are shown as stars (*) and similar to the standard at that point are shown as dot (·). The gap is shown as dash (-). TmTrxR: *T. maritima* TrxR; PhTrxR: *P. horikoshii* TrxR; AeTrxR: *A. pernix* K1 TrxR; SsTrxR: *S. solfataricus* TrxR; EcTrxR: *E. coli* TrxR. Green letters: FAD-binding motifs; blue letters: NAD(P)-binding motif; red letters: redox active center; underlined letters: pyridine nucleotide-disulfide oxidoreductase conserved region.

nucleotide-disulfide oxidoreductase. The purified *T. maritima* Trx was annotated to be Grx-related protein (encoded by TM0868), which is adjacent to TrxR gene, with predicted mass of 25158Da. The protein sequence showed both Grx and Trx folds (Nelson et al. 1999). It has two redox active sites, CQYC at N-terminus and CPYC at C-terminus (Figure 7-5). The BLAST (Altschul et al. 1997) search results showed *T. maritima* Trx had very high similarity (66-67%) to alkyl hydroperoxide reductase subunit F related protein of *Thermoplasma acidophilum* (Ruepp et al. 2000) and Grx-related protein in *P. furiosus* (Robb et al. 2001).

7.4.3 Identification of flavin cofactor of *T. maritima* TrxR

The purified TrxR was yellow, which was an indication of the presence of flavin. The oxidized enzyme solution showed characteristic flavin absorbance maxima: 380 nm and 450 nm. The peaks disappeared upon adding 0.1 mM NADH into the enzyme solution after 5 min (Figure 7-6). A yellowish cofactor was released after the enzyme was mixed with methanol and boiled for 10 min in the dark. This flavin cofactor was further identified as FAD using thin layer chromatography (Figure 7-7). The *T. maritima* TrxR contained 1.88 mol of FAD per mol native enzyme based on the absorbance value at 450 nm and protein amount from which the FAD was extracted. Since *T. maritima* TrxR was a homodimer, each subunit contained approximately one non-covalently bound FAD moiety.

7.4.4 Catalytic properties of the purified TrxR and Trx from *T. maritima*

The purified *T. maritima* TrxR was first characterized with BVOR assay when NADH was used as electron donor. The TrxR exhibited highest activity when pH 9.5, 100 mM glycine-NaOH was used as the assay buffer though it was very active over a broad pH range 8.5-11.0 (Figure 7-8). The enzyme activity was increased along with the elevation of the temperature up to 95^{o}C (Figure 7-9). The TrxR was very thermostable. It retained >60% of the BVOR activity after incubation at 80^{o}C for 28 hours and lost 50% of activity after incubation at 95^{o}C for 9 hours (Figure 7-10). The lost of activity upon heat at 80 and 95^{o}C did not follow first order kinetics. Its activity was dependent on concentrations of both NADH and BV. The catalysis followed Michaelis–Menten kinetics. Apparent K_m value for NADH and apparent V_{max} value were determined to be 73 μM and 1111 U/mg,

```
                    10         20         30         40         50
TmTrx       -MGILSDKDI AYLKDLFGKE LKRKVKIVFF KTEDKTRCQY CEITEQVLEE
TaAHF       MANLIRKEDR EYLKGEFEKY LKNDVDLVVF TSNDEN-CRY CKETVQLATE
AaGrx       --MLLNLDVR MQLKELAQKE FKEPVSIKLF S--QAIGCES CQTAEELLKE
PhGrx       -MGLISEEDK RIIKEEFFSK MVNPVKLIVF IG--KEHCQY CDQLKQLVQE
PfGrx       -MGLISDADK KVIKEEFFSK MVNPVKLIVF VR--KDHCQY CDQLKQLVQE
Clustal Co     ::        :*    .  : . *.: .*        *.  *.   ::  *

                    60         70         80         90        100
TmTrx       LVSVD----- -PKLELEIHD FDSD--KEAV EKYQVEMVPA TILLPEDGKD
TaAHF       VSEIN----- -PKIHLKVYN FDED--KEMV KKYGVEKYPA TIVSKAGVED
AaGrx       TVEVIGEAVG QDKIKLDIYS PFTH--KEET EKYGVDRVPT IVIE--GDKD
PhGrx       LSELT----- -DKLSYEIVD FDTPEGKELA EKYRIDRAPA TTITQ-DGKD
PfGrx       LSELT----- -DKLSYEIVD FDTPEGKELA KRYRIDRAPA TTITQ-DGKD
Clustal Co    .:         *:  .: .       ** . ::* ::  *:   :   . :*

                   110        120        130        140        150
TmTrx       YGIRFYGVPS GHEFGTLIQD IITVSEGKPQ LSEESIQKLQ SLEEPIRISV
TaAHF       GRIVYYGLPS GYEFGSLIED LKNVSMGEAD VSSKAAELIS KIDKPITIKV
AaGrx       YGIRYIGLPA GLEFTTLING IFHVSQRKPQ LSEKTLELLQ VVDIPIEIWV
PhGrx       FGVRYFGIPA GHEFAAFLED IVDVSKGDTD LMQDSKEEVS KIDKDVRILI
PfGrx       FGVRYFGLPA GHEFAAFLED IVDVSREETN LMDETKQAIR NIDQDVRILV
Clustal Co    : : *:*: * ** ::::. :  **  ..: : ..: : :   ::  : * :

                   160        170        180        190        200
TmTrx       FVTPTCPYCP RAVLMAHNMA MAS-----DK IIGEMIEANE YWELSEKFGV
TaAHF       YVTPTCPYCP RAVGTAHKFA LLN-----PN IKGEMIEALE FENEAEEVGV
AaGrx       FVTTSCGYCP SAAVMAWDFA LAN-----DY ITSKVIDASE NQDLAEQFQV
PhGrx       FVTPTCPYCP LAVRMAHKFA IENTKAGKGK ILGDMVEAIE YPEWADQYNV
PfGrx       FVTPTCPYCP LAVRMAHKFA IENTKAGKGK ILGDMVEAIE YPEWADQYNV
Clustal Co  :**.:* ***  *.  * .:* : .        * ..:::* *   : :::  *

                   210        220        230        240
TmTrx       SSVPHIVVNR DPSK--FFVG AYPEKEFINE VLRLAKG--- -----
TaAHF       SSVPHIVINN DVT----FIG AYPDDQFAEY VMEAYDHQ-- -----
AaGrx       VGVPKIVINK GVA---EFVG AQPENAFLGY IMAVYEKLKR EKEQA
PhGrx       MAVPKIVIQV NGEDKVQFEG AYPEKMFLEK LLSALS---- -----
PfGrx       MAVPKIVIQV NGEDRVEFEG AYPEKMFLEK LLSALS---- -----
Clustal Co   .**:**::  .      * * * *:. *    ::   .
```

Figure 7-5 Alignment of amino acid sequences of *T. maritima* Trx and its homologues.

The alignment was plotted with reference to a standard sequence, i.e. the partial sequence of *T. maritima* Trx at the top. Any residues in a column which are identical to the standard at that point are shown as stars (*) and similar to the standard at that point are shown as dot (·). The gap is shown as dash (-). TmTrx: *T. maritima* Trx; TaAHF, *Thermoplasma acidophilum* Alkyl hydroperoxide reductase subunit F related protein; PfGrx, *P. furiosus* Grx-related protein; AaGrx, *A. aeolicus* Grx-like protein; PhGrx, *P. horikoshii* Grx-like protein.

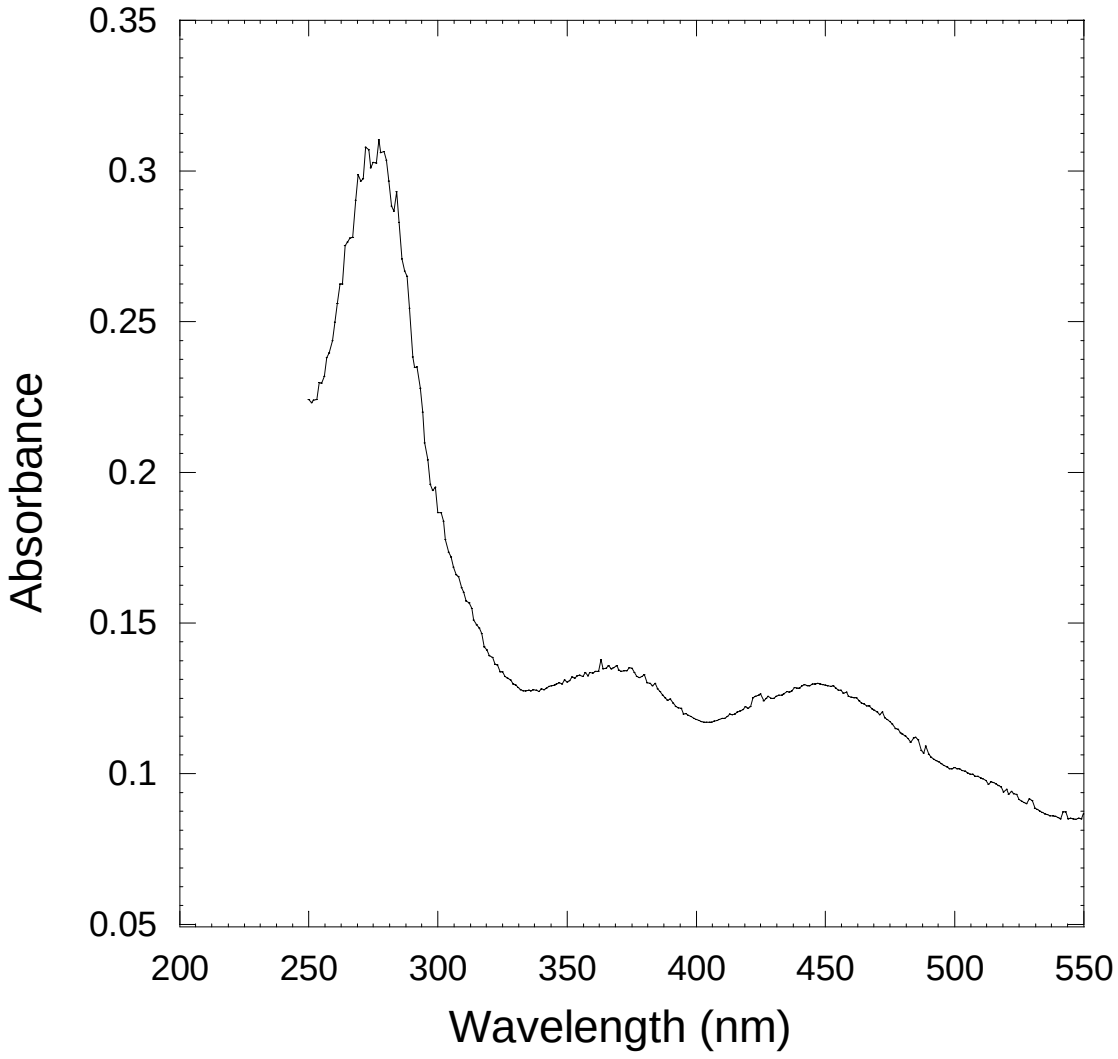

Figure 7-6 Spectrum of *T. maritima* TrxR.

The oxidized enzyme solution (0.11 mg in 1 ml pH 7.8, 50 mM Tris-HCl buffer) in a quartz cuvette was scanned to obtain an absorption spectrum from 190 nm to 600 nm using Varian Bio 50 UV-visible spectrophotometer.

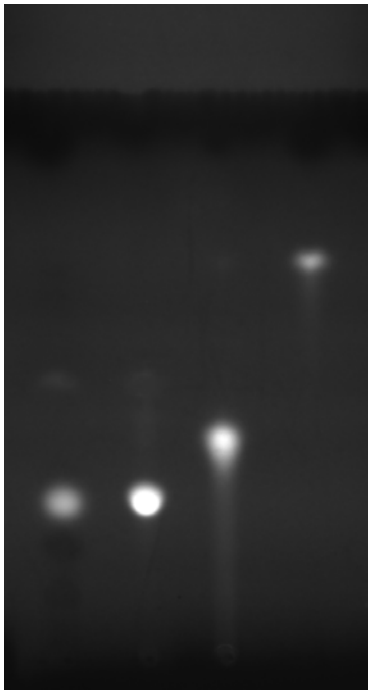

Figure 7-7 Flavin cofactor analysis of *T. maritima* TrxR.

The extracted sample from *T. maritima* TrxR was ascended on thin-layer plate in dark together with commercial standards.Lane 1, extracted sample from *T. maritima* TrxR; lane 2, FAD; lane 3, FMN; lane 4, riboflavin.

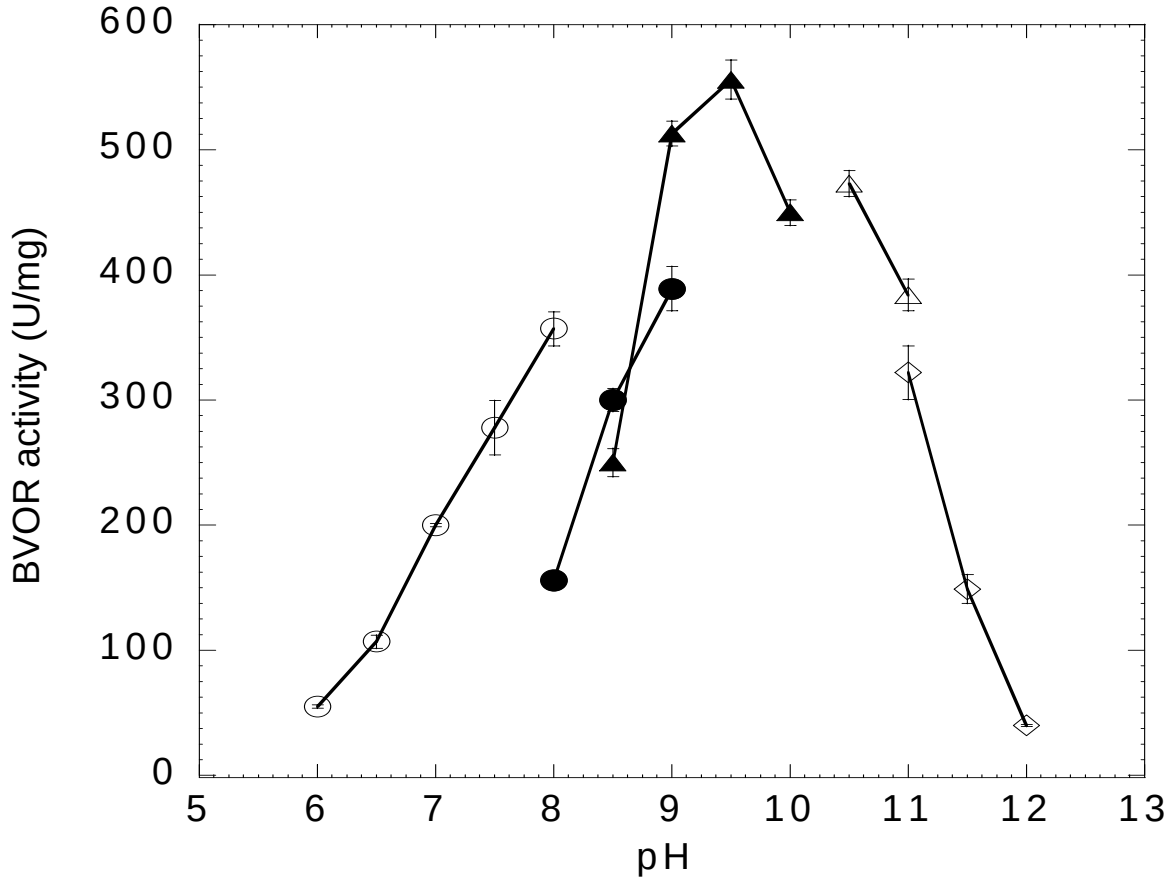

Figure 7-8 pH dependency of the purified TrxR from *T. maritima* using NADH as electron donor.

The activity was assayed at 80°C with NADH-dependent BV reduction. Open circles, 100 mM sodium phosphate buffer, pH 6.0-8.0; filled circles, 100 mM glycylglycine-NaOH buffer pH 8.0-9.0; filled triangles, 100 mM glycine-NaOH buffer pH 8.5-10.0; open triangles, 100 mM CAPS buffer pH 10.0-11.0; open diamonds, 100 mM sodium phosphate buffer pH 11.0-12.0.

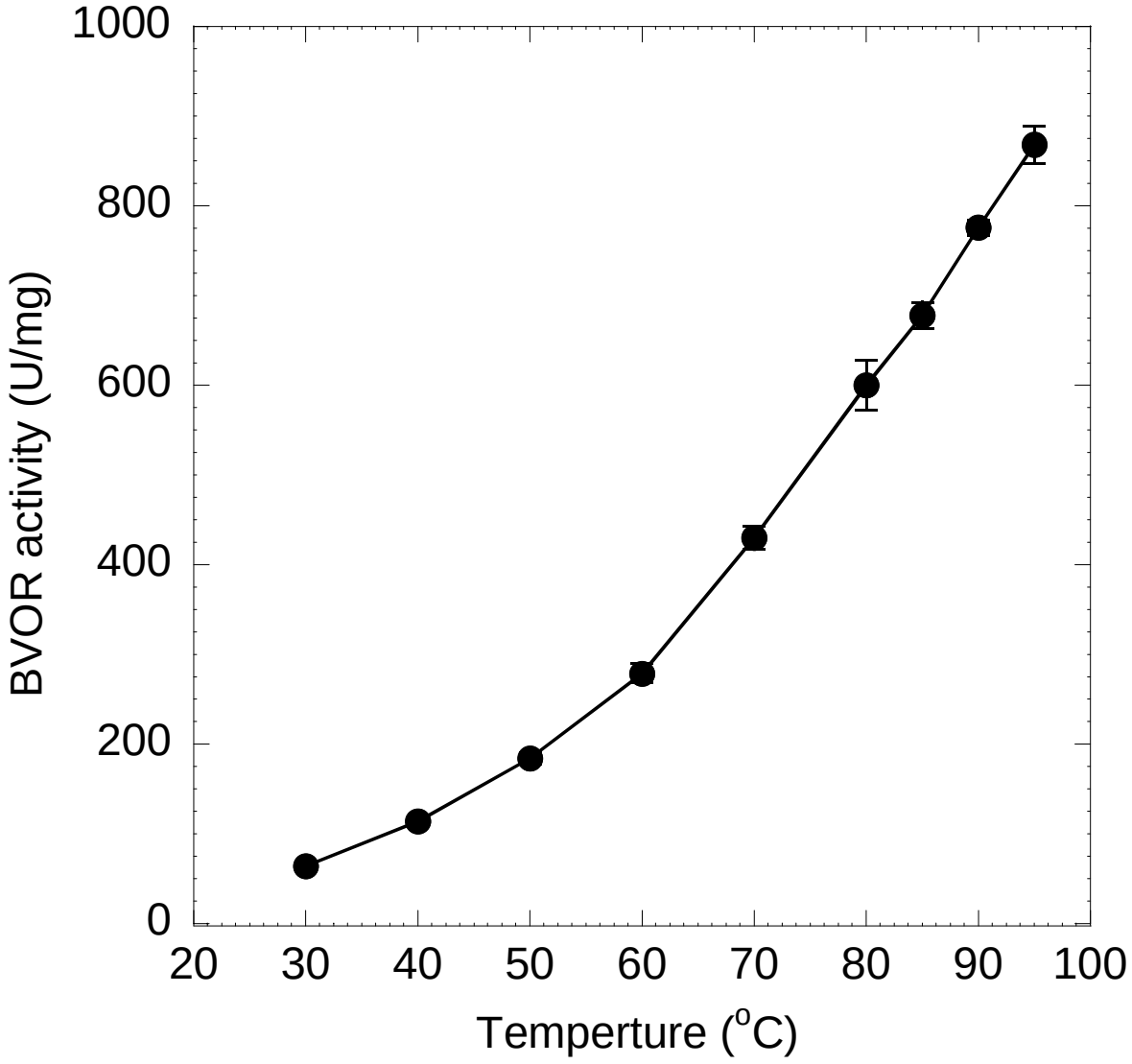

Figure 7-9 Temperature dependency of the purified TrxR from *T. maritima*.

The activity was determined using standard BVOR assay with temperature varying from 30 to 95°C.

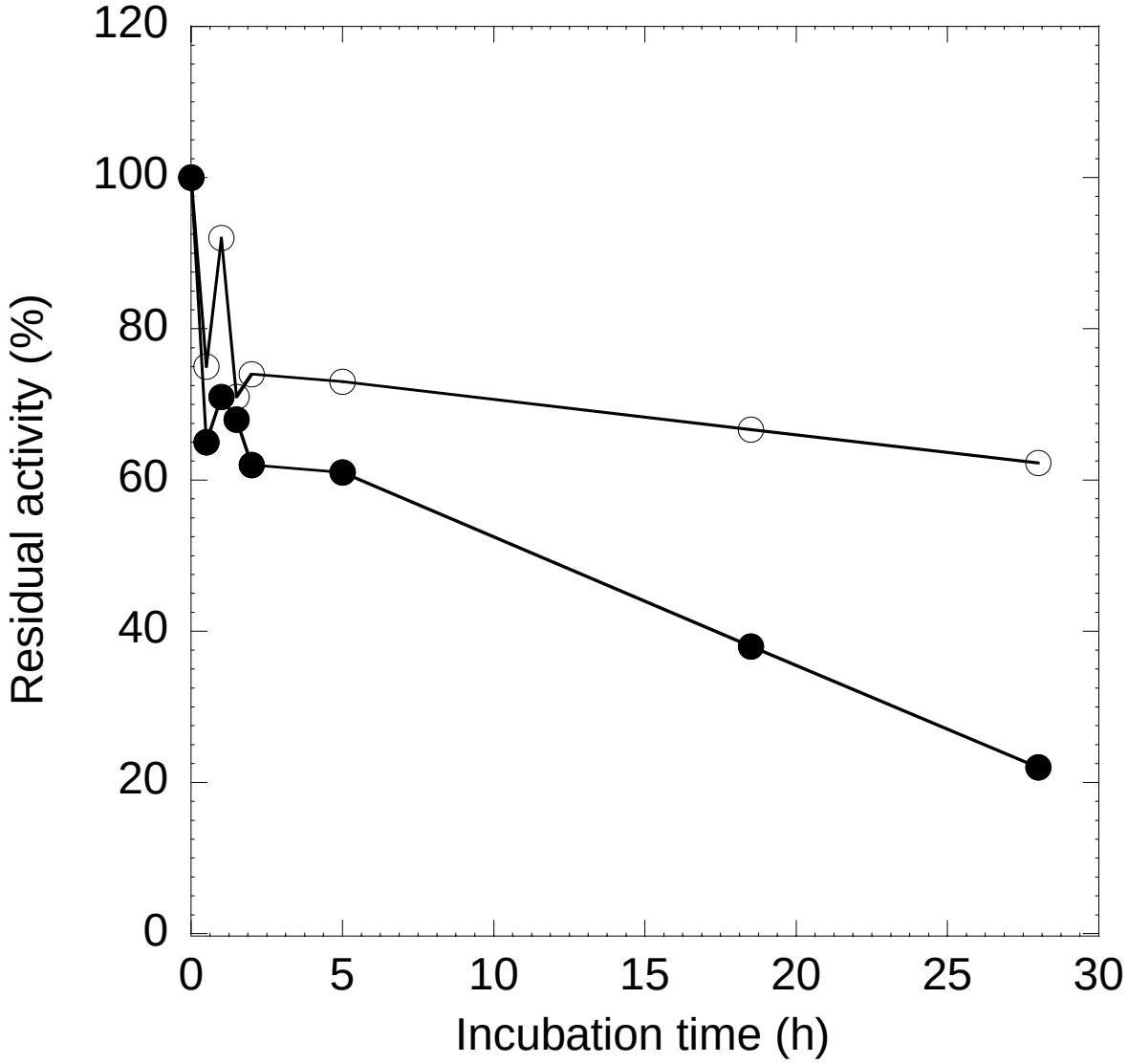

Figure 7-10 Thermostability of the purified TrxR from *T. maritima*.

The purified TrxR (0.06 mg ml^{-1}) in buffer A containing 0.1 M NaCl was incubated at 80°C (open circles) and 95°C (filled circles), respectively. The residual activities were assayed under standard BVOR assay conditions. 100% of activity was 690 U/mg.

respectively. Apparent K_m value for BV was determined to be 89 μM. TrxR showed preference of NADH over NADPH in BV reduction. The activity with NADPH was only 11% (pH 7.0, 100 mM sodium phosphate buffer) and 1.4% (pH 9.5, 100 mM glycine-NaOH) of that with NADH. The optimal pH of BVOR was determined to be 6.5 when NADPH was used as electron donor (Figure 7-11). The apparent K_m for NADPH and V_{max} were determined to be 0.78 mM and 115 U/mg, respectively, which was ten times lower than that of NADH. The substrate specificity of *T. maritima* TrxR were also surveyed with *T. maritima* Trx (7.4.6 Trx-TrxR system), oxidized glutathione (GSSG), lipoic acid, lipoamide, Na_2SeO_3, DTNB, and molecular oxygen. Neither lipoamide, lipoic acid, GSSG nor Na_2SeO_3 could be used as substrate for *T. maritima* TrxR. At pH 7.0, when NADH and NADPH were used as electron donors the BVOR activities were 139 and 9.9 U/mg, respectively. Besides BVOR activity, *T. maritima* TrxR also exhibited NAD(P)H oxidase activity. When molecular oxygen was used as electron acceptor, the specific activity was 22.3 U/mg, which is 16% of BVOR activity (139 U/mg) at 50°C. Interestingly, *T. maritima* TrxR could also catalyze the reduction of DTNB directly with NAD(P)H, which is unusual for a low molecular weight TrxR. *T. maritima* TrxR showed preference of NADH over NADPH with all the substrates tested.

7.4.5 Properties of *T. maritima* Trx

Trxs are known to have disulfide reductase activity using insulin as substrate. The reduced ß-chain of insulin precipitates out and causes the increase of turbidity monitored at 650 nm. The assay for reduction of insulin by DTT was performed at 30°C and pH 7.0. The insulin reduction was dependent on the amount of Trx in the assay system (Figure 7-12). Since *T. maritima* Trx has both Trx and Grx fold based on amino acid sequence information, Grx activity was tested with thiotransferase assay. Grx activity was observed with both L-cysteine (4.9 U/mg) and 2-hydroxyethyl disulfide (4.5 U/mg) as substrates.

7.4.6 The Trx-TrxR system

Trx mediated reduction of DTNB and insulin were carried out to see if the purified Trx and TrxR could form a Trx-TrxR system. The results showed that the insulin disulfide bonds were reduced in the presence of *T. maritima* TrxR and Trx when either NADH or NADPH was used as electron donor

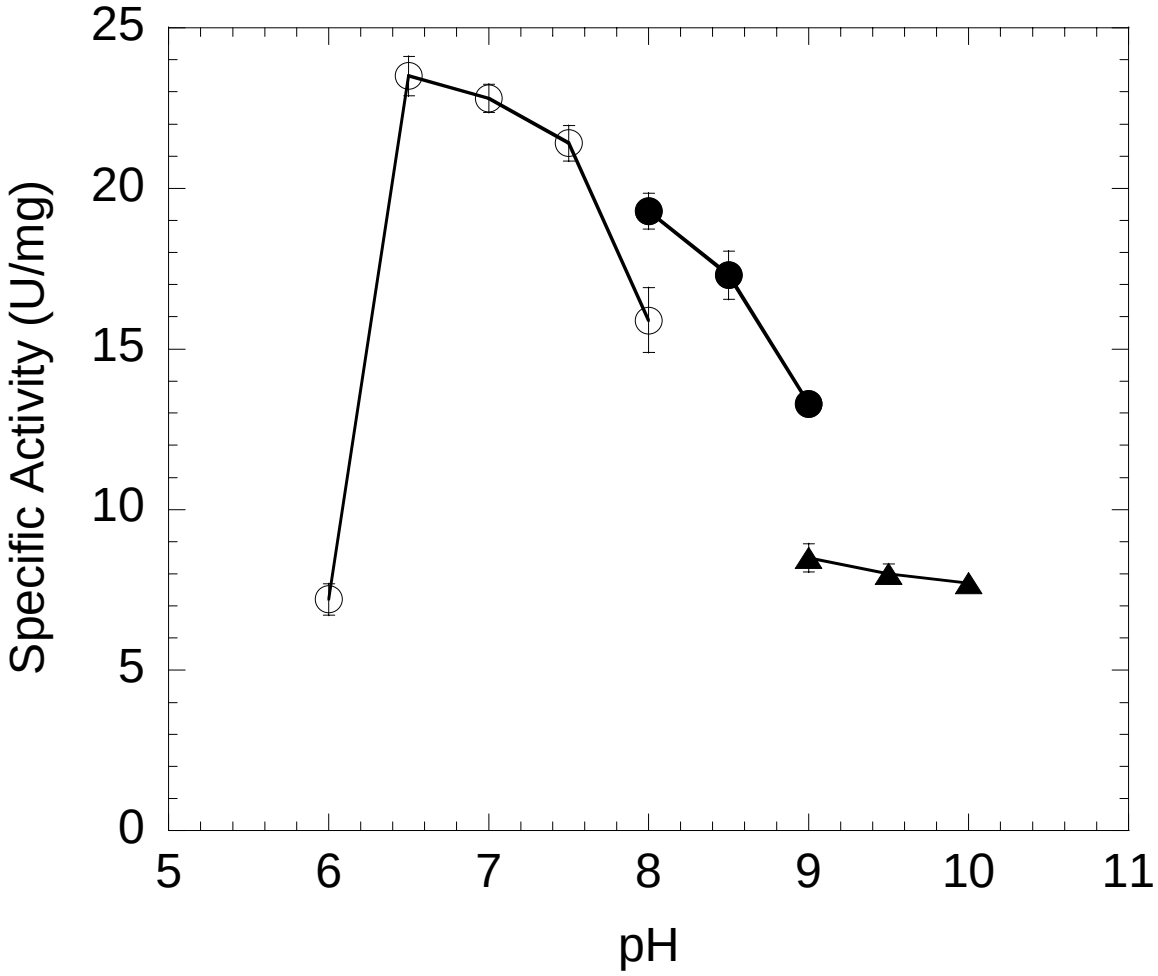

Figure 7-11 pH dependency of the purified TrxR from *T. maritima* using NADPH as electron donor.

The activity was assayed at 80°C with NADPH dependent BV reduction. Open circles, 100 mM sodium phosphate buffer, pH 6.0-8.0; filled circles, 100 mM glycylglycine-NaOH buffer pH 8.0-9.0; filled triangles, 100 mM glycine-NaOH buffer pH 8.5-10.0.

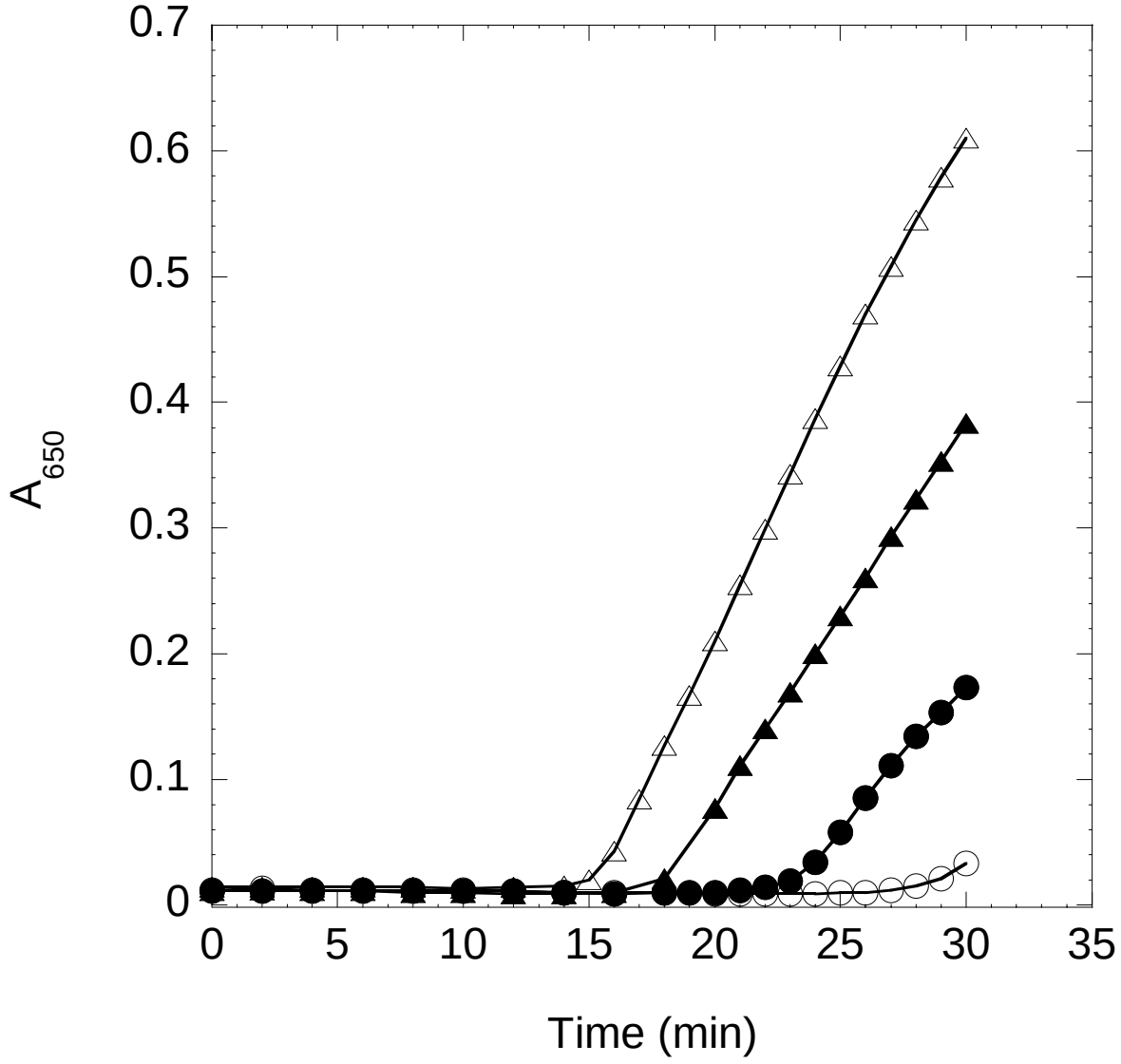

Figure 7-12 Reduction of insulin by *T. maritima* Trx.

The assay mixture contained 1 mM DTT and 1 mg/ml insulin in 100 mM, pH 7.0 sodium phosphate buffer. The reaction was carried out at 30°C by monitoring the increase of absorbance at 650 nm in the absence (open circles), and presence of *T. maritima* Trx (0.15 μM, filled circle; 0.29 μM, filled triangles; 0.58 μM, open triangles).

(Figure 7-13&Figure 7-14). The rate of insulin disulfide bonds reduction was faster when NADH was used as electron donor. The TrxR activity of *T. maritima* TrxR to reduce *T. maritima* Trx was examined using the DTNB coupled assay as well (Figure 7-15). *T. maritima* TrxR apparently formed Trx-TrxR system with *T. maritima* Trx, and the reduction activity of TrxR was dependent on the concentration of Trx (Figure 7-15, column 2-4). There was a very low activity of DTNB reduction in the absence of Trx. These results clearly indicate that *T. maritima* Trx, which has a high homology with *P. furiosus* Grx-like protein, had Trx-like activity and formed a redox system with TrxR in *T. maritima* cell. The system formed by *T. maritima* TrxR and Trx was capable of rapidly reducing both small-molecule (DTNB) and protein (bovine insulin) disulfide-containing substrates in the presence of NADPH or NADH.

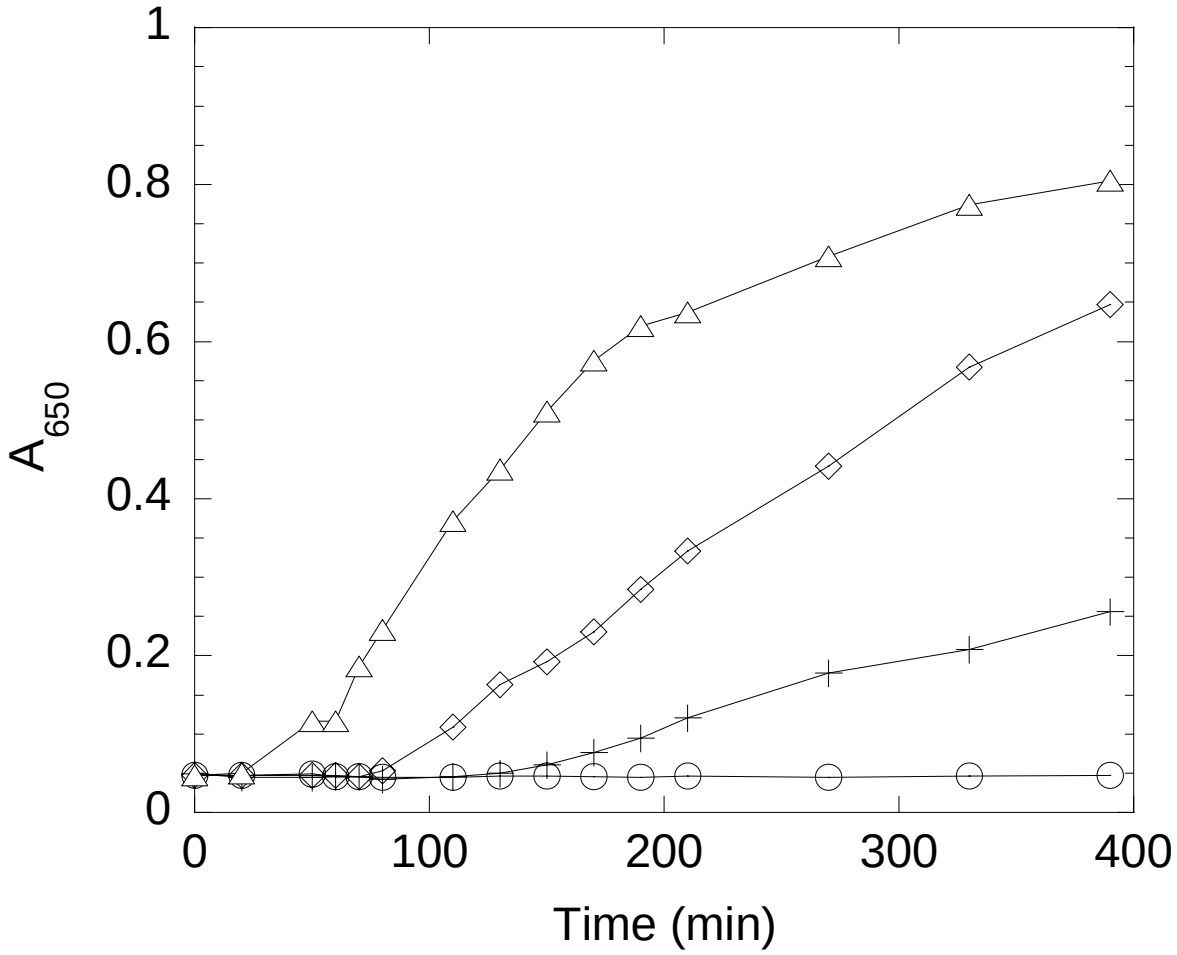

Figure 7-13 Reduction of insulin by Trx-TrxR system with NADH as electron donor.

The assay mixture contained 50 nM Tm TrxR, 0.2 mM NADH, 0.13 mM insulin, and varied amount of *T. maritima* Trx (opened circles, 0 μM; crosses, 0.36 μM; diamonds, 0.72 μM; triangles, 1.44 μM), 1 mM EDTA, in pH 7.0, 100 mM sodium phosphate buffer. The increase of absorbance at 650 nm was monitored at 30^{o}C.

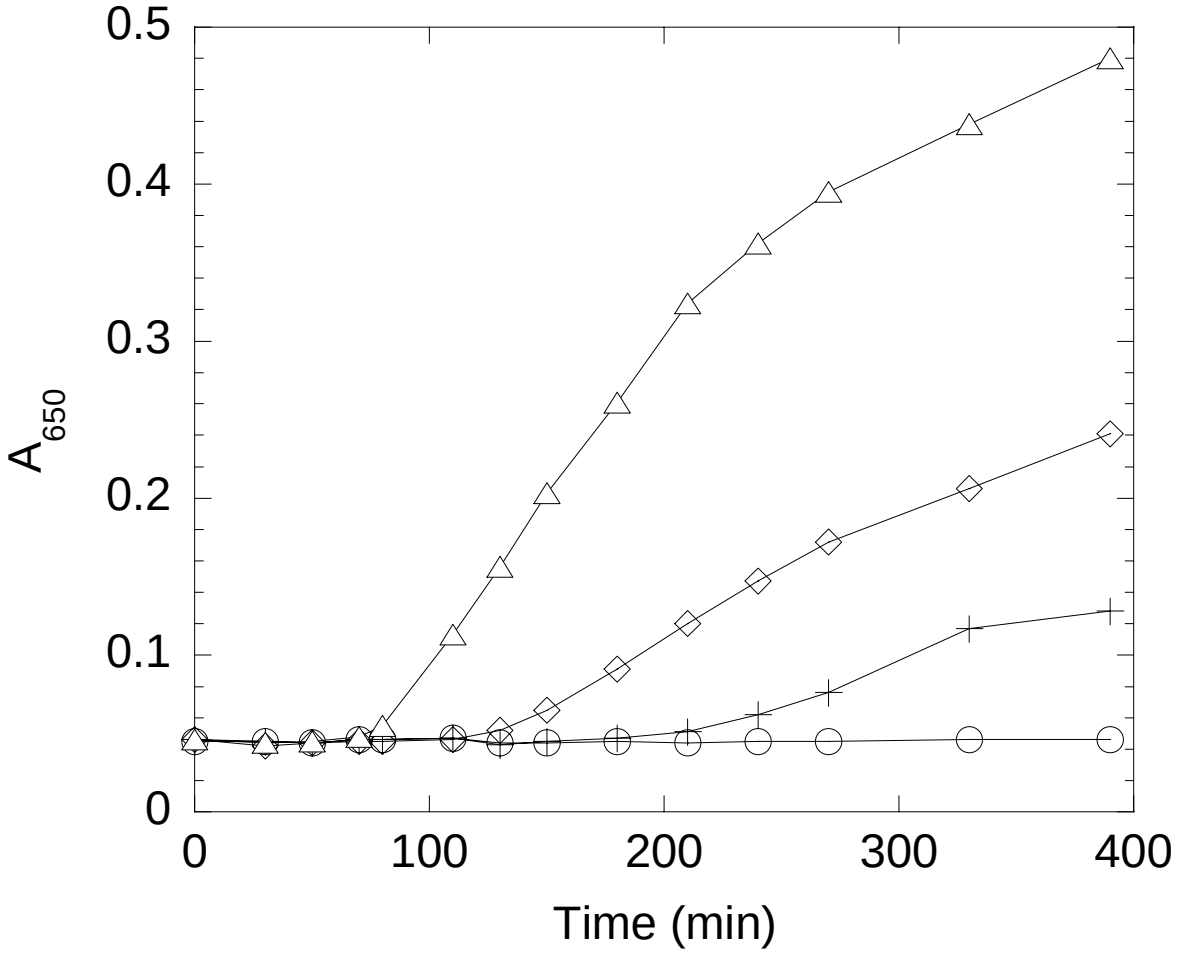

Figure 7-14 Reduction of insulin by Trx-TrxR system with NADPH as electron donor.

The assay mixture contained 50 nM Tm TrxR, 0.2 mM NADPH, 0.13 mM insulin, and varied amount of *T. maritima* Trx (opened circles, 0 μM; crosses, 0.36 μM; diamonds, 0.72 μM; triangles, 1.44 μM), 1 mM EDTA, in pH7.0, 100 mM sodium phosphate buffer. The increase of absorbance at 650 nm was monitored at 30^{o}C.

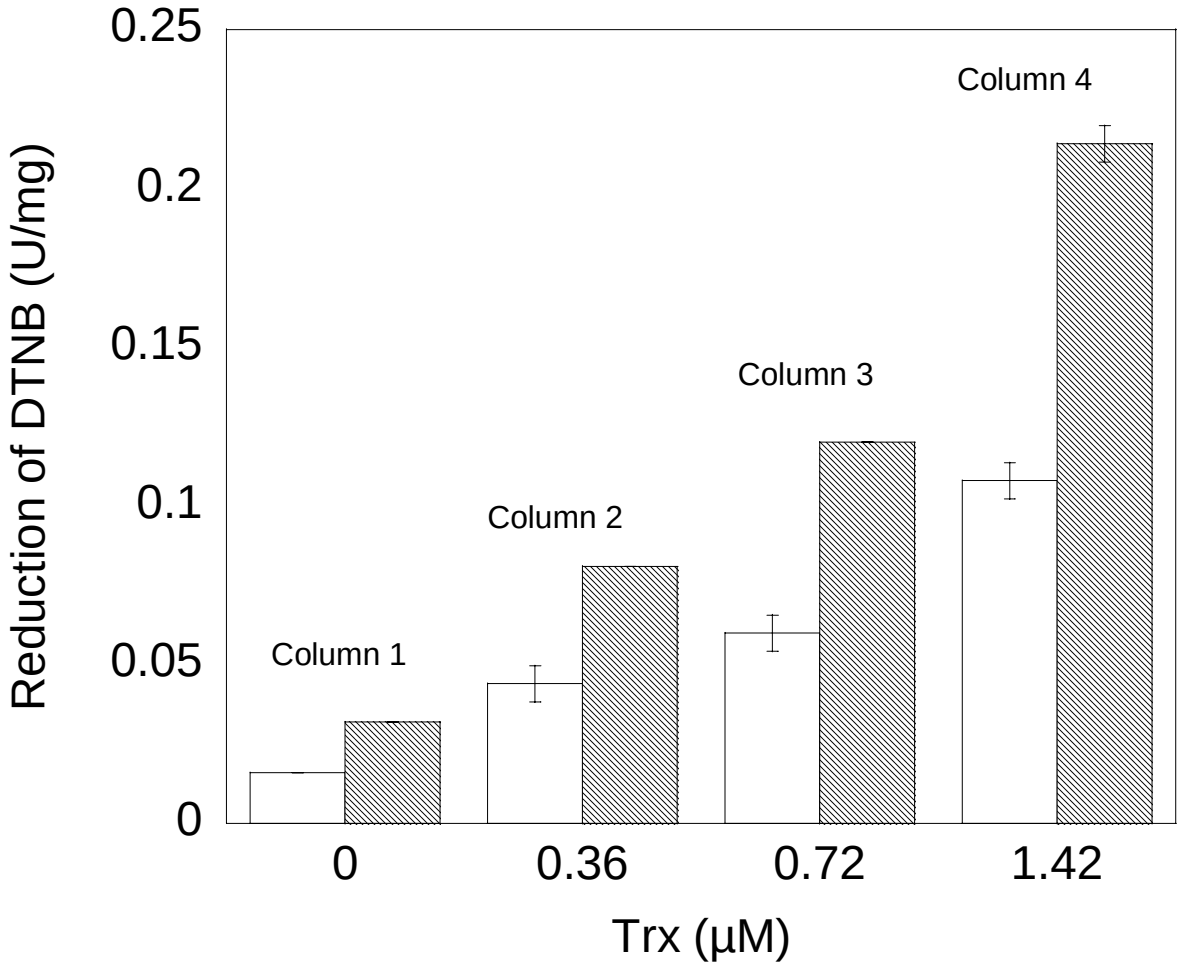

Figure 7-15 Reduction of DTNB by Trx-TrxR system.

The assay mixture contained 50 nM *T. maritima* TrxR, 0.2 mM NAD(P)H (open columns, NADPH; filled columns, NADH), 0.1 mM DTNB, and 0-1.4 μM *T. maritima* Trx (column 1, 0μM; column 2, 0.36 μM; column 3, 0.72 μM; column 4, 1.44 μM), 1 mM EDTA, in pH7.0, 100 mM sodium phosphate buffer. The increase of absorbance at 412 nm was monitored at 30^{o}C.

7.5 DISCUSSION

Trx and TrxR system plays several key roles in maintaining the redox environment of the cell and responding to oxidative stress in all three domains of life (Hirt et al. 2002; Williams et al. 2000). TrxR and Trx were purified and characterized from hyperthermophilic bacterium *T. maritima*. The *T. maritima* TrxR is phylogenetically closer to L-TrxR than H-TrxR. The deduced amino acid sequence is homologous mostly to TrxR from *Carboxydothermus hydrogenoformans* (50% identity and 71% similarity) and shows relatively high homology to *E. coli* TrxR (33% identity and 57% similarity). Similar to other TrxRs (Figure 7-4), this protein has two FAD-binding motifs near the N-terminus (GXGXXA) and C-terminus (GXXAAGD) and one NAD(P)H-binding motif near the middle of the protein (GGGXXA). *T. maritima* TrxR also contains active redox center (CXXC) common in all enzymes showing TrxR activity (Hirt et al. 2002). This active redox center is in a class II pyridine nucleotide-disulfide oxidoreductase active site CATCDGYLFAGKDVIVVGGGD (http://us.expasy.org/cgi-bin/prosite/ScanView.cgi? scanfile=41218312816.scan.gz), which is similar to the conserved motif reported in the Swiss-Prot Prosite Database at the accession number PS00573 (C-x(2)-C-D-[GAS]-x(2,4)-[FYA]-x(4)-[LIVMAT]-x(0,1)-[LIVM](2)-[GI]-[GDS]-[GRD]-[DN]) (http://us.expasy.org/cgi-bin/nicedoc.pl?PS00573). This motif in *T. maritima* TrxR overlaps with NAD(P)H-binding region in the primary structure. The proximity of NAD(P)H-binding region and pyridine nucleotide-disulfide active site is a feature present in L-TrxRs, while in H-TrxRs they are spatially separated (Ruocco et al. 2004). Trx of *T. maritima* has a high sequence homology with the Grx-like protein of *P. furiosus* and alkyl hydroperoxide reductase subunit F related protein of *T. acidophilum*. Furthermore, *T. maritima* Trx has redox-active sequence motif CPYC and CQYC, which suggests that it belongs to the protein-disulfide oxidoreductase family (Guagliardi et al. 1995). *T. maritima* Trx had an insulin reduction and thiotransferase activities, which are similar to Grx-like protein from *P. furiosus* (Guagliard et al. 1995). *T. maritima* Trx showed Trx-like activity that could reduce both insulin and DTNB in the presence of *T. maritima* TrxR and NAD(P)H. Unlike classical Trxs that are smaller (~12 kDa) and have only one CXXC redox-active motif, there is no classical Trx homology gene present in *T. maritima* (Nelson et al. 1999). All Trxs from hyperthermophiles, such as *P. horikoshii* (Kashima and Ishikawa 2003), *A. pernix* (Jeon and Ishikawa 2002), *P. furiosus* (Guagliardi et al. 1995), *Aquifex aeolicus* (Pedone et al. 2006), and *Methanococcus jannaschii* (Lee et al. 2000), *S. solfataricus* (Guagliardi et al. 1994), are around 25 kDa (the one from *A. pernix* is around 37 kDa) and have two redox active motifs (CXXC and CXXC). So far, one Trx from

hyperthermophile, *M. jannaschii*, has similar size to classical Trxs, but contains a Grx-like fold (Lee et al. 2000). This may indicate that hyperthermophiles use Trx containing Grx fold instead of conventional Trx.

The substrate specificity of *T. maritima* TrxR was carried out. It did not show any lipoamide dehydrogenase and glutathione reductase activity, unlike the enzyme from mammals that can catalyze the reduction of lipoic acid efficiently (Arnér et al. 1996). It could catalyze the reduction of *T. maritima* Trx with NADH and NADPH as electron donor which was shown by the reduction of DTNB and insulin, respectively. Interestingly, the purified *T. maritima* TrxR could also catalyze the direct reduction of DTNB with both NADH and NADPH, which is a common feature for H-TrxR (Hirt et al. 2002), not normally found in the L-TrxR. Recently, it has been reported that the L-TrxRs from hyperthermophilic archaea *S. solfataricus*, which was characterized as NADH oxidase previously (Masullo et al. 1996; Ruoco et al. 2004) and *A. pernix* K1 (Jeon and Ishikawa 2002) showed the capability of catalyzing the reduction of DTNB directly. However, there has been no bacterial TrxR showing this property. This indicates that *T. mariitma* TrxR resembles catalytic properties closer to some archaeal and eukaryotic types of TrxRs. The broader substrate spectrum of H-TrxR results from the presence of selenocysteine at the C-terminus (Gly-Cys-Sec-Gly) (Gasdaska et al. 1995; Gladyshev et al. 1996; Tamura and Stadtman 1996). There is no selenocysteine present in *T. maritima* TrxR based on the deduced amino acid sequence (Nelson et al. 1999), *S. solfataricus* TrxR, and *A. pernix* TrxR. The reason for the direct use of DTNB as electron acceptor for those enzymes remains unclear.

This is the first report of Grx-like protein that directly mediates the electron transfer from a TrxR to protein disulfide in hyperthermophilic bacteria. It has been reported that in mesophilic anaerobic bacterium, *C. pasteurianum*, TrxR and Grx homologues are involved in oxidative response (Reynolds et al. 2002). It has been reported that *T. maritima* could tolerate micro molar level of oxygen in the growth media and possesses a highly active H_2O_2-forming NADH oxidase (Yang and Ma 2007). An NADH-dependent peroxidase activity in cell-free extract of *T. maritima* has been demonstrated. Similar to Trx-TrxR system in other organisms, *T. maritima* Trx-TrxR may also provide electrons to thioredoxin peroxidase (TM0807) which would catalyze the reduction of hydrogen peroxide to water, therefore form a complete oxygen defensive pathway.

Chapter 8 Hydrogen Metabolism and Hydrogenases of *Pyrococcus furiosus* and *Thermotoga hypogea*

A manuscript has been prepared for submission based on parts the work described in this chapter.

8.1 ABSTRACT

The hydrogen metabolism in hyperthermophilic archeaon, *Pyrococcus fusiosus*, has attracted very intensive study. The inhibitory effect of hydrogen on the growth of *P. furiosus* was verified. The hydrogenase activity in the cell-free extract resulted from the culture containing external hydrogen in the gas phase was lower than that from the culture without external hydrogen added. The production of ethanol was increased about ten times in the culture containing 100% hydrogen in the gas phase. Two complex flavoproteins functioning as hydrogenase have been purified and characterized previously in *P. furiosus*, which promoted further study of hydrogenase in extremely thermophilic bacterium, *Thermotoga hypogea*. *T. hypogea* is a thermophilic fermentative bacterium able to dispose of the reducing equivalents generated during fermentation by reducing proton to H_2. Activity of hydrogenase was detected in the cell-free extract of *T. hypogea*, from which a hydrogenase was purified to homogeneity by following hydrogen oxidation with BV as electron acceptor using a FPLC system. The purified enzyme was a homotetrameric protein with a subunit of 65 kDa revealed by SDS-PAGE and gel filtration. The purified *T. hypogea* hydrogenase did not contain any flavin as cofactor, but it contained 16 atoms of Fe and 11.6 atoms of acid labile sulfur per mole subunit. It showed both hydrogen uptake and evolution activity. The purified enzyme was very oxygen sensitive and lost 50% of its activity within 3 min exposure to air. Its catalytic properties showed that the hydrogenase had apparent V_{max} values of 1142.0 and 606.9 μmol H_2 oxidized min^{-1} mg^{-1} protein when BV and MV were used as electron acceptors, respectively. Apparent K_m values for MV and BV in H_2 uptake were determined to be 0.17 and 0.24 mM, respectively. The apparent K_m value for MV and apparent V_{max} value in hydrogen evolution were determined to be 1.1 mM and 192.4 μmol min^{-1} mg^{-1}, respectively. The enzyme exhibited pH optima of 10.0 and 8.0 for hydrogen uptake and evolution, respectively, and the optimum temperature for catalytic activity was around 85°C determined by hydrogen oxidation activity. A ferredoxin isolated from *T. hypogea* was identified as the physiological electron carrier for this enzyme assayed by the metronidazole coupled reaction.

8.2 INTRODUCTION

Hydrogenases catalyze the reversible oxidation of hydrogen into two electrons and two protons. Many bacteria and archaea, as well as some unicellular eukaryotes, contain hydrogenases (Adams et al. 1981). Transfer of electrons to hydrogenase with hydrogen production is related to energy conservation in different microorganisms (Nandi and Sengupta 1998). The first hydrogenase purified and characterized was the H_2-evolving enzyme from the anaerobic N_2-fixing bacterium *Clostridium pasteurianum* using ferredoxin as electron donor (Chen and Mortenson 1974). Although hydrogenases from different sources may differ in the aspect of molecular composition, specific activity in catalyzing the hydrogen oxidation and evolution, electron carrier specificity, cofactor content and sensitivity to inactivation by oxygen, they are all iron sulfur proteins except the one from methanogens (Adams 1990a,b; Lyon et al. 2004). Based on metal contents, hydrogenase can be classified into three types: Ni-Fe hydrogenase, Fe-hydrogenase, and iron-sulfur cluster free hydrogenase (Das at el. 2006, Lyon et al. 2004). Majority of known hydrogenases are Ni-Fe hydrogenases, which normally are less active than Fe-hydrogenase and at least have a small subunit (~30 kDa) harbouring Fe-S clusters, a large subunit (~65 kDa) holding the active site, Ni-Fe cluster (Volbeda et al. 1995) and subunits interacting with electron carriers (NAD^+, F_{420}, cytochrome *b*) may be present as well (Albracht 1994). Compared to Ni-Fe hydrogenases, the distribution of Fe-hydrogenases are very limited. So far, they have only been found in anaerobic bacteria, such as *T. maritima* (Verhagen et al. 1999) and *C. pasteurianum* (Peters et al. 1998), and anaerobic eukaryotes, such as protozoan *Trichomonas vaginalis* (Payne et al. 1993). In addition to uptake and evolution of hydrogen, it has been reported that some hydrogenases are also involved in other biological processes, such as transformation of 2, 4, 6-trinitrotoluene in *Clostridium acetobutylicum* (Kutty and Bennett 2006) and against oxidative stress in *Desulfovibrio vulgaris* (Fournier et al. 2004).

P. furiosus is a hyperthermophilic archaeon originally isolated from geothermally heated marine sediments (Fiala and Stetter 1986). It has two soluble FAD-containing Ni-Fe hydrogenases (Bryant and Adams 1989; Ma et al. 1993, 2000). It was assumed that the hydrogen produced during fermentation inhibited the growth, which would be relieved by adding elemental sulfur (Fiala and Stetter 1986; Malik et al. 1989). However, there has been no report about what concentration of hydrogen would have the inhibition effect and how the added hydrogen would affect the activity of NADPH-utilizing enzymes yet. *T. hypogea* belongs to the order of *Thermotogales*, several species of

which are found to produce hydrogen with variety of substrates while tolerating certain level of oxygen (Van Ooteghem et al. 2002, 2004). The potential use of microorganisms for biological hydrogen production makes hydrogen metabolism a promising research area. It has been found that *T. hypogea* can grow on agricultural residues to produce hydrogen, which may have great potential application in biological hydrogen production with renewable materials (Dhanjoon 2005). However, the properties of hydrogenase responsible for the hydrogen production in *T. hypogea* are not known yet. The hydrogenase from *Thermotoga maritima* has been characterized and it is an iron-only hydrogenase composing of three different subunits with molecular weight of 73, 68, and 19 kDa (Verhagen et al. 1999). Although the enzyme has been extensively studied, puzzles still remain. Sequence analysis shows that the *T. maritima* enzyme is a Fe-S-cluster-containing flavoprotein which uses NADH as an electron donor. However, the purified enzyme does not have any flavin and can not use either NAD(P)H or *T. maritima* ferredoxin as electron donor. This chapter describes the effect of external hydrogen on the growth of *P. furiosus* and the purification and characterization of hydrogenase from *T. hypogea*, which may shed further light on understanding of hydrogen metabolism in both hyperthermophilic bacteria and archaea.

8.3 MATERIALS AND METHODS

8.3.1 Growth of *P. furiosus* and *T. hypogea*

P. furiosus (DSM3638) was grown in the media described previously with modification (Raven et al. 1992). The media contained (per liter) 2.5 g of peptone, 2.5 g of yeast extract, 13.8 g of NaCl, 5.0 g of maltose, 5.2 g of N-2-hydroxyethylpiperazine-N'-2-ethanesulfonic acid (HEPES), 10 ml of magnesium salt solution, 1 ml of solution A, 1 ml of solution B, 1 ml of solution C, and 1 mg of resazurin. The pH was adjusted to 7.0. Magnesium salt solution contained (per liter) 180 g of $MgSO_4 \cdot 7H_2O$ and 160 g of $MgCl_2 \cdot 6H_2O$. Solution A contained (per liter) 4 g of tri-sodium citrate, 9 g of $MnSO_4 \cdot 4H_2O$, 2.5 g of $ZnSO_4 \cdot 7H_2O$, 2.5 g of $NiCl_2 \cdot 6H_2O$, 0.13 g of $AlK(SO_4)_2 \cdot 12H_2O$, 0.3 g $CoCl_2 \cdot 6H_2O$, and 0.15 g of $CuSO_4 \cdot 5H_2O$. Solution B contained (per liter) 56 g of $CaCl_2 \cdot 2H_2O$, 25 g of NaBr, 16 g of KCl, 10 g of KI, and 4 g of $SrCl_2 \cdot 6H_2O$. Solution C contained (per liter) 50 g of K_2HPO_4, 7.5 g of H_3BO_3, 3 g of $Na_2WO_4 \cdot 2H_2O$, 0.15 g of $Na_2MoO_4 \cdot 2H_2O$, and 0.005 g of Na_2SeO_3. Different amount of pure H_2 was added to the anoxic media sealed in serum bottles to bring the H_2 concentration to 50, 60 70, 80, 90 and 100% in the gas phase (H_2/N_2+H_2; Vol/Vol). The media were incubated at 95^{o}C after reduced by adding 42 mM of $TiCl_3$ in nitrilotriacetic acid solution prior to inoculation. The growth was monitored by measuring cell density with Genesys 10 Vis spectrophotometer at 600 nm. In order to test the effect of added hydrogen in the growth media on NADPH-dependent enzyme activities, *P. furiosus* was grown in four conditions, 100% H_2 in the gas phase with or without sulfur and 100% N_2 in the gas phase with or without sulfur. The resulting cells from those four conditions were used to prepare cell-free extract with the method reported previously (Ma et al. 2000). Ethanol production in the growth culture was measured with Shimadzu Gas Chromatography after centrifugation at 10,000x*g* for 10 min.

T. hypogea was grown in 125 ml serum bottle containing 50 ml media as described in chapter 3 (3.3.2 Growth of *T. hypogea*). The cultures with either xylose or glucose as carbon source were harvested at mid- and late-exponential phase to determine the growth phase-dependent *T. hypogea* hydrogenase activities in the presence and absence of sodium thiosulphate as electron acceptor. To obtain sufficient *T. hypogea* cell mass for the purification of hydrogenase and ferredoxin, large-scale culture (15 L) was grown routinely at 70^{o}C in the medium described previously (Yang and Ma 2005a).

8.3.2 Enzyme assay and protein determination

Hydrogenase was measured by either hydrogen oxidation or evolution. Oxidation of hydrogen was measured with the method described previously (Ma and Adams 2001). The assay was run in hydrogen flushed anaerobic glass cuvette containing 1.6 mM BV or 1 mM MV in anaerobic 50 mM, pH 8.4 N-(2-hydroxyethyl)-piperazine-N'-3-propanesulfonic acid (EPPS)/NaOH buffer. The increase of absorbance at 580 nm was monitored routinely at 80^{o}C during purification. One unit was defined as the enzyme catalyzing the oxidation of 1 μmol hydrogen per minute. $NADP^{+}$, NAD^{+}, MV, BV, and *T. hypoge*a ferredoxin were tested for substrates spectrum of the purified *T. hypogea* hydrogenase. When NAD(P) was used, the absorbance increase of assay mixture containing 0.5 mM NAD(P), purified hydrogenase, and hydrogen gas in pH 8.4 EPPS buffer at 340 nm was monitored at 80^{o}C (Schneider and Schlegel 1976). The utilization of *T. hypogea* ferredoxin as electron acceptor was tested using a metronidazole coupled assay (Chen and Blanchard 1979). The assay mixture contained 2.4 μg *T. hypogea* ferredoxin, 0.25 mM metronidazole, and 2.75 μg *T. hypogea* hydrogenase in pH 8.4, 50 mM EPPS buffer. The decrease of absorbance at 320 nm (ε_{320nm}=9.3 $mM^{-1}cm^{-1}$) was monitored at 80^{o}C. Glutamate dehydrogenase (GDH) activity was determined in anaerobic glass cuvette by monitoring glutamate dependent reduction of $NADP^{+}$ spectrometrically at 340 nm and 80^{o}C for *P. furiosus* cell-free extract under different growth conditions (Ma et al. 1994a).

Hydrogen evolution was measured with the method described previously (Ma et al. 1994b) at 80^{o}C by the production of hydrogen gas with Buck GC using SDT-reduced MV as electron donor. The assay mixture in 8 ml vial contained 10 mM SDT, 1 mM MV, and 2.3 μg purified enzyme in 2 ml pH 8.4, 50 mM EPPS buffer. The amount of hydrogen (μmol) produced was calculated based on a standard curve obtained under the same condition. One unit of hydrogenase was defined as the enzyme catalyzing the production of 1 μmol hydrogen per minute. In addition to MV, NADH, NADPH, and POR reduced ferredoxin were also tested as a substrate for hydrogen evolution. Sulfur reductase was measured with the method described previously (Ma et al. 1993). 0.1 g sublimed sulfur was added to 8 ml vial containing 2 ml 50 mM EPPS buffer pH 8.4. The vials were degassed routinely to make them anaerobic. SDT and enzyme were added to the preheated vial to make final concentration of 0.8 mM of SDT and 0, 2, 4 or 10 μg purified *T. hypogea* hydrogenase. The mixtures were incubated at 70^{o}C. At different intervals, aliquots of the assay mixture were removed and assayed for hydrogen sulfide by methylene blue formation (Chen and Mortenson 1977). The purity of ferredoxin was monitored by measuring the absorbance ratio at 390 and 280 nm during purification (Blamey et al.

1994). Protein concentration was determined using Bradford method with bovine serum albumin as standard protein (Bradford 1976).

8.3.3 Purification of hydrogenase and ferredoxin from *T. hypogea*

All the purification procedures were carried out anaerobically. Cell-free extract was prepared from 50 g frozen cells and applied to a pre-equilibrated DEAE-Sepharose Fast Flow (5 x 10 cm, Amersham Biotech, Quebec, Canada) using buffer A (50 mM Tris-HCl pH 7.8, 5% [vol/vol] glycerol, 2 mM SDT, and 2 mM DTT). The column was eluted using a gradient of NaCl (0-0.5 M, 500ml) at flow rate of 3 ml/min. Hydrogenase started to elute out as 0.15 M NaCl was applied to the column. Active hydrogenase-containing fractions were pooled and loaded onto a HAP column (Bio-Rad, 2.6 x 10 cm) equilibrated with buffer A. Hydrogenase started to elute out as 0.05 M potassium phosphate was applied to the column. The active fractions were pooled and loaded to Phenyl-Sepharose HP column (2.6 x 8 cm, Amersham Biotech, Quebec, Canada). The column was eluted with a continuous gradient of $(NH_4)_2SO_4$ (0.8-0 M) at a flow rate of 2 ml/min. Hydrogenase activity started to elute out as 0.0 M ammonium sulphate was applied the column. Part of the activity-containing fractions was concentrated with ultra filtration (Amicon Ultra filter, PM 30 membrane) to 3 ml and applied to Superdex 200 column (2.6 x 60 cm, Amersham Biotech, Quebec, Canada) equilibrated with buffer A containing 100 mM KCl. The column was eluted with the same buffer at a flowrate of 3 ml/min. Fractions containing high hydrogenase activity were combined, desalted with ultra filtration, and applied to Q-Sepharose HP column (1 x 10 cm, Amersham Biotech). The column was eluted with linear gradient of NaCl (0-0.5 M) at a flowrate of 1 ml/min. Hydrogenase was eluted out when 0.2 M NaCl was applied to the column. Fractions containing pure hydrogenase as revealed by SDS-PAGE (Laemmli 1970) were concentrated using ultra filtration (Amicon Ultra filter, YM 10 membrane) and stored in liquid nitrogen till use. The purification procedures of ferredoxin were the same as for the purification of hydrogenase, up to the HAP column. Ferredoxin did not bind to HAP column very well. It started to elute out when the potassium phosphate salt was just applied. The ferredoxin-containg fractions were pooled and concentrated using ultra filtration (Amicon Ultra filter, YM 3 membrane) to 10 ml and loaded to Superdex 200 column. The ferredoxin-containing fractions were pooled and loaded to Q-Sepharose column. Ferredoxin was eluted out as 0.3 M of NaCl was applied to the column. The fractions containing purified ferredoxin revealed by SDS-PAGE were

concentrated with ultra filtration (Amicon Ultra filter, YM 3 membrane) and stored at -20^{o}C untill use.

8.3.4 Flavin cofactor analysis

The purified hydrogenase was scanned to check the characteristic peaks of flavin in quartz cuvette from 190 nm to 600 nm (Varian Bio 50 UV-visible spectrophotometer). Then the enzyme used for scanning was extracted for flavin and identified by thin layer chromatography using the method reported previously (Yang and Ma 2005a). Details were described in Chapter 3 (3.3.8 Flavin cofactor analysis).

8.3.5 Metal and sulfur determination

The enzyme sample in Buffer A was concentrated and washed with freshly prepared anaerobic Tris-HCl buffer (pH 7.8, 10 mM) containing 2 mM DTT in the anaerobic chamber using Microcon YM-10 (Millipore, MA, USA) to remove SDT that interferes with metal determination. The oxygen level in the chamber was 1.4 ppm when the experiment was carried out. The presence of Fe and Ni was determined using ICP-MS (Chemical Analysis Laboratory, University of Georgia, USA). Acid labile sulfur was determined using methylene blue formation method described previously (Beinert 1983). The details were described in the materials and methods of Chapter 6 (6.3.4 Iron and acid labile sulfur determination).

8.3.6 Molecular mass determination

The native molecular mass of *T. hypogea* hydrogenase was estimated by gel filtration on Superdex 200 column (2.6 x 60 cm). The details were described in Chapter 7 (7.3.5 Determination of molecular mass and mass spectrometry)

8.4 RESULTS

8.4.1 Effect of hydrogen on *P. furiosus*

P. furiosus was grown in the presence of various amount of hydrogen added in the gas phase before inoculation. There was almost no difference between the culture without added hydrogen and those with 50% (V/V) of hydrogen added. Normally *P. furiosus* produces approximately 30% of hydrogen in the gas phase of a sealed culture bottle. Therefore, the production of hydrogen should not be a factor to inhibit growth under normal growth conditions. The severe inhibition appeared when the hydrogen concentration went up to as high as 80%. However, even with 100% of hydrogen added to the gas phase, *P. furiosus* was still able to grow. In order to understand how the high concentration of hydrogen may shift the electron flow in *P. furiosus*, activities of three enzymes related to the utilization of NADPH, hydrogenase, GDH, and alcohol dehydrogenase, were measured. Ethanol production was used as an indicator for the presence of alcohol dehydrogenase since the enzymatic activity was below the limit of assay method. The results were presented in Table 8-1. Hydrogenase was lower in the cells grown in the presence of hydrogen, while there was no significant difference among GDH activities under all growth conditions tested. The production of ethanol was greatly enhanced by the addition of hydrogen especially when there was no sulfur present.

8.4.2 Purification of *T. hypogea* hydrogenase and ferredoxin

Hydrogen oxidation activity was found to be present in the cell-free extract of *T. hypogea* grown in the presence of sodium thiosulfate or NaCl (Figure 8-1). The hydrogenase activity was higher at mid-log phase than that at later log phase in both cells grown on glucose and xylose. Cell-free extract prepared from 50 g frozen cells grown on glucose was applied to DEAE column. *T. hypogea* hydrogenase activity was eluted as a single peak after DEAE, HAP and Phenyl-Sepharose column. The enzyme was eluted completely after more than 13 column volume (520 ml) buffer A was applied to Phenyl-Sepharose column after the $(NH_4)_2SO_4$ gradient, which indicates that the enzyme had a strong interaction with the column. Since the protein composition of the fractions on SDS-PAGE was quite different, the fractions were split and concentrated with ultra filtration individually. The resulting concentrates were loaded to Superdex 200 individually. The concentrate from the fractions that were eluted out first on Phenyl-Sepharose resulted in two activity peaks corresponding to the molecular weight of 250 kDa and 125 kDa, respectively, and that from the fractions that were eluted

Table 8-1 Effect of added hydrogen in the gas phase on enzyme activities and ethanol production in *P. furiosus*

Enzymes measured	Growth conditions			
	$+S^o, +H_2$[b]	$+S^o, +N_2$[c]	$-S^o, +H_2$	$-S^o, +N_2$
Hydrogenase(U/mg)	1.601±0.11	8.7±0.52	3.09±0.12	5.48±0.21
GDH[a](U/mg)	4.77±0.25	5.58±0.30	3.49±0.22	3.43±0.18
Ethanol (μmol/10^8cells)	4.06±0.27	3.93±0.12	37.39±1.72	ND

[a] GDH stands for glutamate dehydrogenase.

[b] S^o stands for elemental sulfur in the media and H_2 stands for 100% H_2 in the gas phase.

[c] N_2 stands for 100% of N_2 in the gas phase.

ND stands for not detectable.

+ stands for added.

- stands for ommited

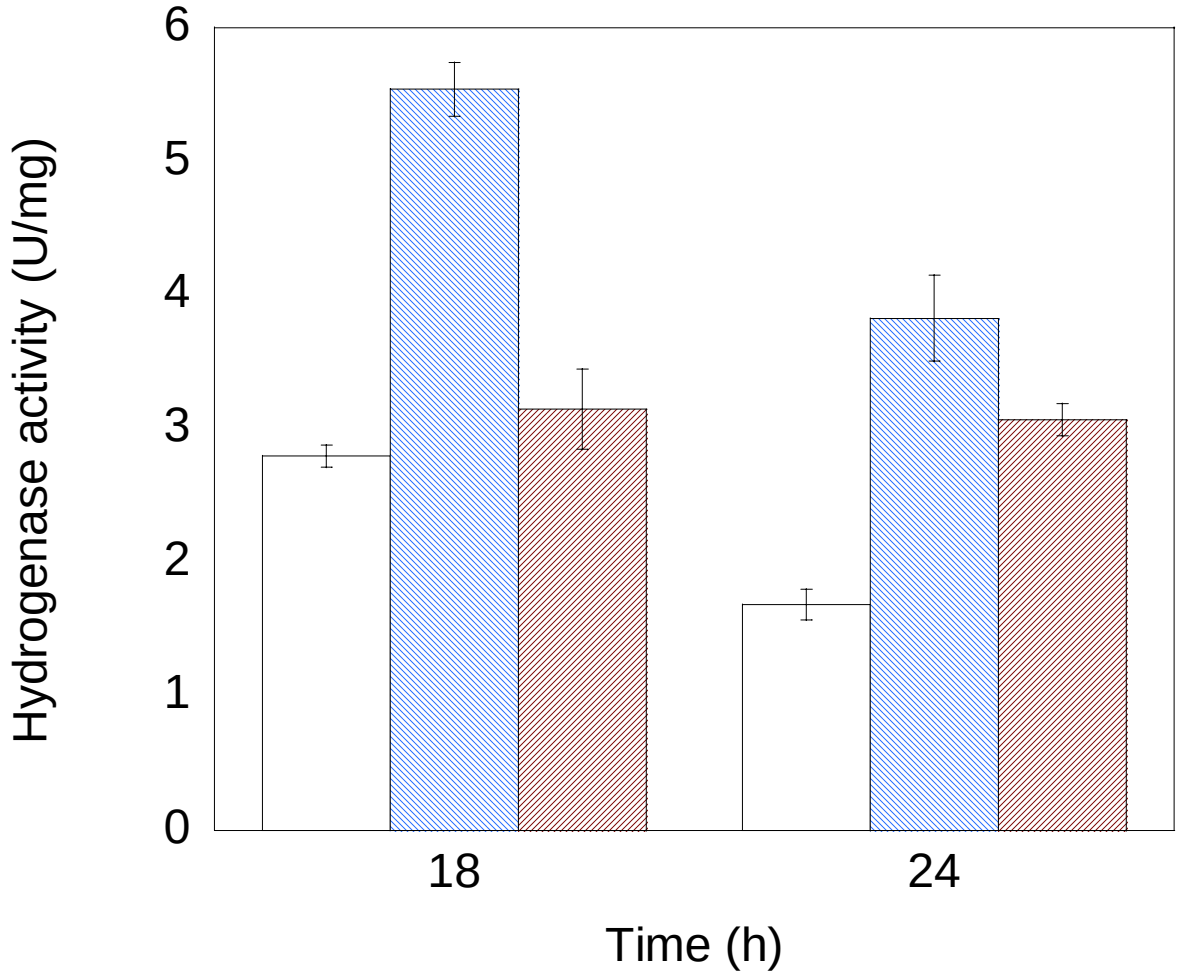

Figure 8-1 Hydrogenase activities in the cells of *T. hypogea* from different growth conditions.

The cell-free extract was made from the culture incubated for 18 and 24 hours from glucose grown cells in the presence of sodium thiosulfate (White), from xylose grown cells in the presence of sodium thiosulfate (Red lines) and glucose grown cells in the presence of NaCl (Red lines).

out later from Phenyl-Sepharose column resulted in only one peak (250 kDa) on Superdex 200 column. The active fractions of the 250 kDa peak were used for further purification and loaded onto Q-Sepharose column. The hydrogenase was purified after Q-Sepharose column revealed by a single band with molecular mass of 65 kDa on SDS-PAGE (Figure 8-2). The enzyme was purified 126-fold after 5 chromatography columns, indicating this enzyme is present in the cell in a quantity slightly less than 1% (Table 8-2). Amino-terminal sequence analysis of the purified hydrogenase gave rise to a single sequence (AGVTVEINGK) that shows no similarity to the two hydrogenases purified from *P. furiosus* (Ma et al. 2000). It shows significant similarity to the sequence near the N-terminus of Fe-hydrogenase in *Clostridium thermocellum* (11 GIPVEING 18; http://genome.ornl.gov/microbial/cthe/) and putative NADP reducing hydrogenase subunit D which would result in a single subunit in *T. maritima* (28 ADVTVVING 36; Nelson et al. 1999). However, none of them has been characterized yet. Ferredoxin was purified after Q-Sepharose column revealed by a single band around 10 kDa on 20% SDS-PAGE, which is similar to the ferredoxin from *T. maritima*. The purified *T. hypogea* ferredoxin with $A_{390/290}$ ratio between 0.85 and 0.87 was used in later electron carrier assay for hydrogenase.

8.4.3 Physical properties of *T. hypogea* hydrogenase

The oxidized form of purified hydrogenase was scanned with Varian spectrophotometer from 190-600 nm. There was no characteristic flavin absorbance peak around 375 and 450 nm. The solution contained the purified hydrogenase was very brownish. After the sample was boiled with hot methanol in the dark for 10 min, the brownish color disappeared and it did not show significant absorbance at 450 nm. The concentrated supernatant was applied on thin layer chromatography to further identify the presence of flavin cofactor. There was no flavin found in the extract (Figure 8-3). Therefore, the purified *T. hypogea* hydrogenase does not contain any flavin cofactor. Since the brownish color of the purified enzyme may have been an indication of the presence of iron-sulfur center, metal content and labile-sulfur were determined. Although the sample was treated in anaerobic chamber (1.4 ppm O_2), the hydrogenase lost its activity completely after the filtration and washing steps, indicating the purified enzyme was extremely oxygen-sensitive. There was 16 g-atoms of iron per subunit, no nickel detected from *T. hypogea* hydrogenase using ICP-MS. The results from methylene blue formation showed that the enzyme contained 11 g-atoms of acid labile sulfur per subunit. Therefore, the purified *T. hypogea* hydrogenase was a Fe-hydrogenase.

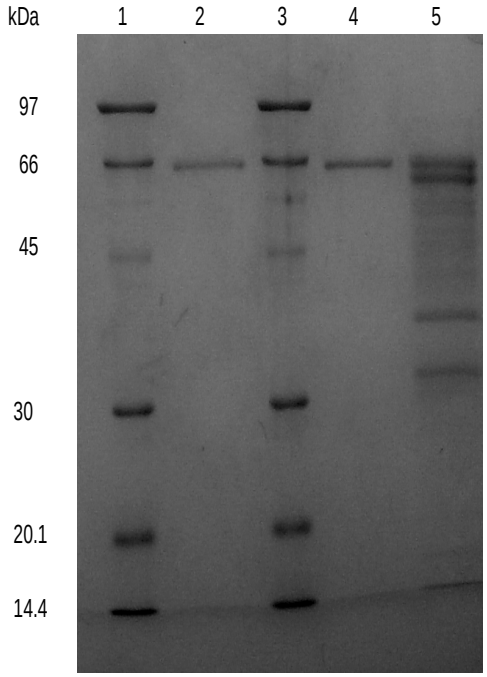

Figure 8-2 SDS-PAGE of *T. hypogea* hydrogenase.

Lane 1 and 3, low molecular standards with molecular weight indicated; lane 2 and 4, purified *T. hypogea* hydrogenase 0.7 and 1.2 μg, respectively; lane 5, 2.8 μg partially purified *T. hypogea* hydrogenase (fractions from gel filtration column).

Table 8-2 Purification of hydrogenase from *T. hypogea*

Purification steps	Total protein (mg)	Total units (U)	Sp act (U/mg)	Purification fold	Recovery (%)
Cell-free extract	1643	13332	8.11	1	100
DEAE-Sepharose	246	6786	27.6	3.4	51
HAP	88	13900	158	19.5	104
Phenyl-Sepharose	22.7	8093	357	44	61
Gel filtration	3.3	3255	986	122	24
Q-Sepharose	1.01	1031	1021	126	8

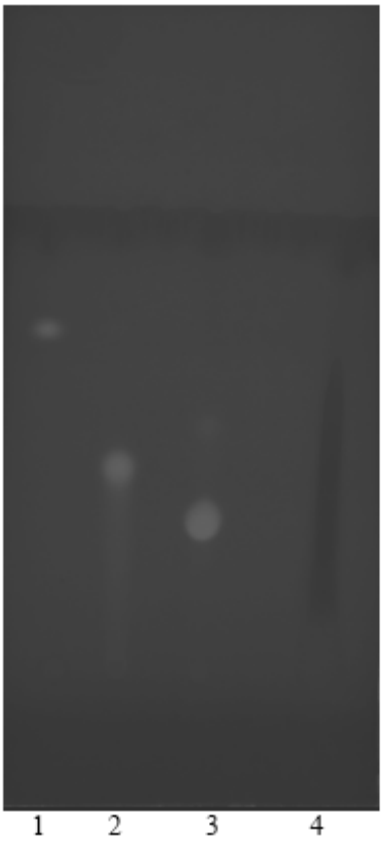

Figure 8-3 Thin layer chromatography of *T. hypogea* hydrogenase extract.

The extracted sample from *T. hypogea* hydrogenase was ascended on thin layer plate in dark together with commercial standards. Lane 1, riboflavin; lane 2, FMN; lane 3, FAD; lane 4, extract of *T. hypogea* hydrogenase.

Thermostability of *T. hypogea* hydrogenase was determined by monitoring its temperature-dependent change of hydrogen oxidation activity with MV. The activity of the purified hydrogenase increased along with the elevation of assay temperature up to 85^{o}C (Figure 8-4). The activity decreased rapidly when the temperature rose to 90^{o}C, which could be caused either by the instability of the enzyme or the low solubility of hydrogen gas at high temperature. Therefore, all other assays performed at 80^{o}C. The time required for a loss of 50% of activity of hydrogenase was approximately 40 and 15 min at 70^{o}C and 85^{o}C, respectively (Figure 8-5) and which did not follow first order kinetics. During purification, it was found that *T. hypogea* hydrogenase activity decreased very quickly whenever the enzyme was exposed to oxygen, even a trace amount. When the enzyme was centrifuged in the anaerobic chamber, where the oxygen level was 1.4 ppm, to prepare sample for metal and sulfur analysis, it lost its activity completely during 2 hours exposure. The enzyme lost its 50% activity around 3 min while it was exposed to ambient air directly (Figure 8-6). Therefore, the purified *T. hypogea* hydrogenase was extremely oxygen sensitive, which is a common feature for iron hydrogenase. The enzyme from *T. maritima* lost 50% of its activity within 10 s exposure to air (Juszczak et al. 1991).

8.4.4 Catalytic properties of *T. hypogea* hydrogenase

The optimal pH for hydrogen oxidation with MV as electron acceptor was determined to be 10.0, while that of the evolution of hydrogen was around 8.0 (Figure 8-7), which is very similar to the reported pH optima of *T. maritima* hydrogenase (Juszczak et al. 1991). The ratio of hydrogen evolution activity to hydrogen oxidation activity at pH 8.0 was found to be 0.4. The activities of hydrogen oxidation by *T. hypogea* hydrogenase under various conditions are shown in Table 8-3. *T. hypogea* hydrogenase could reduce both MV and BV with a preference of BV over MV. Neither NAD^+ nor $NADP^+$ could be reduced under the same assay conditions. Unlike the enzyme from *T. maritima*, *T. hypogea* hydrogenase could reduce ferredoxin with a specific activity of 3.3 U/mg when 0.17 μM ferredoxin was used in the metronidazole coupled assay. For the hydrogen evolution assay, SDT-reduced MV was used as electron donor. NAD(P)H could not be used as substrate either for the purified enzyme or for the cell-free extract to produce hydrogen, while reduced *T. hypogea* ferredoxin could serve as electron donor for the purified hydrogenase to produce H_2 (Figure 8-8). It appears that the purified hydrogenase could also use electrons directly from POR, but ferredoxin stimulated the hydrogenase activity.

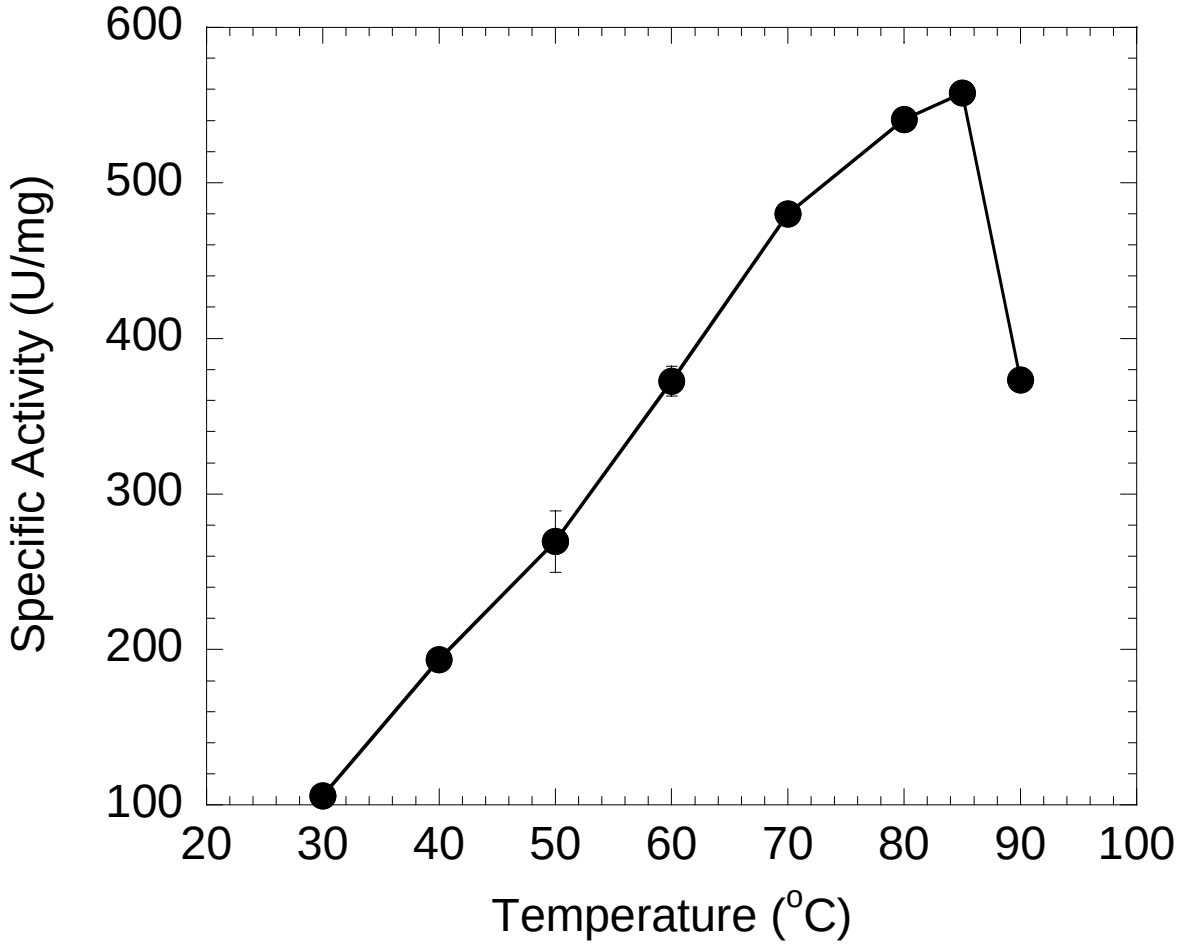

Figure 8-4 Thermoactivity of purified *T. hypogea* hydrogenase.

The oxidation of hydrogen with MV as electron acceptor for *T. hypogea* hydrogenase was carried out with the method described in Material and Methods (8.3.2) with the temperature varying from 30 to 90°C.

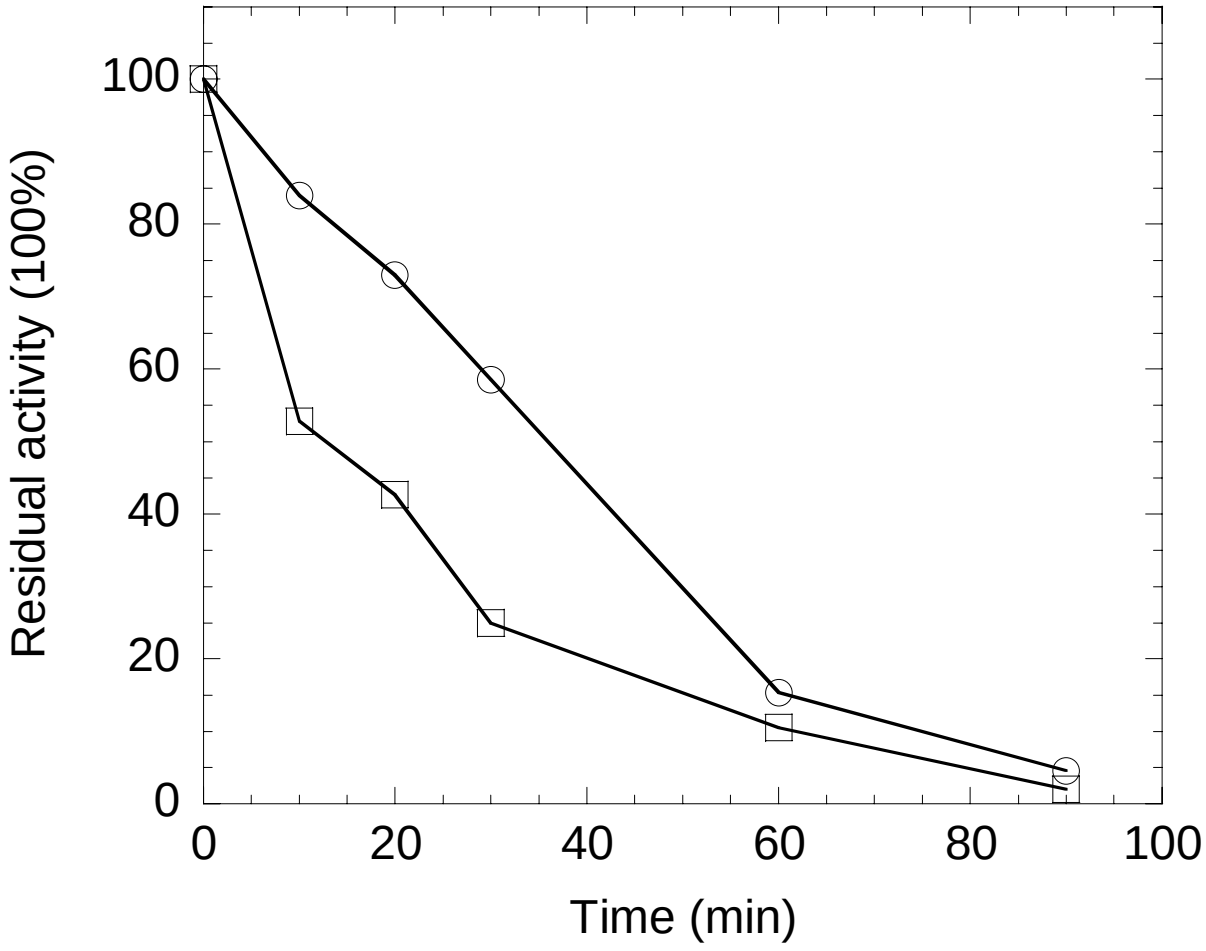

Figure 8-5 Thermostability of purified *T. hypogea* hydrogenase.

Purified *T. hypogea* hydrogenase 0.015 mg/ml in buffer A containg 100 mM KCl was incubated in a sealed small vial anaerobically at 70^{o}C (circles) and 85^{o}C (squares). The residual activity of hydrogen oxidation with BV as electron acceptor was carried out at different time intervals with standard assays. 100% of activity was 1000 U/mg when BV was used as electron acceptor.

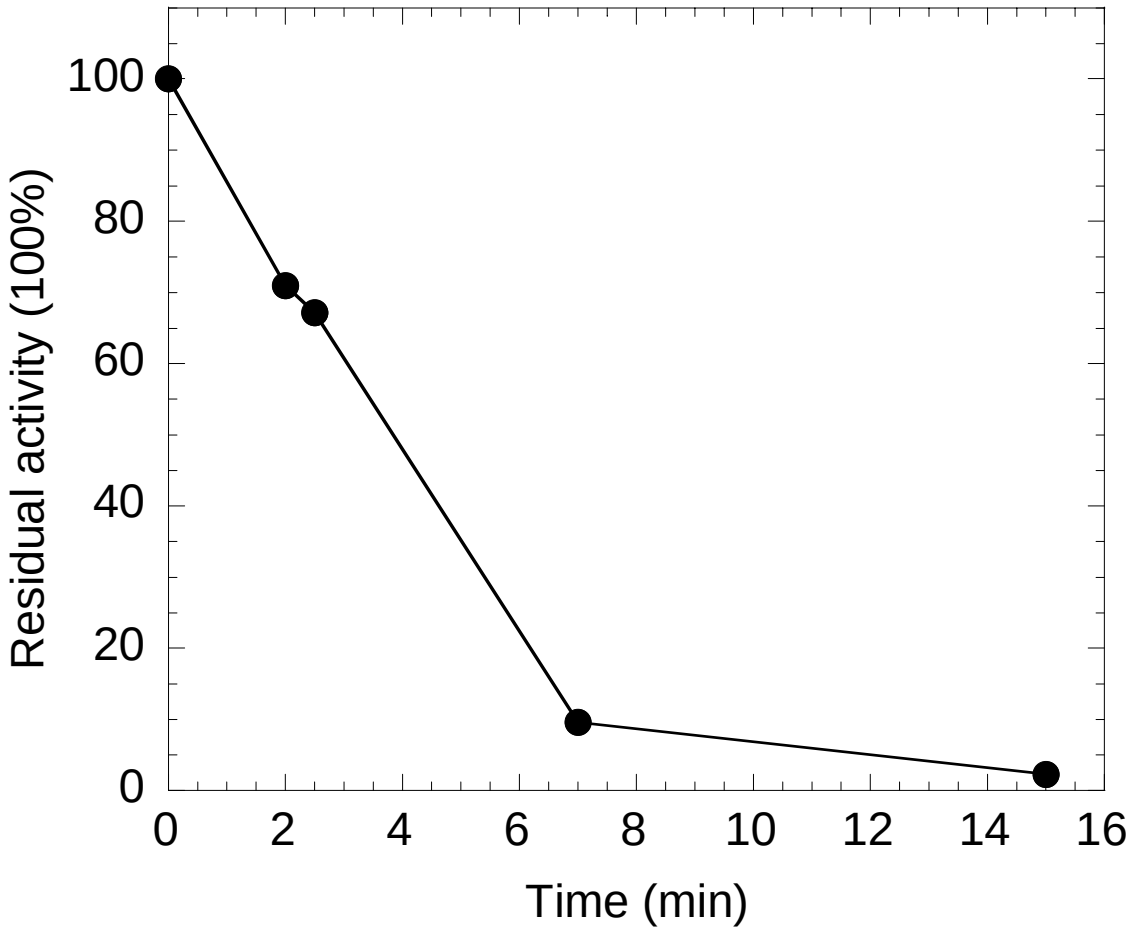

Figure 8-6 Oxygen sensitivity of purified *T. hypogea* hydrogenase.

Purified hydrogenase in buffer A was exposed to ambient air and the residual activity of hydrogen oxidation with BV as electron donor was carried out at different time intervals at 80^{o}C. 100% of activity was 1000 U/mg when BV was used as electron acceptor.

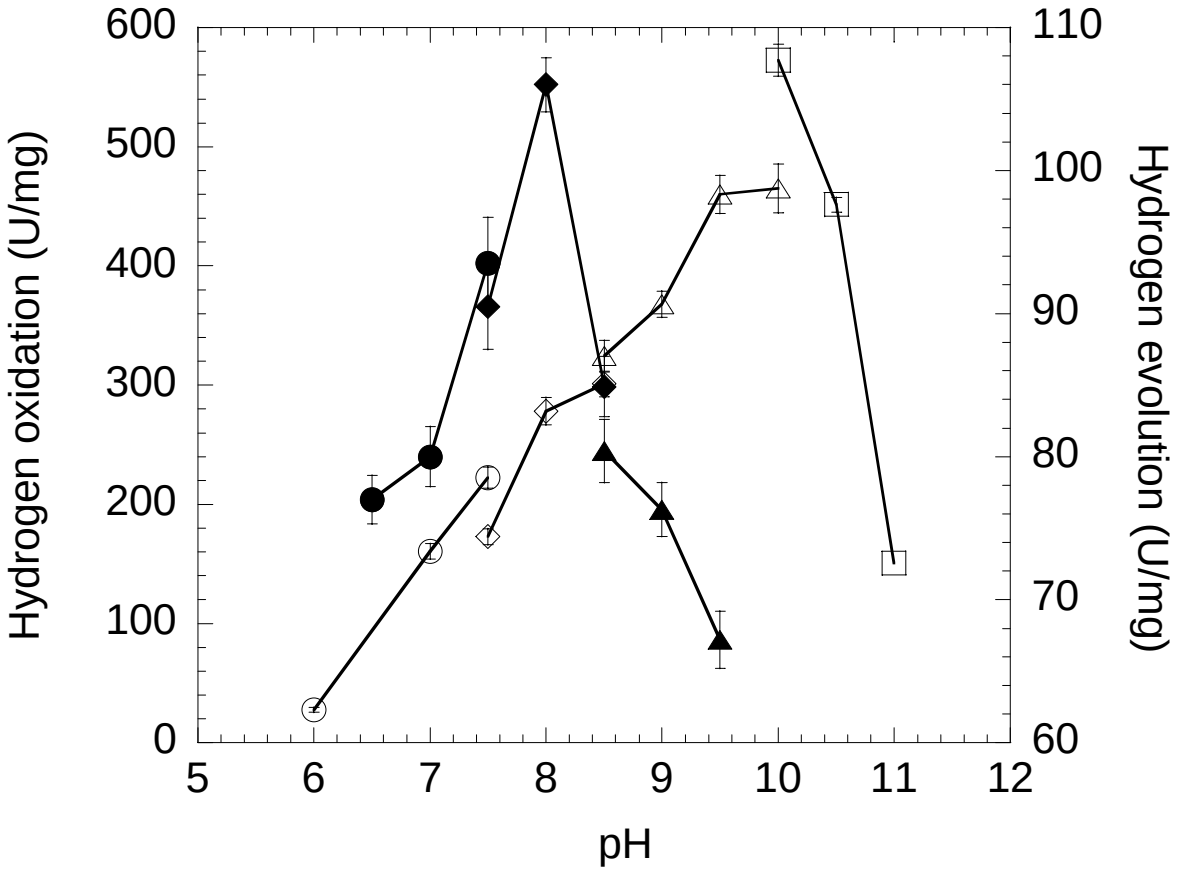

Figure 8-7 Optimal pH determination of purified *T. hypogea* hydrogenase.

The optimal pHs for hydrogen evolution (filled) and oxidation (open) of hydrogenase were determined with 100 mM sodium phosphate pH 6.0-8.0, 100 mM EPPS pH 7.5-8.5, 100 mM glycine-NaOH pH 8.5-10.0, and 100 mM 3-(cyclohexylamino)-1-propanesulfonic acid (CAPS) pH 10.0-11.0 as described in section 8.3.2.

Table 8-3 Utilization of different electron acceptors in H_2 oxidation

Electron acceptors	Concentration (mM)	Specific activity (U/mg)
Ferredoxin	$1.7x10^{-4}$	3.3±0.09
NADP	0.5	0
NAD	0.5	0
MV	1	301±7.5
BV	1	1000±19.6

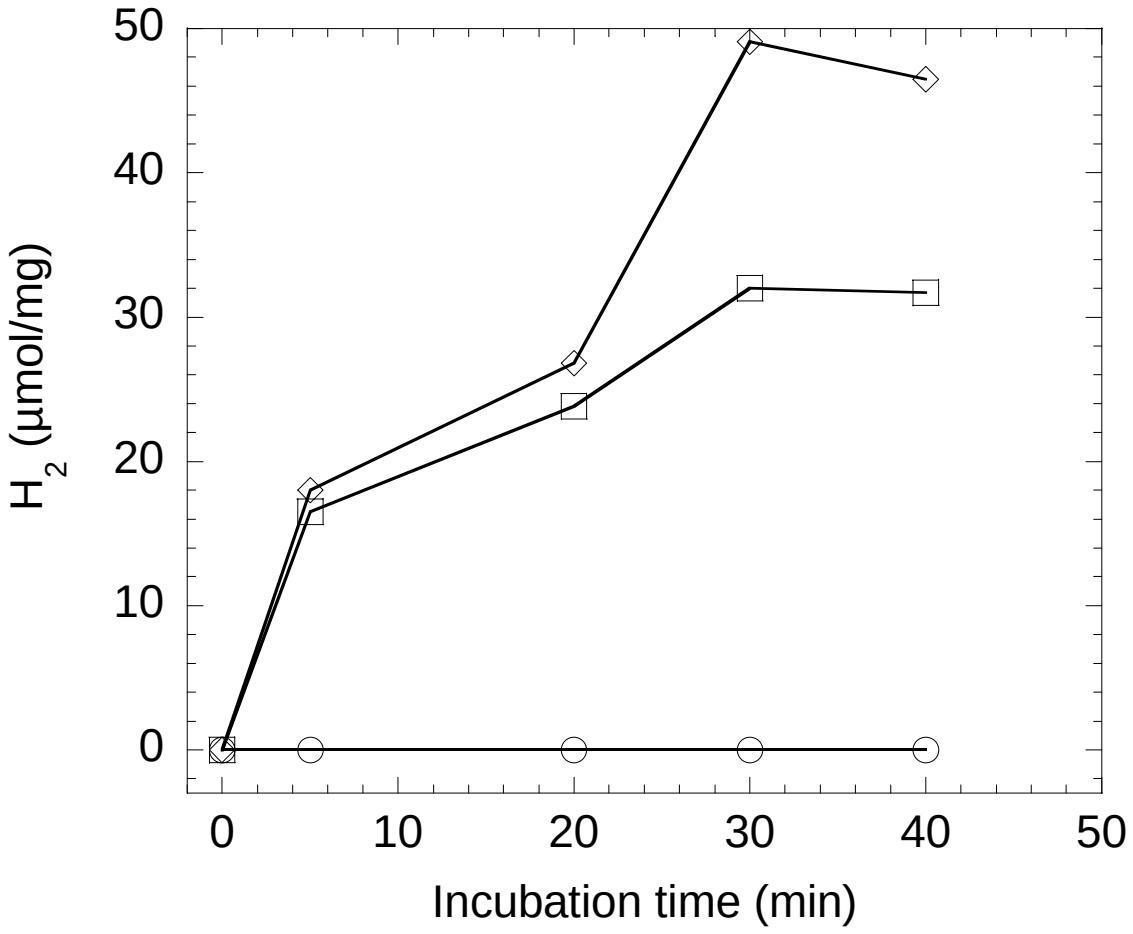

Figure 8-8 Hydrogen evolution with reduced ferredoxin as substrate catalyzed by purified *T. hypogea* hydrogenase.

Hydrogen production using ferredoxin reduced by POR as electron donor was measured with Buck Gas Chromatography. Details were described section 8.3.2. Circles, without both hydrogenase and ferredoxin added; squares, with hydrogenase and without ferredoxin added; diamonds, with both hydrogenase and ferredoxin added.

It has been reported that cytoplamic hydrogenases from some hyperthermophiles, such as *P. furiosus* can function as both hydrogenase and sulfur reductase (Ma et al. 1993, 2000). *T. hypogea* can reduce elemental sulfur to produce hydrogen sulfide (Fardeau et al. 1997). The sulfur reductase assay, therefore, was carried out. However, there was no sulfur reductase activity detectable for purified *T. hypogea* hydrogenase.

The hydrogen uptake activity of *T. hypogea* hydrogenase was dependent on both hydrogen and MV (BV) concentrations (Figure 8-9**,** Figure 8-10&Figure 8-11). The data were fitted to Michaelis-Menten kinetics using SigmaPlot10. Apparent K_m value for hydrogen and V_{max} value were determined to be 0.43 mM and 662.8 μmol min^{-1} mg^{-1}, respectively. Apparent K_m values for MV and BV and apparent V_{max} values were determined to be 0.17 and 0.24 mM; and 606.9 and 1142 μmol min^{-1} mg^{-1}, respectively. The hydrogen evolution activity was dependent on the concentration of MV. The catalysis followed Michaelis-Menten kinetics (Figure 8-12). The apparent K_m value and apparent V_{max} value were determined to be 1.1 mM and 192.4 μmol min^{-1} mg^{-1}, respectively. The K_m value for MV in hydrogen evolution is very close to that (1.25 mM) of hydrogenase II from *P. furiosus* (Ma et al. 2000), and two times lower than that of hydrogenase from *T. maritima* (Juszczak et al. 1991).

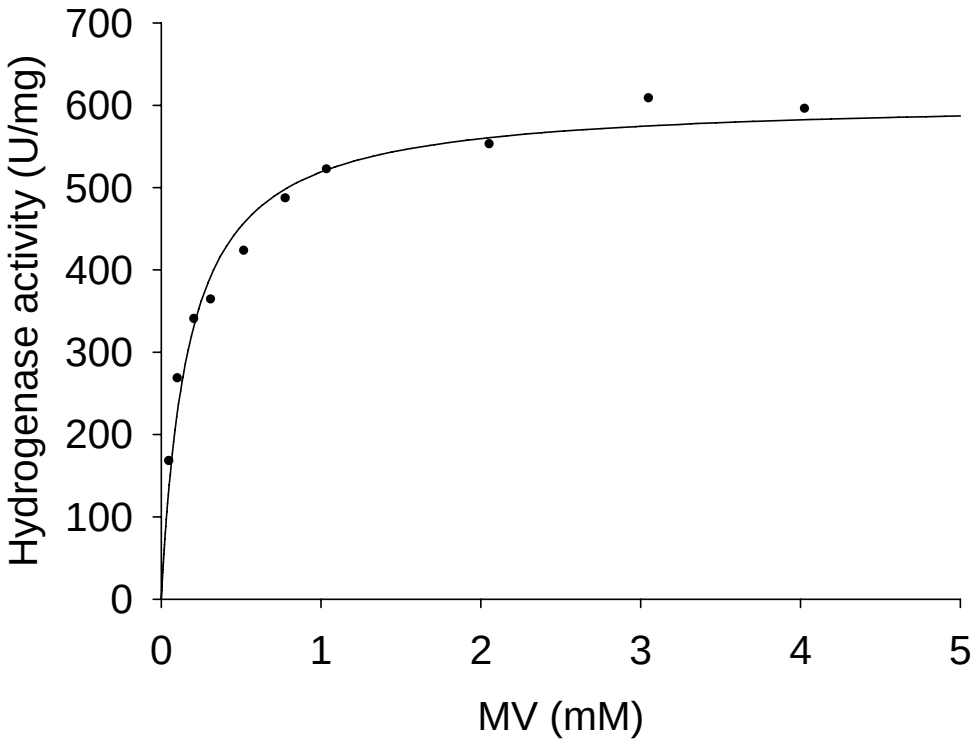

Figure 8-9 MV dependency of purified *T. hypogea* hydrogenase for hydrogen uptake.

The uptake activity of hydrogenase was measured at 80^{o}C with MV concentration varied from 0 to 4 mM. The results were fitted to Michaelis-Menten kinetics using SigmaPlot10.

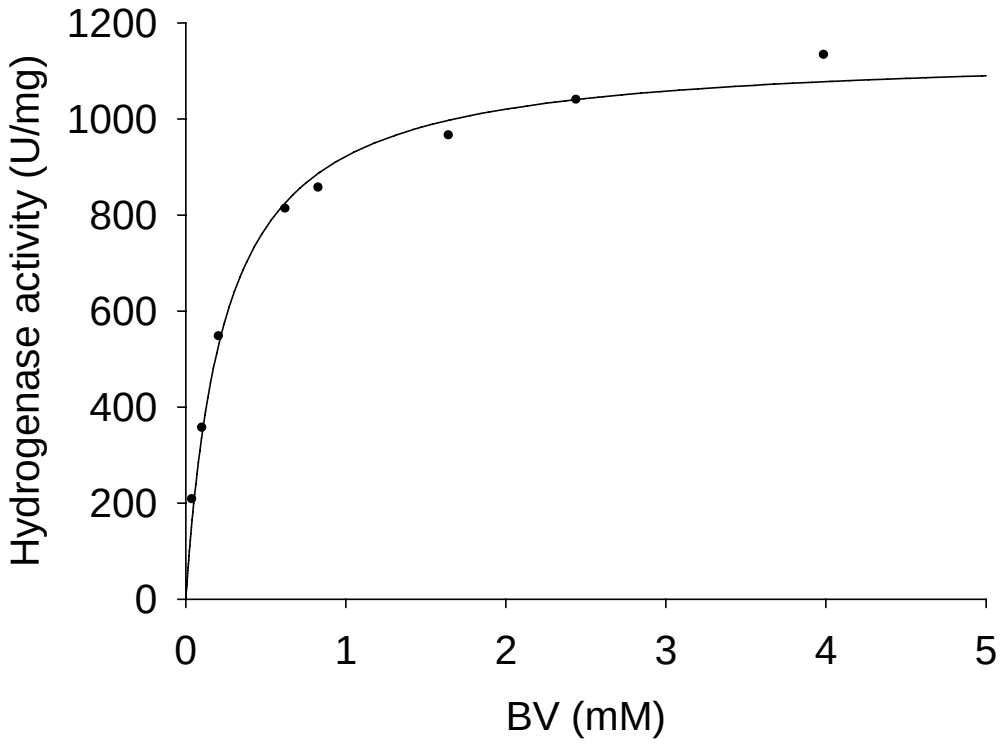

Figure 8-10 BV dependency of purified *T. hypogea* hydrogenase for hydrogen uptake.

The uptake activity of hydrogenase was measured at 80^{o}C with BV concentration varied from 0 to 4 mM. The results were fitted to Michaelis-Menten kinetics using SigmaPlot10.

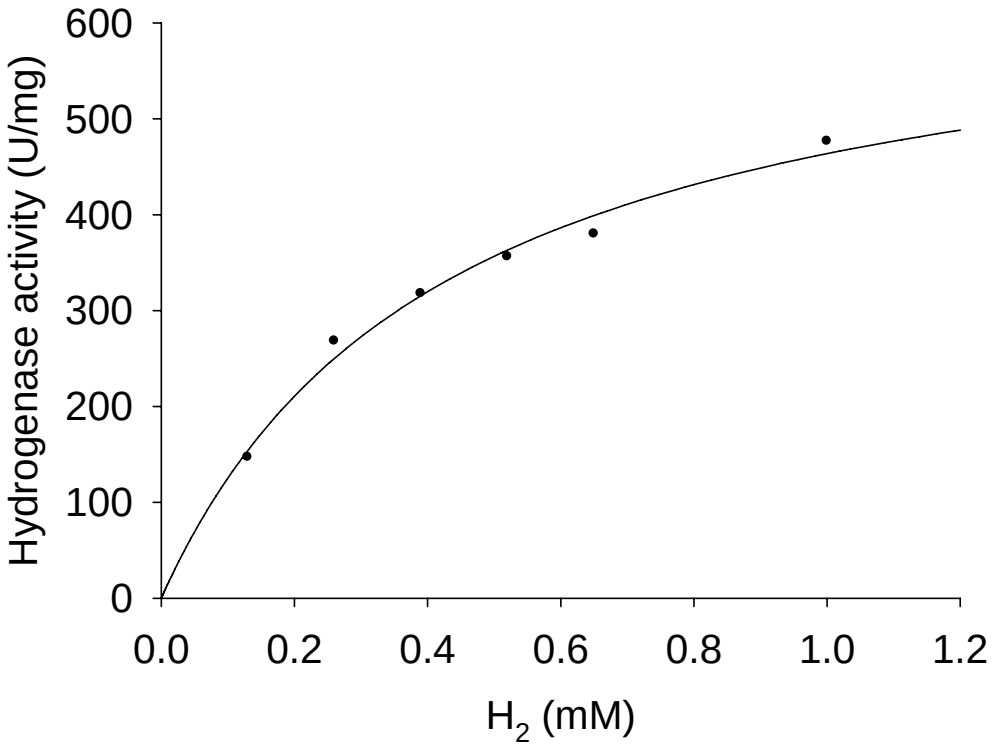

Figure 8-11 H_2 dependency of purified *T. hypogea* hydrogenase for hydrogen uptake.

The uptake activity of hydrogenase was measured at 80^{o}C with H_2 concentration varied from 0 to 1 mM. The results were fitted to Michaelis-Menten kinetics using SigmaPlot10.

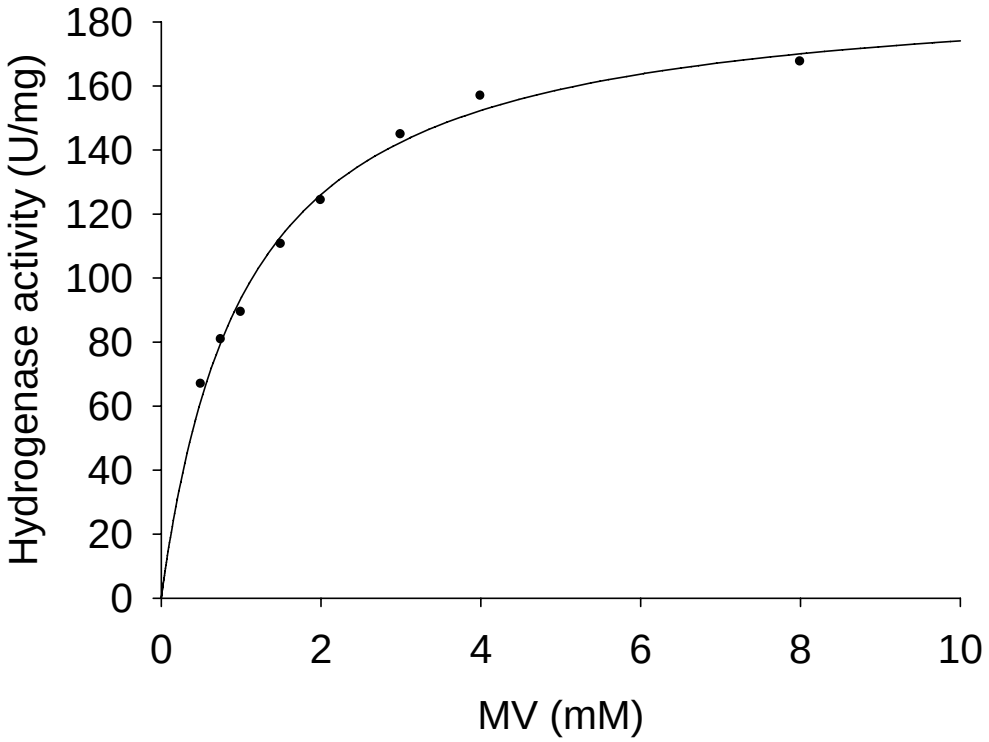

Figure 8-12 MV dependency of purified *T. hypogea* hydrogenase for hydrogen evolution.

Hydrogen evolution was measured at 80^{o}C by the production of hydrogen gas with Buck GC using SDT-reduced MV as electron donor. The results were fitted to Michaelis-Menten kinetics using SigmaPlot10.

8.5 DISCUSSION

It was found that the growth of *P. furiosus* was not inhibited by H_2 in the gas phase up to 50% (v/v). Its growth in the hydrogen atmosphere (100% hydrogen) could still achieve half of the growth in the absence of any added hydrogen in the culture containing both maltose and peptides. Previous study has shown that *P. furiosus* cannot grow in the hydrogen atmosphere without sulfur added in the media and without carbohydrate added (Malik et al. 1989). Our results showed that *P. furiosus* could grow in the 100% of hydrogen in the gas phase in a complex media containing peptone and maltose in the presence or absence of sulfur. It indicates that the inhibition of the growth by hydrogen may be related more to the metabolism of peptides. The cells grown in the hydrogen environment showed lower hydrogenase activity (Table 8-1). Since there is no inhibition of the purified hydrogenase activity by hydrogen (Ma et al. 1994, 2000), the lower hydrogenase activity may result from the lower level expression of hydrogenase. The ethanol production was greatly increased when there was hydrogen present in the gas phase. However, it was not the case if sulfur was present in the growth media, indicating elemental sulfur is a preferred electron acceptor compared to aldehyde or proton.

Hydrogenases in *P. furiosus*, the most studied model organism of hyperthermophilic archaea, have been extensively studied (Bryant and Adams 1989; Ma et al. 1993, 2000; Sapra et al. 2000; Silva et al. 2000). However, the study of hydrogenase in thermophilic bacteria is scarce. *T. hypogea* is a strictly anaerobic, fermentative bacterium that grows optimally at 70^{o}C and maximally up to 90^{o}C by fermenting carbohydrates and peptides to produce acetate, CO_2, and H_2 (Fardeau et al. 1997). It has great potential as a candidate for microbial hydrogen production since *T. hypogea* can utilize various substrates including the renewable agricultural residues. Hydrogenase activity was detected in the anaerobically prepared cell-free extract. It was higher in the xylose grown cell than that from glucose grown cells in the same growth phase. The activity at mid-log phase was higher than that at later log-phase, indicating hydrogenase is a growth related enzyme. The hydrogen oxidation activity of 8.1 U/mg in *T. hypogea*, is comparable to 5.4 U/mg in *P. furiosus* (Ma et al. 2000), 1.4 U/mg in *T. maritima* (Juszczak et al. 1990), 14 U/mg in *Clostridium pasteurianum* (Adams and Mortenson 1984), much lower than 72.5 U/mg in *Thermoanaerobacter tengcongensis* (Soboh et al. 2004) and 104 U/mg in *Desulfovibrio vulgaris* cytoplasmic fraction (van der Western et al. 1978).

The enzyme was purified 126-fold after 5 chromatographic columns and was slightly less than 1% in the cell (Table 8-2). The amount of hydrogenase present in *T. hypogea* cell-free extract is three times lower than that in *T. maritima* (Juszczak et al. 1991), while the purified enzyme (550 U/mg) is ten times more active than that of *T. maritima* hydrogenase (56 U/mg). The hydrogenase from *T. maritim*a was first identified as a homotetramer with subunit weight of 68 kDa, and later on corrected to be a heterotrimeric protein (Juszczak et al. 1991; Verhagen et al. 1999). Hydrogenase from *T. hypogea* showed different behaviour on chromatography columns compared to that from *T. maritima*. The enzyme exhibited very strong interaction with Phenyl-Sepharose column indicating that *T. hypogea* hydrogenase was more hydrophobic. *T. maritima* hydrogenase showed three peaks on gel filtration column with apparent M_r values of 120,000, 280,000 and 60,000 Da, while the purified *T. hypogea* hydrogenase only had one peak with apparent Mr value of 250 kDa. The SDS-PAGE (Figure 8-2) of the gel filtration fraction did have two bands close to 67 kDa, similar to the pure enzyme of *T. maritma*. However, the second band disappeared after Q-Sepharose column, and resulting enzyme had higher specific activity (Table 8-2). The hydrogenase from *T. hypogea* is therefore different from that of *T. maritma* in the aspect of molecular composition since it is a true homotetramer. Although the distribution of Fe-hydrogenase among microorganisms is very limited compared to that of Ni-Fe hydrogenases, a few characterized Fe-hydrogenase are very diverse with respect to subunit composition, iron sulfur content and enzymatic activity (Table 8-4). Like most Fe-hydrogenases, there was no flavin cofactor identified in the purified *T. hypogea* hydrogenase. The only known Fe-hydrogenase containing flavin is the NADH-dependent enzyme from *T. tengcongensis*, which is a heterotetramer containing an NAD(P)H dehydrogenase homologue (Soboh et al. 2004).

T. hypogea hydrogenase was very oxygen sensitive. It lost 50% of activity within 3 minutes when exposed to air, which is a common feature for Fe-hydrogenases. The $t_{1/2}$ of inactivation of the Fe-hydrogenase from *T. maritima* is only 10 s (Juszczak et al. 1991) and the extreme oxygen sensitivity caused a lot of unsuccessful purifications before the strictly anaerobic techniques were applied in the early 1970's (Adams 1990a). Study shows that the extreme oxygen sensitivity is caused by the direct binding of oxygen to one of the iron species located in the catalytic center (Hall et al. 1995). The purified *T. hypogea* hydrogenase could use the oxidized MV, BV, and *T. hypogea* ferredoxin for hydrogen oxidation, and reduced MV and *T. hypogea* ferredoxin for hydrogen evolution. The hydrogen evolution activity of *T. hypogea* hydrogenase with SDT-reduced MV is one fifth of the hydrogen oxidation activity, only one tenth when BV was used for hydrogen oxidation, indicating this

Table 8-4 Properties of Fe-hydrogenases

	C. pasteurianum		*Megasphaera elsdenii*	*D. vulgaris*	*T. maritima*	*T. hypogea*	*T. tengcongensis*
	I	II					
Oxygen sensitivity	Yes	Yes	Yes	No	Yes	Yes	Yes
$t_{1/2}$	5 min	30 min	NA	-	10 sec	3 min	NA
Molecular weight (kDa)	Monomer 62	Monomer 55	Monomer 58	Dimmer 46+10	Trimer 73 /68/19	Tetramer 65 k	Tetramer 65/64/20/14
V_{max}, H_2 uptake (U/mg)	24000	34000	9000	50,000	69	588/ MV 1100/BV	1700
V_{max}, H_2 evolution (U/mg)	5500	10	7000	4600	164	185	1700
Substrates for H_2 evolution	MV Ferredoxin	MV Ferredoxin	MV Ferredoxin	MV cytochrome c_3	MV	MV Ferredoxin	MV NADH
g atoms Fe/mol	20.1±0.7	13.8±0.4	15.6±2.7	9-15	32	16	NA
g atoms S^{2-}/mol	17.8±1.2	11.4±0.2	15.5±2.4	≈13	28.2±0.5	11.7	NA
Flavin	No	No	No	No	No	No	FMN
Ref.	Adams 1990a; Chen and Blanchard 1978				Juszczak et al. 1991	This work	Soboh et al. 2004

enzyme might be involved in hydrogen uptake. The hydrogenase from *T. maritima* shows similar ratio in hydrogen uptake and evolution (Juszczak et al. 1991; Verhagen et al. 1999). *T. hypogea* hydrogenase could use ferredoxin as electron carrier in hydrogen uptake and hydrogen evolution, which is similar to *C. pasteurianum* and *M. elsdenii* (Adams 1990b). It suggests that the purified Fe-hydrogenase of *T. hypogea* may be involved in hydrogen production in the cell with reduced ferredoxin generated during fermentation as substrate.

Chapter 9 General Conclusions

Flavoproteins are ubiquitous enzymes catalyzing oxidoreduction reactions. They are well studied in mesophiles and are known for being involved in various essential processes such as energy metabolism, DNA biosynthesis, against oxidative stress, redox regulation etc (Müller 1991). Their involvement in the metabolism of hyperthermophiles was studied and presented in this report. It was estimated that 4.89%, 5.97% and 8.02% of the ORFs based on motif search and 2.21%, 1.88% and 3.63% of the ORFs based on the match of annotated sequences to experimentally characterized flavoproteins could potentially encode flavoproteins in *P. furiosus*, *T. maritima* and *E. coli*, respectively.

9.1 Flavoproteins involved in oxygen defensive system of *Thermotoga* species

As reported in this thesis, it was found that *T. maritima* and *T. hypogea* could tolerate up to 5.5 and 4.1 μM of dissolved oxygen in the media under continuous shaking conditions, which was unexpected for the obligate anaerobes. An NADH oxidase that can reduce molecular oxygen to hydrogen peroxide or water was detected in *Thermotoga* species. This enzyme was purified and characterized from *T. hypogea* and *T. maritima*. Both enzymes were FAD-containing proteins with native molecular mass around 100 kDa and catalyzed the production of hydrogen peroxide exclusively by reducing oxygen. In the cell-free extract of *T. hypogea* and *T. maritima*, NADH-dependent peroxidase activities had been detected, indicating that both NADH oxidase and NADH peroxidase may act as a system that has the ability to reduce accidentally encountered oxygen to water. The *T. maritima* NADH oxidase was a heterodimer and contained one [2Fe-2S]-center in the large subunit, which was a new type of NADH oxidase identified in hyperthermophiles. The NADH oxidase from *T. maritima* was highly active and oxygen sensitive, indicating it may play some regulatory role to adjust the amount of NADH oxidase expressed in the cell. An accurate and easy way to measure hydrogen peroxide in the NADH oxidase mixture was formulated based on the principle of lability of NADH and stability of hydrogen peroxide under acidic conditions.

9.2 Flavoproteins involved in redox regulation system

As reported in this thesis, a Trx-TrxR system, which is responsible for thiol regulation and oxidative stress protection in cells, was found in *T. maritima*. In contrast to the oxidized environment in the cell surface, the inside of the cell is kept reduced and proteins contain many free sulfhydryl groups (Arnér and Holmgren 2000; Gilbert 1990). As the major ubiquitous disulfide reductase, Trx is very important for maintaining proteins in their reduced state. Disulfide bonds in protein are very important either as

structural features to stabilize protein or part of catalytic cycles (Ritz and Beckwith 2001). Trx and TrxR from *T. maritima* were purified and characterized. TrxR from *T. maritima* was a 67 kDa homodimeric FAD-containing enzyme and showed typically physical properties of bacterial TrxR, but had distinct biochemical properties with respect to catalyzing the direct reduction of DTNB. The purified Trx from *T. maritima* was a monomer with a molecular weight of 23 kDa estimated by gel filtration and 31 kDa estimated by SDS-PAGE, which is bigger than conventional Trx from mesophiles and close to a group of disulfide reductase in hyperthermophiles. *T. maritima* Trx- TrxR system could reduce both insulin and DTNB using either NADH or NADPH as electron donor, which is the first one described in hyperthermophilic bacteria.

9.3 Multi functionality of flavoproteins in hyperthermophiles

As reported in this thesis, the flavoproteins investigated showed multi functionality. In addition to its ability to reduce oxygen with NADH, the NADH oxidase from *T. hypogea* exhibited DLDH activity, which is one component of the glycine decarboxylase system. However, the physiological significance of this activity in *T. hypogea* is not clear since *T. hypogea* could not grow with glycine as sole carbon and energy source and there was no GDC activity detectable. Apart from the high activity towards reduction of oxygen, the NADH oxidase from *T. maritima* demonstrated FAD-GPDH activity, which is a key component in the glycerol catabolism. It could also oxidize *sn*-G-3-P with molecular oxygen to produce hydrogen peroxide and dihydroxyacetone phosphate. It was verified that *T. maritima* could grow with glycerol as sole carbon and energy source. The TrxR from *T. maritima* shows the capability to catalyze the reduction of molecular oxygen with either NADH or NADPH as electron donor. Both TrxR and NADH oxidase from *T. maritima* showed FNOR activity, which is crucial for fermentative hyperthermophiles to convert the reducing equivalent, reduced ferredoxin, generated during fermentation to NAD(P)H. This enzyme is important for recycling ferredoxin and generating NAD(P)H for biosynthesis. The FNOR in *P. furiosus* is bifunctional as well (Ma and Adams 1994). Besides its FNOR activity, the enzyme also functions as a sulfide dehydrogenase. This property of FNOR in hyperthermophiles may represent a new feature of this enzyme from this group of microorganisms. The multi functionality of flavoproteins in hyperthermophiles may compensate for the less overall quantity of flavoproteins compared to that in mesophiles based on the predictions.

9.4 Hydrogen metabolism in hyperthermophiles

Hydrogen metabolism is crucial for hyperthermophilic and heterotrophic anaerobes especially in the absence of electron acceptors such as elemental sulfur or sodium thiosulphate. It was demonstrated that *P. furiosus* could grow well in the presence of 50% of hydrogen in the gas phase, which was the same as that of the growth in the absence of hydrogen. The growth in the hydrogen atmosphere could reach more than 50% of that in the absence of hydrogen, indicating *P. furiosus* is not sensitive to hydrogen inhibition. Some NADPH-utilizing enzymes such as hydrogenase and alcohol dehydrogenase were affected by the presence of 100% added hydrogen to the gas phase of the growth media. Since the hydrogenases in *P. furiosus* are FAD-containing complex proteins (Bryant and Adams 1989; Ma et al. 2000), effort was made to study the hydrogenase in hyperthermophilic bacterium, *T. hypogea*, which is promising bacterium for microbial hydrogen production. The growth related hydrogenase activity was detected in *T. hypogea* and it showed higher activity from xylose grown cells than glucose grown cells. The hydrogenase was purified following hydrogen oxidation activity using BV as electron acceptor. Unlike the enzymes from archeaon, *P. furiosus*, this hydrogenase was not a flavin-containing protein. The purified hydrogenase was a Fe-hydrogenase and able to utilize ferredoxin as electron carrier for hydrogen evolution and uptake, indicating it is a very important enzyme in hydrogen metabolism in *T. hypogea*.

Flavoproteins have been extensively studied in mesophiles. However, little is known about their full functions in hyperthermophiles. Clearly, this study has demonstrated biochemical properties of flavoproteins including NADH oxidase, DLDH, FAD-GPDH, and TrxR, and their functions in hyperthermophilic bacteria *Thermotoga* species. It suggested that the results not only shed light on the involvement of flavoproteins in important biological process such as oxygen detoxification and energy conservation in hyperthermophiles, but also to provide the comparison of the studied flavoprotein to their mesophilic counterparts and to understand those enzyme from the perspective of evolution.

Chapter 10 References

Achenbach-Richter, L., R. Gupta, K.O. Stetter, and C.R. Woese. 1987. Were the original eubacteria thermophiles? Syst. Appl. Microbiol. 9:34-39.

Adams, M.W.W. 1990a. The structure and mechanism of iron-hydrogenases. Biochim. Biophys. Acta 1020:115-145.

Adams, M.W.W. 1990b. The metabolism of hydrogen by extremely thermophilic, sulfur-dependent bacteria. FEMS Microbiol. Rev. 75:219-238.

Adams, M.W.W. 1994. Biochemical diversity among sulfur-dependent, hyperthermophilic microorganisms. FEMS Microbiol. Rev. 15:261-277.

Adams, M.W.W., and R.M. Kelly. 1998. Finding and using hyperthermophilic enzymes. Trends Biotechnol. 16:329-332.

Adams, M.W.W., and L.E. Mortenson. 1984. The purification of hydrogenase II (uptake hydrogenase) from the anaerobic N_2-fixing bacterium *Clostridium pasteurianum*. Biochim. Biophys. Acta 766:51-61.

Adams, M.W.W., L.E. Mortenson, and J.-S. Chen. 1981. Hydrogenase. Biochim. Biophys. Acta 1981. 594:105-176.

Adams, M.W.W., F.B. Perler, and R.M. Kelly. 1995. Extremoenzymes: expanding the limits of biocatalysis. Biotechnol. 13:662-668.

Albracht, S.P.J. 1994. Nickel hydrogenases: in search of the active site. Biochim. Biophys. Acta 1188:167-204.

Alexandre, S., J. Telegdi, I. Boutelet, S. Julein, and J.C. Vincent. 1992. An enzymatic determination of hydrogen peroxide by using spectrophotometry. C.R. Acad. Sci. III 315: 85-91.

Altschul, S.F., T.L. Madden, A.A. Schäffer, J. Zhang, Z. Zhang, W. Miller, and D.J. Lipman. 1997. Gapped BLAST and PSI-BLAST: a new generation of protein database search programs. Nucleic Acids Res. 25:3389-3402.

Amend, J.P., and E.L. Shock. 2001. Energetics of overall metabolic reactions of thermophilic and hyperthermophilic archaea and bacteria. FEMS Microbiol. Rev. 25:175-243.

Andreesen, J.R. 1994. Glycine metabolism in anaerobes. Antonie van Leeuwenhoek 66:233-237.

Argyrou, A., and J.S. Blanchard. 2004. Flavoprotein disulfide reductases: advances in chemistry and function. Prog. Nucleic Acid Res. Mol. Biol. 78:89-142.

Argyrou, A., G.X. Sun, B.A. Palfey, and J.S. Blanchard. 2003. Catalysis of diaphorase reactions by *Mycobacterium tuberculosis* lipoamide dehydrogenase occurs at the EH_4 level. Biochemistry 42:2218-2228.

Arinze, I.J. 2005. Facilitating understanding of the purine nucleotide cycle and the one-carbon pool: Part II Metabolism of the one-carbon pool. Biochem. Mol. Biol. Edu. 33:255-259.

Arnér, E.S.J., and A. Holmgren. 2000. Physiological functions of thioredoxin and thioredoxin reductase. Eur. J. Biochem. 267:6102-6109.

Arnér, E.S.J., J. Nordberg, and A. Holmgren. 1996. Efficient reduction of lipoamide and lipoic acid by mammalian thioredoxin reductase. Biochem. Biophys. Res. Commun. 225:268-274.

Arner, E.S., L. Zhong, and A. Holmgren. 1999. Preparation and assay of mammalian thioredoxin and thioredoxin reductase. Methods Enzymol. 300:226-239.

Arunachalam, U., V. Massey, and C.S. Vaidyanathan. 1992. p-Hydroxyphenylacetate-3-hydroxylase: a two protein component enzyme. J. Biol. Chem. 267:25848-25855.

Baker, A., C.M. Payne, M.M. Briehl, and G. Powis. 1997. Thioredoxin, a gene found overexpressed in human cancer, inhibits apoptosis *in vitro* and *in vivo*. Cancer Res. 57:5162-5167.

Balch, W.E., G.E. Fox, L.J. Magrum, C.R. Woese, and R.S. Wolfe. 1979. Methanogens: reevaluation of a unique biological group. Microbiol. Rev. 43:260-296.

Balk, M., J. Weijma, and A.J.M. Stams. 2002. *Thermotoga lettingae* sp. nov., a novel thermophilic, methanol-degrading bacterium isolated from a thermophilic anaerobic reactor. Int. J. Syst. Evol. Microbiol. 52:1361-1368.

Ballou, D.P., B. Entsch, and L.J. Cole. 2005. Dynamics involved in catalysis by single-component and two-component flavin-dependent aromatic hydroxylases. Biochem. Biophys. Res. Comm. 338:590-598.

Bao, Q., Y. Tian, W. Li, Z. Xu, Z. Xuan, S. Hu, W. Dong, J. Yang, Y. Chen, Y. Xue, Y. Xu, X. Lai, L. Huang, X. Dong, Y. Ma, L. Ling, H. Tan, R. Chen, J. Wang, J. Yu, and H. Yang. 2002. A complete sequence of the *T. tengcongensis* genome. Genome Res. 12:689-700.

Barker, H.A. 1981. Amino acid degradation by anaerobic bacteria. Annu. Rev. Biochem. 50:23-40.

Barnard, G.F., and M. Akhtar. 1979. Mechanistic and stereochemical studies on the glycine reductase of *Clostridium sticklandii*. Eur. J. Biochem. 99:593-603.

Barnett, J.A., R.W. Rayne, and D.Y. Yarrow. 1983. Yeasts: characteristics and identification. Cambridge University Press, Cambridge.

Barns, S.M., C.F. Delwhiche, J.D. Palmer, and N.R. Pace. 1996. Perspectives on archaeal diversity, thermophily and monophyly from environmental rRNA sequences. Proc. Natl. Acad. Sci. USA 93:9188-9193.

Barns, S.M., R.E. Fundyga, M.W. Jeffries, and N.R. Pace. 1994. Remarkable archaeal diversity detected in a Yellowstone National Park hot spring environment. Proc. Natl. Acad. Sci. USA 91:1609-1613.

Baross, J.A., and J.F. Holden. 1996. Overview of hyperthermophiles and their heat-shock proteins. Adv. Prot. Chem. 48:1-34.

Bauer, M.W., S.B. Halio, and R.M. Kelly. 1996. Proteases and glycosyl hydrolases from hyperthermophilic microorganisms. Adv. Pro. Chem. 48:271-310.

Baughn, A.D., and M.H. Malamy. 2004. The strict anaerobe *Bacteroides fragilis* grows in and benefits from nanomolar concentrations of oxygen. Nature 427:441-444.

Bäumer, S., T. Ide, C. Jacobi, A. Johann, G. Gottschalk, and U. Deppenmeier. 2000. The $F_{420}H_2$ dehydrogenase from *Methanosarcina mazei* is a redox-driven proton pump closely related to NADH dehydrogenases. J. Biol. Chem. 275:17968-17973.

Beinert, H. 1983. Semi-micro methods for analysis of labile sulfide and of labile sulfide plus sulfane sulfur in unusually stable iron-sulfur proteins. Anal. Biochem. 131:373-378.

Berg, A., and A. de Kok. 1997. 2-oxo acid dehydrogenase multienzyme complexes: The central role of the lipoyl domain. Biol. Chem. 378:617-634.

Bindoli, A., and M.P. Rigobello. 2002. Mitochondrial thioredoxin reductase and thiol status. Methods Enzymol. 347:307-316.

Blamey, J.M., and M.W.W. Adams. 1994. Characterization of an ancestral type of pyruvate ferredoxin oxidoreductase from the hyperthermophilic bacterium, *Thermotoga maritima*. Biochemistry 33:1000-1007.

Blamey, J.M., S. Mukund, and M.W.W. Adams. 1994. Properties of a thermostable 4 Fe-ferredoxin from the hyperthermophilic bacterium *Thermotoga maritima*. FEMS Microbiol. Lett. 121:165-170.

Blattner, F.R., G. Plunkett III, C.A. Bloch, N.T. Perna, V. Burland, M. Riley, J. Collado-Vides, J.D. Glasner, C.K. Rode, G.F. Mayhew, J. Gregor, N.W. Davis, H.A. Kirkpatrick, M.A. Goeden, D.J. Rose, B. Mau, and Y. Shao. 1997. The complete genome sequence of *Escherichia coli* K-12. Science 277:1453-1462.

Blyth, A.W. 1879. The composition of cows' milk in health and disease. J. Chem. Soc. 35:530-539.

Bork, P., and T.J. Gibson. 1996. Applying motif and profile searches. Methods Enzymol. 266:162-184.

Bornemann, S., M.K. Ramjee, S. Balasubramanian, C. Abell, J.R. Coggins, D.J. Lowe, and R.N.F. Thorneley. 1995. *Escherichia coli* chorismate synthase catalyzes the conversion of (6S)-6-fluoro-5-enolpyruvylshikimate-3-phosphate to 6-fluorochorismate. J. Biol. Chem. 270:22811-22815.

Bourguignon, J., V. Merand, S. Rawsthorne, E. Forest, and R. Douce. 1996. Glycine decarboxylase and pyruvate dehydrogenase complexes share the same dihydrolipoamide dehydrogenase in pea leaf mitochondria: evidence from mass spectrometry and primary-structure analysis. Biochem. J. 313:229-234.

Bradford, M.M. 1976. A rapid and sensitive method for the quantification of microgram quantities of protein utilizing the principle of protein-dye binding. Anal. Biochem. 72:248-254.

Bronnenmeier, K., A. Kern, W. Liebl, and W.L. Staudenbauer. 1995. Purification of *Thermotoga maritima* enzymes for the degradation of cellulosic materials. Appl. Environ. Microbiol. 61:1399-1407.

Brown, N.L., S.J. Ford, R.D. Pridmore, and D.C. Fritzinger. 1983. Nucleotide sequence of a gene from the *Pseudomonas* transposon Tn501 encoding mercuric reductase. Biochemistry 22:4089-4095.

Brüggemann, H., S. Bäumer, W.F. Fricke, A. Wiezer, H. Liesegang, I. Decker, C. Herzberg, R. Martinez-Arias, R. Merkl, A. Henne, and G. Gottschalk. 2003. The genome sequence of *Clostridium tetani*, the causative agent of tetanus disease. Proc. Natl. Acad. Sci. USA 100:1316-1321.

Bryant, F.O., and M.W.W. Adams. 1989. Characterization of hydrogenase from the hyperthermophilic archaebacterium, *Pyrococcus furiosus*. J. Biol. Chem. 264:5070-5079.

Bryk, R., P. Griffin, and C. Nathan. 2000. Peroxynitrite reductase activity of bacterial peroxiredoxins. Nature 407:211-215.

Bunik, V.I. 2003. 2-oxo acid dehydrogenase complexes in redox regulation: role of the lipoate residues and thioedoxin. Eur. J. Biochem. 270:1036-1042.

Carothers, D.J., G. Pons, and M.S. Patel. 1989. Dihydrolipoamide dehydrogenase: functional similarities and divergent evolution of the pyridine nucleotide-disulfide oxidoreductases. Arch. Biochem. Biophys. 268:409-425.

Carrillo, N., and E.A. Ceccarelli. 2003. Open questions in ferredoxin-$NADP^+$ reductase catalytic mechanism. Eur. J. Biochem. 270:1900-1915.

Casero, E., M. Darder, K. Takada, H.D. Abruna, F. Pariente, and E. Lorenzo. 1999. Electrochemically triggered reaction of a surface-confined reagent: mechanistic and EQCM characterization of redox-active self-assembling monolayers derived from 5,5'-dithiobis(2-nitrobenzoic acid) and related materials. Langmuir. 15:127-134.

Cashman, J.R. 2005. Some distinctions between flavin-containing and cytochrome P450 monooxygenases. Biochem. Biophys. Res. Commun. 338:599-604.

Chae, H.Z., S.J. Chung, and S.G. Rhee. 1994. Thioredoxin-dependent peroxide reductase from yeast. J. Biol. Chem. 269:27670-27678.

Chen, J.-S., and D.K. Blanchard. 1978. Isolation and properties of a unidirectional H_2-oxidizing hydrogenase from the strictly anaerobic N_2-fixing bacterium *Clostridium pasteurianum* W5. Biochem. Biophys. Res. Commun. 84:1144-1150.

Chen, J.-S., and D.K. Blanchard. 1979. A simple hydrogenase-linked assay for ferredoxin and flavodoxin. Anal. Biochem. 93:216-222.

Chen, J.-S., and L.E. Mortenson. 1974. Purification and properties of hydrogenase from *Clostridium pasteurianum* W5. Biochim. Biophys. Acta 371:283-298.

Chen, J.-S., and L.E. Mortenson. 1977. Inhibition of methylene blue formation during determination of the acid-labile sulfide of iron-sulfur protein samples containing dithionite. Anal. Biochem. 79:157-165.

Chhabra, S.R., K.R. Shockley, S.B. Conners, K.L. Scott, R.D. Wolfinger, and R.M. Kelly. 2003. Carbohydrate-induced differential gene expression patterns in the hyperthermophilic bacterium *Thermotoga maritima*. J. Biol. Chem. 278:7540-7552.

Chhabra, S.R., K.R. Shockley, D.E. Ward, and R.M. Kelly. 2002. Regulation of endo-acting glycosyl hydrolases in the hyperthermophilic bacterium *Thermotoga maritima* grown on glucan- and mannan-based polysaccharides. Appl. Environ. Microbiol. 68:545-554.

Childs, R.E., and W.G. Bardsley. 1975. The steady-state kinetics of peroxidase with 2,2'-azino-di-(3-ethylbenzthiazoline-6-sulphonic acid) as chromogen. Biochem. J. 145:93-103.

Chiu, M. 2006. Quantitative and comparative study of flavoproteins among mesophilic and hyperthermophilic microorganisms. B.Sc. Thesis. Univ. of waterloo, ON, Canada.

Coats, J.H., G.P. Li, M.S. Kuo, and D.A. Yurek. 1989. Discovery, production, and biological assay of an unusual flavenoid cofactor involved in lincomycin biosynthesis. J. Antibiot. 42:472-474.

Cohen, G.N., V. Barbe, D. Flament, M. Galperin, R. Heilig, O. Lecompte, O. Poch, D. Prieur, J. Quérellou, R. Ripp, J.-C. Thierry, J. van der Oost, J. Weissenbach, Y. Zivanovic, and P.

Forterre. 2003. An integrated analysis of the genome of the hyperthermophilic archaeon *Pyrococcus abyssi*. Mol. Microbiol. 47:1495-1512.

Cole, S.T., K. Eiglmeier, S. Ahmed, D. Honore, L. Elmes, W.F. Anderson, and J.H. Weiner. 1988. Nucleotide sequence and gene-polypeptide relationship of the glpABC operon encoding the anaerobic *sn*-glycerol-3-phosphate dehydrogenase of *Escherichia coli* K-12. J. Bacteriol. 170:2448-2456.

Cole, E.S., C.A. Lepp, P.D. Holohan, and T.P. Fondy. 1978. Isolation and characterization of flavin-linked glycerol-3-phosphate dehydrogenase from rabbit skeletal muscle mitochondria and comparison with the enzyme from rabbit brain. J. Biol. Chem. 253:7952-7959.

Coulter, E.D., N.V. Shenvi, and D.M. Kurtz Jr. 1999. NADH peroxidase activity of rubrerythrin. Biochem. Biophys. Res. Commun. 255:317-323.

Cromartie, T.H., and C.T. Walsh. 1976. *Escherichia coli* glyoxalate carboligase: Properties and reconstitution with 5-deazaFAD and 1, 5-dihydrodeazaFADH_2. J. Biol. Chem. 251:329-333.

Daiyasu, H., T. Hiroike, Y. Koga, and H. Toh. 2002. Analysis of membrane stereochemistry with homology modeling of *sn*-glycerol-1-phosphate dehydrogenase. Protein Eng. 15:987-995.

Danson, M.J., K. Conroy, A. McQuattie, and K.J. Stevenson. 1987. Dihydrolipoamide dehydrogenase from *Trypanosoma brucei* characterization and cellular location. Biochem. J. 243:661-665.

Das, D., T. Dutta, K. Nath, S.M. Kotay, A.K. Das, and T.N. Veziroglu. 2006. Role of Fe-hydrogenase in biological hydrogen production. Curr. Sci. 90:1627-1637.

Davies, G.J., S.J. Gamblin, J.A. Littlechild, and H.C. Watson. 1993. The structure of a thermally stable 3-phosphoglycerate kinase and a comparison with its mesophilic equivalent. Proteins 15:283-289.

de Kok, A., A.F. Hengeveld, A. Martin, and A.H. Westphal. 1998. The pyruvate dehydrogenase multi-enzyme complex from gram-negative bacteria. Biochim. Biophys. Acta 1385:353-366.

de Vos, W.M., S.W.M. Kengen, W.G.B. Voorhorst, and J. van der Oost. 1998. Sugar utilization and its control in hyperthermophiles. Extremophiles 2:201-205.

Dhanjoon, J.K. 2005. Growth on biopolymers and purification and characterization of a xylanase of *Thermotoga hypogea*. M.Sc. Thesis. Univ. Waterloo, ON, Canada.

Diaz, P.I., P.S. Zilm, and A.H. Rogers. 2002. *Fusobacterium nucleatum* supports the growth of *Porphyromonas gingivalis* in oxygenated and carbon-dioxide-depleted environments. Microbiology 148:467-472.

Diêp Lê, K.H., and F. Lederer. 1991. Amino acid sequence of long chain α-hydroxy acid oxidase from rat kidney, a member of the family of FMN-dependent α-hydroxy acid-oxidizing enzymes. J. Biol. Chem. 266:20877-20881.

Dietrichs, D., and J.R. Andreesen. 1990. Purification and comparative studies of dihydrolipoamide dehydrogenases from the anaerobic, glycine-utilizing bacteria *Peptostreptococcus glycinophilus*, *Clostridium cylindrosporum*, and *Clostridium sporogenes*. J. Bacteriol. 172:243-251.

Dietrichs, D., M. Meyer, B. Schmidt, and J.R. Andreesen. 1990. Purification of NADPH-dependent electron-transferring flavoproteins and N-terminal protein sequence data of dihydrolipoamide dehydrogenase from anaerobic, glycine-utilizing bacteria. J. Bacteriol. 172:2088-2095.

Dolin, M.I. 1959. Oxidation of reduced diphosphopyridine nucleotide by *Clostridium perfringens* I. Relation of peroxide to the over-all reaction. J. Bacteriol. 77:383-392.

Donoghue, N.A., D.B. Norris, and P.W. Trudgill. 1976. The purification and properties of cyclohexanone oxygenase from *Nocardia globerula* CL1 and *Acinetobacter* NCIB 9871. Eur. J. Biochem. 63:175-192.

Douce, R., J. Bourguignon, M. Neuburger, and F. Rébeillé. 2001. The glycine decarboxylase system: a fascinating complex. Trends Plant Sci. 6:167-176.

Driskill, L.E., K. Kusy, M.W. Bauer, and R.M. Kelly. 1999. Relationship between glycosyl hydrolase inventory and growth physiology of the hyperthermophile *Pyrococcus furiosus* on carbohydrate-based media. Appl. Environ. Microbiol. 65:893-897.

Duetz, W.A., and B. Witholt. 2004. Oxygen transfer by orbital shaking of square vessels and deepwell microtiter plates of various dimensions. Biochem. Eng. J. 17:181-185.

Dym, O., and D. Eisenberg. 2001. Sequence-structure analysis of FAD-containing proteins. Protein Sci. 10:1712-1728.

Ellman, G.L. 1959. Tissue sulfhydryl groups. Arch. Biochem. Biophys. 82:70-77.

Engelkirk, P.G., J. Duben-Engelkirk, and V.R. Dowell. 1992. Principles and practice of clinical anaerobic bacteriology. Star Publishing Company, Belmont, California.

Erauso, G., A.-L. Reysenbach, A. Godfroy, J.-R. Meunier, B. Crump, F. Partensky, J.A. Baross, V. Marteinsson, G. Barbier, N.R. Pace, and D. Prieur. 1993. *Pyrococcus abyssi* sp. nov., a new hyperthermophilic archaeon isolated from a deep-sea hydrothermal vent. Arch. Microbiol. 160:338-349.

Fardeau, M.L., B. Ollivier, B.K.C. Patel, M. Magot, P. Thomas, A. Rimbault, F. Rocchiccioli, and J.L. Garcia. 1997. *Thermotoga hypogea* sp. nov., a xylanolytic, thermophilic bacterium from an oil-producing well. Int. J. Syst. Bacteriol. 47:1013-1019.

Fiala, G., and K.O. Stetter. 1986. *Pyrococcus furiosus* sp. nov. represents a novel genus of marine heterotrophic archaebacteria growing optimally at 100^{o}C. Arch. Microbiol. 145:56-61.

Fisher, A.J., F.M. Raushel, T.O. Baldwin, and I. Rayment. 1995. Three-dimensional structure of bacterial luciferase from *Vibrio harveyi* at 2.4Å resolution. Biochemistry 34:6581-6586.

Fournier, M., Z. Dermoun, M.-C. Durand, and A. Dolla. 2004. A new function of the *Desulfovibrio vulgaris* Hildenborough [Fe] hydrogenase in the protection against oxidative stress. J. Biol. Chem. 279:1787-1793.

Fraaije, M.W., and A. Mattevi. 2000. Flavoenzymes: diverse catalysts with recurrent features. Trends Biochem. Sci. 25:126-132.

Fraaije, M.W., R.H.H. van den Heuvel, W.J.H. van Berkel, and A. Mattevi. 1999. Covalent flavinylation is essential for efficient redox catalysis in vanillyl-alcohol oxidase. J. Biol. Chem. 274:35514-35520.

Freudenberg, W., D. Dietrichs, H. Lebertz, and J.R. Andreesen. 1989a. Isolation of an atypically small lipoamide dehydrogenase involved in the glycine decarboxylase complex from *Eubacterium acidaminophilum*. J. Bacteriol. 171:1346-1354.

Freudenberg, W., F. Mayer, and J.R. Andreesen. 1989b. Immunocytochemical localization of proteins P1, P2, P3 of glycine decarboxylase, all involved in anaerobic glycine metabolism of *Eubacterium acidaminophilum*. Arch. Microbiol. 152:182-188.

Friedman, M. 1999. Chemistry, nutrition and microbiology of D-amino acids. J. Agric. Food. Chem. 47:3457-3479.

Fritz, G., A. Roth, A. Schiffer, T. Büchert, G. Bourenkov, H.D. Bartunik, H. Huber, K.O. Stetter, P.M.H. Kroneck, and U. Ermler. 2002. Structure of adenylylsulfate reductase from the hyperthermophillic *Archaeoglobus fulgidus* at 1.6-Å resolution. Proc. Natl. Acad. Sci. USA 99:1836-1841.

Fucci, L., C.N. Oliver, M.J. Coon, and E.R. Stadtman. 1983. Inactivation of key metabolic enzymes by mixed-function oxidation reactions: possible implication in protein turnover and ageing. Proc. Natl. Acad. Sci. USA 80:1521-1525.

Fukui, T., H. Atomi, T. Kanai, R. Matsumi, S. Fujiwara, and T. Imanaka. 2005. Complete genome sequence of the hyperthermophilic archaeon *Thermococcus kodakaraensis* KOD1 and comparison with Pyrococcus genomes. Genome Res. 15:352-363.

Galperin, M.Y., K.M. Noll, and A.H. Romano. 1996. The glucose transport system of the hyperthermophilic anaerobic bacterium *Thermotoga neapolitana*. Appl. Environ. Microbiol. 62:2915-2918.

Gan, Z.-R., and W.W. Wells. 1986. Purification and properties of thioltransferase. J. Biol. Chem. 261:996-1001.

Gasdaska, P.Y., J.R. Gasdaska, S. Cochran, and G. Powis. 1995. Cloning and sequencing of a human thioredoxin reductase. FEBS Lett. 373:5-9.

Gassner, G.T., M.L. Ludwig, D.L. Gatti, C.C. Correll, and D.P. Ballou. 1995. Flavoprotein structure and mechanism 7: structure and mechanism of the iron-sulfur flavoprotein phthalate dioxygenase reductase. FASEB J. 9:1411-1418.

Ghisla, S., and V. Massey. 1989. Mechanisms of flavoprotein-catalyzed reactions. Eur. J. Biochem. 181:1-17.

Gilbert, H.F. 1990. Molecular and cellular aspects of thiol-disulfide exchange. Adv. Enzymol. Relat. Areas Mol. Biol. 63:69-172.

Gladyshev, V.N., K.-T. Jeang, and T.C. Stadtman. 1996. Selenocysteine, identified as the penultimate C-terminal residue in human T-cell thioredoxin reductase, corresponds to TGA in the human placental gene. Proc. Natl. Acad. Sci. USA 93:6146-6151.

Gomes, C.M., R.S. Lemos, M. Teixeira, A. Kletzin, H. Huber, K.O. Stetter, G. Schäfer, and S. Anemüller. 1999. The unusual iron sulfur composition of the *Acidianus ambivalens* succinate dehydrogenase complex. Biochim. Biophys. Acta 1411:134-141.

Gomes, C.M., and M. Teixeira. 1998. The NADH oxidase from the thermoacidophilc archaea *Acidianus ambivalens*: isolation and physicochemical characterization. Biochem. Biophy. Res. Commun. 243:412-415.

Gonzälez, J.M., Y. Masuchi, F.T. Robb, J.W. Ammerman, D.L. Maeder, M. Yanagibayashi, J. Tamaoka, and C. Kato. 1998. *Pyrococcus horikishii* sp. nov., a hyperthermophilic archaeon isolated from hydrothermal vent at the Okinawa Trough. Extremophiles 2:123-130.

Greer, S., and R.N. Perham. 1986. Glutathione reductase from *Escherichia coli*: cloning and sequence analysis of the gene and relationship to other flavoprotein disulfide oxidoreductases. Biochemistry 25:2736-2742.

Grinblat, L., C.M. Sreider, and A.O. Stoppani. 1991. Superoxide anion production by lipoamide dehydrogenase redox-cycling: effect of enzyme modifiers. Biochem. Int. 23:83-92.

Grunden, A.M., F.E. Jenney, Jr., K. Ma, M. Ji, M.V. Weinberg, and M.W.W. Adams. 2005. *In vitro* reconstitution of an NADPH-dependent superoxide reduction pathway from *Pyrococcus furiosus*. Appl. Environ. Microbiol. 71:1522-1530.

Guagliardi, A., V. Nobile, S. Bartolucci, and M. Rossi. 1994. A thioredoxin from the extreme thermophilic archaeon *Sulfolobus solfataricus*. Int. J. Biochem. 26:375-380.

Guagliardi A., D. de Pascale, R. Cannio, V. Nobile, S. Bartolucci, and M. Rossi. 1995. The purification, cloning, and high level expression of a glutaredoxin-like protein from the hyperthermophilic archaeon *Pyrococcus furiosus*. J. Biol. Chem. 270:5748-5755.

Hall, D.O., S.A. Markov, Y. Watanabe, and K.K. Rao. 1995. The potential applications of cyanobacterial photosynthesis for clean technologies. Photosyn. Res. 46:159-167.

Harmych, S., R. Arnette, and R. Komuniecki. 2002. Role of dihydrolipoyl dehydrogenase (E3) and a novel E3-binding protein in the NADH sensitivity of the pyruvate dehydrogenase complex from anaerobic mitochondria of the parasitic nematode, Ascaris suum. Mol. Biochem. Parasitol. 125:135-146.

Hedrick, D.B., R.D. Pledger, D.C. White, and J.A. Baross. 1992. In situ microbial ecology of hydrothermal vent sediments. FEMS Microbiol. Ecol. 101:1-10.

Hentall, P.L., N. Flowers, and T.D.H. Bugg. 2001. Enhanced acid stability of a reduced nicotinamide adenine dinucleotide (NADH) analogue. Chem. Commun. 20:2098-2099.

Herles, C., A. Braune, and M. Blaut. 2002. Purification and characterization of an NADH oxidase from *Eubacterium ramulus*. Arch. Microbiol. 178:71-74.

Higgins, D.G., and P.M. Sharp. 1988. CLUSTAL: a package for performing multiple sequence alignment on a microcomputer. Gene 73:237-244.

Hille, R., and T. Nishino. 1995. Flavoprotein structure and mechanism 4: xanthine oxidase and xanthine dehydrogenase. FASEB J. 9:995-1003.

Hirt, R.P., S. Müller, T.M. Embley, and G.H. Coombs. 2002. The diversity and evolution of thioredoxin reductase: new perspectives. Trends Parasitol. 18:302-308.

Holmgren, A. 1977. Bovine thioredoxin reductase system. Purification of thioredoxin reductase from calf liver and thymus and studies of its function in disulfide reduction. J. Biol. Chem. 252:4600-4606.

Holmgren, A. 1979. Thioredoxin catalyzes the reduction of insulin disulfides by dithiothreitol and dihydrolipoamide. J. Biol. Chem. 254:9627-9632.

Holmgren, A. 1985. Thioredoxin. Annu. Rev. Biochem. 54:237-271.

Huber, H., M.J. Hohn, R. Rachel, T. Fuchs, V.C. Wimmer, and K.O. Stetter. 2002. A new phylum of archaea represented by a nanosized hyperthermophilic symbiont. Nature 417:63-67.

Huber, R., T.A. Langworthy, H. König, M. Thomm, C.R. Woese, U.B. Sleytr, and K.O. Stetter. 1986. *Thermotoga maritima* sp. nov. represents a new genus of unique extremely thermophilic eubacteria growing up to 90°C. Arch. Microbiol. 144:324-333.

Huber, R., P. Stoffers, J.L. Cheminee, H.H. Richnow, and K.O. Stetter. 1990. Hyperthermophilic archaebacteria within the crater and open-sea plume of erupting Macdonald seamount. Nature 345:179-182.

Huber, R., T. Wilharm, D. Huber, A. Trincone, S. Burggraf, H. Konig, R. Rachel, I. Rockinger, H. Fricke, and K.O. Stetter. 1992. *Aquifex pyrophilus* gen. nov., sp. nov., represents a novel group of marine hyperthermophilic hydrogen-oxidizing bacteria. Syst. Appl. Microbiol. 15:340-351.

Ichinohe, A., S. Kure, S. Mikawa, T. Ueki, K. Kojima, K. Fujiwara, K. Linuma, Y. Matsubara, and K. Sato. 2004. Glycine cleavage system in neurogenic regions. Eur. J. Neurosci. 19:2365-2370.

Igamberdiev, A.U., N.V. Bykova, W. Ens, and R.D. Hill. 2004. Dihydrolipoamide dehydrogenase from porcine heart catalyzes NADH-dependent scavenging of nitric oxide. FEBS Lett. 568:146-150.

Jannasch, H.W., R. Huber, S. Belkin, and K.O. Stetter. 1988. *Thermotoga neapolitana* sp. nov. of the extremely thermophilic, eubacterial genus *Thermotoga*. Arch. Microbiol. 150:103-104.

Jeanthon, C., A.-L. Reysenbach, S. L'Haridon, A. Gambacorta, N.R. Pace, P. Glénat, and D. Prieur. 1995. *Thermotoga subterranea* sp. nov., a new thermophilic bacterium isolated from a continental oil reservoir. Arch. Microbiol. 164:91-97.

Jeon, S.-J, and K. Ishikawa. 2002. Identification and characterization of thioredoxin and thioredoxin reductase from *Aeropyrum pernix* K1. Eur. J. Biochem. 269:5423-5430.

Jiang, Y., Q. Zhou, K. Wu, X-Q. Li, and W-L. Shao. 2006. A highly efficient method for liquid and solid cultivation of the anaerobic hyperthermophilic eubacterium *Thermotoga maritima*. FEMS Microbiol. Lett. 259:254-259.

Jolley, K.A., D.G. Maddocks, S.L. Gyles, Z. Mullan, S.-L. Tang, M.L. Dyall-Smith, D.W. Hough, and M.J. Danson. 2000. 2-oxoacid dehydrogenase multienzyme complexes in the halophilic Archaea? Gene sequences and protein structural predictions. Microbiology 146:1061-1069.

Jolley, K.A., E. Rapaport, D.W. Hough, M.J. Danson, W.G. Woods, and M.L. Dyall-Smith. 1996. Dihydrolipoamide dehydrogenase from the halophilic archaeon *Haloferax volcanii*: homologous overexpression of the cloned gene. J. Bacteriol. 178:3044-3048.

Joo, H.S., and S.S. Kim. 2001. Purification and characterization of the anabolic acetolactate synthase III from *Serratia marcescens* ATCC25419. J. Biochem. Mol. Biol. 34:244-249.

Juszczak, A., S. Aono, and M.W.W. Adams. 1991. The extremely thermophilic eubacterium, *Thermotoga maritima*, contains a novel iron-hydrogenase whose cellular activity is dependent on tungsten. J. Biol. Chem. 266:13834-13841.

Kanai, A., A. Sato, J. Imoto, and M. Tomita. 2006. Archaeal *Pyrococcus furiosus* thymidylate synthase 1 is an RNA-binding protein. Biochem. J. 393:373-379.

Karrer, P., K. Schöpp, and F. Benz. 1935. Synthesis of flavins IV. Helv. Chim. Acta 18:426-429.

Karthikeyan, S., Q. Zhou, F. Mseeh, N.V. Grishin, A.L. Osterman, and H. Zhang. 2003. Crystal structure of human riboflavin kinase reveals a β barrel fold and a novel active site arch. Structure 11:265-273.

Kashefi, K., and D.R. Lovley. 2003. Extending the upper temperature limit for life. Science 301:934-934.

Kashima, Y., and K. Ishikawa. 2003. A hyperthermostable novel protein-disulfide oxidoreductase is reduced by thioredoxin reductase from hyperthermophilic archaeon *Pyrococcus horikoshii*. Arch. Biochem. Biophys. 418:179-185.

Käslin, S.A., S.E. Childers, and K.M. Noll. 1998. Membrane-associated redox activities in *Thermotoga neapolitana*. Arch. Microbiol. 170:297-303.

Kato, K., P. Walde, H. Mitsui, and N. Higashi. 2003. Enzymatic activity and stability of D-fructose dehydrogenase and sarcosine dehydrogenase immobilized onto giant vesicles. Biotech. Bioeng. 84:415-423.

Kawasaki, S., J. Ishikura, D. Chiba, T. Nishino, and Y. Niimura. 2004. Purification and characterization of an H_2O-forming NADH oxidase from *Clostridium aminovalericum*: existence of an oxygen-detoxifying enzyme in an obligate anaerobic bacteria. Arch. Microbiol. 181:324-330.

Kelley, R.L., and C.A. Reddy. 1986. Purification and characterization of glucose oxidase from ligninolytic cultures of *Phanerochaete chrysosporium*. J. Bacteriol. 166:269-274.

Kengen, S.W.M., J. van der Oost, and W.M. de Vos. 2003. Molecular characterization of H_2O_2-forming NADH oxidases from *Archaeoglobus fulgidus*. Eur. J. Biochem.70:2885-2894.

Kengen, S.W.M., F.A.M. de Bok, N.-D. van Loo, C. Dijkema, A.J.M. Stams, W.M. de Vos. 1994. Evidence for the operation of a novel Embden–Meyerhof pathway that involves ADP-dependent kinases during sugar fermentation by *Pyrococcus furiosus*. J. Biol. Chem. 269:17537-17541.

Kern, P.A., R.B. Simsolo, and M. Fournier. 1999. Effect of weight loss on muscle fiber type, fiber size, capillarity, and succinate dehydrogenase activity in humans. J. Clin. Endocrinol. Metab. 84:4185-4190.

Kisaki, T., N. Yoshida, and A. Imai. 1971. Glycine decarboxylase and serine formation in spinach leaf mitochondrial preparation with reference to photorespiration. Plant Cell Physiol. 12:275-288.

Kistler, W.S., and E.C.C. Lin. 1972. Purification and properties of the flavine-stimulated anaerobic L-α-glycerophosphate dehydrogenase of *Escherichia coli*. J. Bacteriol. 112:539-547.

Kito, M., and L.I. Pizer. 1969. Purification and regulatory properties of the biosynthetic L-glycerol 3-phosphate dehydrogenase from *Escherichia coli*. J. Biol. Chem. 244:3316-3323.

Klein, A.R., H. Berk, E. Purwantini, L. Daniels, and R.K. Thauer. 1996. *Si*-face stereospecificity at C5 of coenzyme F_{420} for F_{420}-dependent glucose-6-phosphate dehydrogenase from *Mycobacterium smegmatis* and F_{420}-depedent alcohol dehydrogenase from *Methanoculleus thermophilicus*. Eur. J. Biochem. 239:93-97.

Koning, S.M., M.G.L. Elferink, W.N. Konings, and A.J. Driessen. 2001. Cellobiose uptake in the hyperthermophilic archaeon *Pyrococcus furiosus* is mediated by an inducible, high-affinity ABC transporter. J. Bacteriol. 183:4979-4984.

Koning, S.M., W.N. Konings, and A.J. Driessen. 2002. Biochemical evidence for the presence of two α-glucoside ABC-transport systems in the hyperthermophilic archaeon *Pyrococcus furiosus*. Archaea 1:19-25.

Konno, R., and Y. Yasumura. 1992. D-amino-acid oxidase and its physiological function. Int. J. Biochem. 24:519-524.

Ksenzhek, O.S., and S.A. Petrova. 1983. Electrochemical properties of flavins in aqueous solutions. Bioelectrochem. Bioenerg. 11:105-127.

Kuhn, R., K. Reinemund, and F. Weygand. 1934. Synthese des lumi-lactoflavins. Ber. Chem. Ges. 67:1460-1462.

Kuo, M.S., D.A. Yurek, J.H. Coats, and G.P. Li. 1989. Isolation and identification of 7, 8-didemethyl-8-hydroxy-5-deazariboflavin, an unusual cosynthetic factor in Streptomycetes, from *Streptomyces lincolnensis*. J. Antibiot. 42:475-478.

Kurzban, G.P., J. Howarth, G. Palmer, and H.W. Strobel. 1990. NADPH-cytochrome P-450 reductase: Physical properties and redox behavior in the absence of the FAD moiety. J. Biol. Chem. 265:12272-12279.

Kutty, R., and G.N. Bennett. 2006. Studies on inhibition of transformation of 2,4,6-trinitrotoluene catalyzed by Fe-only hydrogenase from *Clostridium acetobutylicum*. J. Ind. Microbiol. Biotechnol. 33:368-376.

Laemmli, U.K. 1970. Cleavage of structural proteins during the assembly of the head of bacteriophage T4. Nature 227:680-685.

Lange, C., L. Marvin, and A. Marcual. 1994. Determination of the amino acid sequence of apamin by tandem Mass Spectrometry. Rapid Commun. Mass Spectrom. 8:539-543.

Langkau, B., P. Vock, V. Massey, G. Fuchs, and S. Ghisla. 1995. 2-aminobenzoyl-CoA monooxygenase/reductase evidence for two distinct loci catalyzing substrate monooxygenation and hydrogenation. Eur. J. Biochem. 230:676-685.

Larsson, C., I-L. Pahlman, R. Ansell, M. Rigoulet, L. Adler, and L. Gustafsson. 1998. The importance of the glycerol-3-phosphate shuttle during aerobic growth of *Saccharomyces cerevisiae*. Yeast 14:347-357.

LaRue, T.A., and J.F Spencer. 1967. The utilization of D-amino acids by yeasts. Can. J. Microbiol. 13:777-788.

Laurent, T.C., E.C. Moore, and P. Reichard. 1964. Enzymatic synthesis of deoxyribonucleotides: IV. Isolation and characterization of thioredoxin, the hydrogen donor from *Escherichia coli*. J. Biol. Chem. 239:3436-3444.

Leahy, J.G., P.J. Batchelor, and S.M. Morcomb. 2003. Evolution of the soluble diiron monooxygenases. FEMS Microbiol. Rev. 27:449-479.

Lee, D.Y., B-Y. Ahn, and K-S. Kim. 2000. A thioredoxin from the hyperthmophilic archaeon *Methanococcus jannaschii* has a glutaredoxin-like fold but thioredoxin-like activities. Biochemistry 39:6652-6659.

Lin, E.C.C. 1976. Glycerol dissimilation and its regulation in bacteria. Annu. Rev. Microbiol. 30:535-578.

Lin, X.-L., and R.H. White. 1986. Occurrence of coenzyme F_{420} and its γ-monoglutamyl derivative in nonmethanogenic archaebacteria. J. Bacteriol. 168:444-468.

Lindgren, V., and L. Rutberg. 1974. Glycerol metabolism in *Bacillus subtilis*: gene-enzyme relationships. J. Bacteriol. 119:431-442.

Liu, Z., O. Niwa, T. Horiuchi, R. Kurita, and K. Torimitsu. 1999. NADH and glutamate on-line sensors using Os-gel-HRP/GC electrodes modified with NADH oxidase and glutamate dehydrogenase. Biosens. Bioelectron. 14:631-638.

López-Huertas, E., F.J. Corpas, L.M. Sandalio, and L.A. Del Río. 1999. Characterization of membrane polypeptides from pea leaf peroxisomes involved in superoxide radical generation. Biochem. J. 337:531-536.

Lyon, E.J., S. Shima, R. Boecher, R.K. Thauer, F.-W. Grevels, E. Bill, W. Roseboom, and S.P.J. Albracht. 2004. Carbon monoxide as an intrinsic ligand to iron in the active site of the iron-sulfur-cluster-free hydrogenase H_2-forming methylenetetrahydromethanopterin dehydrogenase as revealed by infrared spectroscopy. J. Am. Chem. Soc. 126:14239-14248.

Ma, K., and M.W.W. Adams. 1994. Sulfide dehydrogenase from the hyperthermophilic archaeon *Pyrococcus furiosus*: a new multifunctional enzyme involved in the reduction of elemental sulfur. J. Bacteriol. 176:6509-6517.

Ma, K., and M.W.W. Adams. 1999. A hyperactive NAD(P)H: rubredoxin oxidoreductase from the hyperthermophilic archaeon *Pyrococcus furiosus*. J. Bacteriol. 181:5530-5533.

Ma, K., and M.W.W. Adams. 2001. Hydrogenase I and II from *Pyrococcus furiosus*. Methods Enzymol. 331:208-216.

Ma, K., and M.W.W. Adams. 2001. Ferredoxin: NADP oxidoreductase from *Pyrococcus furiosus*. Methods Enzymol. 334:40-45.

Ma, K., F.T. Robb, and M.W.W. Adams. 1994a. Purification and characterization of NADP-specific alcohol dehydrogenase and glutamate dehydrogenase from the hyperthermophilic archaeon, *Thermococcus litoralis*. Appl. Environ. Microbiol. 60:562-568.

Ma, K., R.N. Schicho, R.M. Kelly, and M.W.W. Adams. 1993. Hydrogenase of the hyperthermophile *Pyrococcus furiosus* is an elemental sulfur reductase or sulfhydrogenase: evidence for a sulfur-reducing hydrogenase ancestor. Proc. Natl. Acad. Sci. USA 90:5341-5344.

Ma, K., R. Weiss, and M.W.W. Adams. 2000. Characterization of hydrogenase II from the hyperthermophilic archaeon *Pyrococcus furiosus* and assessment of its role in sulfur reduction. J. Bacteriol. 181:1864-1871.

Ma, K., Z.H. Zhou, and M.W.W. Adams. 1994b. Hydrogen production from pyruvate by enzymes purified from the hyperthermophilic archeaon, *Pyrococcus furiosus*: a key role for NADPH. FEMS Microbiol. Lett. 122:245-250.

Mack, M., A.P.G.M. van Loon, and H.-P. Hohmann. 1998. Regulation of riboflavin biosynthesis in *Bacillus subtilis* is affected by the activity of the flavokinase/flavin adenine dinucleotide synthetase encoded by ribC. J. Bacteriol. 180:950-955.

Maeda, K., K. Truscott, X.-L. Liu, and R.K. Scopes. 1992. A thermostable NADH oxidase from anaerobic extreme thermophiles. Biochem. J. 284:551-555.

Mäkinen, K.K., and J. Tenovuo. 1982. Observations on the use of guaiacol and 2,2'-azino-di(3-ethylbenzthiazoline-6-sulfonic acid) as peroxidase substrates. Anal. Biochem. 126:100-108.

Malik, B., W-W., Su, H.L. Wald, I.I. Blumentals, and R.M. Kelly. 1989. Growth and gas production for hyperthermophilic archaebacterium, *Pyrococcus furiosus*. Biotechnol. Bioeng. 34:1050-1057.

Malinauskas, A., T. Ruzgas, and L. Gorton. 1999. Tuning the redox potential of riboflavin by zirconium phosphate in carbon paste electrodes. Bioelectrochem. Bioenerg. 49:21-27.

Manstein, D.J., and E.F. Pai. 1986. Purification and characterization of FAD synthetase from *Brevibacterium ammoniagenes*. J. Biol. Chem. 261:16169-16173.

Marcinkeviciene, J., and J.S. Blanchard. 1997. Catalytic properties of lipoamide dehydrogenase from *Mycobacterium smegmatis*. Arch. Biochem. Biophys. 340:168-176.

Marteinsson, V.T., J.-L. Birrien, A.-L. Reysenbach, M. Vernet, D. Marie, A. Gambacorta, P. Messner, U.B. Sleytr, and D. Prieur. 1999. *Thermococcus barophilu*s sp. nov., a new barophilic and hyperthermophilic archaeon isolated under high hydrostatic pressure from a deep-sea hydrothermal vent. Int. J. Syst. Bacteriol. 49:351-359.

Massey, V. 1994. Activation of molecular oxygen by flavins and flavoproteins. J. Biol. Chem. 269:22459-22462.

Massey, V. 1995. Introduction: flavoprotein structure and mechanism. FASEB J. 9:473-475.

Massey, V. 2000. The chemical and biological versatility of riboflavin. Biochem. Soc. Trans. 28:283-296.

Massey, V., and C. Veeger. 1961. Studies on the reaction mechanism of lipoyl dehydrogenase. Biochim. Biophys. Acta 48:33-47.

Masullo, M., G. Raimo, A. Dello Russo, V. Bocchini, and J.V. Bannister. 1996. Purification and characterization of NADH oxidase from the archaea *Sulfolobus acidocaldarius* and *Sulfolobus solfataricus*. Biotechnol. Appl. Biochem. 23:47-54.

Mattevi, A., G. Obmolova, J.R. Sokatch, C. Betzel, and W.G.J. Hol. 1992. The refined crystal structure of *Pseudomonas putida* lipoamide dehydrogenase complexed with NAD^+ at 2.45 Å resolution. Proteins 13:336-351.

McCormick, J.R.D., and G.O. Morton. 1982. Identity of cosynthetic factor 1 of *Streptomyces aureofaciens* and fragment FO from coenzyme F_{420} of *Methanobacterium* species. J. Am. Chem. Soc. 104:4014-4015.

Messner, K.R., and J.A. Imlay. 1999. The identification of primary sites of superoxide and hydrogen peroxide formation in the aerobic respiratory chain and sulfite reductase complex of *Escherichia coli*. J. Biol. Chem. 274:10119-10128.

Mewies, M., W.S. Mcintire, and N.S. Scrutton. 1998. Covalent attachment of flavin adenine dinucleotide (FAD) and flavin mononucleotide (FMN) to enzymes: the current state of affairs. Protein Sci. 7:7-20.

Miki, K., and E.C.C. Lin. 1973. Enzyme complex which couples glycerol-3-phosphate dehydrogenation to fumarate reduction in *Escherichia coli*. J. Bacteriol. 114:767-771.

Miura, R. 2001. Versatility and specificity in flavoenzymes: control mechanisms of flavin reactivity. Chem. Rec. 1:183-194.

Moonen, M.J.H., M.W. Fraaije, I.M.C.M. Rietjens, C. Laane, and W.J.H. van Berkel. 2002. Flavoenzyme-catalyzed oxygenations and oxidations of phenolic compounds. Adv. Synth. Catal. 344:1023-1035.

Moorhead, G.B.G., S.E.M. Meek, P. Douglas, D. Bridges, C.S. Smith, N. Morrice, and C. Mackintosh. 2003. Purification of a plant nucleotide pyrophosphatase as a protein that interferes with nitrate reductase and glutamine synthetase assays. Eur. J. Biochem. 270:1356-1362.

Müller, F. 1991. Free flavins: syntheses, chemical and physical properties. In chemistry and biochemistry of flavoenzymes (Müller, F., Ed), Boca Raton, CRC press. Pp1-71.

Mustacich, D., and G. Powis. 2000. Thioredoxin reductase. Biochem. J. 346:1-8.

Nandi, R., and S. Sengupta. 1998. Microbial production of hydrogen: an overview. Crit. Rev. Microbiol. 24:61-68.

Nelson, K.E., R.A. Clayton, S.R. Gill, M.L. Gwinn, R.J. Dodson, D.H. Haft, E.K. Hickey, J.D. Peterson, W.C. Nelson, K.A. Ketchum, L. McDonald, T.R. Utterback, J.A. Malek, K.D. Linher, M.M. Garrett, A.M. Stewart, M.D. Cotton, M.S. Pratt, C.A. Phillips, D. Richardson, J. Heidelberg, G.G. Sutton, R.D. Fleischmann, J.A. Eisen, O. White, S.L. Salzberg, H.O. Smith, J.C. Venter, and C.M. Fraser. 1999. Evidence for lateral gene transfer between archaea and bacteria from genome sequence of *Thermotoga maritima*. Nature 399:323-329.

Nelson, C.M., M.R. Schuppenhauer, and D.S. Clark. 1992. High-pressure, high-temperature bioreactor for comparing effects of hyperbaric and hydrostatic pressure on bacterial growth. Appl. Environ. Microbiol. 58:1789-1793.

Neveling, U., R. Klasen, S. Bringer-Meyer, and H. Sahm. 1998. Purification of the pyruvate dehydrogenase multienzyme complex of *Zymomonas mobilis* and identification and sequence analysis of the corresponding genes. J. Bacteriol. 180:1540-1548.

Nguyen, T.N., A.D. Ejaz, M.A. Brancieri, A.M. Mikula, K.E. Nelson, S.R. Gill, and K.M. Noll. 2004. Whole-genome expression profiling of *Thermotoga maritima* response to growth on sugars in a chemostat. J. Bacteriol. 186:4824-4828.

Niimura, Y., Y. Nishiyama, D. Saito, H. Tsuji, M. Hidaka, T. Miyaji, T. Watanabe, and V. Massey. 2000. A hydrogen peroxide-forming NADH oxidase that functions as an alkyl hydroperoxide reductase in *Amphibacillus xylanus*. J. Bacteriol. 182:5046-5051.

Niimura, Y., K. Ohnishi, Y. Yarita, M. Hidaka, H. Masaki, T. Uchimura, H. Suzuki, M. Kozaki, and T. Uozumi. 1993. A flavoprotein functional as NADH oxidase from *Amphibacillus xylanus* Ep01: Purification and characterization of the enzyme and structural analysis of its gene. J. Bacteriol. 175:7945-7950.

Nishiyama, Y., V. Massey, K. Takeda, S. Kawasaki, J. Sato, T. Watanabe, and Y. Niimura. 2001. Hydrogen peroxide-forming NADH oxidase belonging to the peroxiredoxin oxidoreductase family: existence and physiological role in bacteria. J. Bacteriol. 183:2431-2438.

Nölling, J., G. Breton, M.V. Omelchenko, K.S. Makarova, Q. Zeng, R. Gibson, H. Lee, J. Dubois, D. Qiu, J. Hitti, Y.I. Wolf, R.L. Tatusov, F. Sabathe, L. Doucette-Stamm, P. Soucaille, M.J. Daly, G.N. Bennett, E.V. Koonin, and D.R. Smith. 2001. Genome sequence and comparative analysis of the solvent-producing bacterium *Clostridium acetobutylicum*. J. Bacteriol. 183:4823-4838.

Page, R.D.M. 1996. TREEVIEW: an application to display phylogenetic trees on personal computers. Computers Applications in the Biosciences. 12:357-358.

Palfey, B.A., and V. Massey. 1996. Flavin-dependent enzymes. In Comprehensive biological catalysis (Sinnott M., Ed.), Vol. III Radical reactions and oxidation/reduction. Academic Press, New York. USA. Pp83-154.

Pan, N., and J.A. Imlay. 2001. How does oxygen inhibit central metabolism in the obligate anaerobe *Bateroides thetaiotaomicron*. Mol. Microbiol. 39:1562-1571.

Park, H.-J., C.O.A. Reiser, S. Kondruweit, H. Erdmann, R.D. Schmid, and M. Sprinzl. 1992. Purification and characterization of a NADH oxidase from the thermophile *Thermus thermophilus* HB8. Eur. J. Biochem. 205:881-885.

Patel, M.S., and L.G. Korotchkina. 2003. Mini-series: modern metabolic concepts: The biochemistry of the pyruvate dehydrogenase complex. Biochem. Mol. Biol. Edu. 31:5-15.

Patel, M.P., J. Marcinkeviciene, and J. S. Blanchard. 1998. *Enterococcus faecalis* glutathione reductase: purification, characterization and expression under normal and hyperbaric O_2 conditions. FEMS Microbiol. Lett. 166:155-163.

Patel, M.S., N.N. Vettakkorumakankav, and T.C. Liu. 1995. Dihydrolipoamide dehydrogenase: activity assays. Methods Enzymol. 252:186-195.

Payne, M.J., A. Chapman, and R. Cammack. 1993. Evidence for an [Fe]-type hydrogenase in the parasitic protozoan *Trichomonas vaginalis*. FEBS Lett. 317:101-104.

Pedone, E., K. D'Ambrosio, G. De Simone, M. Rossi, C. Pedone, and S. Bartolucci. 2006. Insights on a new PDI-like family: structural and functional analysis of a protein disulfide oxidoreductase from the bacterium *Aquifex aeolicus*. J. Mol. Biol. 356:155-164.

Perham, R.N. 2000. Swinging arms and swinging domains in multifunctional enzymes: catalytic machines for multistep reactions. Annu. Rev. Biochem. 69:961-1004.

Peters, J.W., W.N. Lanzilotta, B.J. Lemon, and L.C. Seefeldt. 1998. X-ray crystal structure of the Fe-only hydrogenase (Cpi) from *Clostridium pasteurianum* to 1.8 angstrom resolution. Science 282:1853-1858.

Petrounia, I.P., J. Goldberg, and E.J. Brush. 1994. Transient inactivation of almond mendelonitrile lyase by 3-methyleneoxindole: a photooxidation product of the natural plant hormone indole-3-acetic acid. Biochemistry 33:2891-2899.

Piepersberg, W. 1994. Pathway engineering in secondary metabolite-producing actinomycetes. Crit. Rev. Biotechnol. 14:251-285.

Pilone, M.S. 2000. D-Amino acid oxidase: new findings. Cell. Mol. Life Sci. 57:1732-1747.

Pinkernell, U., B. Nowack, H. Gallard, and U. von Gunten. 2000. Methods for the photometric determination of reactive bromine and chlorine species with ABTS. Water Res. 34:4343-4350.

Pollock, R.J., and L.B. Hersh. 1973. N-methylglutamate synthetase: The use of flavin mononucleotide in oxidative catalysis. J. Biol. Chem. 248:6724-6733.

Ponnudurai, G., M.C.M. Chung, and N.-H. Tan. 1994. Purification and properties of the L-amino acid oxidase from Malayan pit Viper (*Calloselasma rhodostoma*) venom. Arch. Biochem. Biophys. 313:373-378.

Poole, L.B., C.M. Reynolds, Z.A. Wood, P.A. Karplus, H.R. Ellis, and M.L. Calzi. 2000. AhpF and other NADH: peroxiredoxin oxidoreductases, homologues of low Mr thioredoxin reductase. Eur. J. Biochem. 267:6126-6133.

Porter, T.D., and C.B. Kasper. 1986. NADPH-cytochrome P-450 oxidoreductase: flavin mononucleotide and flavin adenine dinucleotide domains evolved from different flavoproteins. Biochemistry 25:1682-1687.

Powlowski, J.B., S. Dagley, V. Massey, and D. Ballou. 1987. Properties of anthranilate hydroxylase (deaminating), a flavoprotein from *Trichosporon cutaneum*. J. Biol. Chem. 262:69-74.

Purwantini, E., and L. Daniels. 1996. Purification of a novel coenzyme F_{420}-dependent glucose-6-phosphate dehydrogenase from *Mycobacterium smegmatis*. J. Bacteriol. 178:2861-2866.

Quail, M.A., P. Jordan, J.M. Grogan, J.N. Butt, M. Lutz, A.J. Thomson, S.C. Andrews, and J.R. Guest. 1996. Spectroscopic and voltammetric characterization of the bacterioferretin-associated ferredoxin of *Escherichia coli*. Biochem. Biophys. Res. Commun. 229:635-642.

Raven, N., N. Ladwa, D. Cossar, and R. Sharp. 1992. Continuous culture of the hyperthermophilic archaeum *Pyrococcus furiosus*. Appl. Microbiol. Biotechnol. 38:263-267.

Ravot, G., M. Magot, M.-L. Fardeau, B.K.C. Patel, G. Prensier, A. Egan, J.-L. Garcia, and B. Ollivier. 1995. *Thermotoga elfii* sp. nov., a novel thermophilic bacterium from an African oil-producing well. Int. J. Syst. Bacteriol. 45:308-314.

Reed, L.J. 1974. Multienzyme complexes. Acc. Chem. Res. 7:40-46.

Reed, L.J., and M.L. Hackert. 1990. Structure-function relationships in dihydrolipoamide acyltransferases. J. Biol. Chem. 265:8971-8974.

Reed, L.J., M. Koike, M.E. Levitch, and F.R. Leach. 1958. Studies on the nature and reactions of protein-bound lipoic acid. J. Biol. Chem. 232:143-158.

Reed, D.W., J. Millstein, and P.L. Hartzell. 2001. H_2O_2-forming NADH oxidase with diaphorase (cytochrome) activity from *Archaeoglobus fulgidus*. J. Bacteriol. 183:7007-7016.

Reinards, R., J. Kubicki, and H.D. Ohlenbusch. 1981. Purification and characterization of NADH oxdase from membranes of *Archoleplasma laidlawii*, a copper-containing iron-sulfur flavoprotein. Eur. J. Biochem. 120:329-337.

Reynolds, C.M., J. Meyer, and L.B. Poole. 2002. An NADH-dependent bacterial thioredoxin reductase-like protein in conjunction with a glutaredoxin homologue form a unique peroxiredoxin (AhpC) reducing system in *Clostridium pasteurianum*. Biochemistry 41:1990-2001.

Reysenbach, A.-L., and J.W. Deming. 1991. Effects of hydrostatic pressure on growth of hyperthermophilic archaebacteria from the Juan de Fuca Ridge. Appl. Environ. Microbiol. 57:1271-1274.

Ringler, R.L. 1961. Studies on the mitochondrial α-glycerophosphate dehydrogenase: II Extraction and partial purification of the dehydrogenase from pig brain. J. Biol. Chem. 236:1192-1198.

Rinker, K.D., and R.M. Kelly. 1996. Growth physiology of the hyperthermophilic archaeon *Thermococcus litoralis*: development of a sulfur-free defined medium, characterization of an exopolysaccharide, and evidence of biofilm formation. Appl. Environ. Microbiol. 62:4478-4485.

Rinker, K.D., and R.M. Kelly. 2000. Effect of carbon and nitrogen sources on growth dynamics and exopolysaccharide production for the hyperthermophilic archaeon *Thermococcus litoralis* and bacterium *Thermotoga maritima*. Biotechnol. Bioeng. 69:537-547.

Ritz, D., and J. Beckwith. 2001. Roles of thiol-redox pathways in bacteria. Annu. Rev. Microbiol. 55:21-48.

Robb, F.T., D.L. Maeder, J. DiRuggiero, K.M. Borges, and N. Tolliday. 2001a. Glutamate dehydrogenases from hyperthermophiles. In: Methods Enzymol. (Adams M.W.W. and R.M. Kelly, Ed.), Academic Press. vol. 331:26-41.

Robb, F.T., D.L. Maeder, J.R. Brown, J. DiRuggiero, M.D. Stump, R.K. Yeh, R. B. Weiss, and D.M. Dunn. 2001b. Genomic sequence of hyperthermophile, *Pyrococcus furiosus*: implications for physiology and enzymology. Methods Enzymol. 330:134-157.

Robb, F.T., J.-B. Park, and M.W.W. Adams. 1992. Characterization of an extremely thermostable glutamate dehydrogenase: a key enzyme in the primary metabolism of the hyperthermophilic archaebacterium, *Pyrococcus furiosus*. Biochim. Biophys. Acta 1120:267-272.

Ronholm, J. and K. Ma. 2006. Production of acetate from glycerol by *Thermotoga maritima*. Biol 499. Univ. of Waterloo, ON, Canada.

Rosen, G.M., S. Pou, C.L. Ramos, M.S. Cohen, and B.E. Britigan. 1995. Free radicals and phagocytic cells. FASEB J. 9:200-209.

Ross, D., J.K. Kepa, S.L. Winski, H.D. Beall, A. Anwar, and D. Siegel. 2000. NAD(P)H:quinone oxidoreductase 1 (NQO1): chemoprotection, bioactivation, gene regulation and genetic polymorphisms. Chem. Biol. Interact. 129:77-97.

Ruepp, A., W. Graml, M.-L. Santos-Martinez, K.K. Koretke, C. Volker, H.W. Mewes, D. Frishman, S. Stocker, A.N. Lupas, and W. Baumeister. 2000. The genome sequence of the thermoacidophilic scavenger *Thermoplasma acidophilum*. Nature 407:508-513.

Ruocco, M.R., A. Ruggiero, L. Masullo, P. Arcari, and M. Masullo. 2004. A 35 kDa NAD(P)H oxidase previously isolated from the archaeon *Sulfolobus solfataricus* is instead a thioredoxin reductase. Biochimie 86:863-892.

Russel, M., and P. Model. 1988. Sequence of thioredoxin reductase from *Escherichia coli*: relationship to other flavoprotein disulfide oxidoreductases. J. Biol. Chem. 263:9015-9019.

Sakamoto, M., T. Uchimura, and K. Komagata. 1996. Comparison of H_2O-forming NADH oxidase from *Leuconostoc mesenteroides* subsp. mesenteroides NRIC 1541T and *Sporolactobacillus inulinus* NRIC 1133T. J. Ferment. Bioeng. 82:531-537.

Sakuraba, H., S. Goda, and T. Ohshima. 2004. Unique sugar metabolism and novel enzymes of hyperthermophilic archaea. Chem. Rec. 3:281-287.

Sancar, A. 1994. Structure and function of DNA photolyase. Biochemistry 33:2-9.

Sapra, R., M.F.J.M. Verhagen, and M.W.W. Adams. 2000. Purification and characterization of a membrane-bound hydrogenase from the hyperthermophilic archaeon *Pyrococcus furiosus*. J. Bacteriol. 182:3423-3428.

Schäfer, T., and P. Schönheit. 1993. Gluconeogenesis from pyruvate in the hyperthermophilic archaeon *Pyrococcus furiosus*: involvement of reactions of the Embden-Meyerhof pathway. Arch. Microbiol. 159:354-363.

Scherf, U., and W. Buckel. 1993. Purification and properties of an iron-sulfur and FAD-containing 4-hydroxybutyryl-CoA dehydratase/vinylacetyl-CoA Δ3-Δ2-isomerase from *Clostridium aminobutyricum*. Eur. J. Biochem. 215:421-429.

Schicho, R.N., K. Ma, M.W.W. Adams, and R.M. Kelly. 1993. Bioenergetics of sulfur reduction in the hyperthermophilic archaeon *Pyrococcus furiosus*. J. Bacteriol. 175:1823-1830.

Schneider, K., and H.G. Schlegel. 1976. Purification and properties of soluble hydrogenase from *Alcaligenes eutrophus* H16. Biochim. Biophys. Acta 452:66-80.

Schönheit, P., and T. Schäfer. 1995. Metabolism of hyperthermophiles. World J. Microbiol. Biotechol. 11:26-57.

Schröder, C., M. Selig, and P. Schönheit. 1994. Glucose fermentation to acetate, CO_2 and H_2 in the anaerobic hyperthermophilic eubacterium *Thermotoga maritima*: involvement of the Embden-Meyerhof pathway. Arch. Microbiol. 161:460-470.

Schryvers, A., E. Lohmeier, and J.H. Weiner. 1978. Chemical and functional properties of the native and reconstituted forms of the membrane-bound, aerobic glycerol-3-phosphate dehydrogenase of *Escherichia coli*. J. Biol. Chem. 253:783-788.

Schryvers, A., and J.H. Weiner. 1981. The anaerobic *sn*-glycerol-3-phosphate dehydrogenase of *Escherichia coli*: purification and characterization. J. Biol. Chem. 256:9959-9965.

Schumb, W.C. 1949. Stability of concentrated hydrogen peroxide solutions. Ind. Eng. Chem. 41:992-1003.

Schut, G.J., J. Zhou, and M.W.W. 2001. DNA microarray analysis of the hyperthermophilic archaeon *Pyrococcus furiosus*: evidence for a new type of sulfur-reducing enzyme complex. J. Bacteriol. 183:7027-7036.

Schweizer, H.P., and C. Po. 1994. Cloning and nucleotide sequence of the glpD gene encoding *sn*-glycerol-3-phosphate dehydrogenase of *Pseudomonas aeruginosa*. J. Bacteriol. 176:2184-2193.

Segerer, A., A. Neuner, J.K. Kristjansson, and K.O. Stetter. 1986. *Acidianus infernus* gen. nov., sp. nov., and *Acidianus brierleyi* comb. nov.: facultatively aerobic, extremely acidophilic thermophilic sulfur-metabolizing archaebacteria. Int. J. Syst. Bacteriol. 36:559-564.

Selig, M., K.B. Xavier, H. Santos, and P. Schönheit. 1997. Comparative analysis of Embden-Meyerhof and Enter-Doudoroff glycolytic pathways in hyperthermophilic archaea and the bacterium *Thermotoga*. Arch. Microbiol. 167:217-232.

Shames, S.L., B.E. Kimmel, O.P. Peoples, N. Agabian, and C.T. Walsh. 1988. Trypanothione reductase from *Trypanosoma congolense*: gene isolation, primary sequence determination, and comparison to glutathione reductase. Biochemistry 27:5014-5019.

Shen, W., Y. Wei, M. Dauk, Z. Zheng, and J. Zou. 2003. Identification of a mitochondrial glycerol-3-phosphate dehydrogenase from *Arabidopsis thaliana*: evidence for a mitochondrial glycerol-3-phosphate shuttle in plants. FEBS Lett. 536:92-96.

Shevchenko, A., M. Wilm, O. Vorm, and M. Mann. 1996. Mass spectrometric sequencing of proteins from silver-stained polyacrylamide gels. Anal. Chem. 68:850-858.

Shimizu, T., K. Ohtani, H. Hirakawa, K. Ohshima, A. Yamashita, T. Shiba, N. Ogasawara, M. Hattori, S. Kuhara, and H. Hayashi. 2002. Complete genome sequence of *Clostridium perfringens*, an anaerobic flesh-eater. Proc. Natl. Acad. Sci. USA 99:996-1001.

Siegel, L.M., P.S. Davis, and H. Kamin. 1974. Reduced nicotinamide adenine dinucleotide phosphate sulfite reductase of Enterobacteria III. The *Escherichia coli* hemoflavoprotein: catalytic parameters and the sequence of electron flow. J. Biol. Chem. 249:1572-1586.

Silva, P.J., E.C.D. van den Ban, H. Wassink, H. Haaker, B. de Castro, F.T. Robb, and W.R. Hagen. 2000. Enzymes of hydrogen metabolism in *Pyrococcus furiosus*. Eur. J. Biochem. 267:6541-6551.

Smith, E.T., and M.W.W. Adams. 1994. Identification of an unusual paramagnetic species and of three [2Fe-2S] clusters in the iron-only hydrogenase from the hyperthermophilic bacterium *Thermotoga maritima*. Biochim. Biophys. Acta 1206:105-112.

Smith, E.T., J.M. Blamey, Z.H. Zhou, and M.W.W. Adam. 1995. A variable-temperature direct electrochemical study of metalloproteins from hyperthermophilic microorganisms involved in hydrogen production from pyruvate. Biochemistry 34:7161-7169.

Snoep, J.L., M.R. de Graef, A.H. Westphal, A. de Kok, M.J.T. de Mattos, and O.M. Neijssel. 1993. Differences in sensitivity to NADH of purified pyruvate dehydrogenase complexes of *Enterococcus faecalis*, *Lactococcus lactis*, *Azotobacter vinelandii* and *Escherichia coli*: implications for their activity *in vivo*. FEMS Microbiol. Lett. 114:279-284.

Soboh, B., D. Linder, and R. Hedderich. 2004. A multisubunit membrane-bound [NiFe] hydrogenase and an NADH-dependent Fe-only hydrogenase in the fermenting bacterium *Thermoanaerobacter tengcongensis*. Microbiology 150:2451-2463.

Sodek, L., and W.J. da Silva. 1977. Glutamate synthase: a possible role in nitrogen metabolism of the developing maize endosperm. Plant Physiol. 60:602-605.

Sparrow, L.G., P.P.K. Ho, T.K. Sundaram, D. Zach, E.J. Nyns, and E.E. Snell. 1969. The bacterial oxidation of vitamin B6: VII. Purification, properties, and mechanism of action of an oxygenase which cleaves the 3-hydroxypyridine ring. J. Biol. Chem. 244:2590-2600.

Speich, N., C. Dahl., P. Heisig, A. Klein, F. Lottspeich, K.O. Stetter, and H.G. Truper. 1994. Adenylylsulphate reductase from the sulphate-reducing archaeon *Archaeoglobus fulgidus*:

cloning and characterization of the genes and comparison of the enzyme with other iron-sulphur flavoproteins. Microbiology 140:1273-1284.

Spencer, R., J. Fisher, and C. Walsh. 1976. Preparation, characterization, and chemical properties of the flavin coenzyme analogues 5-deazariboflavin, 5-deazariboflavin 5'-diphosphate, and 5-deazariboflavin 5'-diphosphate, 5'→5'-adenosine ester. Biochemistry 15:1043-1053.

Stanley, R.J. 2001. Advances in flavin and flavoprotein optical spectrometry. Antioxid. Redox Signal. 3:847-866.

Stanton, T.B., and N.S. Jensen. 1993. Purification and characterization of NADH oxidase from *Serpulina* (*Treponema*) *hyodysenteriae*. J. Bacteriol. 175:2980-2987.

Stetter, K.O. 1982. Ultrathin mycelia-forming organisms from submarine volcanic areas having an optimum growth temperature of 105°C. Nature 300:258-260.

Stetter, K.O. 1996. Hyperthermophilic prokaryotes. FEMS Microbiol. Rev. 18:149-158.

Stetter, K.O. 2006. History of discovery of the first hyperthermophiles. Extremophiles 10:357-362.

Stott, K., K. Saito, D.J. Thiele, and V. Massey. 1993. Old yellow enzyme: the discovery of multiple isozymes and a family of related proteins. J. Biol. Chem. 268:6097-6106.

Straub, F.B. 1939. Isolation and properties of a flavoprotein from heart muscle tissue. Biochem. J. 33:787-792.

Sunna, A., M. Moracci, M. Rossi, and G. Antranikian. 1997. Glycosyl hydrolases from hyperthermophiles. Extremophiles 1:2-13.

Suzuki, A., and D.B. Knaff. 2005. Glutamate synthase: structural, mechanistic and regulatory properties, and role in the amino acid metabolism. Photosynth. Res. 83:191-217.

Sylvester, D.R., E. Alvarez, A. Patel, K. Ratnam, H. Kallender, and N.G. Wallis. 2001. Identification and characterization of UDP-N-acetylenolpyruvylglucosamine reductase (MurB) from the gram-positive pathogen *Streptococcus pneumonia*. Biochem. J. 355:431-435.

Takahata, Y., M. Nishijima, T. Hoaki, and T. Maruyama. 2001. *Thermotoga petrophila* sp. nov. and *Thermotoga naphthophila* sp. nov., two hyperthermophilic bacteria from the Kubiki oil reservoir in Niigata, Japan. Int. J. Syst. Evol. Microbiol. 51:1901-1909.

Tamura, T., and T.C. Stadtman. 1996. A new selenoprotein from human lung adenocarcinoma cells: purification, properties, and thioredoxin reductase activity. Proc. Natl. Acad. Sci. USA 93:1006-1011.

Tessier, A.J., G.W. Dombi, and D.L. Bouwman. 1996. Thermostability of purified human pancreatic α-amylase is increased by the combination of Ca^{+} and human serum albumin. Clinica Chimica Acta 252:11-20.

Thorpe, C., and J.-J.P. Kim. 1995. Structure and mechanism of action of the acyl-CoA dehydrogenase. FASEB J. 9:718-725.

Toomey, D., and S.G. Mayhew. 1998. Purification and characterisation of NADH oxidase from *Thermus aquaticus* YT-1 and evidence that it functions in a peroxide-reduction system. Eur. J. Biochem. 251:935-945.

Toyoda, T., R. Kobayashi, T. Sekiguchi, K. Koike, M. Koike, and A. Takenaka. 1998a. Crystallization and preliminary X-ray analysis of pig E3, lipoamide dehydrogenase. Acta Cryst. D54:982-985.

Toyoda, T., K. Suzuki, T. Sekiguchi, L.J. Reed, and A. Takenaka. 1998b. Crystal structure of eukaryotic E3, lipoamide dehydrogenase from yeast. J. Biochem. 123:668-674.

Trower, M.K., R.M. Buckland, and M. Griffin. 1989. Characterization of an FMN-containing cyclohexanone monooxygenase from a cyclohexane-grown *Xanthobacter* sp. Eur. J. Biochem. 181:199-206.

Tsai, C.S. 1980. Kinetic studies of multifunctional reactions catalysed by lipoamide dehydrogenase. Int. J. Biochem. 11:407-413.

Tuininga, J.E., C.H. Verhees, J. van der Oost, S.W.M. Kengen, A.J.M. Stams, and W.M. de Vos. 1999. Molecular and biochemical characterization of the ADP-dependent phosphofructokinase from the hyperthermophilic archaeon *Pyrococcus furiosus*. J. Biol. Chem. 274:21023-21028.

Tzeng, S.F., M.P. Bryant, and R.S. Wolfe. 1975a. Factor 420-dependent pyridine nucleotide-linked formate metabolism of *Methanobacterium ruminantium*. J. Bacteriol. 121:192-196.

Tzeng, S.F., R.S. Wolfe, and M.P. Bryant. 1975b. Factor 420-dependent pyridine nucleotide-linked hydrogenase system of *Methanobacterium ruminantium*. J. Bacteriol. 121:184-191.

van der Western, H.M., S.G. Mayhew, and C. Veeger. 1978. Separation of hydrogenase from intact cells of *Desulfovibrio vulgaris*: purification and properties. FEBS Lett. 86:122-126.

van Eys, J., B.J. Nuenke, and M.K. Patterson, Jr. 1959. The nonprotein component of α-glycerophosphate dehydrogenase. Physical and chemical properties of the crystalline rabbit muscle enzyme. J. Biol. Chem. 234:2308-2313.

Van Ooteghem, S.A., S.K. Beer, and P.C. Yue. 2001. Hydrogen production by the thermophilic bacterium, *Thermotoga neapolitana*. Proceedings of the 2001 DOE Hydrogen Program Review. NREL/CP-570-30535.

Van Ooteghem, S.A., S.K. Beer, and P.C. Yue. 2002. Hydrogen production by the thermophilic bacterium *Thermotoga neapolitana*. Appl. Biochem. Biotechnol. 98-100:177-189.

Van Ooteghem, S.A., A. Jones, D. van der Lelie, B. Dong, and D. Mahajan. 2004. H_2 production and carbon utilization by *Thermotoga neapolitana* under anaerobic and microaerobic growth conditions. Biotech. Lett. 26:1223-1232.

Verhagen, M.F.J.M., T. O'Rourke, and M.W.W. Adams. 1999. The hyperthermophilic bacterium, *Thermotoga maritima*, contains an unusually complex iron-hydrogenase: amino acid sequence analyses versus biochemical characterization. Biochim. Biophys. Acta 1412:212-229.

Verhagen, M.F.J.M., T.W. O'Rourke, A.L. Menon, and M.W.W. Adams. 2001. Heterologous expression and properties of the γ-subunit of the Fe-only hydrogenase from *Thermotoga maritima*. Biochim. Biophys. Acta 1505:209-219.

Vermilion, J.L., D.P. Ballou, V. Massey, and M.J. Coon. 1981. Separate roles for FMN and FAD in catalysis by liver microsomal NADPH-cytochrome P-450 reductase. J. Biol. Chem. 256:266-277.

Vettakkorumakankav, N.N., and K.J. Stevenson 1992. Dihydrolipoamide dehydrogenase from *Haloferax volcanii* gene cloning, complete primary structure, and comparison to other dihydrolipoamide dehydrogenases. Biochem. Cell Biol. 70:656-662.

Vieille, C., J.M. Hess, R.M. Kelly, and J.G. Zeikus. 1995. xylA cloning and sequencing and biochemical characterization of xylose isomerase from *Thermotoga neapolitana*. Appl. Environ. Microbiol. 61:1867-1875.

Vieille, C., and G.J. Zeikus. 2001. Hyperthermophilic enzymes: sources, uses, and molecular mechanism for thermostability. Microbiol. Mol. Biol. Rev. 65:1-43.

Volbeda, A., M.-H. Charon, C. Piras, E.C. Hatchikian, M. Frey, and J.C. Fontecilla-Camps. 1995. Crystal structure of the nickel-iron hydrogenase from *Desulfovibrio gigas*. Nature. 373:580-587.

Voraberger, H. 2004. Optical techniques for determination and sensing of hydrogen peroxide in industrial and environmental samples. In: Optical Sensors: Industrial, Environmental and

Diagnostic Applications (R. Narayanaswamy and O.S. Wolfbeis, Ed.), Springer, Berlin, and London. pp. 391-408.

Walker, J.L., and D.J. Oliver. 1986. Glycine decarboxylase multienzyme complex: Purification and partial characterization from pea leaf mitochondria. J. Biol. Chem. 261:2214-2221.

Wanner, C., and J. Soppa. 2002. Functional role for a 2-oxo acid dehydrogenase in the halophilic archaeon *Haloferax volcanii*. J. Bacteriol. 184:3114-3121.

Warburg, O., and W. Christian. 1933. The yellow enzyme and its function. Biochem. Z. 266:377-411.

Ward, D.E., C.J. Donnelly, M.E. Mullendore, J. van der Oost, W.M. de Vos and E.J. Crane III. 2001. The NADH oxidase from *Pyrococcus furiosus*: implications for the protection of anaerobic hyperthermophiles against oxidative stress. Eur. J. Biochem. 268:5816-5823.

Weinberg, M.V., F.E. Jenney, Jr., X. Cui, and M.W.W. Adams. 2004. Rubrerythrin from the hyperthermophilic archaeon *Pyrococcus furiosus* is a rubredoxin-dependent, iron-containing peroxidase. J. Bacteriol. 186:7888-7895.

Weiss, D.S., and R.K. Thauer. 1993. Methanogenesis and the unity of biochemistry. Cell 72:819-822.

Whitby, L.G. 1953. A new method for preparing flavin adenine dinucleotide. Biochem. J. 54:437-442.

Wiame, J.M., S. Bourgeois, and R. Lambion. 1954. Oxidative dissimilation of glycerol studied with variants of *Bacillus subtilis*. Nature 174:37-38.

Wilkinson, K.D., and C.H. Williams, Jr. 1981. NADH inhibition and NAD activation of *Escherichia coli* lipoamide dehydrogenase catalyzing the NADH-lipoamide reaction. J. Biol. Chem. 256:2307-2314.

Williams, C.H. Jr. 1992. Lipoamide dehydrogenase, glutathione reductase, thioredoxin reductase, and mercuric ion reductase: A family of flavoenzyme transhydrogenases. In Chemistry and Biochemistry of Flavoenzymes (Müller F., ed.) vol. 3. 121-211. CRC press, Boca Raton. FL.

Williams, C.H. Jr., L.D. Arscott, S. Müller, B.W. Lennon, M.L. Ludwig, P.-F. Wang, D.M. Veine, K. Becker, and R.H. Schirmer. Thioredoxin reductase: two modes of catalysis have evolved. Eur. J. Biochem. 267:6110-6117.

Williams, C.H. Jr., L.D. Arscott, and G.E. Schulz. 1982. Amino acid sequence homology between pig heart lipoamide dehydrogenase and human erythrocyte glutathione reductase. Proc. Natl. Acad. Sci. USA 79:2199-2201.

Wilson, R.L., L.T. Stauffer, and G.V. Stauffer. 1993. Roles of the GcvA and PurR proteins in negative regulation of the *Escherichia coli* glycine cleavage enzyme system. J. Bacteriol. 175:5129-5134.

Windberger, E., R. Huber, A. Trincone, H. Fricke, and K.O. Stetter. 1989. *Thermotoga thermarum* sp. nov. and *Thermotoga neapolitana* occurring in African continental solfataric springs. Arch. Microbiol. 151:506-512.

Wolfe, R.S. 1991. My kind of biology. Annu. Rev. Microbiol. 45:1-36.

Yang, X., and K. Ma. 2005a. Purification and characterization of an NADH oxidase from extremely thermophilic anaerobic bacterium *Thermotoga hypogea*. Arch. Microbiol. 183:331-337.

Yang, X., and K. Ma. 2005b. Determination of hydrogen peroxide generated by reduced nicotinamide adenine dinucleotide oxidase. Anal. Biochem. 344:130-134.

Yang, X., and K. Ma. 2007. Characterization of an exceedingly active NADH oxidase from anaerobic hyperthermophilic bacterium *Thermotoga maritima*. J. Bacteriol. 189:3312-3317.

You, I.-S., D. Ghosal, and I.C. Gunsalus. 1991. Nucleotide sequence analysis of the Pseudomonas putida PpG7 salicylate hydroxylase gene (nahG) and its 3'-flanking region. Biochemistry 30:1635-1641.

Ziegler, D.M. 1990. Flavin-containing monooxygenases: enzymes adapted for multisubstrate specificity. Trends Pharmacol. Sci. 11:321-324.

Ziegler, D.M. 1991. The 1990 Bernard B. Brodie award lecture: unique properties of the enzymes of detoxification. Drug Metab. Dispos. 19:847-852.

Zillig, W., I. Holz, H.-P. Klenk, J. Trent, S. Wunderl, D. Janekovic, E. Imsel, and B. Haas. 1987. *Pyrococcus woesei*, sp. nov., an ultra-thermophilic marine archaebacterium, representing a novel order, *Thermococcales*. Syst. Appl. Microbiol. 9:62-70.

Zindel, U., W. Freudenberg, M. Rieth, J.R. Andreesen, J. Schnell, and F. Widdel. 1988. *Eubacterium acidaminophilum* sp. nov., a versatile amino acid-degrading anaerobe producing or utilizing H_2 or formate: description and enzyme studies. Arch. Microbiol. 150:254-266.